

F. A. M. de Haan

*Department of Soils and Fertilizers, State Agricultural University,  
Wageningen*

## The interaction of certain inorganic anions with clays and soils



1965 *Centre for Agricultural Publications and Documentation  
Wageningen*

2064104

The author was awarded the degree of Doctor of Agricultural Sciences, State Agricultural University, Wageningen, The Netherlands, on a thesis with the same title and contents.

# Contents

SYMBOLS FREQUENTLY USED	5
1 GENERAL INTRODUCTION	7
2 THEORETICAL PART	11
2.1 The negative adsorption of anions by clays	11
2.1.1 <i>Introduction, present literature</i>	11
2.1.2 <i>Calculation of the negative adsorption in single-salt systems</i>	12
2.1.3 <i>Derivation of the equations pertaining to mixed ionic systems at relatively high moisture content</i>	15
2.1.4 <i>Derivation of expressions for the negative adsorption of anions in systems with interacting double layers</i>	28
2.1.5 <i>The relation between <math>\delta^-</math> and <math>\Gamma</math>, and <math>\Gamma^-</math> and <math>\delta^-</math></i>	35
2.1.6 <i>Some remarks on the validity of the model chosen for the calculations of negative adsorption</i>	40
2.2 The positive adsorption of anions	41
2.2.1 <i>Electrostatic attraction by positively charged sites on the colloid</i>	43
2.2.2 <i>Specific adsorption of anions</i>	45
3 EXPERIMENTAL PROCEDURES AND MATERIALS	49
3.1 Introduction	49
3.1.1 <i>Required accuracy of the determinations</i>	50
3.2 The potentiometric chloride titration	52
3.3 The use of radioisotopes in the adsorption experiments	53
3.3.1 <i>The activity determinations</i>	55
3.3.2 <i>Simultaneous determination of the adsorption of two or more different anions</i>	56
3.4 Design of the anion adsorption experiments	57
3.4.1 <i>Verification of the method</i>	60
3.4.2 <i>The applicability of differences in half life to a differentiation between two isotopes</i>	61
3.5 The determination of the specific surface area from the retention of ethylene glycol	63
3.6 Materials	65
3.6.1 <i>Clays</i>	65
3.6.2 <i>Soils</i>	66

4	RESULTS ON ANION INTERACTION WITH CLAYS	71
4.1	Experiments with montmorillonite	71
4.1.1	<i>Comparison of the negative adsorption of chloride, as measured by the titration method and by the tracer method</i>	71
4.1.2	<i>The negative adsorption of chloride in mixed cationic systems</i>	73
4.1.3	<i>Simultaneous determination of the adsorption of <math>\text{Cl}^-</math> and <math>\text{SO}_4^{2-}</math> in Na-systems</i>	75
4.1.4	<i>The positive adsorption of sulfate at low concentration level</i>	76
4.1.5	<i>The influence of phosphate on the positive adsorption of sulfate</i>	78
4.1.6	<i>Simultaneous determination of the adsorption of <math>\text{Cl}^-</math> and <math>\text{SO}_4^{2-}</math> at different degrees of Ca saturation of the clay</i>	80
4.1.7	<i>The adsorption of phosphate on montmorillonite</i>	84
4.1.7.1	<i>General considerations</i>	84
4.1.7.2	<i>Simultaneous determination of the adsorption of chloride and phosphate on Na-montmorillonite</i>	85
4.1.7.3	<i>The influence of pyrocatechol and fluoride on the positive adsorption of phosphate</i>	87
4.1.7.4	<i>The influence of sodiumsilicate on the phosphate adsorption</i>	89
4.1.7.5	<i>The influence of the pH on the phosphate adsorption</i>	93
4.1.7.6	<i>The release of phosphate against silicate as a function of time</i>	95
4.1.8	<i>Simultaneous determination of the adsorption of three anions on Na-montmorillonite</i>	97
4.1.9	<i>The reduction of the negative adsorption of chloride due to the interaction of double layers</i>	99
4.1.10	<i>Determination of the chloride exclusion by Clayspur montmorillonite</i>	101
4.2	Experiments with illite	102
4.2.1	<i>Measurement of chloride exclusion. Determination of the specific surface area</i>	102
4.2.2	<i>Simultaneous determination of the adsorption of chloride and sulfate in Na-illite systems</i>	103
4.2.3	<i>Determination of the specific surface area after removal of the organic matter</i>	105
4.2.4	<i>The adsorption of phosphate on Na-illite before and after removal of the organic matter</i>	106
4.2.5	<i>Reduction of the negative adsorption of sulfate in Na-illite systems with interacting double layers</i>	108
4.2.6	<i>Determination of the specific surface area of the total fraction &lt; 2 <math>\mu</math> of Winsum illite</i>	108
4.3	Experiments with kaolinite	109
4.3.1	<i>The interaction between chloride and Na-kaolinite</i>	109
4.3.2	<i>The positive adsorption of phosphate on Na-kaolinite</i>	112
4.4	Analysis of the phosphate adsorption data	112

5	THE INTERACTION OF CHLORIDE AND PHOSPHATE WITH SOILS	121
5.1	Chloride interaction measurements	121
5.1.1	<i>Determination of the specific surface area according to the exclusion of chloride</i>	121
5.1.2	<i>Specific surface area determination of 3 soils over a wider range of electrolyte levels</i>	123
5.1.3	<i>The influence of the removal of free iron oxides on the chloride exclusion by Sticky soil and Na-laterite</i>	125
5.1.4	<i>Comparison between the results of the ethylene glycol retention method and the anion exclusion method</i>	126
5.2	Phosphate adsorption measurements	129
5.2.1	<i>Determination of the phosphate adsorption isotherms</i>	129
5.2.2	<i>The influence of pH on the phosphate adsorption by two soils</i>	133
	SUMMARY	135
	SAMENVATTING	139
	ACKNOWLEDGEMENT	145
	LITERATURE	147
	APPENDICES	153

## Symbols frequently used

$C_0$	concentration in equilibrium solution (mmol/ml)
$\sum C$	total ionic concentration in double layer (mmol/ml)
$\sum C_s$	total ionic concentration at the solid-liquid interface (mmol/ml)
$\sum C_0$	total ionic concentration in equilibrium solution (mmol/ml)
$N_0$	total ionic concentration in equilibrium solution (me./ml)
$f^{++}$	equivalent concentration fraction of divalent cations
$f^{=}$	equivalent concentration fraction of divalent anions
$f^{\equiv}$	equivalent concentration fraction of trivalent anions
$\Gamma$	surface charge density (me./cm <sup>2</sup> )
$\Gamma^-$	amount of monovalent anion excluded per unit surface area (me./cm <sup>2</sup> )
$\psi$	electric potential
$k$	Boltzmann constant
$T$	absolute temperature
$e$	electronic charge
$z^-$	valence of anion expressed as positive number
$1/u^{z^-}$	Boltzmann factor for anion of valence $z^-$ ( $= \exp(z^- e\psi/kT)$ )
$u_s$	value of $u$ at colloid surface
$u_c$	value of $u$ at central plane between opposing particles
$F$	faraday
$\epsilon$	dielectric constant
$R$	gas constant
$\beta$	$= 8\pi F^2/1,000e RT = 1.06 \times 10^{15}$ cm/mmol at 25° C
$v$	valency of cation
$d^-, d^=$ and $d^{\equiv}$	equivalent distance of exclusion of mono-, di-, and trivalent anion, respectively (Å)
$D/D^{s-}$	reduced thickness of water layer
$\sigma$	surface charge density (e.s.u./cm <sup>2</sup> )
$\rho$	volume charge density (e.s.u./cm <sup>3</sup> )
$V_{ex}$	volume of exclusion (ml/g colloid)
$V_{tot}$	total liquid volume (ml)
$V_{app}$	apparent volume (ml)
$W$	weight of colloid (g)
$A_s^*$ and $A_e^*$	activity of labeling solution and equilibrium solution, respectively (cpm/ml)

$A_0^*$  and  $A_t^*$  activity at time zero and t minutes after time zero, respectively  
(cpm/ml)

$T_{1/2}$  half life of radioisotope (minutes)

C.E.C. cation exchange capacity ( $\mu\text{e./g}$  colloid)

S specific surface area ( $\text{m}^2/\text{g}$  colloid)

## 1. General introduction

A characterization of the transient nutrient status of soil with respect to the plant requires a knowledge of both the amount and activity (or perhaps rather the partial molar Gibb's free energy) of nutrient ions present in soil. As the partial molar Gibb's free energy of an ion in solution is related to the composition of the solution, and more particularly to the concentration of the ion under consideration, it is necessary and satisfactory to determine simultaneously the amount present and the concentration in the equilibrium solution of the soil under varying conditions.

A characteristic feature of soil is its capacity to adsorb (or bind) ions reversibly, at least in part, in amounts far in excess of those present in the ambient solution. As such the adsorption complex of the soil serves as a storage reservoir enabling man to grow plants without daily additions of the necessary nutrient elements. Thus, in order to gain an insight in the changes of the soil with respect to its nutrient status, it is of importance to study the relationship between amount adsorbed and equilibrium concentration of certain nutrient ions under specified conditions. Obviously, the determination of the adsorption isotherms for different ions is the basis of the chemical evaluation of the soil.

The predominant negative charge of the soil solid phase renders cation adsorption the most striking feature of soils. In fact this phenomenon was discovered as early as 1850 by WAY and has been the subject of extensive investigations in soil chemistry ever since (a.o. KERR, 1928; VANSELOW, 1932; VAGELER, 1932; GAPON, 1933; JENNY, 1936; MATTSO, 1942; MAGISTAD, 1944; DAVIS, 1945; KELLEY, 1948; KRISNAMOORTHY and OVERSTREET, 1949; WIKLANDER, 1951; 1952; ERIKSSON, 1952; GAINES and THOMAS, 1953; see also reviews by BOLT, 1960, and BABCOCK, 1963). Much progress has been made in this matter, and functional relationships describing the exchange equilibrium between solution and complex for most common cations (Na, K, Ca, Mg) have been given. With the notable exception of K ions in illitic systems the specificity of the complex for these ions falls within the range predicted from differences in valence and size of the adsorbed cations. This is due to the fact that the adsorption forces are predominantly electrostatic in nature, the hydration energy of the cations being too large to allow dehydration of the cation upon adsorption (again with the notable exception of K ions and the less common Rb and Cs ions).

For practical purposes the above situation is satisfactorily described by a relationship of the form

$$\frac{\gamma_p}{\gamma_q} = K_G \cdot \frac{\sqrt[2]{C_{0p}}}{\sqrt[2]{C_{0q}}} \quad (1.1)$$



usually indicated as the GAPON equation, in which  $\gamma_p$  and  $\gamma_q$  represent the amounts adsorbed, in me. per gram solid, and  $C_{0p}$ ,  $C_{0q}$  the equilibrium concentrations, in mol/l, of the ion species p and q, respectively;  $z_p$  and  $z_q$  equal the valency of the ions involved,  $K_G$  representing the exchange "constant" according to GAPON. In the range of 0-40 per cent monovalent cations at the soil complex  $K_G$  appears to have a fairly constant value, making the equation of interest e.g. in irrigation practice. Experimental determination of  $K_G$  for a soil and the ions under study then allows the prediction of the composition of the adsorbing complex, following the use of irrigation water of a certain quality.

An approach with more theoretical basis is given by the theory of the diffuse electric double layer, known as the GOUY-CHAPMAN theory. According to this the distribution of the cations (anions) close to the surface of the clay particle is represented as a gradually decreasing (increasing) value with the distance from this surface. Further development of this idea and practical applications have been given by SCHOFIELD (1946) and ERIKSSON (1952).

Applying the GOUY-CHAPMAN theory to soil systems several basic assumptions are made, viz:

1. the attraction between ion and colloid is caused by electrostatic forces and no specific attraction exists;
2. the charge of the colloid is homogeneously distributed over the surface;
3. the behavior of the ions in the diffuse double layer is ideal.

Notwithstanding these simplifications good results were obtained applying this theory, as was shown for Na-Ca-systems by BOLT (1955) and PRATT et al (1962), and for K-Ca-systems by LAGERWERFF and BOLT (1959), SUMNER and BOLT (1962), VAN SCHOUWENBURG and SCHUFFELEN (1963).

With respect to anions the situation is entirely different. Usually one finds that the amount adsorbed (or bound) is very much smaller than the amount of adsorbed cations, which is understandable in view of the predominant negative charge of the complex. In fact one should expect (and often finds) that the adsorption is negative, i.e. anions are excluded rather than adsorbed. Nevertheless, certain anions are also adsorbed positively, indicating the presence of some positively charged sites on the complex and/or chemical bonding. Obviously the situation is rather complex in the case of anions, as positive adsorption (or chemical bonding) should always be accompanied by anion exclusion at the negatively charged sites. At the same time, chemical bonding should be expected to be rather specific for certain anions. In summary, anion adsorption should be expected to be small and very specific in contrast to the high magnitude and comparatively low specificity of cation adsorption. This is borne out by the literature, which shows adsorption of certain anions of varying magnitude in specific cases (a.o. ENSMINGER, 1954; KAMPATH et al, 1956; CHAO et al, 1962, 1963; CHANG and THOMAS, 1963). In contrast to other anions the phosphate ion is invariably positively adsorbed (a.o. HASEMAN, 1950; BRELAND and SIERRA, 1962; SISSINGH, 1961). It may be shown, however, that in most cases the negative adsorption still forms a substantial part of the actual adsorption.

As follows from the above and has already been pointed out by DE HAAN and BOLT (1963), a correct interpretation of experimentally determined anion adsorption data requires a correction for the amount excluded by the negatively charged sites. If, for example, a positive adsorption of a certain anion is found from experiment, the measured amount must be enlarged with the negative adsorption to find the correct value of the amount which is positively adsorbed. Thus, the difference between the measured adsorption and the expected negative adsorption constitutes the actual positive adsorption.

For this correction it is imperative that a correct procedure for the calculation of the negative adsorption be available. Accordingly considerable attention has been given to the theoretical derivation (Chapter 2) and experimental verification of this theory of negative adsorption (Chapter 4).

It may also be pointed out that this negative adsorption must be taken into account for a correct evaluation of salt diffusion in soil columns (DUTT and LOW, 1962; BOLT and DE HAAN, 1964). Moreover it provides the basis for the interpretation of the behavior of soils upon pressure filtration (BOLT, 1961 a and b) and the so-called salt sieving effect in soil columns (DERJAGUIN, 1958; KEMPER, 1961). Finally a method for the determination of the specific surface area of soils is based on negative adsorption measurements (SCHOFIELD, 1947): Chapter 5 represents results of these determinations for a number of Dutch soils. Because the anion exclusion is often only a small fraction of the total amount of anions present in the system, much attention has been paid to its experimental evaluation (Chapter 3). Since the phosphate ion is perhaps the most important anion from an agricultural point of view, much of the data concerns phosphate adsorption measurements.

## 2. Theoretical part

### 2.1 The negative adsorption of anions by clays

#### 2.1.1 Introduction, present literature

As was pointed out in Chapter 1 the evaluation of the negative adsorption of anions by clays is a necessary prerequisite for the study of anion adsorption characteristics of clays and soils. This negative adsorption is the direct result of the presence under field conditions of a predominantly negative charge on most soil constituents.

This charge is the result of isomorphic substitutions in the clay lattice and/or proton dissociation-association reactions of surface OH-groups. In the first case the charge has been built-in during the formation of the clay lattice and may be considered to be of a constant magnitude. In the second case the surface charge varies in magnitude and possibly in sign with the concentration of the potential determining H-ion and the electrolyte concentration of the system.

Experimental evidence indicates that the common soil clays of the montmorillonite and illite groups have a net negative charge which does not vary over a pH range from, say, 4 to 8, and which is independent of the electrolyte concentration, indicating that substitution is the prime source of the colloid charges in these cases. A detailed investigation shows, however, that at low pH a small amount of positive charge of variable magnitude is also often present. Most authors agree that these charges are due to proton association at the exposed AlOH-groups along the clay plate edge. This is supported by the fact that for kaolinites (a clay mineral with a relatively large edge surface) indications were found of the presence of a rather considerable positive charge, varying with pH. Although thus the net charge of kaolinite appears to vary with pH, it was shown by CASHEN (1959) that this is interpreted best by assuming the presence of a constant amount of negative charge in addition to a varying amount of positive charge.

As the substitution charge is presumably distributed throughout the lattice, its influence makes itself felt mainly on the planar side of the clay plates. No convincing evidence has been found of the presence of a varying negative charge on these planar sides at pH values below 7-8. Above these pH values, however, the cation exchange capacity of clays tends to increase. This is usually attributed to the dissociation of SiOH-groups along the edges and perhaps along lattice imperfections.

The above considerations indicate that calculations on the distribution of ions in the counter-ion atmosphere of clay particles should be based preferably upon a

model assuming a constant surface charge density. A notable exception to this are the organic colloids in soil. For these the charge is likely pH dependent. Till now very little experimental data have been presented on the cation and anion adsorbing properties of these materials. Presumably the chemical instability of the organic compounds renders a study of the physical chemical properties extremely difficult. Moreover it seems doubtful whether the model of an electric double layer formed on a planar charged surface, which seems very suitable for the description of the ion atmosphere on the planar sides of the clay particles, is applicable to organic compounds. These should perhaps be considered as coiled polymers with a large number of, mainly carboxylic, OH groups.

Leaving the organic colloids out of consideration it thus seems obvious that the GOUY-CHAPMAN theory of the double layer formed on planar surfaces may be used as a point of departure for a calculation of the distribution of anions in the vicinity of the planar side of clay particles. As has been pointed out already in the General Introduction, several approximations are involved in this theory. It will be shown later (cf section 2.1.6) that the error caused by these approximations is unlikely to be of significance insofar as anions are involved.

It should be stated here that the principle of the calculations to be presented is the same as that introduced by SCHOFIELD (1946), KLAARENBECK (1946) and extended by BOLT and WARKENTIN (1958). These calculations, however, were worked out only for systems containing single salts. The main purpose of this theoretical part is to derive expressions for anion exclusion of general applicability to most mixed systems, which are of interest in soil studies, i.e. systems containing mono- and divalent cations and mono-, di-, and trivalent anions (N.B. phosphate ions are present at different valencies at field pH).

As these derivations follow an approach similar to that used by the above authors, the calculation of the negative adsorption in single-salt systems is briefly reviewed first.

### 2.1.2 Calculation of the negative adsorption in single-salt systems

In figure 1 the cation and anion concentrations in the vicinity of a charged clay surface are represented schematically for a system in equilibrium with a single salt solution of a concentration  $C_0$  mol/l. Although both anion and cation concentration reach a finite value at the clay surface, the concentration curves may be extended for mathematical convenience over a distance  $\delta$  beyond the location of the charged surface to the point where  $C^-$  and  $C^+$  reach the values zero and infinity, respectively. At this point the total countercharge reaches infinity. It also represents the point where, for the given ion distribution, an infinitely highly charged surface should be located.

The negative adsorption of anions, in me. per  $\text{cm}^2$  surface area,  $F^-$ , is represented by the cross-hatched area in figure 1. Introducing the distance coordinates  $x$  (measur-

ed from the charged surface) and  $X = x + \delta$ , and following the standard theory of the diffuse double layer, the negative adsorption for systems in which the thickness of the liquid layer greatly exceeds the thickness of the double layer (i.e. suspensions with a relatively high liquid content) is found as:

$$\begin{aligned}\Gamma z^- &= N_0^- \cdot \int_0^\infty \left(1 - \frac{1}{u^{z^-}}\right) dx \\ &= N_0^- \cdot \left\{ \int_0^\infty \left(1 - \frac{1}{u^{z^-}}\right) dX - \int_0^\delta \left(1 - \frac{1}{u^{z^-}}\right) dX \right\}\end{aligned}\quad (2.1)$$

in which  $z^-$  is valence of the anion expressed as a positive number;  $N_0^-$  is the equilibrium concentration of the anion in eq/l and  $1/u^{z^-} = \exp(z^- e\psi/kT)$ , the Boltzmann factor for the anion of valence  $z^-$ , with  $e$  = electronic charge,  $\psi$  = electric potential,  $k$  = Boltzmann constant and  $T$  = absolute temperature.

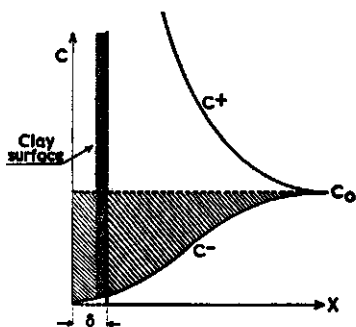


Fig. 1. The ionic distribution at a planar, charged surface

As is indicated in figure 1, the second integral of equation (2.1) may be approximated by  $z^- C_0 \cdot \delta (= N_0^- \cdot \delta)$ . It can be shown that the exact value of this integral may be evaluated, proving that the error due to the approximation introduced in using  $z^- C_0 \cdot \delta$  amounts to less than 3% if the surface charge density  $\geq 10^{-7}$  me. per  $\text{cm}^2$  and  $C_0 \leq 10^{-1}$  molar (cf section 2.1.5). It was also shown by SCHOFIELD, that the distance  $\delta$  is a function of the surface charge density of the clay and may be approximated quite well by the relation:

$$\delta \approx \frac{4}{z^+ \beta \Gamma} \quad (2.2)$$

in which  $\Gamma$  represents the surface charge density, expressed in me. per  $\text{cm}^2$  surface; values of  $\Gamma$  may be estimated for different clays from the C.E.C. and the specific surface area;  $z^+$  represents the valency of the dominant cation in the system and  $\beta$  equals a constant of double layer theory  $= 8\pi F^2/1000 \epsilon RT$ , with  $F$  is the faraday,  $\epsilon$  is dielectric constant and  $R$  is gas constant; at  $25^\circ \text{C}$   $\beta$  equals  $1.06 \times 10^{15}$  cm/mmole. For further details on the relation between  $\Gamma^-$  and  $\delta$  and between  $\delta$  and  $\Gamma$  the reader is referred to section 2.1.5.

Starting with equation (2.1) and using the functional relationship between  $u$  and  $X$  as derived from the solution of the Poisson-Boltzmann equation for the diffuse double layer in the presence of one type of salt SCHOFIELD presented the following equation describing negative adsorption for systems containing a single salt:

$$\frac{\Gamma^-}{N} = \frac{q}{\sqrt{v\beta N}} - \frac{4}{v\beta\Gamma} \quad (2.3)$$

in which  $N$  represents the equilibrium concentration in eq/l and  $v$  the valency of the cation;  $q$  is a constant determined by the ratio of the valencies of the cation and the anion in the system. For the mono-mono-valent case, e.g. NaCl,  $q$  has the value 2.

The equation given by SCHOFIELD is limited to systems without interaction between adjacent double layers.

The extension to a system with interacting double layers has been given by BOLT and WARKENTIN. In evaluating the first integral of equation (2.1) use is made of the expression obtained by the first integration of the Poisson-Boltzmann equation of the electric double layer, viz.:

$$\frac{d(e\psi/kT)}{dX} = \frac{d \ln u}{dX} = \pm \sqrt{\beta} \cdot \sqrt{\sum C - \sum C_0} \quad (2.4)$$

in which  $\sum C$  and  $\sum C_0$  indicate the total ionic concentration in mol/l in the double layer and in the equilibrium solution, respectively.

Combining equations (2.1) and (2.4) one finds:

$$\frac{\Gamma z^-}{N_0^-} = \int_{x=0}^{x=D} \frac{(1-1/u^z) d \ln u}{\sqrt{\beta} \cdot \sqrt{\sum C - \sum C_0}} - \delta \quad (2.5)$$

in which  $D$  = distance from the imaginary position of the charged plate to the central plane between two opposing clay plates.

This equation worked out for a system containing one symmetric salt only of valence  $z$ , with interaction of double layers, leads to the equation as given by the above mentioned authors:

$$\frac{\Gamma z}{zC_0^-} = \int_{\infty}^{u_c} \frac{(1-1/u^z) du^z}{z\sqrt{\beta C_0^-} \cdot \sqrt{u^{2z}(u^z + u^{-z} - u_c^z - u_c^{-z})}} - \delta \quad (2.6)$$

in which  $u_c$  and  $\infty$  represent the value of  $u$  at the central plane and at the plane of infinite charge, respectively.

Solution of the integral of equation (2.6) then gave:

$$\frac{\Gamma z}{zC_0^-} = (D - \delta) - \frac{2\sqrt{u_c^z}}{z\sqrt{\beta C_0^-}} \cdot \{F(\pi/2, \alpha) - E(\pi/2, \alpha)\} \quad (2.7)$$

in which  $F(\pi/2, \alpha)$  and  $E(\pi/2, \alpha)$  represent complete elliptic integrals of the first and second kind, respectively, with  $\alpha = \arcsin 1/u_c^z$ .

### 2.1.3 Derivation of the equations pertaining to mixed ionic systems at relatively high moisture content

Starting with the general equation (2.5) one may arrive at certain special solutions for the negative adsorption of anions, by applying this equation to systems of different, mixed ionic compositions. To show the procedures used the solutions are presented in detail in the Appendices. In the following sections the derivations are given in abridged form for the systems of interest.

Solutions require the writing out of the expression  $(\sum C - \sum C_0)$ , appearing in the integrated Boltzmann equation, for the system chosen, resulting in a polynomial in  $u$ .

For practical purposes two types of systems are chosen for evaluation, symbolized by:

a. +2, +1, -1, -2 and

b. +1, -1, -2, -3,

the numbers representing the valency of the ions, the + or - sign referring to cations and anions, respectively.

It was also attempted to solve the equation for a system containing simultaneously all ionic species present in the systems a) and b). A general solution for this system (which would make the solutions of a) and b) superfluous) appeared to necessitate the use of an electronic computer. As the simultaneous presence of divalent cations and trivalent anions at high concentrations in soils (notably  $\text{Ca}^{2+}$  and  $\text{PO}_4^{3-}$ ) seems improbable this solution was not obtained. In stead an approximate solution was used, valid for systems in which the concentration of trivalent anions is very low in comparison to the total electrolyte level. As will be discussed in section 2.1.3 under c, this solution should be valid even for reasonably high concentrations of the trivalent anion. This system will be symbolized by: c) +2, +1, -1, -2, (-3), the brackets indicating that the trivalent anion is present in small amounts.

*a Solution for systems containing mono- and divalent cations and anions.* As was shown by DE HAAN and BOLT (1963) such a system may be described in the following manner.

If  $N_0$  represents the total salt concentration in eq/l and  $f^{++}$  and  $f^{-}$  stand for the equivalent concentration fractions of the divalent cation and anion, respectively, then the concentrations in eq/l of the different ions are equal to:

$f^{++}N_0$  for the divalent cation  
 $(1-f^{++})N_0$  for the monovalent cation  
 $f^{-}N_0$  for the divalent anion  
 $(1-f^{-})N_0$  for the monovalent anion.

Thus in this case:

$$\sum C - \sum C_0 = N_0 \left\{ \frac{1}{2} f^{++} u^2 + (1 - f^{++}) u + (1 - f^{-}) u^{-1} + \frac{1}{2} f^{-} u^{-2} - \frac{1}{2} (4 - f^{++} - f^{-}) \right\} \quad (2.8)$$

Substitution of (2.8) in (2.5), replacing  $d \ln u$  by  $1/u du$  gives:  
**a 1** for the monovalent anion

$$\frac{\Gamma^-}{(1-f^-)N_0} = \pm \frac{1}{\sqrt{\beta N_0}} \cdot \int_{u=\infty}^{u=1} \frac{(1-1/u)du}{\sqrt{\frac{1}{2}f^{++}u^4 + (1-f^{++})u^3 - \frac{1}{2}(4-f^{++}-f^-)u^2 + (1-f^-)u + \frac{1}{2}f^-}} - \delta^- \quad (2.9)$$

In this equation  $\delta^-$  symbolizes now the exact value of the integral of equation (2.9) between the limits  $u = \infty$  and  $u = u_s$  ( $u_s$  equals the value of  $u$  at the charged surface). In section 2.1.5 the relation between  $\delta^-$  and measurable properties of the system will be discussed in detail, indicating that the replacement of  $\delta^-$  by  $\delta \simeq 4/2\beta\Gamma$  is acceptable for most systems.

Dividing numerator and denominator of (2.9) by  $(u-1)$  this gives:

$$\frac{\Gamma^-}{(1-f^-)N_0} = \pm \frac{2}{\sqrt{\beta N_0}} \cdot \int_{\infty}^1 \frac{du}{u\sqrt{f^{++}u^2 + 2u + f^-}} - \delta^- \quad (2.10)$$

$$= \pm \frac{2}{\sqrt{\beta N_0}} \cdot \int_{\infty}^1 \frac{du}{u\sqrt{A}} - \delta^- \quad (2.11)$$

in which  $A$  designates the second power polynomial in  $u$  of the denominator.

**a 2** For the divalent anion one finds:

$$\frac{\Gamma^-}{f^-N_0} = \pm \frac{1}{\sqrt{\beta N_0}} \times \int_{u=\infty}^{u=1} \frac{(1-1/u^2)du}{\sqrt{\frac{1}{2}f^{++}u^4 + (1-f^{++})u^3 - \frac{1}{2}(4-f^{++}-f^-)u^2 + (1-f^-)u + \frac{1}{2}f^-}} - \delta^- \quad (2.12)$$

which upon simplification yields:

$$\frac{\Gamma^-}{f^-N_0} = \pm \frac{2}{\sqrt{\beta N_0}} \cdot \int_{\infty}^1 \frac{(u+1)du}{u^2\sqrt{A}} - \delta^- \quad (2.13)$$

It is noted that the left hand side of these equations represents the equivalent distance over which no anions appear to be present, i.e. the amount of anions excluded per  $\text{cm}^3$  colloid surface expressed as the number of  $\text{cm}^3$  of solution per  $\text{cm}^2$  surface, which appears to be free of anions. Later in this text this distance will be termed the equivalent distance of exclusion,  $d^-$  (cf also figure 1).

As is shown in Appendix I the solutions of equations (2.11) and (2.13) are, respectively:

$$\frac{\Gamma^-}{(1-f^-)N_0} = \frac{\sqrt{2}}{\sqrt{\beta N_0}}$$



$$\times \left\{ \frac{1}{\sqrt{f^-}} \left[ \sinh^{-1} \left( \frac{\sqrt{f^-} \cdot \sqrt{f^{++} + 2 + f^-}}{\sqrt{1 - f^{++} f^-}} \right) - \sinh^{-1} \left( \frac{\sqrt{f^-} \cdot \sqrt{f^{++}}}{\sqrt{1 - f^{++} f^-}} \right) \right] \right\} - \delta^- \quad (2.14)$$

and

$$\frac{\Gamma^-}{f^- N_0} = \frac{\sqrt{2}}{\sqrt{\beta N_0}} \cdot \left( \frac{\sqrt{f^{++} + 2 + f^-}}{f^-} - \frac{\sqrt{f^{++}}}{f^-} - \frac{1 - f^-}{f^-} \cdot \frac{1}{\sqrt{f^-}} \right) \times \left[ \sinh^{-1} \left( \frac{\sqrt{f^-} \cdot \sqrt{f^{++} + 2 + f^-}}{\sqrt{1 - f^{++} f^-}} \right) - \sinh^{-1} \left( \frac{\sqrt{f^-} \cdot \sqrt{f^{++}}}{\sqrt{1 - f^{++} f^-}} \right) \right] - \delta^- \quad (2.15)$$

For convenience the terms within accolades in equations (2.14) and (2.15), multiplied by  $\sqrt{2}$ , are replaced by the symbols  $Q'_a$  and  $Q''_a$ , respectively, yielding:

$$\frac{\Gamma^-}{(1 - f^-) N_0} = \frac{Q'_a}{\sqrt{\beta N_0}} - \delta^- \quad (2.16)$$

and

$$\frac{\Gamma^-}{f^- N_0} = \frac{Q''_a}{\sqrt{\beta N_0}} - \delta^- \quad (2.17)$$

Thus it appears that the theoretical value for the distance of exclusion of the mono- and divalent anion can be found as the product of  $1/\sqrt{\beta N_0}$  and a factor  $Q'_a$  and  $Q''_a$ , respectively, diminished with  $\delta^-$ .

Since  $Q'_a$  and  $Q''_a$  are dependent upon the ratios of the different ions in the equilibrium solution their respective values were calculated for a large number of combinations of  $f^{++}$  and  $f^-$  (cf Appendix I). The results of this calculation are given in table 1 and presented graphically in figure 2. Because of the relative minor influence

Table 1. Calculated  $Q_a$  values for a system containing mono- and divalent cations and anions (+2, +1, -1, -2)

		$Q'_a$						$Q''_a$					
$f^{++}$	$f^-$	0.0	0.2	0.4	0.6	0.8	1.0	0.0	0.2	0.4	0.6	0.8	1.0
0.0	2.000	1.968	1.938	1.912	1.886	1.862		2.667	2.615	2.572	2.526	2.486	2.449
0.2	1.465	1.441	1.419	1.398	1.379	1.361		2.066	2.028	1.991	1.958	1.920	1.897
0.4	1.296	1.277	1.259	1.242	1.226	1.209		1.854	1.822	1.792	1.764	1.738	1.713
0.6	1.171	1.168	1.153	1.139	1.125	1.109		1.708	1.681	1.655	1.631	1.609	1.588
0.8	1.102	1.088	1.074	1.062	1.050	1.037		1.596	1.573	1.551	1.530	1.510	1.492
1.0	1.035	1.023	1.008	1.000	0.989	0.980		1.507	1.486	1.471	1.448	1.431	1.414

of  $f^-$  only the extremes are presented, corresponding to  $f^- = 0$  and  $f^- = 1$ , respectively. As is shown by the insert of figure 2, linear interpolation is permitted for values of  $f^-$  not given in the main graph.

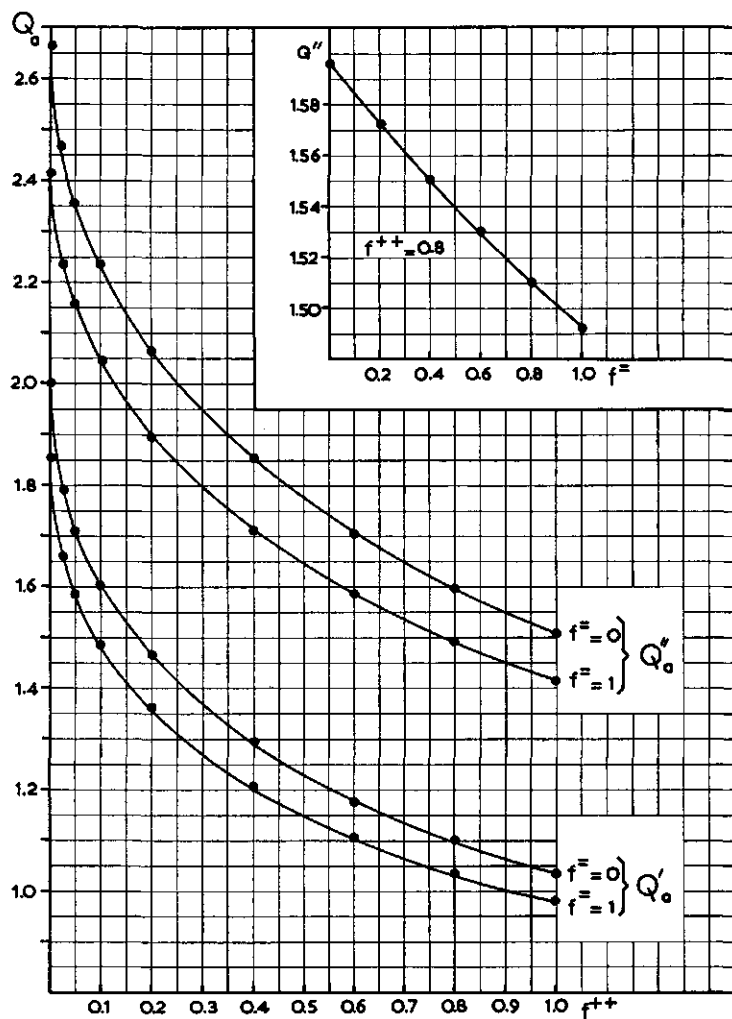


Fig. 2. Calculated values of  $Q'_a$  and  $Q''_a$  for different values of  $f^{++}$  and  $f^{\equiv}$ . The insert shows the linearity of the  $Q$ -terms with different values of  $f^{\equiv}$  at a constant value of  $f^{++}$  (0.8)

**b** Solution for systems containing monovalent cations and mono-, di-, and trivalent anions. Again the total salt concentration in the equilibrium solution is considered to be  $N_0$  eq/l, whereas the equivalent fraction of the mono-, di-, and trivalent anion may now be represented by  $(1 - f^{\equiv} - f^{\equiv})$ ,  $f^{\equiv}$  and  $f^{\equiv}$ , respectively.

**b 1** The monovalent anion. Using equation (2.5) and the expression for  $(\sum C - \sum C_0)$  the negative adsorption of the monovalent anion in this system is found as:

$$\frac{\Gamma^-}{(1 - f^{\equiv} - f^{\equiv})N_0} = \pm \frac{1}{\sqrt{\beta N_0}}$$

$$\times \int_{-\infty}^1 \frac{(1-1/u)du}{\sqrt{u^3 - (2 - \frac{1}{2}f^- - \frac{2}{3}f^{\equiv})u^2 + (1 - f^- - f^{\equiv})u + \frac{1}{2}f^- + \frac{1}{3}f^{\equiv}u^{-1}}} - \delta^- \quad (2.18)$$

Dividing again numerator and denominator by  $(u-1)$  this gives:

$$\frac{\Gamma^-}{(1 - f^- - f^{\equiv})N_0} = \pm \frac{1}{\sqrt{\beta N_0}} \cdot \int_{-\infty}^1 \frac{du}{\sqrt{u^3 + (\frac{1}{2}f^- + \frac{2}{3}f^{\equiv})u^2 + \frac{1}{3}f^{\equiv}u}} - \delta^- \quad (2.19)$$

Equation (2.19) has different solutions all of which may be represented as:

$$\frac{1}{\sqrt{\beta N_0}} \cdot Q_b' - \delta^-.$$

The specific form of these solutions depends on the roots of the cubic equation:

$$B = u^3 + (\frac{1}{2}f^- + \frac{2}{3}f^{\equiv})u^2 + \frac{1}{3}f^{\equiv}u \quad (2.20)$$

As is shown in figure 3 most combinations of  $f^-$  and  $f^{\equiv}$  lead to an equation with

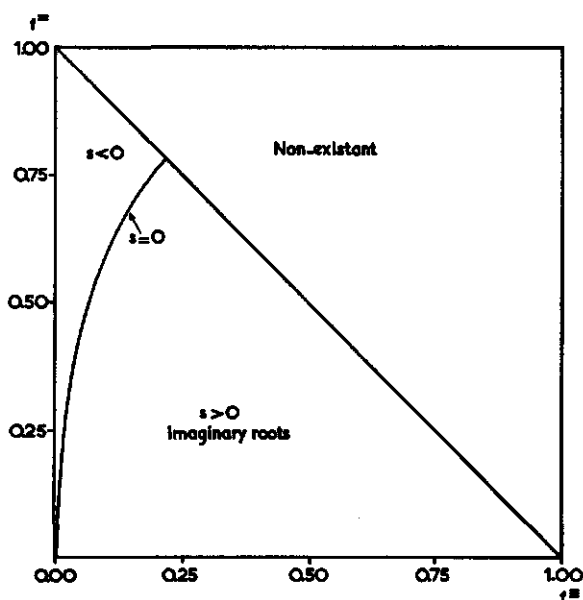


Fig. 3. The occurrence of imaginary and real roots of the polynomial  $B$  as a function of  $f^-$  and  $f^{\equiv}$

one real root,  $u = 0$ , and two imaginary roots. For this case (2.20) is transformed into:

$$B = u \{(u-r)^2 + s^2\}$$

$$\text{with } r = -(\frac{1}{2}f^- + \frac{1}{3}f^{\equiv})$$

$$\text{and } s = \sqrt{\frac{1}{3}f^{\equiv} - (\frac{1}{2}f^- + \frac{1}{3}f^{\equiv})^2}$$

As is shown in Appendix II the solution of the integral of equation (2.19) is then found as:

$$Q'_b = \int_{\infty}^1 \frac{du}{\sqrt{B}} = \frac{-2a}{c} \cdot F(\varphi, k) \quad (2.21)$$

in which  $F(\varphi, k)$  is an incomplete elliptic integral of the first kind, and  $a$ ,  $c$  and  $k$  are known functions of  $r$  and  $s$ , according to:

$$a = -r + s \operatorname{tg} \theta$$

$$c = \sqrt{\frac{4s^3}{\sin^3 2\theta}}$$

$$k = |\sin \theta| \quad \text{with } \theta = \frac{1}{2} \operatorname{arctg} \left( \frac{s}{-r} \right); \quad 0 < \theta < \pi/2$$

The value of  $\varphi$  is found by substituting the integration limits of  $u$  into the equation:

$$u = \frac{a(\cos \varphi + 1)}{1 - \cos \varphi}$$

Table 2. Calculated  $Q_b$  values for a system containing monovalent cations and mono-, di-, and trivalent anions (+1, -1, -2, -3)

		$Q'_b$					
$f^-$	$f \equiv$	0.0	0.2	0.4	0.6	0.8	1.0
0.0		2.000	1.948	1.905	1.866	1.829	1.793
0.2		1.968	1.919	1.876	1.838	1.806	—
0.4		1.939	1.892	1.854	1.819	—	—
0.6		1.912	1.870	1.832	—	—	—
0.8		1.886	1.848	—	—	—	—
1.0		1.863	—	—	—	—	—

		$Q''_b$					
$f^-$	$f \equiv$	0.0	0.2	0.4	0.6	0.8	1.0
0.0		2.667	2.578	2.510	2.449	2.391	2.334
0.2		2.615	2.534	2.469	2.410	2.356	—
0.4		2.572	2.492	2.432	2.378	—	—
0.6		2.526	2.457	2.400	—	—	—
0.8		2.487	2.424	—	—	—	—
1.0		2.450	—	—	—	—	—

		$Q'''_b$					
$f^-$	$f \equiv$	0.0	0.2	0.4	0.6	0.8	1.0
0.0		3.067	2.952	2.857	2.778	2.708	2.648
0.2		3.002	2.906	2.816	2.739	2.674	—
0.4		2.945	2.854	2.773	2.701	—	—
0.6		2.890	2.807	2.729	—	—	—
0.8		2.840	2.760	—	—	—	—
1.0		2.796	—	—	—	—	—

In the case  $B$  has three real roots,  $\alpha_1, \alpha_2, \alpha_3$ , the transformation into an elliptic integral follows a slightly different pattern. One then finds (cf section 1 of Appendix II):

$$Q'_b = 2\lambda \cdot F(\varphi, k) \quad (2.22)$$

with  $\lambda = 1/\sqrt{\alpha_1 - \alpha_3}$  and  $k^2 = (\alpha_2 - \alpha_3)/(\alpha_1 - \alpha_3)$

$\varphi$  is now found by substituting the integration limits into:

$$u = \frac{\alpha_1 - \alpha_2 \sin^2 \varphi}{1 - \sin^2 \varphi}$$

Finally several special combinations of  $f^{\equiv}$  and  $f^{\equiv}$  lead to "degraded" elliptic integrals which may be solved without further substitution (cf Appendix).

The values of  $Q'_b$  corresponding to a large number of combinations of  $f^{\equiv}$  and  $f^{\equiv}$ , as calculated to the above approach, are presented in table 2 and figure 4.

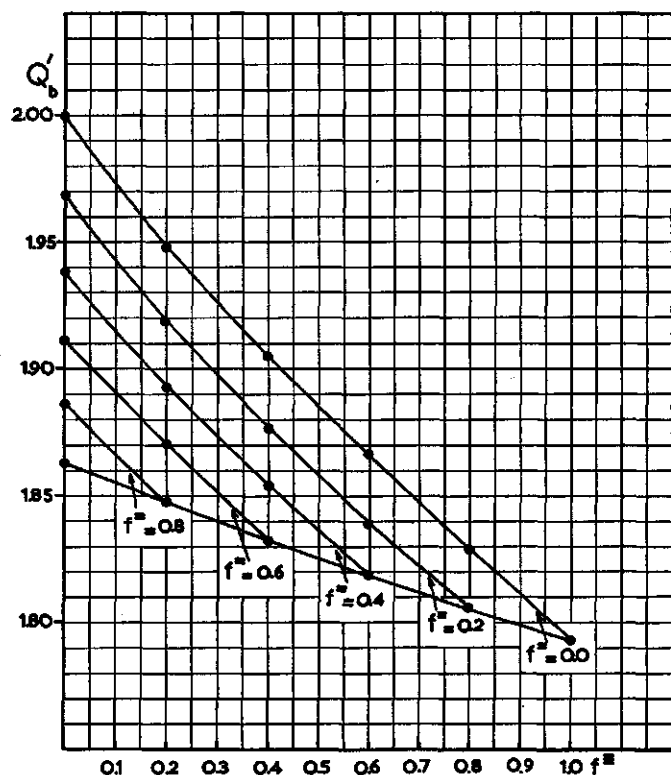


Fig. 4. Calculated values of  $Q'_b$  for different combinations of  $f^{\equiv}$  and  $f^{\equiv}$

**b 2** The divalent anion. For the negative adsorption of the divalent anion in this system one arrives at:

$$\frac{\Gamma^=}{f^=N_0} = \pm \frac{1}{\sqrt{\beta N_0}} \cdot \int_{\infty}^1 \frac{(1-1/u^2)du}{\sqrt{u^3 + (2-\frac{1}{2}f^= - \frac{2}{3}f^=)u^2 + (1-f^= - f^=)u + \frac{1}{2}f^= + \frac{1}{3}f^=u^{-1}}} - \delta^- \quad (2.23)$$

Introducing again the third power polynomial  $B$  this gives:

$$\frac{\Gamma^=}{f^=N_0} = \pm \frac{1}{\sqrt{\beta N_0}} \cdot \int_{\infty}^1 \frac{(u+1)du}{u\sqrt{B}} - \delta^- \quad (2.24)$$

$$= \pm \frac{1}{\sqrt{\beta N_0}} \cdot \left\{ \int_{\infty}^1 \frac{du}{\sqrt{B}} + \int_{\infty}^1 \frac{du}{u\sqrt{B}} \right\} - \delta^- \quad (2.25)$$

which may be written as:

$$= \frac{1}{\sqrt{\beta N_0}} \cdot Q_b'' - \delta^- \quad (2.26)$$

As is shown in section 2 of Appendix II,  $Q_b''$  is found as:

$$Q_b'' = Q_b' + \left\{ -\frac{2}{c} \cdot F(\varphi, k) + \frac{4}{c} \cdot E(\varphi, k) - \frac{4}{c} \cdot \left( \frac{1 - \cos \varphi}{\sin \varphi} \right) \cdot \sqrt{1 - k^2 \sin^2 \varphi} \right\} \quad (2.27)$$

in which  $E(\varphi, k)$  indicates an incomplete elliptic integral of the second kind;  $c$ ,  $\varphi$ , and  $k$  have the same meaning as in equation (2.21). As in the above case,  $Q_b''$  may thus be calculated for any combination of  $f^=$  and  $f^=$ . For several combinations  $Q_b''$  values are given in table 2 and figure 5.

**b 3** The trivalent anion. The negative adsorption of the trivalent anion in this system is found as:

$$\frac{\Gamma^=}{f^=N_0} = \pm \frac{1}{\sqrt{\beta N_0}} \cdot \int_{\infty}^1 \frac{(1-1/u^3)du}{\sqrt{u^3 + (2-\frac{1}{2}f^= - \frac{2}{3}f^=)u^2 + (1-f^= - f^=)u + \frac{1}{2}f^= + \frac{1}{3}f^=u^{-1}}} - \delta^- \quad (2.28)$$

$$= \pm \frac{1}{\sqrt{\beta N_0}} \cdot \int_{\infty}^1 \frac{(u^2+u+1)du}{u^2\sqrt{B}} - \delta^- \quad (2.29)$$

$$= \pm \frac{1}{\sqrt{\beta N_0}} \cdot \left\{ \int_{\infty}^1 \frac{du}{\sqrt{B}} + \int_{\infty}^1 \frac{du}{u\sqrt{B}} + \int_{\infty}^1 \frac{du}{u^2\sqrt{B}} \right\} - \delta^- \quad (2.30)$$

$$= \frac{1}{\sqrt{\beta N_0}} \cdot Q_b''' - \delta^- \quad (2.31)$$

Using a recurrence procedure the third integral of equation (2.30) may be converted into the first and second integral, which have been solved already.

As is shown in section 3 of Appendix II:

$$Q_b''' = \frac{2\sqrt{1+\frac{1}{2}f''+f'''}}{f'''} - \frac{1-f''}{f'''} \cdot Q_b' - \frac{f''+f'''}{f'''} \cdot (Q_b'' - Q_b') \quad (2.32)$$

Calculated values for  $Q_b'''$  are presented in table 2 and figure 6.

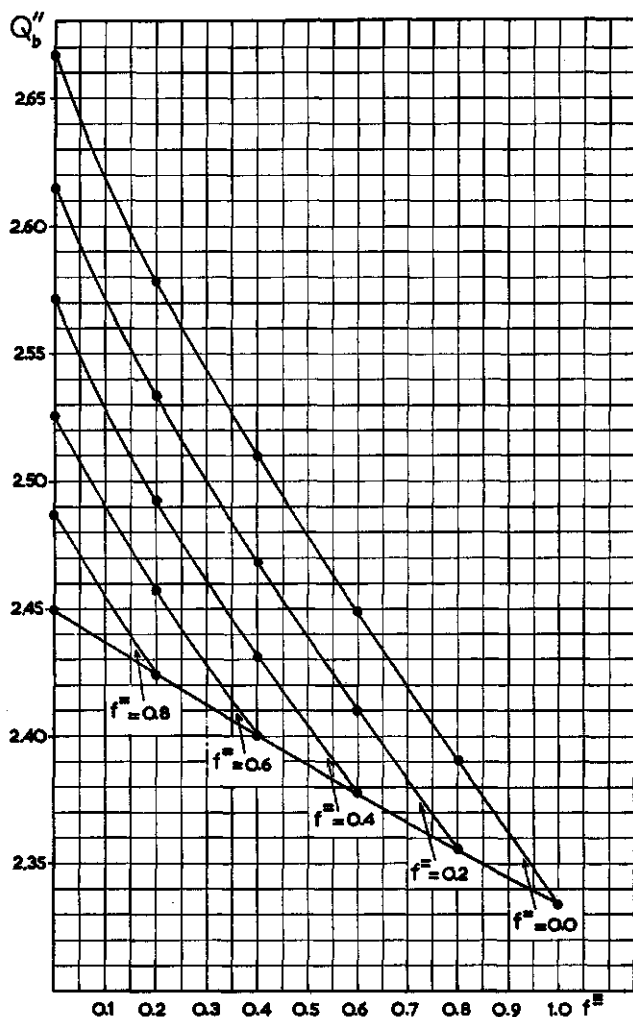
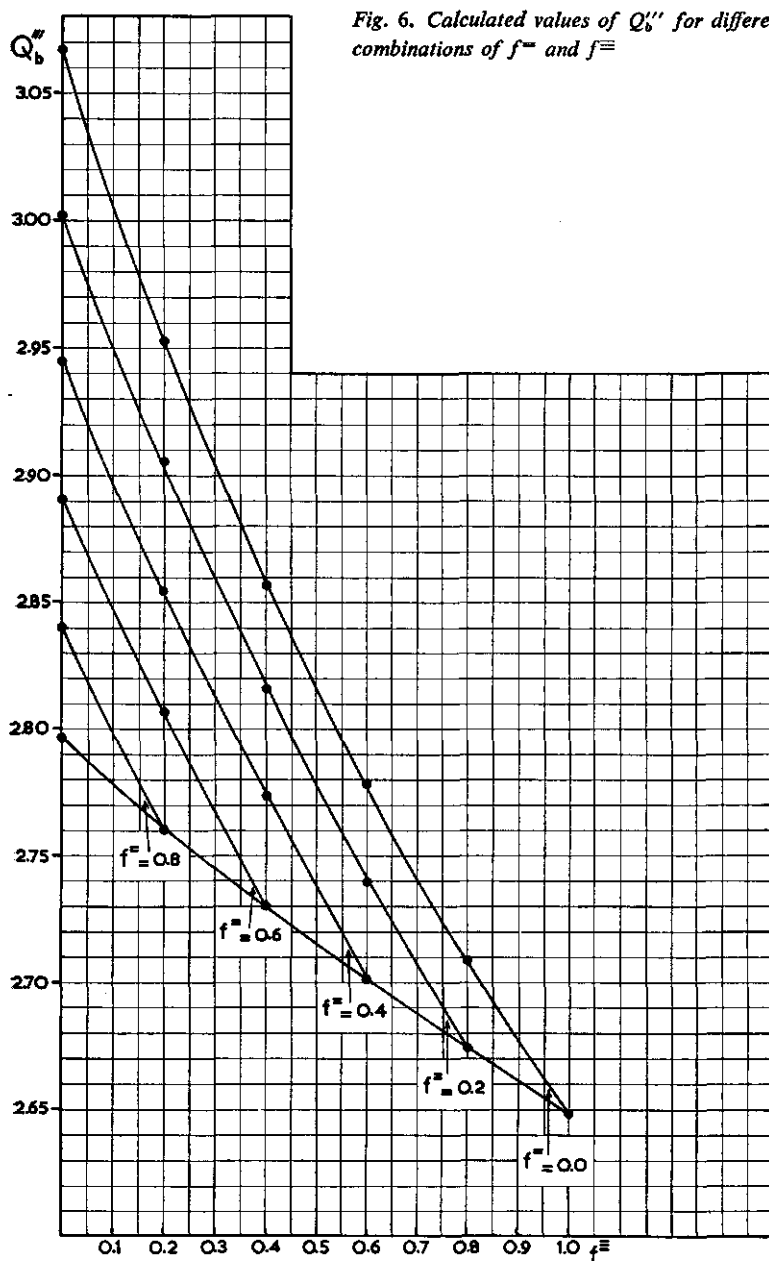


Fig. 5. Calculated values of  $Q_b'''$  for different combinations of  $f''$  and  $f'''$

c *Approximate approach for a quintuple system.* Applying the same procedure as above for a system containing mono- and divalent cations and mono-, di-, and tri-



valent anions the mathematics of the solution of the equations becomes quite complicated. Using the same symbols for the equivalent fractions of the ions as in the foregoing one may put now for the negative adsorption of the monovalent anion:



$$\frac{\Gamma^-}{(1-f^+-f^\equiv)N_0} = \pm \frac{1}{\sqrt{\beta N_0}} \cdot \int_{-\infty}^1 \frac{(1-1/u) d \ln u}{\sqrt{\frac{1}{2}f^{++}u^2 + (1-f^{++})u + (1-f^+-f^\equiv)u^{-1} + \frac{1}{2}f^+u^{-2} + \frac{1}{2}f^\equiv u^{-3} - (2 - \frac{1}{2}f^{++} - \frac{1}{2}f^+ - \frac{1}{2}f^\equiv)}} - \delta^- \quad (2.33)$$

By writing the numerator as  $(u-1)du$  and dividing both the numerator and denominator by  $(u-1)$  one finds:

$$= \pm \frac{1}{\sqrt{\beta N_0}} \cdot \int_{-\infty}^1 \frac{du}{\sqrt{\frac{1}{2}f^{++}u^4 + u^3 + (\frac{1}{2}f^+ + \frac{1}{2}f^\equiv)u^2 + \frac{1}{2}f^\equiv u}} - \delta^- \quad (2.34)$$

Substituting the fourth power polynomial in  $u$  by  $C$  one arrives at:

$$\frac{\Gamma^-}{(1-f^+-f^\equiv)N_0} = \pm \frac{1}{\sqrt{\beta N_0}} \cdot \int_{-\infty}^1 \frac{du}{\sqrt{C}} - \delta^- \quad (2.35)$$

In the same manner as used before one finds for the di- and trivalent anion:

$$\frac{\Gamma^+}{f^+ N_0} = \pm \frac{1}{\sqrt{\beta N_0}} \cdot \left\{ \int_{-\infty}^1 \frac{du}{\sqrt{C}} + \int_{-\infty}^1 \frac{du}{u\sqrt{C}} \right\} - \delta^- \quad (2.36)$$

and

$$\frac{\Gamma^\equiv}{f^\equiv N_0} = \pm \frac{1}{\sqrt{\beta N_0}} \cdot \left\{ \int_{-\infty}^1 \frac{du}{\sqrt{C}} + \int_{-\infty}^1 \frac{du}{u\sqrt{C}} + \int_{-\infty}^1 \frac{du}{u^2\sqrt{C}} \right\} - \delta^- \quad (2.37)$$

To solve the integrals appearing in these equations the roots of the fourth power polynomial in  $u$  must be found, which is hardly possible without using an electronic computer.

As was indicated above it would seem satisfactory for practical purposes (i.e. application to soil systems) to solve the equations for systems in which the concentration of the trivalent anion is small.

In that case  $C \simeq u^2 \cdot A$  and the solutions of (2.35) and (2.36) become identical with those of (2.11) and (2.13), viz.:

$$c1 \quad \frac{\Gamma^-}{(1-f^+-f^\equiv)N_0} \simeq \frac{1}{\sqrt{\beta N_0}} \cdot Q'_a - \delta^-$$

$$c2 \quad \frac{\Gamma^+}{f^+ N_0} \simeq \frac{1}{\sqrt{\beta N_0}} \cdot Q''_a - \delta^-$$

Under the same circumstances the solution of the negative adsorption of the trivalent anion is of the form:

$$c3 \quad \frac{\Gamma^\equiv}{f^\equiv N_0} \simeq \pm \frac{2}{\sqrt{\beta N_0}} \cdot \left\{ \int_{-\infty}^1 \frac{du}{u\sqrt{A}} + \int_{-\infty}^1 \frac{du}{u^2\sqrt{A}} + \int_{-\infty}^1 \frac{du}{u^3\sqrt{A}} \right\} - \delta^- \quad (2.38)$$

Using again a recurrence procedure for the evaluation of the third integral (cf Appendix III), one finds:

$$\frac{\Gamma^{\equiv}}{f^{\equiv} N_0} = \frac{1}{\sqrt{\beta N_0}} \cdot Q_c''' - \delta^- \quad (2.39)$$

in which

$$Q_c''' = \sqrt{2} \left\{ \frac{\sqrt{f^{++} + 2 + f^{\equiv}}}{2f^{\equiv}} + \frac{2f^{\equiv} - f^{++}}{2f^{\equiv}} \cdot \frac{Q_a'}{\sqrt{2}} + \frac{2f^{\equiv} - 3}{2f^{\equiv}} \left( \frac{Q_a'' - Q_a'}{\sqrt{2}} \right) \right\} \quad (2.40)$$

The calculated values of  $Q_c'''$  as a function of  $f^{++}$  and  $f^{\equiv}$  are presented in table 3 and figure 7.

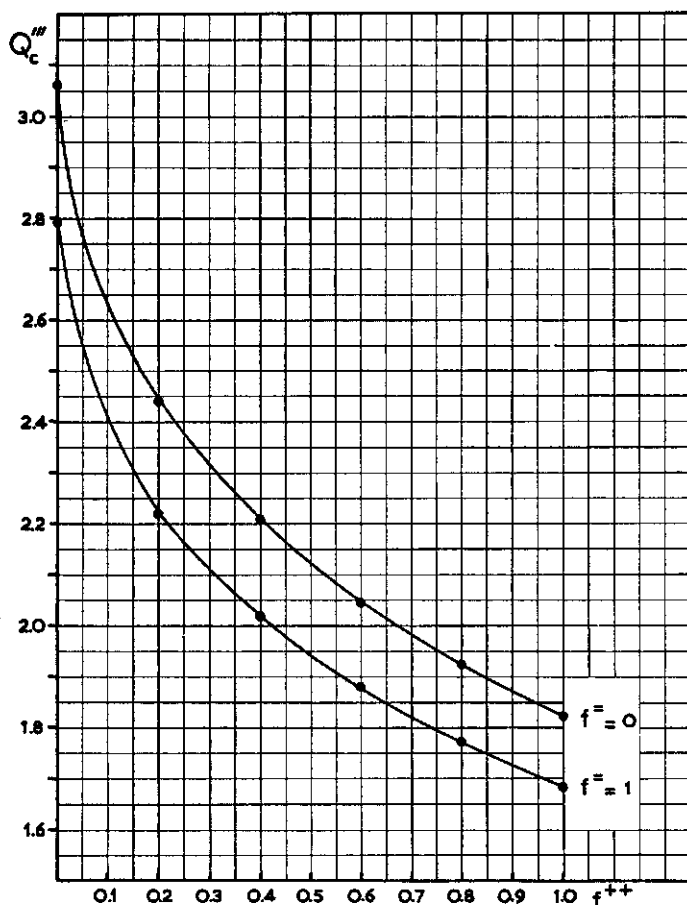


Fig. 7. Calculated values of  $Q_c'''$  for different combinations of  $f^{++}$  and  $f^{\equiv}$

As a check on the validity of the above approximation,  $Q_c'''$ ,  $Q_a''$  and  $Q_a'$  for systems

Table 3. Calculated  $Q'''$  values for a system containing mono- and divalent cations and anions, and trace amounts of trivalent anions (+2, +1, -1, -2, (-3))

$f^{++}$	$f^-$	$Q'''$					
		0.0	0.2	0.4	0.6	0.8	1.0
0.0		3.067	3.009	2.946	2.890	2.840	2.794
0.2		2.442	2.384	2.341	2.298	2.264	2.222
0.4		2.211	2.157	2.122	2.086	2.053	2.019
0.6		2.049	1.999	1.969	1.939	1.910	1.883
0.8		1.929	1.883	1.850	1.825	1.799	1.773
1.0		1.824	1.782	1.755	1.732	1.706	1.687

with  $f^{++} = 0$  were compared with  $Q_b'''$ ,  $Q_b''$  and  $Q_b'$  at different values of  $f^{\equiv}$ . To this purpose a correction factor was calculated, with which the approximate values  $Q_c'''$ ,  $Q_c''$  and  $Q_c'$  must be multiplied to find the exact values  $Q_b$ . In figure 8 these correction factors, expressed as  $Q_{\text{correct}}/Q_{\text{approx.}}$ , are plotted as a function of  $f^{\equiv}$  for different values of  $f^{\equiv}$ . As is evident the approximate values differ less than 6% from the exact values for  $f^{\equiv} = 0$  if  $f^{\equiv} \leq 0.3$ . If  $f^{\equiv}$  has a value of 0.6 one may even go to 0.4 for  $f^{\equiv}$ , the deviation between approximate and exact values still being below 6%. It is shown by this figure that a linear interpolation suffices to connect the exact values with the approximate values.

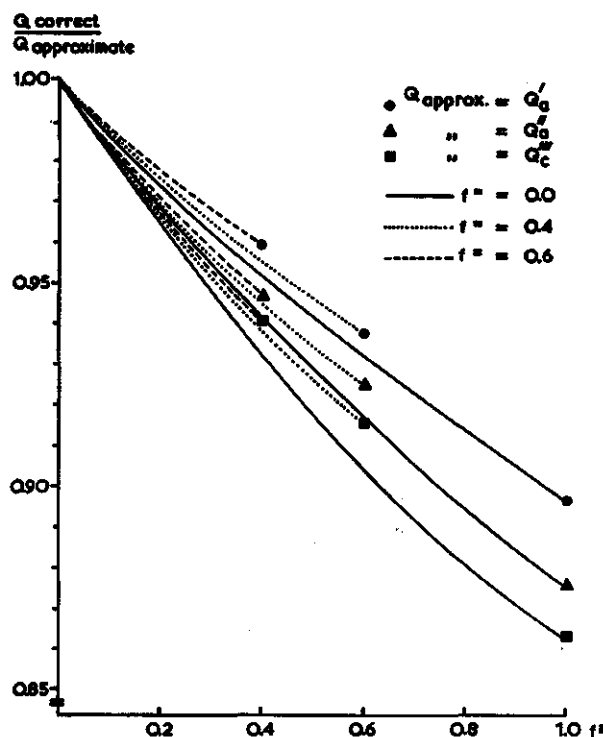


Fig. 8.  
The correction,  $Q_{\text{corr}}/Q_{\text{approx.}}$ , to be applied to the approximate values of  $Q$  (based on the neglect of the trivalent anion) in order to obtain the correct values,  $Q_b$ , as a function of  $f^{\equiv}$  and  $f^{\equiv}$

As the systems containing monovalent cations only are more sensitive towards the error introduced by neglecting the trivalent anion than the divalent cationic systems, the approximations should be equally valid for those systems.

It should be pointed out that in the limiting case where  $f^{\equiv}$  approaches zero the expression  $\Gamma^{\equiv}/f^{\equiv}N_0$  is still well defined as the distance of exclusion of the trivalent anion,  $d^{\equiv}$ . In practice this situation arises when carrier-free amounts of radioactive tracers are used.

#### 2.1.4 Derivation of expressions for the negative adsorption of anions in systems with interacting double layers

All derivations given in section 2.1.3 pertained to systems with a relatively high liquid content, indicating that the thickness of the double layer does not exceed the thickness of the water layer around the colloidal particles. If this condition does not prevail, as may be the case in highly concentrated suspensions of a colloid with a large specific surface area, interaction of the double layers of opposing particles must be taken into account.

In this case the anion concentration is integrated over a distance from the plate to the point midway two opposing plates. The electric potential at the "end" of the double layer is then not equal to zero, but has a certain value,  $\psi_c$ , the subscript  $c$  referring to the central plane between the plates. The corresponding  $u$  value is indicated by  $u_c$ .

It should be pointed out that in a suspension one may not expect all clay plates to be in parallel position with respect to each other. As long as the suspension is not flocculated, the repulsion between adjacent particles must lead to an arrangement which should be very close to parallel for adjacent plates. In flocculated systems (and specifically so at low suspension concentration) parallel arrangement may be absent. In that case one should expect sizable deviations from the calculations based on parallel arrangement.

As the derivations of the expressions for systems with not freely expanded double layers are quite involved, the systems to be considered are less complicated than those of the foregoing section. As will be discussed later the complicated systems may be approximated quite well by certain simplified derivations.

The derivation is given first for a system containing monovalent cations and mono- and divalent anions (+1, -1, -2).

According to the general equation (2.5), applied to this system under the condition of interaction, one finds for the monovalent anion:

$$\frac{\Gamma^-}{(1-f^{\equiv})N_0} = \pm \frac{1}{\sqrt{\beta N_0}} \cdot \int_{\infty}^{u_0} \frac{(1-1/u)du}{u\sqrt{u+(1-f^{\equiv})u^{-1} + \frac{1}{2}f^{\equiv}u^{-2} - u_c - (1-f^{\equiv})u_c^{-1} - \frac{1}{2}f^{\equiv}u_c^{-2}}} - \delta^- \quad (2.41)$$

$$= \pm \frac{1}{\sqrt{\beta N_0}} \cdot \int_{\infty}^{u_c} \frac{(1-1/u)du}{\sqrt{(u-u_c)[u^2-u\{(1-f^-)/u_c+f^-/2u_c^2\}-f^-/2u_c]}} - \delta^- \quad (2.42)$$

Substitution of the form under the root sign in (2.42) by  $I$  gives:

$$= \pm \frac{1}{\sqrt{\beta N_0}} \cdot \int_{\infty}^{u_c} \frac{(1-1/u)du}{\sqrt{I}} - \delta^- \quad (2.43)$$

$$= \pm \frac{1}{\sqrt{\beta N_0}} \cdot \left\{ \int_{\infty}^{u_c} \frac{du}{\sqrt{I}} - \int_{\infty}^{u_c} \frac{du}{u\sqrt{I}} \right\} - \delta^- \quad (2.44)$$

In the same manner the divalent anion is found as:

$$\frac{\Gamma^-}{f^- N_0} = \pm \frac{1}{\sqrt{\beta N_0}} \cdot \int_{\infty}^{u_c} \frac{(1-1/u^2)du}{\sqrt{I}} - \delta^- \quad (2.45)$$

$$= \pm \frac{1}{\sqrt{\beta N_0}} \cdot \left\{ \int_{\infty}^{u_c} \frac{du}{\sqrt{I}} - \int_{\infty}^{u_c} \frac{du}{u^2 \sqrt{I}} \right\} - \delta^- \quad (2.46)$$

Solution of the integrals requires the roots of  $I = 0$ , which are:

$$\alpha_1 = u_c$$

$$\alpha_2 = \frac{1}{2} \left( \frac{1-f^-}{u_c} + \frac{f^-}{2u_c^2} \right) + \frac{1}{2} \sqrt{\frac{(1-f^-)^2}{u_c^2} + \frac{2f^-(1-f^-)}{2u_c^3} + \frac{f^{-2}}{4u_c^4} + \frac{2f^-}{u_c}}$$

$$\alpha_3 = \frac{1}{2} \left( \frac{1-f^-}{u_c} + \frac{f^-}{2u_c^2} \right) - \frac{1}{2} \sqrt{\frac{(1-f^-)^2}{u_c^2} + \frac{2f^-(1-f^-)}{2u_c^3} + \frac{f^{-2}}{4u_c^4} + \frac{2f^-}{u_c}}$$

Substituting the solutions of the integrals appearing in (2.44) (cf Appendix IV) one finds:

$$\frac{\Gamma^-}{(1-f^-)N_0} = \frac{Q'_1}{\sqrt{\beta N_0}} - \delta^- \quad (2.47)$$

with

$$Q'_1 = \frac{2}{\sqrt{u_c - \alpha_3}} \left( 1 - \frac{1}{\alpha_2} \right) \cdot F(\pi/2, k) + \frac{2(u_c - \alpha_2)}{\alpha_2 u_c \sqrt{u_c - \alpha_3}} \cdot \Pi(\pi/2, \rho, k) \quad (2.48)$$

in which

$$k = \sqrt{\frac{\alpha_2 - \alpha_3}{u_c - \alpha_3}}, \quad \rho = \frac{-\alpha_2}{u_c},$$

and  $\Pi(\pi/2, \rho, k)$  = complete elliptic integral of the third kind. This integral has never been tabulated and its value must be calculated from a series expansion.

Using the recurrence procedure indicated earlier the second integral of (2.46) may

be converted into the ones appearing in equation (2.44) (cf Appendix), yielding:

$$\frac{\Gamma^-}{f^- N_0} = \frac{Q_i''}{\sqrt{\beta N_0}} - \delta^- \quad (2.49)$$

in which

$$Q_i'' = \frac{2}{\sqrt{u_c - \alpha_3}} \cdot \left[ \left( 1 + \frac{1-f^-}{\alpha_2 f^-} - \frac{u_c}{f^-} \right) \cdot F(\pi/2, k) + \frac{u_c - \alpha_3}{f^-} \cdot E(\pi/2, k) - \frac{1-f^-}{f^-} \cdot \frac{u_c - \alpha_2}{\alpha_2 u_c} \cdot \Pi(\pi/2, \rho, k) \right] \quad (2.50)$$

The results corresponding to  $f^- = 0.6$  and  $u_c = 2$  are given in table 4 and represented by the crosses 1 and 2 in figure 9.

Table 4. Influence of double layer interaction on negative adsorption.  
(The numbers within brackets refer to calculations, neglecting the presence of anions)

	$1/u_c$	$D \cdot \sqrt{\beta N_0}$	Fraction of original negative adsorption left ( $Q_i/Q_{i(0)}$ )		
			monovalent	divalent	trivalent
$f^- = 0.0$	0.1	0.997 (0.994)	0.473 (0.472)	0.373 (0.371)	0.334 (0.324)
	0.2	1.419 (1.405)	0.638 (0.632)	0.526 (0.524)	0.467 (0.457)
	0.3	1.762	0.748		
	0.4	2.076 (1.987)	0.825 (0.795)	0.729 (0.700)	0.671 (0.635)
	0.5	2.362 (2.221)	0.872 (0.833)	0.806 (0.755)	0.745 (0.696)
	0.6	2.716	0.929		
	0.7	3.090	0.959		
	0.8	3.570 (2.810)	0.972 (0.843)	0.961 (0.801)	0.940 (0.769)
	0.9	4.340	1.000		
$f^- = 0.6$	0.5	2.326	0.901	0.833	

Although the negative adsorption of the anions may be calculated according to the above it seems unlikely that the rather involved application of series expansion of the  $\Pi$  function is warranted from a practical point of view. Thus it was shown in section 2.1.3 that the influence of a varying anionic composition at constant electrolyte level on the equivalent distance of exclusion of the anions (i.e.  $d^-$ ,  $d^=$ ,  $d^{\equiv}$ ) is relatively small. This is understandable since the value of this distance of exclusion is determined by the potential distribution in the double layer. In turn this potential distribution is determined to a large extent by the cationic (i.e. counterionic) composition. This is so because the total charge of the co-ions is usually insignificant in comparison to the charge of the counterions. This condition applies specifically to the system with interacting double layers, the co-ions now being repelled from the entire double layer system (at least if  $u_c \gg 1$ ).

It thus follows that the calculation of the distance of exclusion of the mono- and divalent anions in the above mixed system should be approximated very closely by

the result obtained when assuming that  $f^- \approx 0$ . Applying this condition, the roots of  $I$  are found as:

$$\alpha_1 = u_c \quad \alpha_2 = 1/u_c \quad \alpha_3 = 0.$$

Using these roots the integrals of (2.44) and (2.46) are readily solved in terms of complete elliptic integrals of the first and second kind only (cf Appendix IV), and one finds:

$$Q_i'(f^- = 0) \approx Q_i' = \frac{2(1-u_c)}{\sqrt{u_c}} \cdot F\left(\pi/2, \frac{1}{u_c}\right) + 2\sqrt{u_c} \cdot E\left(\pi/2, \frac{1}{u_c}\right) \quad (2.51)$$

and

$$\begin{aligned} Q_i''(f^- = 0) &\approx Q_i'' \\ &= \left\{ \frac{8}{3\sqrt{u_c}} - \frac{4\sqrt{u_c}}{3} \left(u_c + \frac{1}{u_c}\right) \right\} \cdot F\left(\pi/2, \frac{1}{u_c}\right) + \frac{4\sqrt{u_c}}{3} \left(u_c + \frac{1}{u_c}\right) \cdot E\left(\pi/2, \frac{1}{u_c}\right) \end{aligned} \quad (2.52)$$

Finally the above treatment may be extended to the case of the trivalent anion (again assumed to have negligible influence on the potential distribution of the double layer), yielding:

$$\begin{aligned} Q_i'''(f^\equiv = f^- = 0) &\approx Q_i''' \\ &= \left[ \left\{ 1 + \frac{4}{15} \left(u_c + \frac{1}{u_c}\right) \right\} \frac{2}{\sqrt{u_c}} + \left\{ \frac{3}{5} - \frac{8}{15} \left(u_c + \frac{1}{u_c}\right)^2 \right\} 2\sqrt{u_c} \right] \cdot F\left(\pi/2, \frac{1}{u_c}\right) \\ &\quad - \left\{ \frac{3}{5} - \frac{8}{15} \left(u_c + \frac{1}{u_c}\right)^2 \right\} 2\sqrt{u_c} \cdot E\left(\pi/2, \frac{1}{u_c}\right) \end{aligned} \quad (2.53)$$

The results of the above approximations, together with the exact results obtained for  $f^- = 0.6$  and  $u_c = 2$  are given in table 4 and represented by the solid lines 1, 2 and 3 in figure 9. In table 4 the distance of exclusion is given as a fraction of its value at  $u_c = 1$  (i.e. in the absence of interaction), as a function of  $1/u_c$ . As  $u_c$  is directly related to the half distance between the plates  $D$  and the equilibrium concentration,  $N_0$ , according to:

$$D \cdot \sqrt{\beta N_0} = \frac{2}{\sqrt{u_c}} \cdot F(\pi/2, k) \quad (\text{cf equation 2.44})$$

the value of  $D \cdot \sqrt{\beta N_0}$  (the experimentally accessible measure of the degree of interaction) is also indicated. In figure 9 a plot of  $Q_i/Q_\infty$  against  $D \cdot \sqrt{\beta N_0}$  is given.

Carrying the above approximation to the extreme, one may also venture to estimate the depression of the negative adsorption from the values found for systems in which the anionic concentrations are *all* negligible in comparison to the cationic concentrations (i.e. neglecting also the influence of the monovalent anions). Obviously this approximation will be valid only at fairly high values of  $u_c$ . The equations are much less involved in this case (cf Appendix) and yield:

$$Q_i'(N_0^{z-} = 0) = \left(1 - \frac{1}{2u_c}\right) \frac{\pi}{\sqrt{u_c}} \quad (2.54)$$

$$Q_i''(N_0^{z-} = 0) = \left(1 - \frac{3}{8u_c^2}\right) \frac{\pi}{\sqrt{u_c}} \quad (2.55)$$

$$Q_i'''(N_0^{z-} = 0) = \left(1 - \frac{5}{16u_c^3}\right) \frac{\pi}{\sqrt{u_c}} \quad (2.56)$$

For comparison the values of  $Q_i(N_0^{z-} = 0)/Q_a$  are shown in table 4 (between brackets) together with the corresponding value of  $D \cdot \sqrt{\beta N_0}$  ( $= \pi/\sqrt{u_c}$ ) and plotted as the open symbols in figure 9.

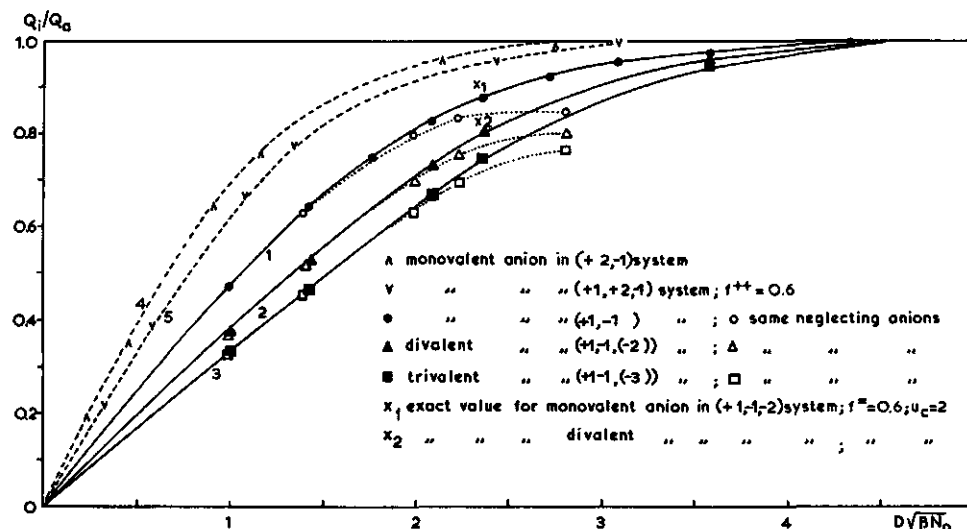


Fig. 9. Depression of the negative adsorption of anions in systems with interacting double layers,  $Q_i/Q_a$ , as a function of  $D \cdot \sqrt{\beta N_0}$ .

It is seen that the neglect of anions does not make any difference up to values of  $D \cdot \sqrt{\beta N_0}$  of 2 (high interaction). Beyond 2, however, a considerable deviation starts to appear, indicating that the approximation introduced leads to a fairly large error in the final result in this region.

In view of the above results, obtained for partial neglect of the anions, the system containing two types of cations warrants further investigation. Deriving the exact expression for a system of the composition  $(+2, +1, -1, u_c \neq 1)$  one finds:

$$\frac{\Gamma^-}{N_0} = \pm \frac{1}{\sqrt{\beta N_0}} \cdot \int_{-\infty}^{u_c} \frac{(1-1/u)du}{\sqrt{(u-u_c)u\{\frac{1}{2}f^{++}u^2 + (1-f^{++} + \frac{1}{2}f^{++}u_c)u - 1/u_c\}}} - \delta^- \quad (2.57)$$



$$= \pm \frac{1}{\sqrt{\beta N_0}} \cdot \sqrt{\frac{2}{f^{++}}} \cdot \left\{ \int_{\infty}^{u_c} \frac{du}{\sqrt{J}} - \int_{\infty}^{u_c} \frac{du}{u\sqrt{J}} \right\} - \delta^- \quad (2.58)$$

The roots of  $J$  are:

$$\alpha_1 = u_c$$

$$\alpha_2 = \left( 1 - \frac{1}{2}u_c - \frac{1}{f^{++}} \right) + \sqrt{\frac{1}{4}u_c^2 - \left( 1 - \frac{1}{f^{++}} \right) u_c + 1 - \frac{2}{f^{++}} + \frac{1}{f^{++2}} + \frac{2}{f^{++}u_c}}$$

$$\alpha_3 = 0$$

$$\alpha_4 = \left( 1 - \frac{1}{2}u_c - \frac{1}{f^{++}} \right) - \sqrt{\frac{1}{4}u_c^2 - \left( 1 - \frac{1}{f^{++}} \right) u_c + 1 - \frac{2}{f^{++}} + \frac{1}{f^{++2}} + \frac{2}{f^{++}u_c}}$$

The general solution of  $Q'_i$  is then given by:

$$Q'_i = \sqrt{\frac{2}{f^{++}}} \left[ \frac{2}{\sqrt{\alpha_1(\alpha_2 - \alpha_4)}} \cdot \left\{ \left( 1 - \frac{1}{\alpha_2} \right) \cdot F(\varphi, k) + \frac{\alpha_1 - \alpha_2}{\alpha_1 \cdot \alpha_2} \cdot \left( \frac{1}{1 - k^2} \cdot E(\varphi, k) - \frac{k^2 \sin \varphi \cos \varphi}{(1 - k^2)\sqrt{1 - k^2 \sin^2 \varphi}} \right) \right\} \right] \quad (2.59)$$

with

$$k^2 = \frac{\alpha_2(\alpha_1 - \alpha_4)}{\alpha_1(\alpha_2 - \alpha_4)}$$

The value of  $\varphi$  is found by filling in the integration limits into:

$$u = \frac{\alpha_2(\alpha_1 - \alpha_4) \sin^2 \varphi - \alpha_1(\alpha_2 - \alpha_4)}{(\alpha_1 - \alpha_4) \sin^2 \varphi - (\alpha_2 - \alpha_4)}$$

$D$  is now found as the first integral of equation (2.58), multiplied with  $\sqrt{2/f^{++}}$ , thus:

$$D \cdot \sqrt{\beta N_0} = \sqrt{\frac{2}{f^{++}}} \cdot \frac{2}{\sqrt{\alpha_1(\alpha_2 - \alpha_4)}} \cdot F(\varphi, k) \quad (2.60)$$

Calculations of  $Q'_i$  were executed for a range of  $u_c$  values for the conditions  $f^{++} = 1$  and  $f^{++} = 0.6$ , respectively, and for a range of  $f^{++}$  values at  $u_c = 2$ .  $Q'_i$  values were compared with the corresponding  $Q'_a$  values (cf table 1). Results are given in table 5 and plotted as the broken lines 4 and 5 in figure 9, respectively.

Combining now all results obtained so far one may plot the reduced value of the negative adsorption (i.e.  $Q_i/Q_a$ ) against the reduced thickness of the water layer (i.e.  $D/D^*$ , in which  $D^* = Q_a/\sqrt{\beta N_0}$ ). This has been done in figure 10. When plotted in this manner the effect of interaction appears to be described satisfactorily for most practical purposes by means of the central line of the "band" in which all points are situated. As a further refinement it may be noted that in the case that the ratio of cationic valence to anionic valence,  $p$ , is greater than one (e.g.  $\text{Cl}^-$  repulsion

in predominantly Ca-systems) the interaction effect is somewhat enlarged (points situated below central line), whereas for  $p$  smaller than one (e.g.  $\text{SO}_4^{2-}$  repulsion in predominantly Na-systems) the interaction effect is depressed.

Table 5. The influence of interaction on the negative adsorption in a (+1, +2, -1) system

	$D \cdot \sqrt{\beta N_0}$						$Q_i/Q_a$					
$1/u_e f^{++}$	1.0	0.8	0.6	0.4	0.2	0.0	1.0	0.8	0.6	0.4	0.2	0.0
0.1	0.222		0.265			0.997	0.199		0.217			0.473
0.2	0.447		0.554			1.419	0.357		0.385			0.638
0.4	0.905		1.054			2.076	0.650		0.663			0.825
0.5	1.152	1.233	1.326	1.500	1.721	2.362	0.759	0.766	0.775	0.820	0.850	0.872
0.8	2.140		2.421			3.570	0.956		0.970			0.972
0.9	2.775		3.097			4.340	0.989		0.998			1.000

Thus finally the general procedure for the calculation of the negative adsorption, pertaining to all systems, reads as follows:

Knowing the composition of the system the negative adsorption (expressed as the distance of exclusion,  $D^{z-}$ ), for the condition  $u_e = 1$  is found from tables 1, 2 and 3 or the figures 2, 4, 5, 6 and 7.

Next the value of  $D$  (thickness of the liquid layer) is calculated from the water content and an estimate of the specific surface area of the colloid. Using the corresponding value  $D/D^{z-}$  one may estimate the reduction of  $D^{z-}$  due to interaction from the "band" presented in figure 10. As follows from figure 10 this reduction is less than about 5 % as long as  $D/D^{z-} \geq 1.5$ .

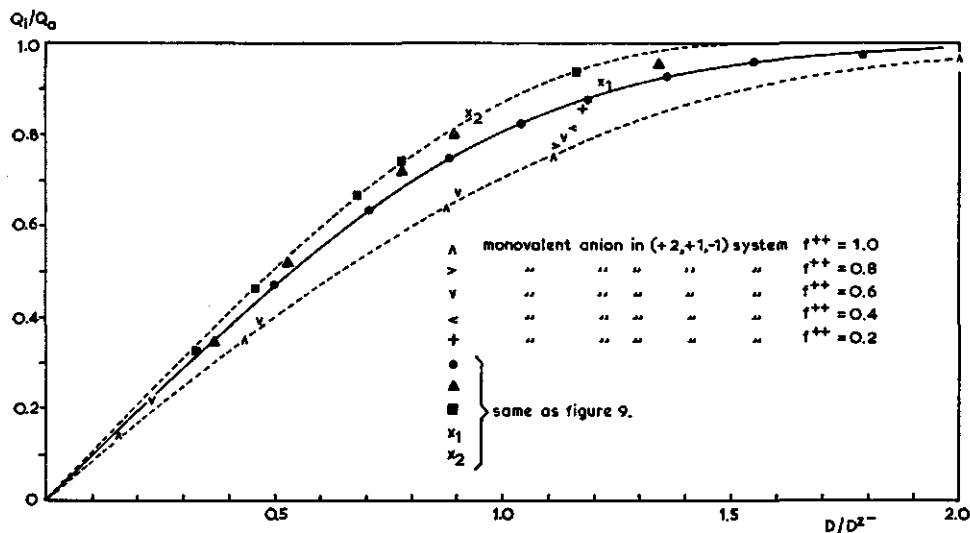


Fig. 10. Depression of the negative adsorption of anions in systems with interacting double layers,  $Q_i/Q_a$ , as a function of the reduced thickness of the water layer,  $D/D^{z-}$  ( $= D \cdot \sqrt{\beta N_0}/Q_a$ )

### 2.1.5 The relation between $\delta^-$ and $\Gamma$ , and $\Gamma^-$ and $\delta^-$

It follows from figure 1 that  $\delta^- (= \int_{\infty}^{u_s} (1 - u^{-2}) dX)$  is very nearly equal to the distance  $\delta$  (the extrapolation of the distance axis to the point where  $u = \infty$ ).

As was pointed out in section 2.1.2 the relation between  $\delta$  and  $\Gamma$  may in turn be approximated by:

$$\delta \simeq \frac{4}{z^+ \beta \Gamma} \quad (2.2)$$

For an evaluation of the validity of the above "double" approximation, the exact relation between  $\delta^-$  and  $\Gamma$  will be presented here. This relation is found by the actual execution of the integrations in the range  $u = \infty$  to  $u = u_s$  (i.e. the value of  $u$  at the colloid surface), in combination with the relation between  $u_s$  and  $\Gamma$  derived below.

The relation meant is considered for a system containing mono- and divalent cations and monovalent anions (+2, +1, -1). Although such calculations could be executed for all systems treated above, such an effort seems unwarranted in view of the fact that, as has been shown in the foregoing, the exact anionic composition has only a small influence on the potential distribution in the entire double layer. Accordingly the influence of the anionic composition on the potential distribution in the range of  $\infty > u > u_s$  must certainly be negligible.

Choosing thus a system of the composition (+2, +1, -1) one proceeds as follows. For a freely expanded double layer the surface charge density may be expressed as:

$$\sigma = \int_{x_s}^{\infty} \rho dX \quad (2.61)$$

in which  $\sigma$  and  $\rho$  represent the surface charge density and volume charge density, in electrostatic units per  $\text{cm}^2$  and per  $\text{cm}^3$ , respectively. Using the Poisson equation for the 1-dimensional case this gives:

$$\begin{aligned} \sigma &= \int_{x_s}^{\infty} -\frac{d^2\psi}{dX^2} \cdot \frac{\epsilon}{4\pi} \cdot dX \\ \sigma &= -\frac{\epsilon}{4\pi} \cdot \left( \frac{d\psi}{dX} \right)_{X=x_s} \end{aligned} \quad (2.62)$$

The surface charge density, expressed in me. per  $\text{cm}^2$ ,  $\Gamma$ , is related to  $\sigma$  by:

$$\Gamma = \frac{1,000\sigma}{N_{A_v} \cdot e},$$

with  $N_{A_v}$  the Avogadro number

$$\Gamma = \frac{1,000\sigma}{F} \quad (2.63)$$

Combining equations (2.62) and (2.63) one finds:

$$\Gamma = - \frac{1,000\varepsilon}{4\pi F} \cdot \left( \frac{d\psi}{dX} \right)_{X=X_s}$$

Introducing the definition of  $\beta$  in this equation (cf section 2.1.2) and replacing again  $\exp(-e\psi/kT)$  by  $u$ , this gives:

$$\Gamma = - \frac{2}{\beta} \cdot \left( \frac{d \ln u}{dX} \right)_{u=u_s} \quad (2.64)$$

Combining with equation (2.4):

$$\Gamma = \frac{2}{\beta} \cdot \sqrt{\beta} \cdot \sqrt{\sum C_s - \sum C_0} \quad (2.65)$$

in which  $\sum C_s$  stands for the total ionic concentration at the solid-liquid interface. Thus for the system under consideration:

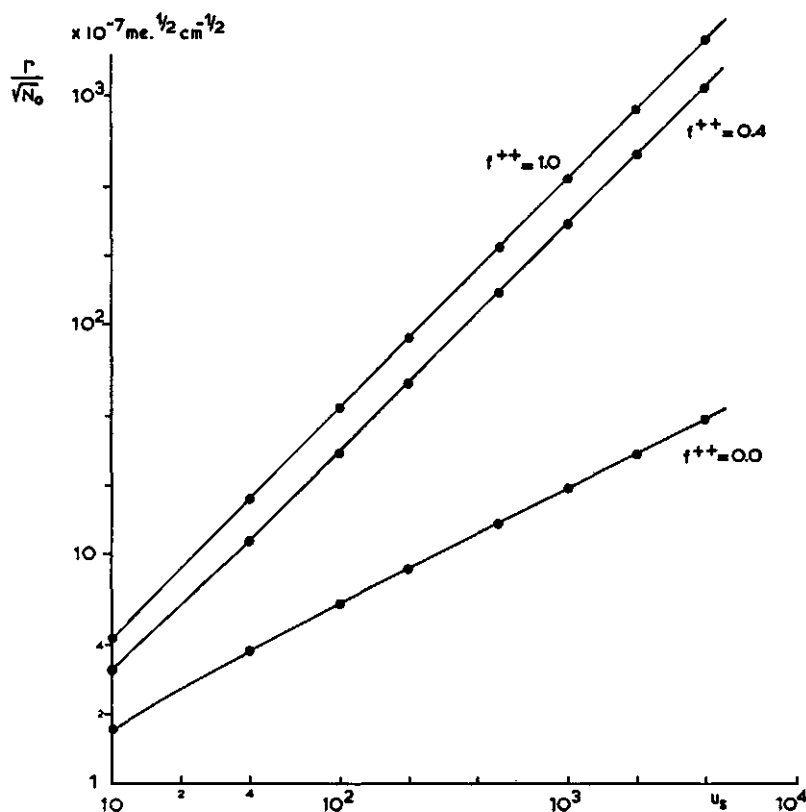


Fig. 11.  $\Gamma/\sqrt{N_0}$  as a function of the Boltzmann factor pertaining to the colloid surface,  $u_s$ .

$$\Gamma = \frac{2}{\sqrt{\beta}} \cdot \sqrt{N_0} \cdot \sqrt{\frac{f^{++}}{2} u_s^2 + (1-f^{++})u_s + \frac{1}{u_s} - (2-\frac{1}{2}f^{++})} \quad (2.66)$$

which equation describes the relation of  $\Gamma$  with  $f^{++}$  and  $u_s$ . Using equation (2.66) values for  $\Gamma/\sqrt{N_0}$  were calculated for different combinations of  $f^{++}$  and  $u_s$ . Results are presented graphically in figure 11.

Applying now the definition of  $\delta^-$  to equation (2.10) one finds:

$$\begin{aligned} \delta^- &= \pm \frac{\sqrt{2}}{\sqrt{\beta N_0}} \cdot \int_{\infty}^{u_s} \frac{du}{u \sqrt{f^{++} u^2 + 2u}} \\ &= \frac{\sqrt{2}}{\sqrt{\beta N_0}} \cdot \left\{ \sqrt{f^{++} + \frac{2}{u_s}} - \sqrt{f^{++}} \right\} \end{aligned} \quad (2.67)$$

A combination of equations (2.66) and (2.67) then leads to the exact relation between  $\delta^-$  and  $\Gamma$ , viz.:

$$\delta^- = \frac{2\sqrt{2}}{\beta\Gamma} \cdot \left\{ \sqrt{f^{++} + \frac{2}{u_s}} - \sqrt{f^{++}} \right\} \cdot \sqrt{\frac{f^{++}}{2} u_s^2 + (1-f^{++})u_s + \frac{1}{u_s} - (2-\frac{1}{2}f^{++})} \quad (2.68)$$

With the use of equation (2.68) and figure 11 values for  $\beta\Gamma \cdot \delta^-$  may be calculated for different values of  $N_0$ . To this purpose values of  $u_s$  corresponding to arbitrarily chosen values of  $\Gamma/\sqrt{N_0}$  are found from figure 11. Results are given in table 6.

Table 6. Comparison between  $\delta^-$ ,  $\delta$  and  $\delta_i^-$  for several values of  $\Gamma/\sqrt{N_0}$

$\Gamma/\sqrt{N_0}$ ( $\text{me.}^{1/2} \text{ cm}^{-1/2}$ )	$\beta\Gamma \cdot \delta^-$			$\beta\Gamma \cdot \delta$			$\beta\Gamma \cdot \delta_i^-$		
	$f^{++} = 0.0$	$f^{++} = 0.4$	$f^{++} = 1.0$	$f^{++} = 0.0$	$f^{++} = 0.4$	$f^{++} = 1.0$	$f^{++} = 0.0$	$u_s = 2$	$u_s = 10$
$5 \times 10^{-7}$	3.942	2.000	1.900	4	2.082	2	3.958	3.049 <sup>1</sup>	
$10 \times 10^{-7}$	3.985	2.004	1.948	4	2.041	2	3.990	3.617	
$20 \times 10^{-7}$	3.996	2.005	1.977	4	2.017	2	4.000	3.881	
$40 \times 10^{-7}$	3.999	2.006	1.983	4	2.010	2	4.000	3.969	

<sup>1</sup>) calculated according to the series expansion of  $\sqrt{L}$ . are  $\cot \sqrt{L}$  for small values of  $L$

As equation (2.68) is quite complicated to apply in practice, an approximate solution was derived, which is easier to handle.

To this purpose the potential distribution in the presence of cations only is used in equation (2.66). This is not unreasonable in view of the fact that at high values for  $u_s$  the third and fourth term under the root sign in equation (2.66) are negligible in comparison with the first and second term. Thus one finds:

$$\delta^- \simeq \delta \simeq \pm \frac{1}{\sqrt{\beta N_0}} \cdot \int_{\infty}^{u_s} \frac{du}{u \sqrt{\frac{1}{2}f^{++}u^2 + (1-f^{++})u}}$$

$$\simeq \frac{1}{\sqrt{\beta N_0}} \cdot \frac{2}{1-f^{++}} \cdot \left( \frac{\sqrt{\frac{1}{2}f^{++}u_s^2 + (1-f^{++})u_s}}{u_s} - \sqrt{\frac{f^{++}}{2}} \right) \quad (2.69)$$

According to equation (2.66) one finds now:

$$\frac{\beta\Gamma}{2} = \sqrt{\beta N_0} \cdot \sqrt{\frac{f^{++}}{2}u_s^2 + (1-f^{++})u_s} \quad (2.70)$$

Combining equations (2.69) and (2.70):

$$\begin{aligned} \frac{\delta \cdot \beta\Gamma}{2} &\simeq \frac{2}{1-f^{++}} \cdot \frac{1}{2} \sqrt{\frac{1}{2}f^{++}u_s^2 + 2(1-f^{++})u_s} \cdot \left\{ \frac{\sqrt{f^{++}u_s^2 + 2(1-f^{++})u_s} - \sqrt{f^{++}u_s^2}}{u_s} \right\} \\ &\simeq \frac{1}{1-f^{++}} \cdot \{ \sqrt{f^{++}u_s + 2(1-f^{++})} \cdot (\sqrt{f^{++}u_s + 2(1-f^{++})} - \sqrt{f^{++}u_s}) \} \end{aligned} \quad (2.71)$$

As follows from (2.70):

$$f^{++}u_s = -(1-f^{++}) + \sqrt{(1-f^{++})^2 + \frac{f^{++}\beta\Gamma^2}{2N_0}}$$

Substituting this into equation (2.71) one arrives at:

$$\begin{aligned} \delta &\simeq \frac{2}{\beta\Gamma} \cdot \left\{ 1 + \sqrt{1 + \frac{f^{++}\beta\Gamma^2}{2N_0(1-f^{++})^2}} - \sqrt{\frac{f^{++}\beta\Gamma^2}{2N_0(1-f^{++})^2}} \right\} \\ &\simeq \frac{2}{\beta\Gamma} \cdot \{ 1 + \sqrt{1+K} - \sqrt{K} \} \end{aligned} \quad (2.72)$$

in which  $K$  thus stands for

$$\frac{f^{++}}{2(1-f^{++})^2} \cdot \beta \left( \frac{\Gamma}{\sqrt{N_0}} \right)^2$$

For  $f^{++} = 1$  one finds  $K = \infty \rightarrow \delta = 2/\beta\Gamma$  and

for  $f^{++} = 0$  one finds  $K = 0 \rightarrow \delta = 4/\beta\Gamma$ .

This thus checks with the approximation as given by SCHOFIELD (cf equation 2.2). Using equation (2.72) one may calculate the approximate  $\delta$  values for different values of  $f^{++}$  and  $\Gamma/\sqrt{N_0}$ . Results are given in table 6.

In figure 12 the percentage deviation between the exact value  $\delta^-$  and the approximate value  $\delta$  is plotted as a function of  $\Gamma/\sqrt{N_0}$ . It is shown that the deviation is less than 3% as long as  $(\Gamma/\sqrt{N_0}) \times 10^{-7} \geq 10$ . Since  $\Gamma$  is of the order of magnitude of  $1-3 \times 10^{-7}$  me. per  $\text{cm}^2$  this condition usually prevails in soil studies, as the equilibrium concentration is normally below 0.5 normal.

Remains a check on the influence of interaction on the approximation used for  $\delta^-$ . As interaction tends to suppress the anionic concentrations everywhere in the system the approximation  $\delta^- \simeq \delta$  will be more valid than in the systems without interaction.

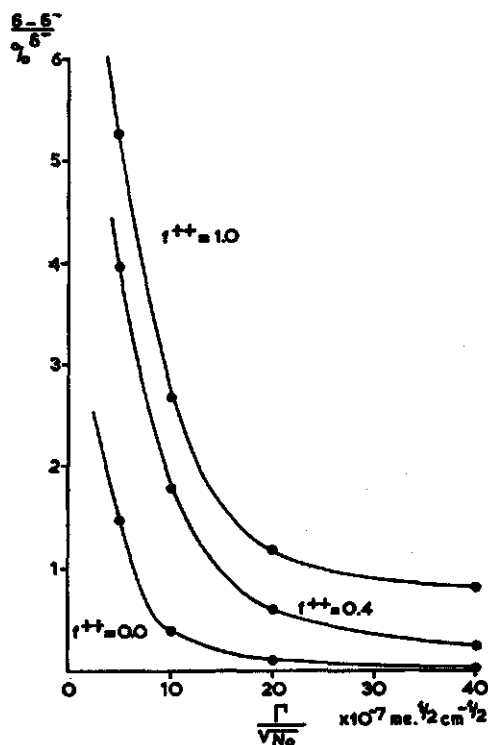


Fig. 12. Percentage deviation of the approximate value,  $\delta$ , from the correct value,  $\bar{\delta}$ , as a function of  $\Gamma/\sqrt{N_0}$ .

Moreover the effect of the anions is now depressed so far that it seems quite warranted to evaluate the influence of interaction by using again the anion-free model. Applying thus the equations (2.69) and (2.70) to such a system containing only cations of valence  $z$  one finds:

$$\begin{aligned}
 \delta_i^- &\simeq \frac{1}{\sqrt{\beta N_0/z}} \cdot \int_{\infty}^{u_i^z} \frac{du}{u\sqrt{u^z - u_c^z}} \\
 &\simeq \frac{1}{\sqrt{\beta N_0}} \cdot \frac{1}{\sqrt{z}} \cdot \int_{\infty}^{u_i^z} \frac{du^z}{u^z \sqrt{u^z - u_c^z}} \\
 &\simeq \frac{2}{\sqrt{\beta N_0}} \cdot \frac{1}{\sqrt{z} \cdot u_c^z} \cdot \text{arc cot} \sqrt{\frac{u_i^z}{u_c^z} - 1}
 \end{aligned} \tag{2.69i}$$

and

$$\frac{\beta \Gamma}{2} = \frac{\sqrt{\beta N_0}}{\sqrt{z}} \cdot \sqrt{u_i^z - u_c^z} \tag{2.70i}$$

Combination then yields:

$$\begin{aligned}\delta_i^- &\simeq \frac{4}{z\beta\Gamma} \cdot \left\{ \sqrt{\frac{u_s^z}{u_c^z} - 1} \cdot \operatorname{arc cot} \sqrt{\frac{u_s^z}{u_c^z} - 1} \right\} \\ &\simeq \frac{4}{z\beta\Gamma} \cdot \sqrt{L} \cdot \operatorname{arc cot} \sqrt{L}\end{aligned}\quad (2.72i)$$

in which  $L$ , according to (2.70i) equals

$$\frac{z\beta}{4u_c^z} \cdot \left( \frac{\Gamma}{\sqrt{N_0}} \right)^2$$

Results for the conditions  $u_c = 2$  and  $u_c = 10$  are given in table 6. Series expansion of  $\sqrt{L} \cdot \operatorname{arc cot} \sqrt{L}$  gives:

$$\left( 1 - \frac{1}{3L} + \frac{1}{5L^2} - \dots \right)$$

indicating that the correction to be applied for interaction will exceed 5 % for  $L < 6$ .

In addition to the above considerations, which indicate that the percentage deviation from the approximate equation

$$\delta^- \simeq \frac{4}{z^+ \beta \Gamma}$$

is usually small, it may also be shown that for most soil colloids (in contrast to colloids with a much lower surface charge density) the actual magnitude of  $\delta^-$  will hardly exceed a few Å units.

Thus one finds for the common clay minerals, viz. montmorillonite, illite and kaolinite, values of  $\Gamma$  of about  $1 \times 10^{-7}$ ,  $3 \times 10^{-7}$  and  $2 \times 10^{-7}$  me./cm<sup>2</sup>, respectively. According to the foregoing this implies that  $\delta^-$  equals about 4 Å (Na-montmorillonite), 2 Å (Ca-montmorillonite, Na-kaolinite) or 1 Å (Ca-kaolinite, Na-illite, Ca-illite).

At the same time the values of the equivalent distance of exclusion,  $d^-$ , as given by the general equation:

$$d^- = \frac{Q}{\sqrt{\beta N_0}} - \delta^-$$

acquire a magnitude of roughly 10–20 Å ( $N_0 = 10^{-1}$  normal), 30–60 Å ( $N_0 = 10^{-2}$  normal), 100–200 Å ( $N_0 = 10^{-3}$  normal) and 300–600 Å ( $N_0 = 10^{-4}$  normal). Thus for soil systems the influence of  $\delta^-$  is usually small, although under saline conditions it should certainly be considered.

### 2.1.6 Some remarks on the validity of the model chosen for the calculations of negative adsorption

As was mentioned before several basic assumptions are involved in the application



of the GOUY-CHAPMAN theory to the description of the ion distribution in the vicinity of a charged surface (cf figure 1).

The assumptions underlying this theory concern a) the neglect of the presence of specific adsorption forces between ion and colloid; b) the neglect of ionic interaction in the double layer; c) the neglect of dielectric saturation effects and d) the neglect of the inhomogeneity of the electric field due to the presence of point charges on the colloid surface. It will be clear that all these effects are acting over a short range and therefore the ensuing disturbance of the ionic distribution is usually limited to a layer of several Å units from the charged surface.

As far as cation adsorption is concerned those first layers are very important since they store a large part of the total counter charge. Thus the application of the GOUY-CHAPMAN theory may lead to notable complications if cations with considerable differences in properties are involved.

With respect to anions the situation is in strong contrast with the above. Due to the anion repulsion by the negatively charged colloid the first layers from the surface contain only very few anions (the anion concentration at the surface amounting to e.g. 1 % of the equilibrium concentration). Specificity factors with respect to anions, although they are conceivably larger than those with respect to cations, will not influence considerably the anion distribution. If a specificity factor of e.g. 5 prevails, which would be disastrous to the application of the model to cation distribution, the anion concentration in the surface layers would increase from 1 to, say, 5 % of the equilibrium concentration. The effect of this on the negative adsorption, however, would still be a hardly detectable quantity, the anion deficit of these first layers having been changed only from 99 % to, say, 95 % of the equilibrium concentration.

The observed fact that often the negative adsorption of anions obeys closely to the relationship as predicted by the GOUY-CHAPMAN theory is in accordance with the above, although it should not be construed to imply that the actual distribution of the anions close to the surface does not differ from the predictions of this theory.

## 2.2 The positive adsorption of anions

In addition to the negative adsorption of anions by soil constituents also a positive adsorption of the latter may occur. This positive adsorption may exceed, or be less than, the ever present anion exclusion. Thus an over-all negative adsorption does not necessarily preclude the presence of a positive adsorption.

It has often been found that the over-all adsorption of anions by soils is positive. In fact, evidence to that effect has been given in specific cases for most common inorganic anions in soil, i.e.  $\text{Cl}$ ,  $\text{SO}_4$  and  $\text{PO}_4$ . The notable exception to this is  $\text{NO}_3$  for which no such data are known. This is probably due to the variability of the concentration of nitrate in soils, which renders accurate adsorption studies of this anion extremely difficult.

Although  $\text{Cl}$  usually appears to be negatively adsorbed, an over-all positive adsorp-

tion has been shown to occur, notably in kaolinitic soils at low pH (SUMNER, 1961). Positive adsorption of Cl by different soil types of Virginia has been described by MATTSON (1927) and THOMAS (1962). Also positive adsorption of  $\text{SO}_4$  has been proved beyond doubt in certain soils, a.o. by KAMPRATH *et al* (1956), LIU and THOMAS (1961) and CHAO *et al* (1962, 1963). In view of the importance of the  $\text{PO}_4$  ion with respect to plant nutrition, extensive investigations have been carried out on the availability of soil phosphorus to plants, as influenced by its adsorption on soil constituents. For this anion data from the literature show invariably an over-all positive adsorption.

In phosphate adsorption studies radioisotopes have been used to a great extent. MCAULIFFE *et al* (1947) measured the disappearance of  $\text{P}^{32}$  from the equilibrium solution as a function of time, after addition of carrier free  $\text{P}^{32}$  to suspensions of phosphate containing soils. They concluded that the radioisotope was diluted with several components of the soil phosphorus, the rates of reaction differing widely for the various components. The inverse experiment, showing the rate of release of  $\text{P}^{32}$  bound by the "soil", was carried out by WIKLANDER (1950). In this experiment the equilibrium solution containing the radioisotope was replaced after a contact time of several days by a synthetic solution of the same composition, except for the absence of the radioisotope, and the increase of the activity in solution was then measured as a function of time. On the basis of different rates of reaction measured in this way, WIKLANDER estimated the distribution of the total soil phosphorus over several different categories.

The determination of the isotopic dilution of  $\text{P}^{32}$  when added to soil under standardized conditions (shaking time, etc.) presumably will give a measure of the "labile pool" of P in soil, i.e. P that is present in such a form that isotopic exchange is effected easily under these conditions. The magnitude of this pool has been termed *E*-value (exchangeable P) and has been used as an estimate of P available to plants.

A variant of this method is the determination of the *L*-value (LARSEN, 1952), in which method the isotopic dilution is measured *in the plant* rather than in the soil dialyzate or extract. This value presumably would provide a measure of the available pool as sampled by the plant. If the *E*- and *L*-value coincide, no difficulties in interpretation seem to be present. Usually they are not identical, in which case the interpretation of the *L*-value becomes somewhat problematic. Thus for  $L > E$  it appears that certain components of P in soil are available to the plant (e.g. by dissolution) while they are not accessible for isotopic exchange. There is no proof, however, to what degree the dilution observed in the plant had already taken place in the soil.

In contrast to the above was the viewpoint taken in this matter by FRIED and DEAN (1952), who proposed that if any premixing of added tracer and soil P could be avoided, the observed *L*-value should be interpreted simply as a measure of the availability of soil P relative to that of the added (labeled) fertilizer P (or vice versa) and should be named *A*-value. RUSSELL *et al*. (1954) described data, which they interpreted as indications that equilibrium between soil phosphorus and fertilizer phosphorus was established in the total phosphate source (pool), from which phosphorus was taken up by the plant. As has been discussed by SISSINGH (1961), constancy of *L* (or *A*) at different levels of P uptake from the same pool is no proof for isotopic equilibrium at the moment of uptake, because phosphate compounds with very low rates of reaction for the isotopic dilution process may be present.

In summary, the interpretation of P uptake data is rather complicated. Although of profound

interest with respect to the characterization of the fertility status of soil as regards P, these data appear to be of very limited value for the evaluation of the interaction between phosphate and soil constituents.

As regards organic anions, a positive adsorption was measured in certain cases, as described by a.o. HOLMES and TOTH (1957; a soil conditioner, S-17, a water soluble polyanion, on montmorillonite, illite and kaolinite), MORTENSEN (1959; hydrolyzed polyacrylonitrile on kaolinite), and FRISSEL (1961; certain herbicides on montmorillonite, illite and kaolinite). With respect to the organic anions, however, considerable misunderstanding exists between "true" adsorption (i.e. adsorption in aqueous suspensions and thus comparable to that occurring in soils under natural conditions) and the adsorption on dry material as measured by infrared analysis and X-ray analysis (FRISSEL, 1961). In the latter case it seems likely that entry of water may often cause desorption of compounds which appear to be adsorbed in the absence of water.

In visualizing the mechanism underlying positive adsorption of anions by soils one may distinguish two types of mechanisms, viz.:

- 1 electrostatic attraction by positively charged sites on the colloidal particles;
- 2 specific adsorption, which term is used to cover all other types of positive anion adsorption, including chemical bonds (chemi-sorption).

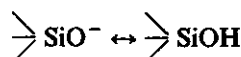
It should be stated that this distinction is hardly a principal one if chemi-sorption prevails, all adsorption forces being then of an electric nature. Quantitatively the results may be entirely different, mainly due to differences in magnitude and specificity of the forces acting.

### 2.2.1 Electrostatic attraction by positively charged sites on the colloid

This mechanism should be considered to be of the same character as the cation adsorption phenomenon, except for the inversion of the sign of the charges of adsorbent and adsorbate. As the negative charge of the clay minerals is usually large in comparison to the positive charge, if present, it is easy to understand that the positive adsorption is often masked by the anion repulsion, especially for the minerals of the montmorillonite and illite groups. Considering minerals with a relatively large positive charge, however, e.g. kaolinites at low pH, the positive adsorption may be of the same order of magnitude as the anion exclusion, which then results in an apparent absence of interaction between the colloidal material and the anions, or in an over-all positive adsorption.

As was pointed out before (cf section 2.1.1) the electric charge of soil colloids is attributed to three main causes, viz. isomorphic substitution, the presence of surface AlOH groups and the presence of surface SiOH groups. The electric charge due to isomorphic substitution has a constant value and is always negative, whereas the charge contributed by the surface AlOH and SiOH groups will vary with the pH and the electrolyte concentration of the system. Of these the SiOH groups are of little

concern as regards anion adsorption, the pK values of the association-dissociation reaction



being around 9. No evidence for the existence of  $\text{>SiOH}_2^+$  groups at pH values above 3.5 has been found (BOLT, 1957). The SiOH groups are situated along the edges of the clay minerals, and possibly also along crystall imperfections on the planar side of the minerals.

FRIPIAT and coworkers (1954, 1957) studied the active surface groups of several colloids, especially kaolinites. For the purpose of the determination of the total number of OH groups present at the surface, the isotopic exchange between surface hydroxyl groups of the solid and the vapor of heavy water was applied. A differentiation between total OH groups and acidic OH groups was made on the basis of the reactivity of the hydroxyl groups with certain organic compounds. The total number of surface OH groups per  $\text{m}\mu^2$  found was very close to the maximum number as calculated by ILER (1955) on the basis of a required space of  $12.5 \text{ \AA}^2$  for each group. While the differences in the cation exchange capacity as influenced by differences in the pH of the system could be explained satisfactorily assuming the formation of  $\text{AlOH}^-$  groups at increasing pH values, the cation exchange capacity itself could not be related quantitatively to the number of OH groups present. As was mentioned before, also for kaolinites indications were found for the presence of a constant negative charge due to isomorphic substitution, which would then constitute at least part of the C.E.C..

SCHOFIELD (1938) reported the positive adsorption of easily exchangeable anions by certain clays at low pH values. The adsorption mechanism was described as an electrostatic attraction between the anions and positively charged aluminum hydroxyde groups.

As has been pointed out by FRISSEL (1961), some speculations can possibly be made about the reversal of the edge charges as a function of the pH in the system. The different pK values of alumina and silica groups being known from experiments (SCHOFIELD and TAILOR, 1954; FRINK and PEECH, 1963) the extrapolation of these data to the clay minerals remains uncertain in view of the fact that here the edge Al atoms are usually bonded by means of an O-bridge to Si atoms. Starting with the structure of gibbsite as a model for the edge Al groups of clay minerals, FRISSEL concluded that the activity of edge aluminum hydroxyde groups of the 1 : 1 type clay minerals (e.g. kaolinite) would be less than that of the 2 : 1 type clay minerals (montmorillonite and illite). The same author suggested that disappearance of the positive charges from the edges would take place at pH values between 5 and 7.

Inasfar as the positive anion adsorption is governed by an electrostatic attraction only it is evident that the positive adsorption will increase with decreasing pH values.

in the influence of the salt concentration on the anion adsorption. To distinguish between its effect at the planar sides and that at the edges. As pointed out in detail before, the charges at the planar sides make themselves felt in conclusion, which was found to be inversely proportional to the square of the concentration. Thus the effect of this on the over-all adsorption would be diminishing with increasing electrolyte concentration.

For positive anion adsorption at the edges one may reason that an increase in the salt level invariably causes an increase of this adsorption. Thus, for a constant determining ion of a positively charged edge has a constant pH value), an increase of the salt concentration leads to a larger surface charge, resulting in a larger positive anion adsorption. In soil colloidal systems tends to decrease with increased salt level, which may favor the increase of the positive adsorption. In as far as the anion adsorption is caused by chemisorption on neutral sites (cf section 2.2.2) an increase of electrolyte concentration will diminish the built-up of a negative charge at these sites. This built-up serving as a limiting factor for the positive adsorption, the reducing effect of the increased electrolyte concentration will cause a decrease of the positive adsorption.

Whether the model of the planar diffuse electric double layer is of much value for the positive adsorption of anions by positively charged sites on the edges, because the edges are rather remote from homogeneously charged, planar surfaces as preassumed in this theory. Moreover, specificity of adsorption is to be larger than in the case of cation adsorption.

#### Specific adsorption of anions

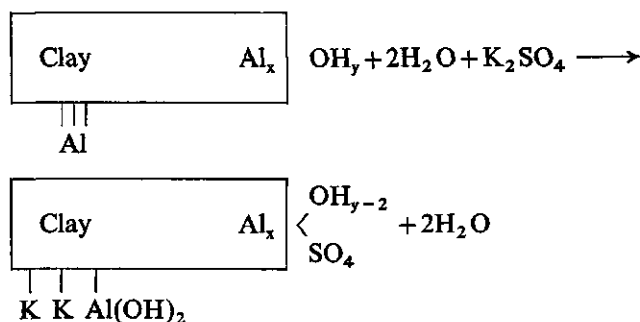
The adsorption of inorganic anions on soil colloids due to specific adsorption is so probable that this mechanism should be considered as chemisorption. A literature review on this subject, presenting a general picture of the present stage of knowledge on this phenomenon, has been given by

who introduced the term "anion penetration" for the chemical reactions which are built-in into a hydroxy alumina structure. According to these authors, the reactions concern a substitution of OH groups by anions and a simultaneous displacement of H ions by cations. Their importance for soil studies is based on the fact that anion penetration is not limited to free aluminum hydroxide only, but also occurs in interlayer alumina of clays, as was proposed by Liu and these authors described the adsorption of sulfate by soils containing exchangeable aluminum groups (at the edge) and exchangeable aluminum (at planar

#### ERRATA:

Page 44: Chapter V. 4: 5th line, read: the moisture suction is  $h$  cm

Page 47: horizontal axis of fig. 19, read:  $\log 100\alpha + \log \psi$



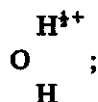
Thus, the exchangeable Al ions at the planar side are supposed to hydrolyze to a hydroxy-aluminum species (cf HSU and RICH, 1960), resulting in the formation of free negatively charged places on the clay on which the cations of the salt involved are adsorbed, while the anions of the salt simultaneously replace hydroxyl groups from the hydroxy-aluminum group at the edge. These supposedly replaced hydroxyl groups neutralize the hydrogen ions resulting from the hydrolysis of the exchangeable Al.

Reactions of the above type are usually stated to be responsible to a large extent for the anion fixation capacity of certain soils and clays (HEMWALL, 1957; MEHLICH, 1961; WADA, 1959). A striking difference between the adsorption under influence of the normal electrostatic adsorption forces and this chemical bonding is that the latter mechanism shows a very high degree of specificity; also in certain cases lack of reversibility was indicated.

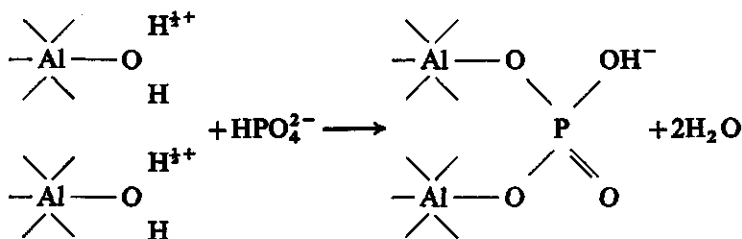
As reported by LIU and THOMAS anion retention is influenced by several factors. A linear relationship existed between the pH of the system and the amount of anions retained. In addition, the type of anion played an important role, sulfate ions being retained in much larger quantities than chloride ions under comparable conditions. This preference was found to be more pronounced at lower pH values. The retention appeared to be time dependent, as after a time lapse of 8 weeks equilibrium was still not established in the sulfate bonding by certain Virginia soils. These observations and the data of RAGLAND and COLEMAN (1960) about the increase of hydrolysis of exchangeable aluminum and of the formation of aluminum hydroxydes in soil systems after the addition of salts were explained by CHANG and THOMAS (1963) by assuming the occurrence of reactions of the "building-in" type as described above. According to the findings of the different authors mentioned above cations and anions are often adsorbed simultaneously, which led them to introduce the term "salt adsorption". This term, however, seems erroneous as not the salt molecules but the separate ions are adsorbed. Moreover cations and anions are adsorbed at different places of the soil complex as described by the chemical reaction given above.

Upon closer consideration it seems questionable whether this rather artificial reaction equation is suitable for the representation of anion bonding. The above authors failed to recognize that no negatively charged OH groups prevailed at the edges under the experimental conditions involved (pH below 6). Starting with a

fresh hydrogen clay (which has not yet been converted in part into an aluminum clay, as happens upon aging), the positive sites at the edges should presumably be represented as:



if now a salt is added, e.g.  $\text{K}_2\text{HPO}_4$ , one should perhaps visualize the anion adsorption reactions as:



Thus a negative charge starts being built-up at the edges upon adsorption. This explains the effect of phosphate as a dispersing agent, as the flocculation due to edge-to-planar-side attachment is now efficiently prevented. Extending this line of thought to the chloride and sulfate ions one must conclude that these are probably adsorbed according to a different mechanism (cf also Chapter 4), because chloride and sulfate salts do not appear to inhibit flocculation.

It is obvious that in the above given example the potassium ions will simultaneously replace H ions at the planar sides, which tends to a decrease of the pH in the system. In case of an Al-clay, part of the exchangeable aluminum will be replaced by K, which results in a comparable tendency of decreasing pH. Indeed, CHANG and THOMAS mentioned that the pH is usually lowered upon anion adsorption.

With respect to the reported stoichiometry of cation and anion adsorption it may be pointed out that a conclusion to the occurrence of this phenomenon requires much more refined determinations than were carried out by the mentioned authors. Moreover, this stoichiometry seems improbable as may be shown in the following manner. Assuming that a salt, e.g.  $\text{K}_2\text{SO}_4$ , is added to an Al-clay, part of the sulfate will presumably be bound and part of the potassium will replace exchangeable aluminum. The amounts of both are dependent on totally different factors; the Al exchange is under the given circumstances predominantly regulated by the preference of the adsorbing complex for Al against K, while the sulfate bonding depends strongly on the number of reactive sites at the edges and/or on the preference for sulfate against the anion which was formerly held by these sites. If one now visualizes the extremely unlikely situation that these factors are acting in such a way that the amounts of K and  $\text{SO}_4$ , which disappear out of the solution, are equal, one should find a different ratio between these amounts if the same salt solution would be added to the Al-clay after partial replacement of the exchangeable Al by e.g. Ca, the preference of Ca

against K presumably being lower than that of Al against K. Due to the fact that the adsorption of the cation and the anion are governed by different, independent factors, one must conclude that the above mentioned stoichiometry, if incidentally observed, should be considered as highly fortuitous.

In combining the two causes of anion adsorption it should be remembered that both mechanisms may occur simultaneously. Chemisorption appears hardly open for calculations based on theoretical models, so if the latter prevails (as seems likely for many anions) only a qualitative insight in the mechanism of positive anion adsorption may be obtained. Pointing to earlier considerations, the available experimental data are not always useful as they may include the sometimes unknown contribution of anion exclusion. Obviously data should be collected which allow correction for this contribution. After such a correction some inference may possibly be made with respect to the bonding mechanism, on the basis of observed specificity, reversibility and the influence of pH and salt concentration.



### 3 Experimental procedures and materials

#### 3.1 Introduction

The experimentally accessible measure of the negative adsorption of anions is the volume of exclusion,  $V_{ex}$ , in ml per gram colloid. This quantity also equals the product of the equivalent distance of exclusion from the negatively charged surface and the corresponding specific surface area of the colloidal particles.

$V_{ex}$  thus represents the volume in which no anions appear to be present; it is related to the anion exclusion,  $\gamma^-$ , in me. per gram colloid, via:

$$V_{ex} = \frac{\gamma^-}{n_0^-} \quad (3.1)$$

in which  $n_0^-$  = equilibrium concentration of the anion involved, in me. per ml.

$V_{ex}$  is found experimentally from the difference between the actual solution volume of the system,  $V_{tot}$ , and the apparent volume in which the anion appears to be dissolved at the equilibrium concentration  $n_0^-$ ,  $V_{app}$ , both expressed in ml per total system, according to:

$$V_{ex} = (V_{tot} - V_{app})/W \quad (3.2)$$

in which  $W$  stands for the amount of solids in the system in grams. As the apparent volume equals the quotient of the total amount of the anion and the equilibrium concentration of this ion, equation (3.2) may be transformed into:

$$V_{ex} = \left( V_{tot} - \frac{\sum(-)}{n_0^-} \right) / W \quad (3.3)$$

in which  $\sum(-)$  represents the total amount of the anion under consideration, expressed in me..

Applying equation (3.3) to a suspension of soil material one finds:

$$V_{ex} = \left( 1 - \frac{n_{sus}^-}{n_0^-} \right) V_{sus}/W \quad (3.4)$$

in which  $V_{sus}$  and  $n_{sus}^-$  represent the volume of solution in the suspension and the average concentration of the anion in the suspension, respectively.  $V_{sus}$  is found by diminishing the total volume of the suspension with the volume of the solids. Thus according to (3.4) the determination of the concentration of the anion in both the suspension and the equilibrium solution leads to  $V_{ex}$ . It will be clear that in the case

of positive adsorption of the anion a negative value is found for  $V_{ex}$ , corresponding to a volume of inclusion,  $V_{inc}$ .

The determination of  $V_{ex}$  necessitates a separation between the suspension and the equilibrium solution. As the anion distribution in the system is easily disturbed if this separation is effected by means of centrifugation, the equilibrium solution should preferably be obtained through the use of dialysis bags (cf BOLT and DE HAAN, 1963). The composition of the equilibrium solution may then be ascertained directly from the contents of the bags. Because equilibrium must be effected now by diffusion of the ions through the cellophane membrane of the bag, it should be expected that more time is required to attain equilibrium. Moreover, this cellophane may interfere with anion adsorption. For these reasons the properties of the bag material as regards diffusion and possible adsorption of the anions were studied in preliminary tests.

As follows from Chapter 2 the volume of exclusion depends strongly on the electrolyte concentration of the system, values for  $V_{ex}$  being higher the lower the concentration. This places a limitation on the experimental procedure, as sometimes values for  $V_{ex}$  of satisfactory magnitude are found only in systems with rather low electrolyte concentration.

### 3.1.1 Required accuracy of the determinations

In soil suspensions at high moisture content  $V_{ex}$  is usually found by a subtraction of two values of nearly the same magnitude and thus the accuracy in the determination of both values must be extremely high to avoid a considerable error in the final result. In accordance with equation (3.2) the absolute error in the determination of  $V_{ex}$  per total system amounts to:

$$\sigma_{V_{ex}} = \sigma_{V_{tot}}^2 + \sigma_{V_{app}}^2 \quad (3.5)$$

in which  $\sigma$  represents the absolute error, subscripts referring to the quantities meant. Thus the relative error in  $V_{ex}$  amounts to:

$$\begin{aligned} \sigma_{V_{ex}}' &= \sqrt{\frac{\sigma_{V_{tot}}'^2 + \sigma_{V_{app}}'^2}{V_{ex}^2}} \\ &= \sqrt{\frac{\sigma_{V_{tot}}'^2 \cdot V_{tot}^2 + \sigma_{V_{app}}'^2 \cdot V_{app}^2}{(V_{tot} - V_{app})^2}} \end{aligned} \quad (3.6)$$

If the apparent volume equals a fraction  $p$  of the actual volume, then:

$$V_{app} = p \cdot V_{tot} \quad (3.7)$$

Substituting this in equation (3.6) one arrives at:

$$\sigma_{V_{ex}}' = \sqrt{\frac{\sigma_{V_{tot}}'^2 + p^2 \cdot \sigma_{V_{app}}'^2}{(1-p)^2}} \quad (3.8)$$

The determination of the actual volume is based on weight data, assuming a specific weight of 1. Taking the weighing procedure as the starting point for the calculation of the error in  $V_{ex}$ , the relative error of  $V_{tot}$  equals the standard deviation  $\sigma'_0$  of the weighing procedure,  $\sigma'_0$  being  $\leq 1\%$ . From this it follows:

$$\sigma'_{V_{ex}} = \sqrt{\frac{\sigma_0'^2 + p^2 \cdot \sigma_{V_{app}}'^2}{(1-p)^2}} \quad (3.9)$$

The apparent volume is found as the quotient of two measured concentrations. The error in these concentration determinations is supposed to be  $a \cdot \sigma'_0$ . Thus one finds for the relative error of the apparent volume:

$$\sigma'_{V_{app}} = \sqrt{2a^2 \cdot \sigma_0'^2} \quad (3.10)$$

Substitution of (3.10) in (3.9) gives:

$$\sigma'_{V_{ex}} = \sqrt{\frac{\sigma_0'^2 + 2a^2 \cdot p^2 \cdot \sigma_0'^2}{(1-p)^2}} \quad (3.11)$$

Since the volume of exclusion is expressed per gram of colloid (cf  $W$  in equation 3.3), whereas the colloid content of the system is determined on weight basis, the final relative error of  $V_{ex}$  becomes:

$$\sigma'_{V_{ex}} = \sigma'_0 \cdot \sqrt{\frac{3 + 2a^2 \cdot p^2}{(1-p)^2}} \quad (3.12)$$

With the use of equation (3.12) the relative error of  $V_{ex}$ , relative to  $\sigma'_0$ , may be calculated for different values of  $a$  and  $p$ . Results of these calculations are presented in figure 13. This figure indicates that the error of  $V_{ex}$  is rather sensitive to the value of  $a$  in the range  $p \geq 0.7$ . The  $p$  value, however, is fixed by the system chosen, viz. nature and amount of clay present. In order to attain equilibrium between suspension and dialyzate in a reasonable time period the suspension must be sufficiently fluid, which means that the limit of the clay content in the case of e.g. Na-montmorillonite is about 2 %. The maximum volume of exclusion to be expected then amounts to roughly 10–20 % of the total volume, thus  $p$  being 0.8–0.9. As follows from figure 13 little is gained by decreasing the error in the concentration determination below that of the weighing ( $\sigma'_0$ ). The weighing procedure being the easiest to execute with great accuracy one should nevertheless limit the  $a$  value to unity or at the most two. Under the present conditions the value of  $p$  is obviously the limiting factor for the accuracy that may be obtained.

For the concentration determination of chloride ions in both the suspension and the dialyzate an excellent method exists, viz. the potentiometric chloride titration, which method may be executed with a relative error of less than 1 % as long as the concentration equals or exceeds  $2 \times 10^{-4}$  N (cf section 3.2). For the determination of the negative adsorption of other anions, however, e.g. sulfate and phosphate, no methods of comparable accuracy could be found. In this case (and also for chloride

at lower concentrations) the determination of  $V_{ex}$  with the help of radionuclides proved to be quite satisfactory.

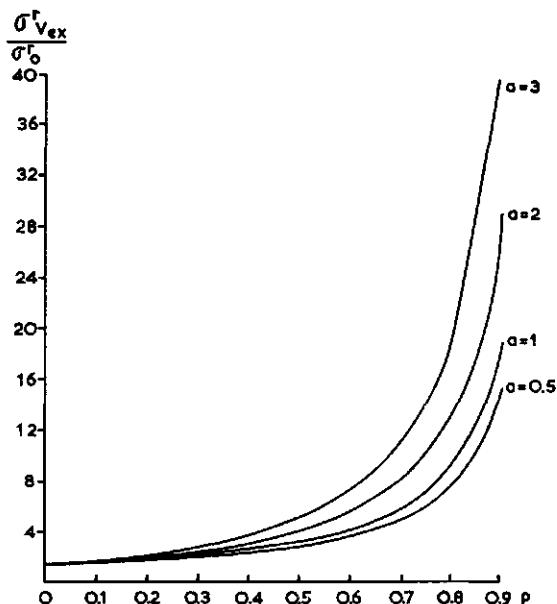


Fig. 13. The percentage error of the experimentally determined quantity  $V_{ex}$  relative to the "basic" error in the analytical determinations,  $\sigma_o^r$ , as a function of  $p$  and  $a$ .

### 3.2 The potentiometric chloride titration

For the determination of the negative adsorption of chloride the method used by BOLT (1961) may be applied.

Weighed aliquots of both the suspension and the equilibrium solution are brought at a  $\text{NH}_4\text{NO}_3$  concentration of 0.5 N. The titration is executed with a Ag-AgCl electrode prepared according to BROWN (1934), which is placed in the unknown. The calomel electrode, placed in a solution of 0.5 N  $\text{NH}_4\text{NO}_3$ , is used as reference electrode. This solution is connected with the unknown by means of an agar bridge containing 0.5 N  $\text{NH}_4\text{NO}_3$ . Additions of a  $\text{AgNO}_3$  solution of known normality are measured by means of a plunger type micro buret. The sample is titrated under continuous stirring. Following each addition the electric potential between the Ag-AgCl electrode and the calomel electrode is measured by means of a Pye potentiometer. The titration is executed in a constant temperature room.

Plotting after each titration the observed values of the potential against the additions of the  $\text{AgNO}_3$  solution one may attempt to determine the experimental equivalence point from the steepest slope of the curve in this figure. For reasons of accuracy, however, an "absolute" potential method was applied to the determination of the end-point of the titration. To this purpose each series of titrations was preceded and followed by a separate determination of the electric potential at the equivalence

point, titrating a set of NaCl solutions of known normality under comparable conditions as the samples. It was found that under the conditions of the experiments, the equivalence potential would vary only 1/2-1 mV during a single day.

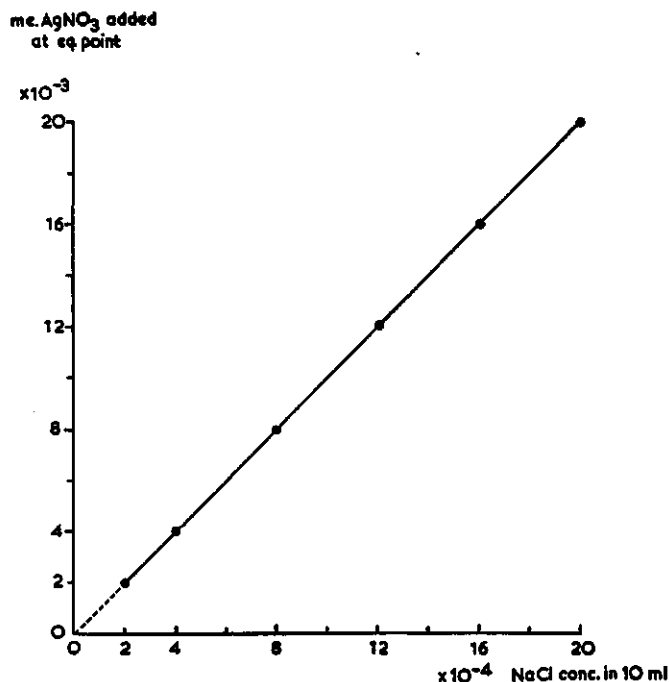


Fig. 14. Verification of the accuracy of the potentiometric chloride titration.

It appeared from the data shown in figure 14, that in this way chloride concentrations of about  $2 \times 10^{-4}$  N can be determined with sufficiently high accuracy (error  $\leq 1\%$ ), provided the titration is executed in solution. This figure presents titration data of standard NaCl solutions of different, known concentrations with a AgNO<sub>3</sub> solution of known normality, using the equivalence potential as derived from separate titrations of a set of standards at 0.01 normal concentration.

### 3.3 The use of radioisotopes in the adsorption experiments

The experimental evaluation of the negative adsorption of chloride at concentration levels below  $2 \times 10^{-4}$  N necessitates the use of radioactive chloride. The application of radionuclides for adsorption studies in soils has been described a.o. by SUMMER and BOLT (1962), CHAO *et al* (1962) and ØIEN *et al* (1959). Some specific problems arising when using radionuclides with extreme half lives ( $K^{42}$  and  $K^{40}$ ) have been discussed in detail by DE HAAN *et al* (1964).

The experimental procedure reads in principle as follows. A solution containing the ion of interest, labeled with a radioisotope of this ion, is added to the system under study. Isotopic equilibrium (which implies that the radioisotope is equally distributed over all atoms of the same species throughout the system) is acquired by means of agitation. After equilibration the activity of the equilibrium solution is measured. The ratio of the added activity to the (radio)activity-concentration in the equilibrium solution, equals the apparent volume in which the radioisotope is homogeneously distributed, according to:

$$V_{app} = \frac{V_a \cdot A_a^*}{A_e^*} \quad (3.13)$$

in which  $V_a$  represents the added amount of the labeling solution and  $A_a^*$  and  $A_e^*$  are the activity-concentrations, in counts per minute per ml, of the labeling solution and the equilibrium solution, respectively. It will be clear that positive or negative adsorption of the ion results in an apparent volume which is larger or smaller, respectively, than the actual volume. The volume of inclusion or exclusion is found in the normal way as the difference between the actual and the apparent volume (cf equation 3.2).

Table 7. Some relevant data of the radionuclides used

Radio nuclide	Half life	Type of radiation	Disintegration energy (MeV)	Commercial form
Cl <sup>36</sup>	3.03 × 10 <sup>5</sup> year	β <sup>-</sup>	0.714	2n HCl
S <sup>35</sup>	87.2 days	β <sup>-</sup>	0.167	as sulfate in aqueous solution
P <sup>32</sup>	14.2 days	β <sup>-</sup>	1.71	as orthophosphate in dilute hydrochloric acid

Radionuclides of interest for the anion adsorption experiments are radioisotopes of Cl, S and P, of which some data are given in table 7. When using these radioisotopes for the execution of the experiments, a commercially available source is diluted with distilled water (or a suitable salt solution) to a labeling solution of the desired composition. Weighed amounts of this solution are added to the system and to a known amount of a suitable standard salt solution. Determination of the activity-concentration of the standard solutions yields the value of  $A_a^*$ , taking into account the dilution factor employed.

The application of radioisotopes often allows measurements at extremely low concentration levels, especially if the isotope is available in carrier free form. This may be demonstrated with the following example, concerning carrier free P<sup>32</sup>. A suitable activity-concentration of the solution is about 0.1 micro curie per ml, corresponding to a disintegration rate of roughly 2 × 10<sup>5</sup> disintegrations per minute. For one gram of a pure radioisotope the disintegration rate amounts to:

$$\frac{0.693}{T_{\frac{1}{2}}} \cdot \frac{6 \times 10^{23}}{A} \cdot \frac{1}{3.7 \times 10^{10}} \text{ curie} = 1.13 \times 10^{13} \cdot \frac{1}{A \cdot T_{\frac{1}{2}}} \text{ curie} \quad (3.14)$$

in which A and  $T_{\frac{1}{2}}$  represent the atom weight and the half life of the radioisotope, respectively. Applying (3.14) to  $P^{32}$  one finds an activity per gram of pure  $P^{32}$  of:

$$\frac{1.13 \times 10^{13}}{32 \times 20,448} \mu\text{C/gram}$$

This then means that the P concentration of a solution containing 0.1  $\mu\text{C}$  carrier free  $P^{32}$  per ml amounts to:

$$\frac{3.2 \times 20,448}{1.13 \times 10^{13}} = 5.8 \times 10^{-15} \text{ gram P/ml}$$

As the  $P^{32}$  is present as phosphate, the phosphate concentration in a system in which carrier free  $P^{32}$  is used at an activity concentration of 0.1  $\mu\text{C/ml}$  is roughly  $2 \times 10^{-15}$  mmol/ml.

### 3.3.1 The activity determinations

For the activity determinations amounts of about one half milliliter of the solutions are weighed onto an aluminum planchet of special shape. Next the planchet is put on a brass ring, placed on a hotplate, and its content is evaporated till dryness. Then the activity measurement is executed by means of normal counting equipment with a G.M. end-window tube. The efficiency of the counter array used was about 10–15 %.

Because the radioactive disintegration is a random process the accuracy of the activity determination depends on the number of disintegrations recorded. The error equals the square root of the total count number, which implies that at least 10,000 disintegrations must be registered to keep the error within one percent with a probability of 68.3 %. To be on the safe side all samples were counted till 40,000.

In addition errors are introduced during the sample preparation procedure. These are caused by irregularities of the dried sample and inhomogeneity of the mica window of the G. M. tube. The latter fact may contribute considerably to the inaccuracy if soft  $\beta$ -emitters are involved, e.g.  $S^{35}$  (cf table 7). To minimize the error caused by irregularities, each sample should preferably be counted in different positions, e.g. by rotating the sample between three separate countings over 120 degrees. Earlier investigations on this subject (BOLT and PIETERS, 1964) indicated that the application of the described procedure results in an error in the mean value of the count rate of 0.35 % for most radionuclides, if 10 samples of each solution are counted. This means that the error in the single sample amounts to 1 % under these conditions.

For the present investigations it appeared to be satisfactory to prepare three samples of each unknown and standard solution, taking three countings of each sample. Later it was established that the error resulting from taking one counting of nine

different samples was equal to or smaller than that in the situation above. This was evidently important since an automatic sample changer (Philips, type PW 4001) became available during the course of this work. A test of this equipment indicated small, but significant differences between the count data obtained from the same sample when placed at different positions in the chain of sample holders. By thoroughly checking the equipment, however, correction factors could be established for this effect.

Using these and taking all precautions mentioned above, it was found eventually that for the radionuclides of interest sufficient accuracy could be obtained (error  $\leq 1\%$ ) if only five samples of each solution were counted.

Because of the long half life of  $\text{Cl}^{36}$ , and also of  $\text{S}^{35}$  (cf table 7) time corrections are not necessary for a comparison of the count data of one experiment, if all activity determinations of the same experiment are carried out within 1, or at the most 1.5 day. When using  $\text{P}^{32}$ , however, corrections for radioactive decay are required. This may be done by back calculating all count data of the same experiment to zero time. A more practical solution of this problem is given by counting the unknown and the standard that belongs to it directly after each other. To this purpose the samples of unknown and standard were always placed in consecutive positions in the sample changer.

### 3.3.2 Simultaneous determination of the adsorption of two or more different anions

Application of the potentiometric titration of chloride, combined with the tracer method for another anion, allows the simultaneous measurement of the adsorption of two different anions in the same system. In the specific case of systems containing chloride, sulfate and phosphate, the following techniques appear to be possible.

The difference between the disintegration energies of  $\text{S}^{35}$  and  $\text{P}^{32}$  (cf table 7) may be used for a differentiation between the activities of both radioisotopes, if present in one solution. This possibility was tested with the help of a Tricarb liquid scintillation counter with a channel analyzer<sup>1</sup>. Several testruns showed, however, that the accuracy of the activity determinations according to this procedure was far below the required level.

A second possibility to differentiate between the two radionuclides above is given by their difference in half life, viz. 87.2 days for  $\text{S}^{35}$  and 14.2 days for  $\text{P}^{32}$ . The relation between the activity of a radioisotope in a sample at a time  $t$  minutes after zero time,  $A_t^*$ , and at zero time,  $A_0^*$ , is given by:

$$A_t^* = A_0^* \cdot \exp \left( -\frac{t \cdot \ln 2}{T_{\frac{1}{2}}} \right) \quad (3.15)$$

<sup>1</sup>) Kindly supplied by ITAL, Wageningen.



Using equation (3.15) one may calculate the activities of both isotopes in a sample containing a mixture of the two from the count data, assessed at known time intervals. It will be clear that the determination of the activity-concentration is less accurate in this case than for a single radioisotope. This may be remedied in part by repeating the countings at several times (cf also section 3.4.2).

### 3.4 Design of the anion adsorption experiments

In the experiments polyethylene bottles were used to prevent breakage during the equilibration period. The systems to be studied were assembled in the following way.

First an amount of the labeling solution is brought into the bottles. Next different salt solutions of known normality are added to attain the desired solution composition. Following the addition of a suspension of the clay material under study, two dialysis bags, each containing about 15 ml distilled water, are added. All additions are weighed on an analytical balance.

For the bags a dialysis tubing material with a flat width of 15/16 inch, a diameter inflated of 5/8 inch and a wall thickness of 0.0008 inch was used. The tubing was cut into pieces of equal length, which were shaken in distilled water. The water was renewed periodically until no change in the electric conductivity was found. For use in the experiments the pieces of tubing were knotted to form bags, which were filled with distilled water. Previous to the addition of the bags to the systems the outside was dried with the help of adsorbing paper. A correction was applied for the dry weight of the dialysis bag material.

In the present experiments the amounts were chosen such, that the actual volume of solution,  $V_{tot}$ , was about 130 ml. For reasons of accuracy each system was accompanied by its own standard solution, having roughly the same composition as the system.

After the weighings, the bottles are agitated to attain an equilibrium state throughout the system. End-over-end shaking turned out to be the most effective for this purpose. Since equilibrium must be established by diffusion of the ions into the dialysis bag, the time required for equilibration may be expected to be longer at lower electrolyte level. It was found that a shaking time of one week suffices to attain equilibrium for all ions of interest, even at the lowest electrolyte level used (about  $10^{-4}$  N).

After equilibration the dialysis bags are removed from the bottle and the contents are pipetted off into a test tube. In the case of the tracer method preferably at least 5 samples are prepared of each bag contents and compared with 5 samples of the standard, resulting in  $V_{app}$  according to equation (3.13). In the case of the potentiometric chloride titration 5 ml aliquots of both the suspension and the dialyzate are titrated, resulting in  $n_{ms}^-$  and  $n_0^-$  of equation (3.4). Substitution of these data, together with the weighing data, into equations (3.2) and (3.4), respectively, allows the calculation of the volume of exclusion (inclusion). It should be noted that according to this procedure  $V_{ex}$  is found in grams per gram of clay. Employing a solution density of 1.00 the data are given as  $V_{ex}$  in milliliters per gram of clay.

Because of possible dilution of the suspensions via osmosis from the bags the weight concentrations of the suspensions were determined after removal of the bags in the case of the potentiometric chloride titration.

By using the contents of the two bags for separate determinations, duplicate values of  $V_{ex}$  were found. The comparison between the duplicates was used to verify that equilibrium had been established.

The dialyzate remaining after preparation of the samples was used for the measurement of the electric conductivity. The total salt concentration,  $N_0$ , was estimated from the conductivity, using International Critical Tables.

In those cases where the measured value of  $V_{ex}$  deviates from the calculated value (indicating the presence of positive adsorption) the equilibrium concentration of the anion concerned must be determined. For the chloride ion the potentiometric titration can be used to this purpose. The concentrations of sulfate and phosphate may be found from radio analysis if the specific activity is known. This is the case if the concentration of the anion involved in the suspension is zero or has a known value.

This method fails if the amount of the specific anion in the added suspension is unknown, which situation usually arises when soils are employed, especially with respect to phosphate. The concentration in the equilibrium solution must then be found in a separate determination by means of chemical analysis. In the present experiments phosphate concentrations were determined colorimetrically with the ammonium-molybdate method, employing a Beckman spectrophotometer. Sulfate was never present in the suspensions in detectable quantities.

The determination of  $N_0$ , combined with the concentrations of the ion species studied, allows the calculation of  $f$ -values, i.e. the equivalent concentration fractions.  $Q$ -values may then be found as described in Chapter 2. The experimental value of  $V_{ex}$  may then be plotted versus  $Q/\sqrt{\beta N_0}$ . The slope of this line yields the specific surface area of the colloidal material involved, provided positive adsorption is absent, whereas the intercept equals  $\delta^-$ .

It should be noted that for the calculation of the  $f$ - and  $Q$ -values the *equivalent* concentrations of the ions must be known, whereas *molar* concentrations are found from the chemical analyses. With respect to phosphate this may give rise to complications, since P may be present as mono-, di-, or trivalent anion, depending on the pH of the system.

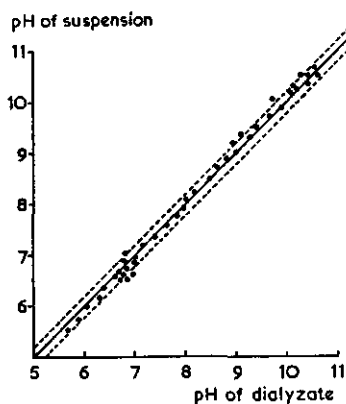


Fig. 15. Comparison between pH values of suspensions and corresponding dialyzates for a series of systems

Although one thus needs the pH of the equilibrium solution, this determination was difficult in the present case because of the small volume of the dialysis bags. Thus it was examined whether the pH of the dialyzate could be approximated by the pH of the suspension. To this purpose the suspension pH, as measured by means of an Electrofact pH meter, type 6C50/4A, was compared with the pH of the dialyzate, for several series of systems. Results are presented in figure 15. This figure gives a weak indication of the occurrence of a suspension effect. The differences between suspension- and dialyzate-pH values, however, were usually within the range of the experimental error of the pH measurement, and thus the use of the suspension-pH values was assumed to be sufficiently accurate.

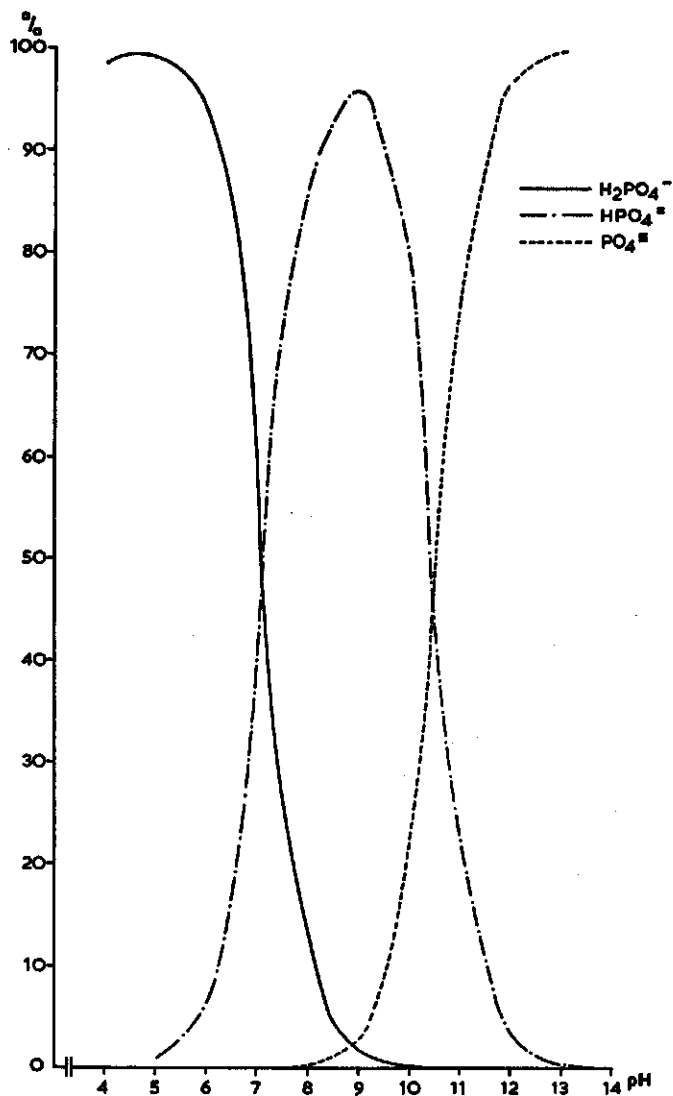


Fig. 16. The distribution of total P over mono-, di-, and tri-valent phosphate ions as a function of pH

At a known pH one may calculate the distribution of total P over the different ion species from the following formulae:

$$\text{fraction as } \text{H}_2\text{PO}_4^- = P \left\{ \frac{\text{H}^3 \cdot K_1}{\text{H}^3 + \text{H}^2 \cdot K_1 + \text{H} \cdot K_1 \cdot K_2 + K_1 \cdot K_2 \cdot K_3} \right\}$$

$$\text{fraction as } \text{HPO}_4^{2-} = P \left\{ \frac{\text{H} \cdot K_1 \cdot K_2}{\text{H}^3 + \text{H}^2 \cdot K_1 + \text{H} \cdot K_1 \cdot K_2 + K_1 \cdot K_2 \cdot K_3} \right\}$$

$$\text{fraction as } \text{PO}_4^{3-} = P \left\{ \frac{K_1 \cdot K_2 \cdot K_3}{\text{H}^3 + \text{H}^2 \cdot K_1 + \text{H} \cdot K_1 \cdot K_2 + K_1 \cdot K_2 \cdot K_3} \right\}$$

in which H represents the concentration of H ions and  $K_1$ ,  $K_2$  and  $K_3$  stand for the first, second and third dissociation constant of phosphoric acid, respectively. For these constants the values as given by Handbook of Chemistry and Physics (1963) were used, viz.:

$$K_1 = 7.52 \times 10^{-8}$$

$$K_2 = 6.23 \times 10^{-8}$$

$$K_3 = 2.2 \times 10^{-13}$$

The calculated distribution of total P over the different ion species as a function of pH is presented graphically in figure 16. For lack of practical interest the range of undissociated phosphoric acid is not plotted. Although the above figures preassume activity coefficients equal to unity, the corrections for systems up to 0.01 N NaCl were small enough to warrant their neglect. Corrections for temperature deviations were assumed not to be necessary since all measurements were conducted at room temperature.

### 3.4.1 Verification of the method

It is evident that any interaction of the ions under study with materials used in the experiments other than the colloid will invalidate the adsorption studies. Thus preliminary experiments were carried out to check the possible adsorption of the anions by the polyethylene bottles and the dialysis tubing material.

For chloride and sulfate interaction could not be detected, even at the lowest concentration used (i.e. carrier free  $\text{S}^{35}$  as sulfate). Phosphate, however, was adsorbed by the bottles to a considerable extent. This was first tested out by using a solution containing carrier free  $\text{P}^{32}$  (in the absence of dialysis tubing). The activity concentration of this solution was followed as a function of shaking time. The solid line of figure 17 indicates that after one week only 50 % of the original activity remained in solution, indicating severe adsorption. This adsorption may be depressed considerably by the addition of an amount of "cold" phosphate. At phosphate levels of  $10^{-5}$ ,  $3 \times 10^{-5}$ ,  $6 \times 10^{-5}$  and  $10^{-4}$  N, respectively, (calculated from additions of a  $\text{Na}_3\text{PO}_4$  solution <sup>1)</sup>) the activity left in solution amounted to 92, 95, 98 and 100 percent, respectively, of the original activity.

<sup>1)</sup> In the following the phosphate concentration is usually indicated as normality, expressed as  $\text{Na}_3\text{PO}_4$ . The concentration in molarity is in these cases simply found by dividing the numbers presented by a factor 3.

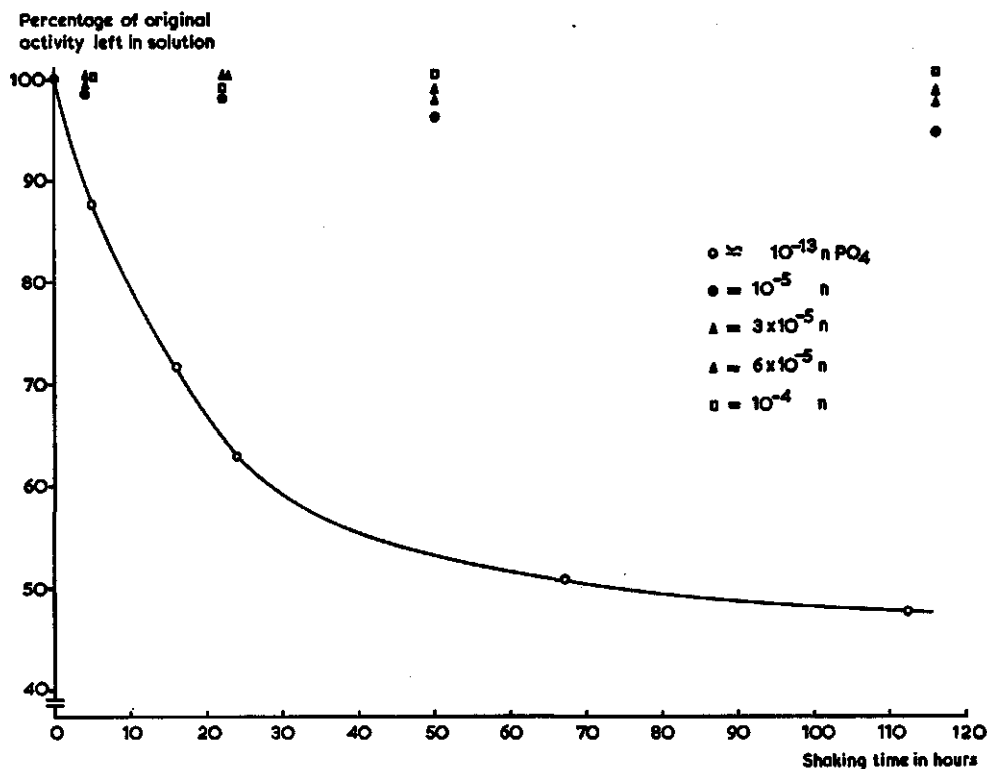


Fig. 17. The adsorption of  $\text{P}^{32}$  on the polyethylene bottles used in the experiments, as a function of time and phosphate concentration

The dialysis bags may also adsorb phosphate. From a repeat of the above experiment in the presence of dialysis bags it was found that the total adsorption of phosphate on bottle and bags became negligible at phosphate concentrations of at least  $10^{-4}$  N (cf figure 18). In accordance with this experience this minimum phosphate level was maintained in all experiments in which  $\text{P}^{32}$  was employed.

#### 3.4.2 The applicability of differences in half life to a differentiation between two isotopes

In a separate experiment it was verified whether the application of differences in half life suffices for a differentiation between two isotopes, present in a mixture, as was suggested in section 3.3.2. To this purpose three series of solutions, A, B and C, were prepared from two labeling solutions, viz. one containing  $\text{S}^{35}$  and one containing  $\text{P}^{32}$ . Each series consisted of 5 systems with a total electrolyte level varying from  $5 \times 10^{-4}$  to  $10^{-2}$  N, divided equally over sulfate and phosphate. To series

*A* an aliquot of the  $S^{35}$  labeling solution was added and to *B* an aliquot of the  $P^{32}$  labeling solution, whereas to series *C* both  $S^{35}$  and  $P^{32}$  were added. After mixing, 5 samples were prepared from each system.

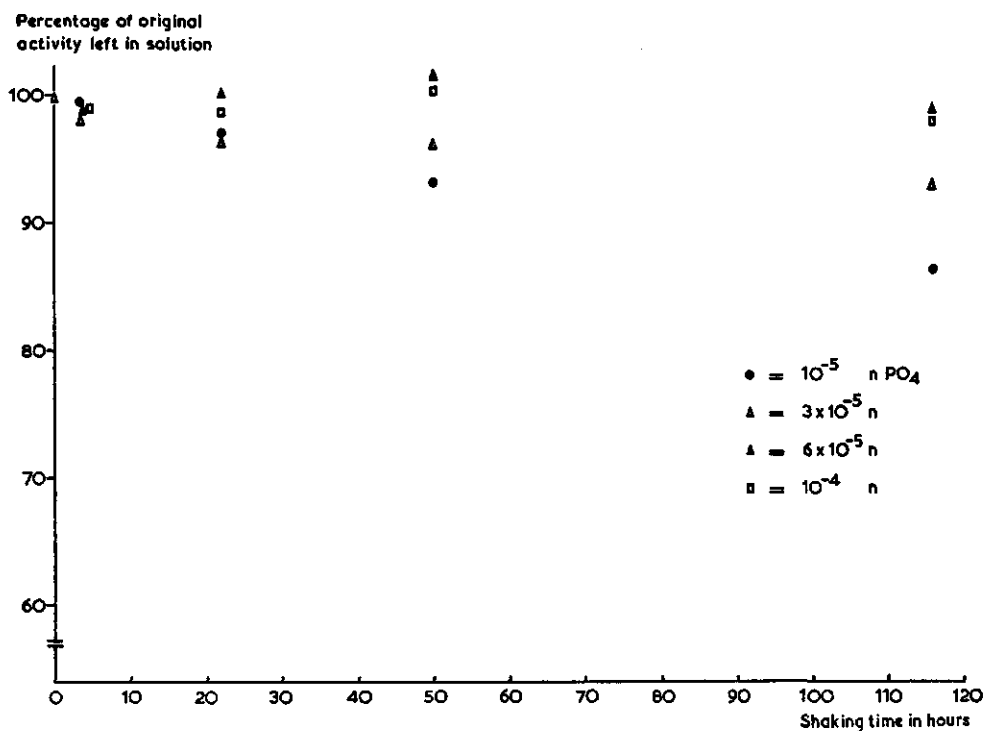


Fig. 18. The combined adsorption of  $P^{32}$  on the polyethylene bottles and the dialysis bag material, as a function of time and phosphate level

From the count data of *A* and *B*, which served as standards, the expected count rate of *C* could be calculated. Samples of series *C* were then counted twice at an interval of 20 days. The experimental contribution of both isotopes to the observed count rate could be found by solving the equations:

$$\begin{aligned}
 S_0 + P_0 &= X_0 \\
 S_t + P_t &= X_t
 \end{aligned}
 \tag{3.16}$$

in which  $S$ ,  $P$  and  $X$  stand for the count rate attributed to  $S^{35}$ , count rate attributed to  $P^{32}$ , and total count rate, respectively. The subscripts 0 and  $t$  refer to zero time and the time at which the samples were counted for the second time. Applying equation (3.15),  $S_t$  and  $P_t$  may readily be expressed in  $S_0$  and  $P_0$ , respectively, indicating that equations (3.16) may be solved after one repeat of the counting procedure.

The comparison of measured and calculated values of  $S_0$  and  $P_0$  is given in figure 19. The first part of this figure represents the deviation between the experimental total count rate of the samples of series C and the expected total count rate according to the standard solutions A and B. This deviation turned out to be about 0.5 %.

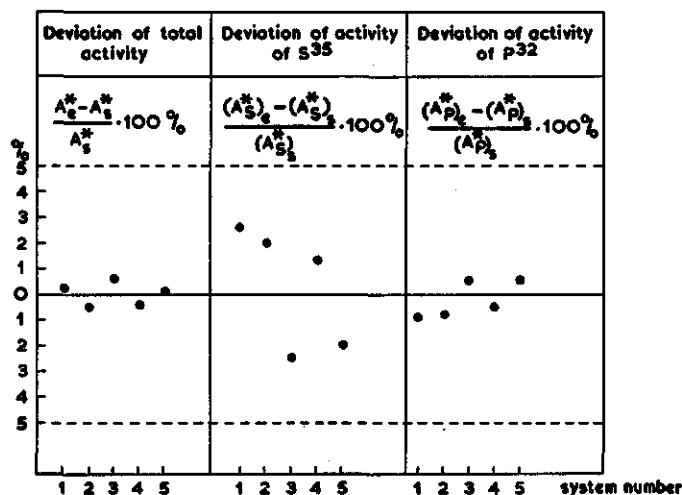


Fig. 19. The error in the measurements of the count rates of  $S^{35}$  and  $P^{32}$  when present in the same solution. The separate activities were calculated on the basis of differences in half life

The second and third part present the deviation between the count rates of  $S^{35}$  and  $P^{32}$ , respectively, as calculated according to the standard solutions and as calculated according to the decay method. As expected, the deviations are higher in this case but they still have a reasonably low value, indicating that the described method may be employed to the determination of the activities of two isotopes, present in one solution.

Naturally, this method is applicable only if the half lives of the isotopes involved differ sufficiently. The accuracy of the measurement will be higher the larger the change in activity ratio of both components of the mixture during the time interval between the two countings. Preferably one should adjust the ratio of activities at time "zero" such that the short lived isotope dominates strongly. In addition the second counting should be delayed until the activity of the short lived isotope has decreased substantially; the activity of the latter should then constitute only a minor fraction of the total activity.

### 3.5 The determination of the specific surface area from the retention of ethylene glycol

The application of ethylene glycol retention to the determination of the specific surface area of clays was introduced by DYAL and HENDRICKS (1950). Briefly this

method reads as follows. Clay samples of known weight, which have been dried over  $P_2O_5$  in vacuum, are thoroughly wetted with ethylene glycol. Next the excess of glycol is removed by molecular distillation in vacuum over anhydrous  $CaCl_2$ . The distillation is continued until a monolayer of ethylene glycol remains, as is indicated by a low rate of loss of the glycol. From the weighing data and a factor representing the amount of glycol required to form a monolayer on one  $m^2$  of surface (0.00031 g according to the above authors) the specific surface area of the clay may be calculated. A complication arising with this method is that the end-point of the desorption process is not distinct. DYAL and HENDRICKS proposed that the desorption would be finished at the moment that the rate of loss is smaller than 0.020 gram glycol per gram clay per 7 hours.

The method was applied to soils by BOWER and GESCHWEND (1952). They proposed that the desorption process should be considered as completed if less than 3-4 % of the glycol present on the soil is desorbed per hour.

An equilibrium method was introduced by MARTIN (1955), who found that the amount of glycol retained by clays became constant with time, if the desiccator in which the equilibration is established contains a free surface of glycol in addition to anhydrous  $CaCl_2$ . MARTIN, however, did not attempt to relate his data to the specific surface area of the clay.

Following MARTIN's approach, a modification of the method of DYAL and HENDRICKS was introduced by BOWER and GOERTZEN (1959). This modification is based on the principle - following from the relevant theory of BRUNAUER, EMMETT and TELLER (1938) - that monolayer coverage will occur at a certain vapor pressure. For convenience, although rather arbitrarily, these authors selected the vapor pressure of a  $CaCl_2$ -glycol solvate for this purpose.

The method reads as follows:

Amounts of about 0.5 gram of the samples are brought into weighing flasks and dried over  $P_2O_5$ . Then about 1 ml of redistilled ethylene glycol is added and the samples are allowed to stand for at least 24 hours to ensure a complete saturation of the clay. Next the samples are placed in a vacuum desiccator, which is connected with a vacuum pump capable of reducing pressure to 0.05 mm Hg. Also a  $CaCl_2$ -glycol solvate is placed in the desiccator. This solvate is prepared by adding about 100 grams of  $CaCl_2$ , dried at  $210^\circ C$ , to roughly 20 ml of the glycol. Next the desiccator is evacuated. After standing 48 hours under vacuum the samples are weighed periodically at time intervals of about 5-8 hours until two successive weighings agree within a few tenths of a mg. BOWER and GOERTZEN showed that this procedure yields a retention value for Ca-montmorillonite corresponding to the known surface area at the surface coverage suggested by DYAL and HENDRICKS.

The above method was tested on the surface determination of Ca-montmorillonite, Na-montmorillonite and Na-illite. Determinations were executed two times, in triplicate. Results are given in table 8. Although the data within each series agree quite good with each other, fairly large differences are found between the results of the two repeats, except for the Ca-montmorillonite. Moreover, there is found a large difference between the specific surface areas of Ca-montmorillonite and Na-montmorillonite, indicating that the ionic composition of the clay has an important



Table 8. Surface area determination according to the ethylene glycol retention method

	Surface area ( $m^2/gram$ )		
	Ca-montmorillonite	Na-montmorillonite	Na-illite
1)	880	695	251
	876	686	250
	880	685	255
2)	880	723	310
	885	763	329
	906	—	303
mean value	883	710	277

influence on the results of surface-area determinations according to the ethylene glycol retention method.

### 3.6 Materials

The materials involved in the anion adsorption experiments may be divided into two groups, viz. fairly pure clays, and soils. Results on both are discussed in the Chapters 4 and 5, respectively.

#### 3.6.1. Clays

In order to check the theoretical considerations as given in Chapter 2, the anion interaction between chloride, sulfate and phosphate and certain clays was investigated. Clay samples were chosen such that the three main types of clay minerals, viz. montmorillonite, illite and kaolinite, were present at a high degree of purity.

The montmorillonite employed was a bentonite from Osage, Wyoming; in addition a Clayspur montmorillonite was used in one experiment. The illite used was Winsum illite from Groningen, The Netherlands, whereas the kaolinite was Drybranch

Table 9. Cation exchange capacity and mineralogical composition of the clays used

Clay	C.E.C. (me./g clay)	Mineralogical composition <sup>1</sup> in %			
		montmorillonite	illite	kaolinite	quartz
montmorillonite (Osage)	0.95	97	—	—	3
illite (Winsum)	0.46	5—10	80	5	10—5
kaolinite (Drybranch)	0.089	5	—	95	—

<sup>1</sup>) determined by means of X-ray diffraction; the data were kindly supplied by Dr. J. CH. L. FAVEJEE

kaolinite from the U.S.A.. Data on the cation exchange capacity and on the mineralogical composition are given in table 9.

The original clay was suspended in water and the fraction  $< 2\mu$  was collected by syphoning off. Stock suspensions of the clays with homoionic Na composition were prepared in the following way. First the suspension was treated with a HCl solution (pH 2-3) in order to dissolve carbonates, if present. To prevent decomposition of the clay the low pH was maintained for a short time-period only, viz. at the most 10-15 minutes. After adjusting the pH to its original value (with NaOH), the suspension was passed consecutively through columns containing Na-resin and Cl-resin (amberlite). Amounts of resin and contact time between clay and resin were chosen such that a homoionic Na-Cl-composition was ensured (BOLT and FRISSEL, 1960). Ca-clays were prepared from the above Na-clays by repeated treatment with  $\text{CaCl}_2$  solution. Finally an alternating treatment with small amounts of H- and OH-resin was applied to remove salt from the suspensions, followed by readjustment of pH, if necessary. If a specified, mixed ionic composition was required a part of the stock suspension in Ca-form was treated with a precalculated amount of Na-resin according to the method described in the above reference.

### 3.6.2 Soils

In addition to pure clays, samples of 12 different soils of The Netherlands were employed in the anion adsorption studies. The sampling spots of the soils are presented on the map in figure 20 and a short description of each of the soils is given below. For further details the reader is referred to "Soils of the Netherlands" (EDELMAAN, 1950).



Fig. 20. Location of the 12 Dutch soils used in the experiments

1. **STICKY SOIL (Kleeaarde):** A very specific soil, present only at small spots on slopes of hills in Southern Limburg. Its name is based on its extreme sensitivity to tillage, which can be executed successfully only over a small range of moisture contents. The soil material is supposed to be the weathering product of soft lime stone layers from the Senone, usually containing small pieces of flint.

The sample was taken at a depth of 10–20 cm. The color changes from 10 YR 7/4 when dry to 10 YR 5/4 when wetted. The pH(H<sub>2</sub>O) is 7.2, the pH(KCl) 6.4. Clay content about 35 %.

2. **LOESS SOIL:** These soils cover the major part of Southern Limburg and are connected with the extensive loess area of Germany, Belgium and France. The soil material is supposed to be of aeolian origin. As its most pronounced property the constancy of its texture and mineralogical composition over wide-spread areas is mentioned. The textural composition has a very distinct maximum between 2 and 50  $\mu$ .

The sample was taken at a depth of 10–40 cm. The color changes from 10 YR 6/3 when dry to 10 YR 4/4 when wet. The pH(H<sub>2</sub>O) is 6.3, the pH(KCl) 5.6.

3. **WILHELMINAPOLDER SOIL:** The sample was taken in one of the so-called "new-land polders" of Southern Beveland. These polders are characterized by a flat topography and a regular parcelling which is not connected with the forms of the landscape. They are mostly agricultural soils of very high quality. The soil material consists of sea deposits, usually rich in lime. Embankment of these polders was performed at the time that the height of deposition reached the high-water level.

The depth of sampling was 10–30 cm. The color varies from 10 YR 6/3 when dry to 10 YR 4/2 when wet. The pH(H<sub>2</sub>O) is 7.7, the pH(KCl) 7.3. Clay content about 25 %.

4. **OSS SOIL:** This is a sample of a fairly heavy clay deposit of the river Meuse. These river clay soils have been deposited in the pleistocene erosion valley of the Meuse and have a maximum depth of a few metres.

Depth of sampling was 10–30 cm. The color changes from 10 YR 6/3 when dry to 10 YR 4/2 when wet. The pH(H<sub>2</sub>O) is 5.6, the pH(KCl) 4.8. Clay content about 50 %.

5. **RIVER BASIN CLAY SOIL:** The river basin clays are heavy deposits of the rivers Rhine and Meuse and their branches. Their drainage is usually quite poor as they are surrounded by higher levee soils.

The depth of sampling was 5–30 cm. The color varies from 10 YR 4/1 when dry to 10 YR 3/1 when wet. The pH(H<sub>2</sub>O) is 5.4, the pH(KCl) 4.8. Clay content about 50 %.

6. **GRIEND SOIL:** An estuary soil, formed in the fresh water tidal area of the Meuse delta. The subsoil consists of river clay and peat on which in the first stage of the silting up process a layer of coarse river sand is deposited, thus forming fairly extensive sand banks. On these banks reaching a height that they run dry at ebb-tide, a vegetation develops which in turn promotes the silting up until the land becomes sufficiently high to allow the growth of willows. These soils covered with the specific vegetation of chiefly willows are entitled Griend soils. Depth of sampling was 5–15 cm. The color changes from 10 YR 7/2 in the dry state to 10 YR 4/2 when wetted. The pH(H<sub>2</sub>O) is 7.6, the pH(KCl) 7.1. Clay content about 25 %.

7. **MUNNIKELAND SOIL:** This soil is also found as the subsoil of the Griend soils. In this case, however, the old landscape of river clay and peat (in this case river clay) is still on the surface and has not been covered by younger deposits.

Depth of sampling was 10–20 cm. The color varies from 10 YR 7/3 when dry to 10 YR 4/3 when wet. The pH(H<sub>2</sub>O) is 5.9, the pH(KCl) 5.4. Clay content about 25 %.

8. **RANDWIJK SOIL:** A river levee soil of the Rhine, one of the river clay soils characterized by the presence of one or more sandy layers somewhere in the profile.

The depth of sampling was 10–20 cm. The color changes from 10 YR 8/3 when dry to 10 YR 3/3 when wet. The pH(H<sub>2</sub>O) is 7.1, the pH(KCl) 6.4. Clay content about 35 %.

9. **WOLFSWAARD SOIL:** Belongs to the so-called foreland soils which are situated between the riverbed (i.e. Rhine) and the high dikes. The foreland soils are usually flooded a few times a year, the water leaving a thin clay cover of several mm thickness.

The depth of sampling was 10–30 cm. The color varies from 5 Y 6/1 when dry to 5 Y 4/1 when wet. The pH(H<sub>2</sub>O) is 7.4, the pH(KCl) 6.8. Clay content about 40 %.

10. **Y-POLDER SOIL:** These polders are situated along the bay of the Y. Formerly the area consisted chiefly of peat, which has been washed away for the major part. Moreover, dune sand is found in the subsoil, alternating with remnants of the peat. A fairly heavy clay layer, rich in lime, has been deposited on this subsoil of varying composition. These polders form the most fertile part of the Netherlands.

The sample was taken at a depth of 5–15 cm. The color varies from 2.5 Y 6/2 in the dry state to 2.5 Y 4/2 when wetted. The pH(H<sub>2</sub>O) is 7.2, the pH(KCl) 6.7. Clay content about 55 %.

11. **N.O.P. SOIL (North-east polder soil):** The subsoil of this polder has also been peat, covering the pleistocene sand. The peat was washed away over extensive areas. A layer of very fine sand, poor in colloid content (so-called "sloef"), was deposited later. The most recent sediment, forming the surface soil at the sampling spot, consists of a light marine clay, rich in lime.

The depth of sampling was 10–30 cm. The color changes from 5 Y 6/1 when dry to 5 Y 4/2 when wet. The pH(H<sub>2</sub>O) is 7.7, the pH(KCl) 7.3. The clay content is about 20 %.

12. **WINSUM SOIL:** This soil can be compared with the so-called "knip" clay, which is a subrecent sea deposit from brackish sea water. The most striking property of these soils is the high percentage of sodium and magnesium at the adsorption complex, which causes a strong tendency to dispersion.

The sample was taken at a depth of 20–40 cm. The color varies from 5 Y 7/1 when dry to 5 Y 5/1 when wet. The pH(H<sub>2</sub>O) is 7.0, the pH(KCl) 6.2. Clay content about 40 %.

Air-dry aggregates of the above soils with a diameter of 2–4 mm were brought on Büchner filters and percolated with a solution of about 2 normal NaCl to attain a homoionic composition of the adsorption complex. To ensure an over-all wetting of the aggregates and to prevent the enclosure of air bubbles, the samples were completely wetted from below before starting the percolation procedure. In order to dissolve carbonates the first part of the NaCl solution was acidified with HCl to pH 4. The passage of the salt solution was continued until the leachate was free of Ca.

Next a solution of about 50 % ethyl alcohol was used to remove excess salt. The soils were then dried at 105°C, suspended in distilled water and the fraction < 50μ was separated by wet sieving. The anion adsorption experiments were conducted on this sodium saturated fraction < 50 μ.

The textural composition of this fraction was measured by pipetting off parts of the soil suspension at different depths and times, applying Stoke's law. For the measurement of the cation exchange capacity parts of the sodium saturated soil were brought into the Ca form by treatment with CaCl<sub>2</sub> solution. Then the C.E.C. was determined by employment of the isotopic dilution of Ca<sup>45</sup>, using the formula:

$$\text{C.E.C.} = \left( \frac{V_a \cdot A_a^*}{A_e^*} - V_{tot} \right) \cdot n_0^{++} / W$$

in which all symbols have the meaning as described before. If  $n_0^{++}$  represents the

Table 10. Particle size distribution and cation exchange capacity of the fraction < 50 $\mu$  of 12 Dutch soils

Soil	Percentage weight of the separates						C.E.C. ( $\mu\text{e.}/\text{g soil}$ )
	50–20 $\mu$	20–10 $\mu$	10–5 $\mu$	5–2 $\mu$	2–0.5 $\mu$	< 0.5 $\mu$	
1. Sticky soil	17.9	11.0	6.3	10.2	16.4	38.1	147
2. Loess soil	62.2	14.0	3.8	1.7	7.1	11.4	70
3. Wilhelmina polder soil	32.5	9.0	8.2	6.7	16.7	27.2	261
4. Oss soil	4.4	6.5	10.4	13.0	30.2	34.9	217
5. River basin clay soil	6.9	8.8	11.7	11.0	22.4	39.1	514
6. Griend soil	19.9	14.6	14.6	13.4	16.0	21.4	178
7. Munnikeland soil	23.0	15.8	18.3	12.4	16.5	14.0	186
8. Randwijk soil	21.6	14.7	12.2	6.4	18.2	27.5	219
9. Wolfswaard soil	15.4	9.3	11.6	10.3	18.6	35.2	250
10. Y-polder soil	1.9	9.5	10.9	12.7	22.3	42.6	319
11. North-east polder soil	38.7	15.1	10.4	5.1	10.1	20.3	178
12. Winsum soil	28.8	10.4	7.9	5.2	12.1	35.4	228

concentration of Ca in the equilibrium solution in  $\mu\text{e.}/\text{ml}$  the cation exchange capacity is found in  $\mu\text{e.}$  per gram of soil. Results are given in table 10.

## 4 Results on anion interaction with clays

The theoretical considerations and mathematical derivations as presented in Chapter 2 were compared with experimental results. To this purpose several series of experiments were carried out. In order to facilitate the interpretation of the experimental data, a considerable number of these experiments were limited to relatively simple systems, containing only fairly pure clays. The results of these first series are discussed below.

### 4.1 Experiments with montmorillonite

If not stated otherwise, the clay involved in the experiments described in this section was the Osage montmorillonite, total fraction  $< 2\mu$ .

#### 4.1.1 Comparison of the negative adsorption of chloride, as measured by the titration method and by the tracer method

A first test run was designed to check the agreement between the two methods available for the determination of the exclusion volume of chloride. To this purpose all systems were labeled with  $\text{Cl}^{36}$ . In conjunction with the application of the tracer method two standard solutions were also prepared, one at low and one at high activity. At the same time, both suspension and dialyzate were titrated. The combined results of the two methods are given in table 11 and plotted in figure 21.

The slope of the line in this figure indicates that the specific surface area of the montmorillonite used amounts to  $700 \text{ m}^2$  per gram clay. This is an acceptable value for the fraction  $< 2\mu$ .

The agreement between the results of both methods is excellent for most points; however, a small difference exists at the lowest salt level. This discrepancy must be attributed to difficulties with the potentiometric titration at this low concentration. In connection with this it must be kept in mind that the titration values presented result from the difference between two determinations, viz. one in the suspension and one in the dialyzate.

Figure 21 also indicates the absence of a significant influence of the activity level of the standard solutions. Accordingly, the following experiments were carried out

Table 11. The negative adsorption of  $\text{Cl}^-$  by Na-montmorillonite (Osage) as determined by the tracer method and the titration method; duplicates refer to different dialysis bags. ( $f^{++} = 0$ ;  $f^- = 0$ ;  $Q' = 2.000$ )

No.	$N_0$ (me./ml)	$Q'/\sqrt{\beta N_0}$ (Å)	$V_{ex}$ (ml/g clay <sup>1)</sup> )		
			Tracer method		Titration method
			standard low act.	standard high act.	
1	$4.17 \times 10^{-4}$	301	20.34 22.24	19.62 21.54	23.52 24.91
2	$9.50 \times 10^{-4}$	199	13.72 14.67	12.90 13.87	13.23 13.92
3	$1.32 \times 10^{-3}$	169	11.62 11.49	11.97 11.84	11.34 11.90
4	$3.00 \times 10^{-3}$	112	7.19 7.45	7.58 7.84	7.55 7.78
5	$5.71 \times 10^{-3}$	81	4.51 4.54	4.95 4.91	5.32 5.40
6	$1.03 \times 10^{-2}$	61	3.20 3.91	3.63 4.33	3.59 3.99

<sup>1)</sup> volumes of exclusion were calculated from determinations on weight basis assuming a solution density of 1.00 g/ml.

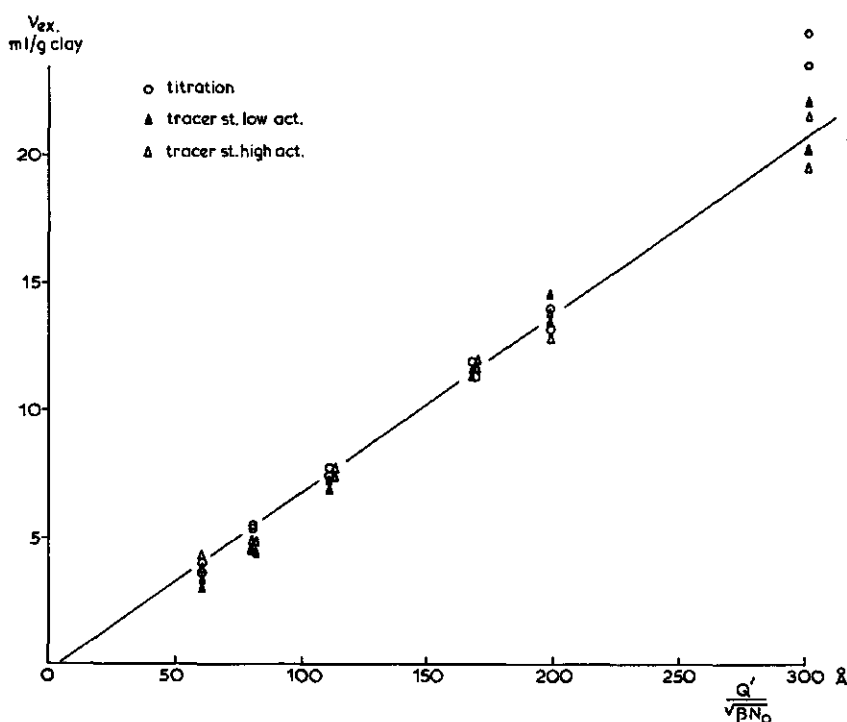


Fig. 21. Comparison between the results of chloride exclusion by Na-montmorillonite as measured according to the titration method and the tracer method

at one activity level only. To ensure maximum accuracy the activity levels of unknowns and standards were always made to be roughly the same.

#### 4.1.2 The negative adsorption of chloride in mixed cationic systems

As was discussed in Chapter 2 the cationic composition of the system will influence the negative adsorption of anions to a great extent. This influence is related to the extent of the diffuse electric double layer. At a given electrolyte level the valency of the cations appears to be a dominant factor in this respect.

These effects were investigated in an experiment comprising three series of systems with chloride (labeled with  $\text{Cl}^{36}$ ) as the anion. In series I a homoionic Na-clay was used, in series III a homoionic Ca-clay, whereas in series II the composition of the clay complex was 50% Na and 50% Ca. The specified ionic composition was maintained in all points of series II. This was achieved by the addition of salt solutions during the preparation of the systems in such a manner that the reduced activity ratio of the cations remained constant (cf equation 1.1). Thus the ionic composition of each system had a known value, allowing the evaluation of  $Q'$  values according to figure 2.

The results are given in table 12. The mean values of the duplicate measurements are presented graphically in figure 22. It is seen that all points are scattered around the line of  $700 \text{ m}^2/\text{gram}$  (within experimental error), indicating that the anion is behaving in accordance with theoretical expectations.

Table 12. The negative adsorption of  $\text{Cl}^-$  by I: Na-montmorillonite (Osage); II: Na-Ca-montmorillonite; III: Ca-montmorillonite. Characterization of the systems:  $f^- = 0$ ;  $f^+ = 0$

No.	$N_0$ (me./ml)				$Q'/\sqrt{\beta N_0}$ (Å)			$V_{\infty}$ (ml/g clay)		
	I ( $f^{++} = 0$ )	II	$f^{++}$	III ( $f^{++} = 1$ )	I	II	III	I	II	III
1	$6.78 \times 10^{-4}$	$7.01 \times 10^{-4}$	< 0.000	$6.91 \times 10^{-4}$	236	232	121	15.83 15.79	16.21 16.08	7.91 7.73
2	$1.01 \times 10^{-3}$	$1.08 \times 10^{-3}$	< 0.000	$1.13 \times 10^{-3}$	193	187	95	13.17 13.14	12.63 12.34	6.10 6.15
3	$1.40 \times 10^{-3}$	$1.52 \times 10^{-3}$	0.001	$1.36 \times 10^{-3}$	164	157	86	11.36 11.28	11.46 10.97	5.48 5.39
4	$2.23 \times 10^{-3}$	$2.35 \times 10^{-3}$	0.005	$2.40 \times 10^{-3}$	130	121	65	8.70 8.40	8.61 8.22	3.92 4.03
5	$3.85 \times 10^{-3}$	$3.72 \times 10^{-3}$	0.009	$3.88 \times 10^{-3}$	99	94	51	6.84 6.75	6.44 6.40	3.20 3.14
6	$1.20 \times 10^{-3}$	$1.11 \times 10^{-3}$	0.022	$1.30 \times 10^{-3}$	56	52	28	3.49 3.53	4.06 3.53	1.46 1.57

The dotted line of figure 22 stands for the calculated chloride exclusion of the Ca-montmorillonite, based on a specific surface area of  $700 \text{ m}^2/\text{g}$ . This line runs parallel to the one for Na systems at a



distance of 2 Å, because of the difference between the  $\delta$  values for Na- and Ca-montmorillonite systems. The line for Na-Ca-montmorillonite should lie in between the dotted and the solid lines but is not shown for practical reasons. It is noted that the points of series III (Ca-system) are slightly below the Ca-line. Since the deviation is still within experimental error it does not seem warranted to draw conclusions herefrom at this stage of the experiments.

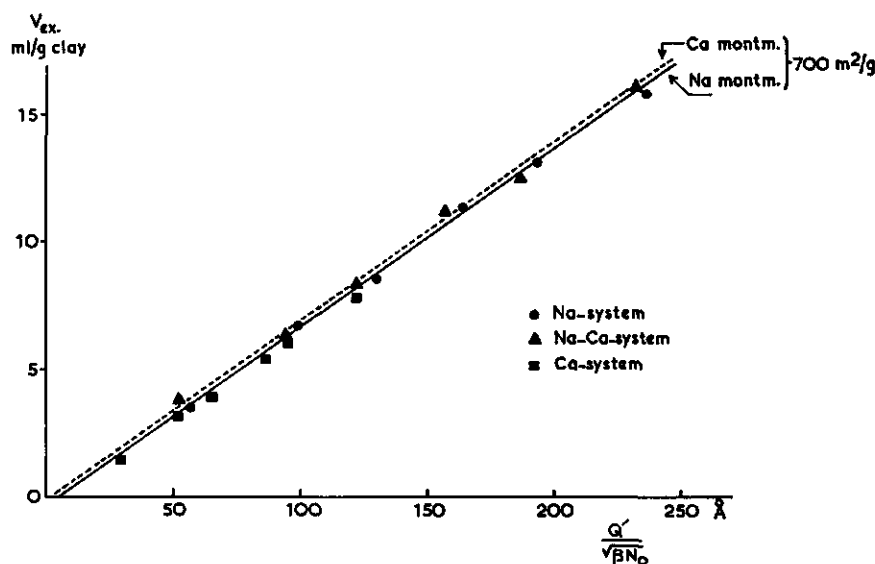


Fig. 22. The exclusion of chloride in mixed cationic montmorillonite systems

BOLT and WARKENTIN (1956) have also described data on the negative chloride adsorption by a Na- and a Ca-bentonite. They plotted the measured values of the exclusion volume against  $2/v^+ \sqrt{\beta N_0}$ , with  $v^+$  = valency of the dominant cation in the system. When presented in this way, different lines are found for the Na and the Ca samples. If, however, as calculated from the experimental data tabulated by the above authors, a plot is made of the  $V_{ex}$  values as a function of  $Q'/\sqrt{\beta N_0}$  ( $Q'$  being 2.000 in the Na case and 1.035 in the Ca case) the points of both systems again follow roughly the same line; two Ca-points at high salt level show a small deficit in  $V_{ex}$ .

The above observations contradict the findings of EDWARDS and QUIRK (1962), who recorded a considerable decrease of the chloride repulsion by Ca-montmorillonite as compared to the exclusion by the same clay when used in the Na form. This was interpreted as the result of condensation of clay crystals to larger units. It must be concluded that the montmorillonite as used in the present experiment did not indicate such a "plate-condensation", at least not at a significant degree (cf also section 4.1.6). The fact that centrifugation during preparation was avoided in these experiments – in contrast to the procedure used by EDWARDS and QUIRK – may perhaps explain the observed difference in behavior.

#### 4.1.3 Simultaneous determination of the adsorption of $\text{Cl}^-$ and $\text{SO}_4^{2-}$ in Na-systems

In this experiment the adsorption of the mono- and divalent anion were determined simultaneously, applying the titration method for chloride and the tracer method for sulfate. Appropriate salt levels and ionic compositions of the systems were acquired by additions of different amounts of both NaCl and  $\text{Na}_2\text{SO}_4$  solutions. Values for  $f^-$  varied from 0.05 to 0.99. The results are presented in table 13 and figure 23.

Table 13. The negative adsorption of  $\text{Cl}^-$  and  $\text{SO}_4^{2-}$  by Na-montmorillonite (Osage) ( $f^{++} = 0$ ;  $f^{\equiv} = 0$ )

No.	$N_0(\text{me./ml})$	$f^-$	$Q'$	$Q''$	$Q'/\sqrt{\beta N_0} (\text{\AA})$	$Q''/\sqrt{\beta N_0} (\text{\AA})$	$V_{\infty}(\text{ml/g clay})$	
							$\text{Cl}^-$	$\text{SO}_4^{2-}$
1	$4.30 \times 10^{-4}$	0.58	1.91	2.53	283	374	20.35	-29.90
2	$8.25 \times 10^{-4}$	0.99		2.45		262	20.51	-24.81
3	$1.25 \times 10^{-3}$	0.60		2.53		220		17.89
4	$2.75 \times 10^{-3}$	0.30	1.95	2.59	114	152	7.07	17.45
5	$4.82 \times 10^{-3}$	0.13		2.63		117	7.53	14.69
6	$1.00 \times 10^{-2}$	0.05	1.99	2.66	61	82	3.89	15.97
							3.90	10.16
								10.28
								8.25
								8.64
								8.27
								6.61

Again a good agreement is found, except for sulfate point no 1 (lowest salt level, not plotted in figure 23). The situation of the points with respect to the  $700 \text{ m}^2/\text{gram}$  line indicates that both  $\text{Cl}^-$  and  $\text{SO}_4^{2-}$  are excluded in accordance with theoretical expectations, at least in the range plotted. The small discrepancy of sulfate point no 6 is attributed to the high electrolyte level of the system involved. This may influence the accuracy of the activity determinations. Since the salt concentration of the system represented by this point lies in the range where self-absorption of  $\text{S}^{35}$  begins to play an important role, even a small difference between the electrolyte levels of standard solution and dialyzate could cause a considerable error in the final result.

Sulfate point no 1 (cf table 13) shows a considerable deviation from the line, viz. an inclusion volume of about 27 ml per gram clay. This thus means the appearance of positive sulfate adsorption. It is understandable that positive adsorption enters in here, because in this system the total amount of sulfate present was small in comparison to the anion adsorption capacity of the clay. To substantiate this supposition the positive sulfate adsorption was investigated in a separate experiment.

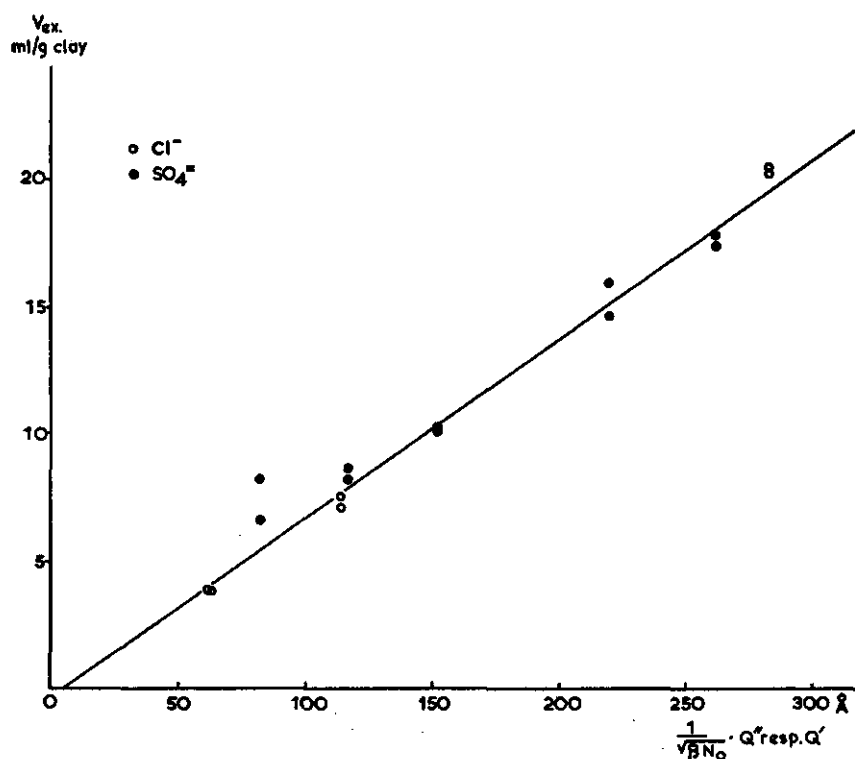


Fig. 23. Simultaneously measured exclusion of chloride and sulfate by Na-montmorillonite

#### 4.1.4 The positive adsorption of sulfate at low concentration level

A series of systems was prepared in which the total electrolyte level was maintained at a value of about  $4 \times 10^{-4}$  normal, using labeled  $\text{SO}_4^{2-}$  at concentration levels varying between "carrier free" and  $4 \times 10^{-4}$  normal. The major part of the experiment was done with Na-clay; also a limited number of points were determined in Na-Ca systems. The results are given in table 14 and are plotted, together with the

Table 14. The positive adsorption of  $\text{SO}_4^{2-}$  by montmorillonite (Osage). The data represent the mean value of two dialysis bags

No.	System	pH	$N_0(\text{me./ml})$	$f^-$	$Q''$	$Q''/\sqrt{\beta N_0}(A)$	$V_{ex}(\text{ml/g clay})$
1	Na	6.30	$4.3 \times 10^{-4}$	0.58	2.53	374	-27.4
2	Na	6.25	$4.1 \times 10^{-4}$	0.53	2.55	384	-21.6
3	Na	6.15	$4.2 \times 10^{-4}$	0.70	2.50	375	-8.5
4	Na	6.20	$4.2 \times 10^{-4}$	0.99	2.45	367	+7.4
	Na-Ca	6.15	$2.8 \times 10^{-4}$	$0(f^{++} = 0.006)$	2.66	491	-34.2
	Na	6.30	$2.6 \times 10^{-4}$	0	2.67	505	-34.1
	Na	6.20	$2.5 \times 10^{-4}$	0	2.67	530	-36.7

mean values of the sulfate data of table 13, in figure 24. This figure shows that indeed positive sulfate adsorption becomes apparent at very low sulfate levels. From these data one may estimate the amount of positively adsorbed sulfate by multiplying the "deficit" in  $V_{ex}$  - as compared to the negative adsorption line found from the chloride measurements - with the actual sulfate concentration. Using all data presented it

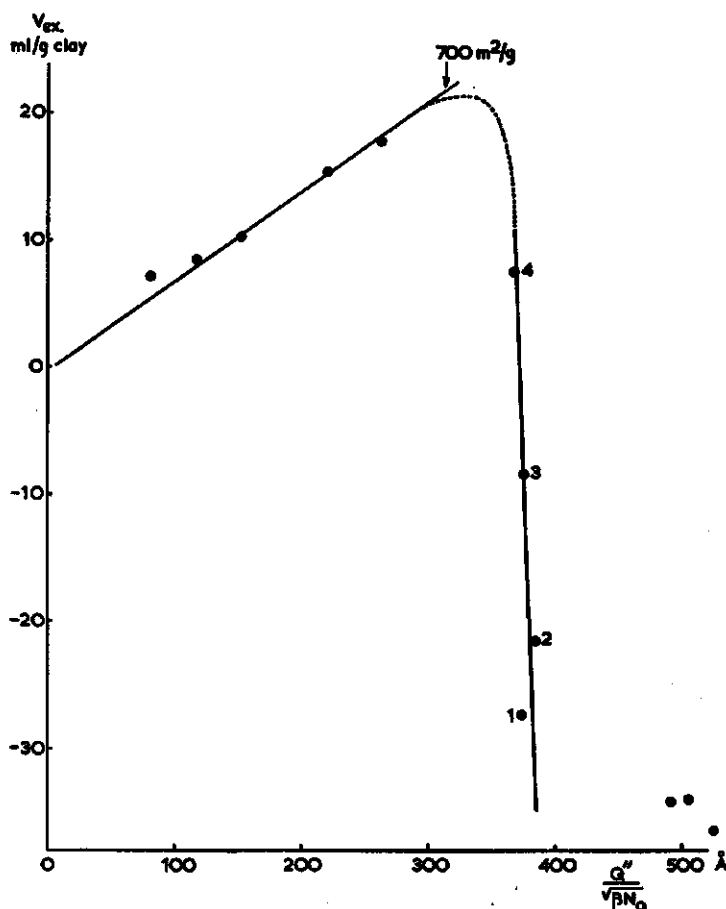


Fig. 24. The positive adsorption of sulfate on Na-montmorillonite at low sulfate concentrations

would seem that the positive adsorption is less than about  $10^{-3}$  me. per gram clay, point no 2 of table 13 still being on the line within a 1 ml range. Applying the same approach to the data of table 11 one finds that the positive adsorption of chloride in the absence of sulfate is also less than about  $10^{-3}$  me. per gram clay. In the presence of  $SO_4^{2-}$ , the positive adsorption of chloride, if present at all, was even less than  $0.4 \times 10^{-3}$  me. per gram clay (cf point no 1 of table 13). This suppression is logical because a divalent anion will compete quite strongly with the monovalent chloride.

Although the above data are insufficient to give precise numbers about positive adsorption, it may be concluded that the clay exhibits indeed a small positive adsorption of sulfate. This can be detected only provided the total amount of sulfate present per gram clay is small. Thus for low suspension concentrations the determination of sulfate adsorption is greatly facilitated by the use of radioisotopes.

Although the same would appear to hold for the detection of positive chloride adsorption, in practice this is not so. In fact the specific activity of  $\text{Cl}^{36}$  as obtained from commercial sources is so low, that relatively large additions of "cold" chloride in the labeling solution are necessary to yield a reasonable count rate of the samples. As a result the chloride concentration becomes then too high to render the detection of positive chloride adsorption possible, if present.

#### 4.1.5 The influence of phosphate on the positive adsorption of sulfate

In section 4.1.4 the competition between sulfate and chloride with respect to positive adsorption of these anions on clays was mentioned already. It seems evident that under comparable conditions the sulfate adsorption will exceed that of chloride. If the adsorption process is of the electrostatic type, the relative amounts adsorbed can be expected to be a function of the reduced ratio of the activities of the ions in solution. Thus in that case a preference of sulfate above chloride should be expected due to the difference in valency and size of these ions. If chemi-sorption prevails, a preference should be expected for that anion which fits best into the clay lattice, as will be determined by the ionic structure. Therefore one should expect a preference of sulfate above chloride also in case of the occurrence of chemi-sorption, both the ionic structure and size of the sulfate ion being much more alike the  $\text{SiO}_4$  groups in the clay. Thus, regardless of the adsorption mechanism involved, it seems likely that sulfate will be preferred above chloride.

Extending this line of thought to the phosphate ion one may reason that in the case of electrostatic adsorption there should be a preference of sulfate above phosphate

Table 15. The influence of phosphate on the positive adsorption of sulfate (Na-montmorillonite, Osage)

No.	pH	$\text{Na}_2\text{PO}_4$ conc. (me./ml)	$N_0$ (me./ml)	$1/\sqrt{\beta N_0}$ (Å)	$Q''/\sqrt{\beta N_0}$ (Å)	$V_{22} \text{SO}_4^{2-}$ (ml/g clay)
1	6.40	—	$4.68 \times 10^{-4}$	142	380	—28.04 —28.10 —28.16
2	6.35	$10^{-7}$	$4.75 \times 10^{-4}$	141	378	—20.13 —19.81 —19.49
3	6.40	$10^{-6}$	$4.61 \times 10^{-4}$	143	382	12.14 12.23 12.32
4	6.20	$10^{-5}$	$4.75 \times 10^{-4}$	141	378	26.80 26.20 25.59
5	6.25	$10^{-4}$	$4.81 \times 10^{-4}$	140	374	26.39 26.10 25.81
6	6.52	$2 \times 10^{-4}$	$6.34 \times 10^{-4}$	122	322	22.18 22.24 22.29

since the size of the phosphate ion is larger and the valency equal to or lower (at intermediate pH values) than that of sulfate. As regards chemi-sorption, it appears difficult to make a prediction about the preference on the basis of size and structure alone.

In view of the above it was investigated at which concentration level phosphate is able to compete with sulfate and suppress its positive adsorption by the clay. To this purpose the sulfate adsorption at a concentration of about  $10^{-6}$  N was measured at increasing additions of phosphate, corresponding to 0,  $10^{-7}$ ,  $10^{-6}$ ,  $10^{-5}$ ,  $10^{-4}$  and  $2 \times 10^{-4}$  N, as  $\text{Na}_3\text{PO}_4$ . Results are given in table 15 and plotted

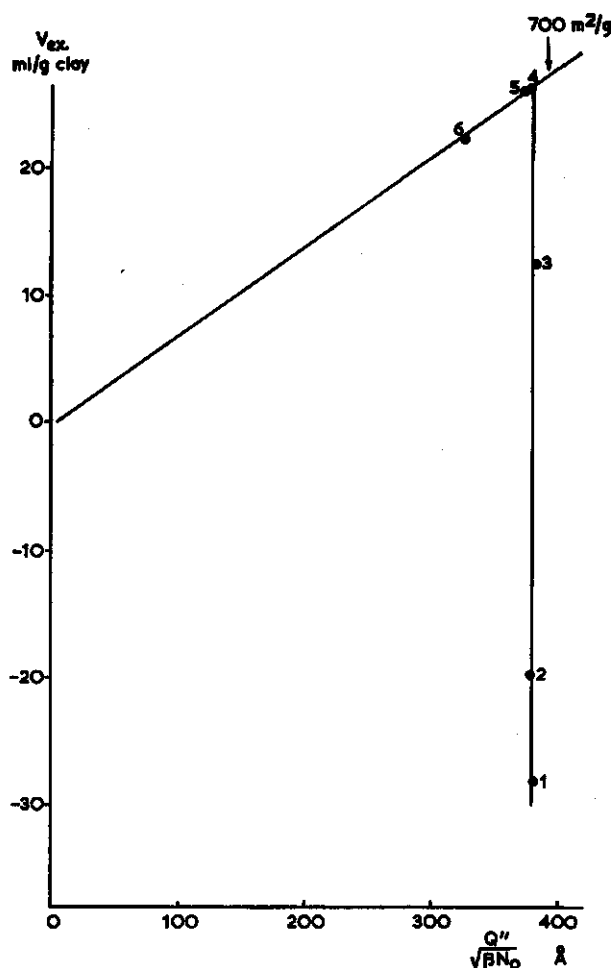


Fig. 25. The influence of phosphate on the positive adsorption of sulfate

in figure 25. It is seen that the lowest phosphate addition decreases the inclusion volume of sulfate with roughly 8 ml (about one quarter), indicating that at least 80 % of the added phosphate had been used for replacement of sulfate at the clay. At

a level of  $10^{-6}$  N phosphate one finds sulfate to be negatively adsorbed, but the point (no 3 of figure 25) is below the  $700 \text{ m}^2/\text{g}$  line, indicating that in fact a positive sulfate adsorption still prevails. The depression of sulfate adsorption in comparison to the adsorption at zero phosphate treatment amounts to 80 % in this case. At  $10^{-5}$  N phosphate, sulfate is excluded in accordance with theory.

Although the above data are certainly not conclusive for a quantitative approach (e.g. the sulfate concentration is an uncertain factor, since small amounts of sulfate may be present in the clay in excess of the added amount) one may attempt to estimate the preference of phosphate above sulfate. Expressing amounts adsorbed and in solution in mols, one finds that phosphate is preferentially adsorbed above sulfate with a factor of roughly 5. This is so notwithstanding the fact that at the pH values measured (cf table 15) phosphate is present for about 50 % as a monovalent anion. In view of the considerations presented at the beginning of this section this allows the conclusion that the phosphate adsorption should probably be looked upon as a reaction of the chemi-sorption type.

As to the likelihood of chemi-sorption of sulfate, it is mentioned that the high solubility of aluminum sulfate suggests that chemi-sorption of sulfate on the clay is less likely; in contrast, aluminum phosphate is much less soluble. Of course this difference in solubility must be ascribed again to differences in the ionic structure and size of both ions. It may thus be concluded that the adsorption of sulfate is probably limited to an electrostatic attraction between sulfate ions and positively charged spots on the clay, whereas the phosphate adsorption should definitely be considered as a chemi-sorption process, at least in part.

Aside from the above considerations, the present experiment shows that very low concentrations of phosphate are sufficient to prevent positive sulfate adsorption.

#### 4.1.6 Simultaneous determination of the adsorption of $\text{Cl}^-$ and $\text{SO}_4^{2-}$ at different degrees of Ca saturation of the clay

This experiment was set up to check the applicability of the derived equations for mixed ionic systems, containing both mono- and divalent cations and anions. In series I a clay was used with a composition of 80 % Ca and 20 % Na at the adsorption complex. By means of additions of NaCl,  $\text{CaCl}_2$  and  $\text{Na}_2\text{SO}_4$  solutions (the last tagged with  $\text{S}^{35}$ ) a series of 7 systems was prepared with different  $f^{++}$  and  $f^-$  values. Again the composition of the clay complex was kept constant throughout the series, by adding the salt solutions while maintaining a constant reduced activity ratio. The clay used in series II was a 100 % Ca clay. In this case various salt levels and values for  $f^-$  were obtained by additions of  $\text{CaCl}_2$  and  $\text{CaSO}_4$  solutions. Results are shown in table 16 and figure 26.

The  $\text{Cl}^-$  points at the lower electrolyte levels are consistent with previous experience, but at the higher concentrations a small deficit of  $V_{\text{ex}}$  is apparent. All sulfate points (and also chloride points at high salt concentrations) show a considerable deviation

from the 700 m<sup>2</sup>/g line. This discrepancy is not attributed to positive anion adsorption, since values for positive adsorption would then be much too high in view of the Na systems studied. The results seem more likely to be indicative for the effect of coagulation of the clay.

In interpreting the above data it should be remembered that the degree of coagulation of a clay depends on at least two factors, viz. the electrolyte concentration of the equilibrium solution and the composition of the adsorption complex (KOENIGS, 1961). Both an increasing electrolyte level and increasing Ca saturation tend to diminish the expansion of the electric double layer, thus facilitating a contact between the

Table 16. Simultaneous determination of the negative adsorption of Cl<sup>-</sup> and SO<sub>4</sub><sup>2-</sup> in systems with different cationic composition. (Osage montmorillonite) Series I: 80 % Ca on the adsorption complex; Series II: 100 % Ca on the adsorption complex

No.	N <sub>0</sub> (me./ml)	f <sup>++</sup>	f <sup>-</sup>	Q'	Q''	Q'/√βN <sub>0</sub> (A)	Q''/√βN <sub>0</sub> (A)	V <sub>∞</sub> (ml/g clay)		
								measured		
								Cl <sup>-</sup>	SO <sub>4</sub> <sup>2-</sup>	SO <sub>4</sub> <sup>2-</sup>
I.1	8.64 × 10 <sup>-4</sup>	0.02	0	1.796	2.461	187	258	13.2	14.2	> 12.4
.2	1.30 × 10 <sup>-3</sup>	0.03	0.98		2.220		190		11.4	> 10.5
.3	2.32 × 10 <sup>-3</sup>	0.06	0.49	1.640	2.234	104	142	7.2	7.4	> 6.8
.4	4.44 × 10 <sup>-3</sup>	0.11	0.47	1.527	2.121	70	98	5.0	3.6	> 4.6
.5	9.75 × 10 <sup>-3</sup>	0.20	0.44	1.400	1.980	45	63	2.2	2.2	2.2
.6	1.24 × 10 <sup>-2</sup>	0.24	0.43	1.372	1.952	38	54	1.9	1.3	1.9
.7	2.66 × 10 <sup>-2</sup>	0.39	0.38	1.273	1.810	24	35	1.0	0.9	1.0
II.1	6.44 × 10 <sup>-4</sup>	1.00	0.47	1.005	1.460	122	177	8.6	8.1	> 8.0
.2	1.01 × 10 <sup>-3</sup>	1.00	0.46	1.005	1.461	98	142	6.7	5.8	> 6.4
.3	1.72 × 10 <sup>-3</sup>	1.00	0.53	1.002	1.458	74	108	4.6	4.1	> 4.8
.4	3.20 × 10 <sup>-3</sup>	1.00	0.62	0.999	1.446	54	79	2.6	1.9	2.5
.5	6.01 × 10 <sup>-3</sup>	1.00	0.37	1.011	1.473	40	58	1.4	1.0	1.2
.6	1.30 × 10 <sup>-2</sup>	1.00	0.17	1.025	1.489	28	41	0.8	0.6	0.8

positively charged edges and the negatively charged planar sides of the clay particles. As a result one may then expect the formation of larger units, consisting of two or more elementary particles attached to each other. Since the negatively charged surface with freely expanded double layers decreases upon coagulation the negative adsorption must become progressively lower with increasing coagulation. The distance of exclusion of divalent anions being larger than that of monovalent anions under comparable conditions, one may visualize that there should be a stage of coagulation at which the repulsion of divalent anions is being depressed already, whereas the monovalent anion is still excluded to the same degree as in the absence of coagulation. It would thus seem that the observed decrease of negative adsorption is caused again by the interaction of double layers. In contrast with highly concentrated suspensions of a dispersed colloid, in which the elementary particles are supposed to be surrounded by a water layer of roughly the same thickness, the coagulation type of interaction is hardly open for a quantitative approach, since in this case the



suspension should be considered to be inhomogeneous with larger units of clay particles of different magnitude occurring at irregular spacings. This renders the estimate of the degree of interaction from the suspension properties (clay content, specific surface area and electrolyte level) impossible.

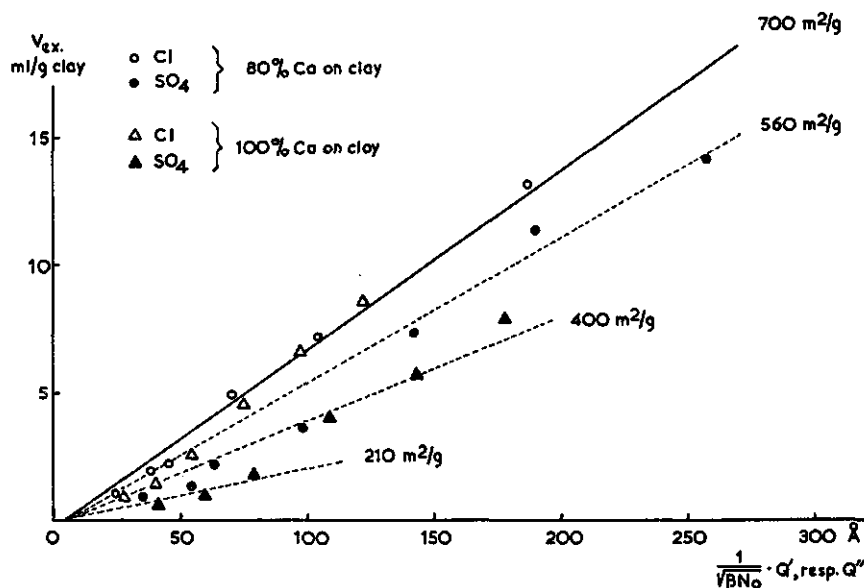


Fig. 26. Simultaneously measured exclusion of chloride and sulfate by montmorillonite at different cationic compositions

On the other hand one may attempt to estimate from experimental data the equivalent degree of interaction, according to figures 9 and 10.

Considering the data of this experiment qualitatively, it is found that the  $\text{Cl}^-$  points 1, 3 and 4 of the 80 % Ca clay (2 has not been determined because of the low chloride level) and the  $\text{Cl}^-$  points 1, 2 and 3 of the 100 % Ca clay are on the 700  $\text{m}^2/\text{g}$  line, indicating that for both clays chloride is behaving as expected, as long as the electrolyte level is not higher than about  $4.5 \times 10^{-3}$  N for the 80 % Ca clay and about  $2 \times 10^{-3}$  N for the 100 % Ca clay. In view of the above given reasons for coagulation it is reasonable that the maximum permissible electrolyte level to prevent deviations from the negative adsorption line is lower in the homoionic Ca-case than for the specified composition of 80 % Ca and 20 % Na on the clay.

The sulfate points 1, 2 and 3 of the 80 % Ca system come roughly to the same line as the chloride points 5, 6 and 7 of the 80 % Ca system and chloride point 4 of the 100 % Ca case, which line indicates a specific surface area of 560  $\text{m}^2/\text{g}$  (equal to a decrease in the negative adsorption of 20 %). Thus sulfate in the 80 % Ca system up to a salt level of about  $2.3 \times 10^{-3}$  N shows approximately the same reduction as chloride in the same system at concentrations of about  $2.5 \times 10^{-3}$  N and as chloride in the 100 % Ca system at a salt concentration of about  $3.2 \times 10^{-3}$  N.

The line of 400  $\text{m}^2/\text{g}$  in figure 26 indicates that the decrease (45 %) for sulfate in the mixed cationic

system up to electrolyte levels of  $2.7 \times 10^{-3}$  N is roughly the same as that for sulfate in the homoionic Ca systems up to levels of  $1.7 \times 10^{-3}$  N and that for chloride in this system up to electrolyte levels of  $1.3 \times 10^{-3}$  N. Finally the 100 % Ca system shows a decrease for sulfate of 70 % at salt concentrations of  $3.2 \times 10^{-3}$  to  $1.3 \times 10^{-3}$  N (sulfate points 4, 5 and 6 of series II on the 210 m<sup>2</sup>/g line).

An attempt to a semi-quantitative approach leads to the following considerations. The depression of  $V_{ex}$  of the chloride ions may be calculated for each system and expressed as the ratio between the measured  $V_{ex}$  value and the theoretically expected  $V_{ex}$  value for the system involved. This ratio should equal  $Q'_i/Q'_a$  values as described in section 2.1.4. According to figure 9 one may then calculate the equivalent thickness of the water layer. With regard to the chloride points without deviation one must conclude that this thickness is at least about 1.5 times the theoretical distance of exclusion. Accepting these minimum values for the water layer thickness, one may compute the expected values of  $V_{ex}$  for the sulfate ions; these are presented in the last column of table 16. A comparison between the measured and the calculated values in this table shows a fairly good agreement, indicating that the influence of coagulation on the negative adsorption of sulfate relative to that of chloride could be interpreted in this manner.

In evaluating the above approach it should be kept in mind that the accuracy of the determinations constituted a limiting factor, especially in the range of high electrolyte levels; a volume of exclusion of 1.3 ml per gram clay corresponds to only about 2 per cent of the total volume.

The formation of larger clay units upon coagulation can take place in different ways, viz. according to a condensation mechanism and a flocculation mechanism. If the first mentioned mechanism occurs, the clay plates are supposedly being bonded together in parallel position at fairly close distance, thus forming more or less layered chains of platelets (KOENIGS, 1961). On the other hand, a so-called cardhouse flocculation (VAN OLPHEN, 1951,) with the platelets not in parallel position with respect to each other but situated in all crossing planes, may prevail if an edge penetration may occur at any place at the planar side of the clay plate. Experimental evidence indicates that this type of flocculation will be met especially at high electrolyte level and/or a high degree of Ca saturation of the clay.

If the condensation type prevails, part of the clay surface is hardly available for anion repulsion, which would lead to a lower specific surface area as measured according to negative adsorption data. The  $\text{Cl}^-$  and  $\text{SO}_4^{2-}$  points should then be expected to come to this same line of smaller specific surface area. According to the above data, however, one finds the chloride and sulfate points at different lines, indicating that presumably the coagulation is predominantly of the cardhouse flocculation type in the systems studied. This was substantiated by the observation that the systems 1-6 of series II showed a gradual decrease of the flocculation volume from about 90 to about 50 ml per gram clay, if the suspensions were allowed to stand for two days.

#### 4.1.7 The adsorption of phosphate on montmorillonite

##### 4.1.7.1 General considerations

When studying the behavior of phosphate ions in contact with soil colloids, a difficulty arises with respect to the interpretation of the experimental data. The presence of phosphate as mono-, di- or trivalent anions depends strongly on the pH of the system (cf figure 16) and in most cases a mixture of the three, or at least two species occurs. This makes a plot of the measured values of the exclusion volume versus the distance of exclusion for each anion of different valency (as has been used in the foregoing sections) impossible, since one cannot distinguish between the different species by means of  $P^{32}$ . Therefore another method of interpretation was applied, which may be described briefly in the following way.

From the count rates of the standard solutions one may calculate the activity of the labeling solution and thus the total activity added to each system. Since the montmorillonite used did not contain any phosphate (at least not in a detectable amount) the total amount of P present in each system was known from the additions of phosphate solutions, and thus the specific activity of phosphate had a known value. This then means that the phosphate concentration of the equilibrium solution, expressed in  $\mu\text{g P/ml}$ , can be found in this case from this specific activity and the count rates of the dialyzates. A multiplication of the difference between the actual and the apparent volume with the equilibrium concentration results in a value for the over-all adsorption of phosphate, expressed as  $\mu\text{g P/g clay}$ . This over-all adsorption may be positive or negative, depending again on whether a volume of inclusion or exclusion, respectively, is found.

From the pH one finds the distribution of total P over  $\text{H}_2\text{PO}_4^-$ ,  $\text{HPO}_4^{2-}$  and  $\text{PO}_4^{3-}$ , which allows the calculation of  $f$  values, provided  $N_0$  is known. In these  $f$  values also other ions present in the system are incorporated. Then the  $Q$  values are found, which allow the calculation of the theoretical value for the volume of exclusion for the mono-, di- and trivalent phosphate anion, using the established value of  $700 \text{ m}^2/\text{g}$  for the specific surface area of the clay. Multiplication of each of these exclusion volumes with the corresponding phosphate concentration in the dialyzate yields the amount of each species, expected to be excluded per gram clay. The total theoretical negative adsorption,  $\gamma^-$ , in  $\mu\text{g P}$  per gram clay, is then found as the summation of the values for the different species.

The difference between the theoretically expected value, and the measured value, of  $\gamma^-$  then equals the actual amount of phosphate positively adsorbed. Expressed again in  $\mu\text{g P/g clay}$  this quantity is indicated as "net positive adsorption" in tables 17 and following. The expression "net adsorption" was chosen to indicate that the observed adsorption (either positive or negative) was corrected for the anion exclusion.

#### 4.1.7.2 Simultaneous determination of the adsorption of chloride and phosphate on Na-montmorillonite

In this experiment the adsorption of chloride and phosphate was measured simultaneously in 3 series of systems, the total electrolyte concentration gradually increasing within each series. In series *A* the phosphate concentration was kept roughly constant at a value of  $5 \times 10^{-4}$  N by additions of precalculated amounts of a  $\text{Na}_3\text{PO}_4$  solution. In series *B* the chloride concentration was kept constant and low, the phosphate concentration increasing. Series *C* was set up such that the electrolyte level gradually increased, part of the salt being chloride and part phosphate. The experimental results are given in table 17.

Comparing the measured  $V_{ex}$  values of chloride with the theoretically expected values for the monovalent anions (given in table 17 for  $\text{H}_2\text{PO}_4^-$ ), it is seen that chloride is negatively adsorbed again in accordance with expectations. Because of the low chloride level of series *B*, values for  $V_{ex}$  of  $\text{Cl}^-$  have not been determined in this series.

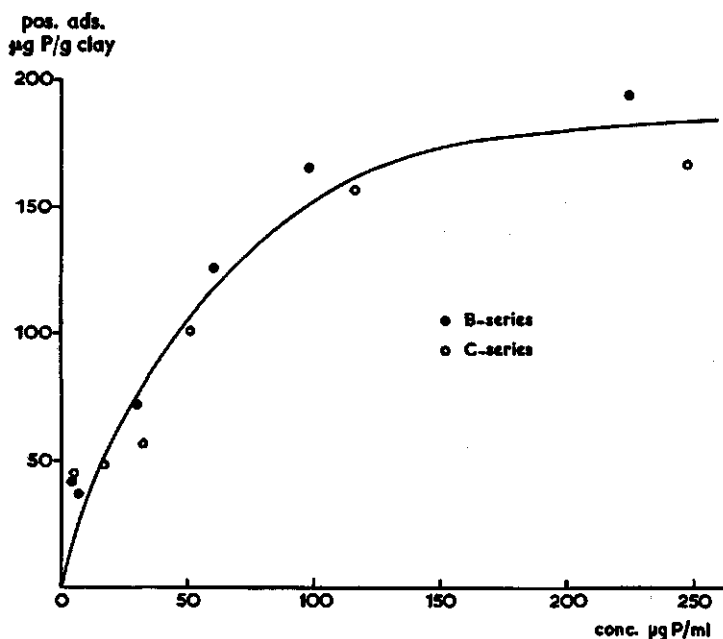


Fig. 27. Phosphate adsorption isotherm for montmorillonite (net adsorption plotted against concentration in equilibrium solution)

The phosphate data of series *B* and *C* show a gradual increase of the net P adsorption with increasing phosphate concentration. Figure 27 represents an adsorption isotherm in which the "net adsorption" is plotted as a function of the concentration in solution. For an analysis of this adsorption isotherm reference is made to section 4.4.

Table 17. Simultaneous determination of the adsorption of chloride and phosphate by Na-montmorillonite (Oso Series A: Phosphate concentration constant (low), chloride concentration increasing; Series B: Chloride concen

No.	pH	$N_0$ (me./ml)	P conc. in eq. sol. ( $\mu\text{g P/ml}$ )	$1/\sqrt{\beta N_0}$ ( $\text{\AA}$ )	$f^-$	$f^+$	$f^{\equiv}$	$d^-$	$d^+$ ( $\text{\AA}$ )	$d^{\equiv}$
A.1	6.85	$6.48 \times 10^{-4}$	4.5	121	0.87	0.13	—	240	319	366
.2	6.61	$8.38 \times 10^{-4}$	4.2	106	0.93	0.07	—	211	282	323
.3	6.90	$2.70 \times 10^{-3}$	3.6	59	0.97	0.03	—	118	157	181
.4	6.75	$5.67 \times 10^{-3}$	3.2	41	1.0	—	—	82	109	126
.5	7.10	$9.60 \times 10^{-3}$	3.1	31	1.0	—	—	62	83	95
.6	7.22	$1.86 \times 10^{-2}$	2.8	22	1.0	—	—	44	59	68
B.1	6.63	$7.00 \times 10^{-4}$	4.4	116	0.92	0.08	—	231	308	353
.2	6.80	$8.02 \times 10^{-4}$	6.8	108	0.84	0.16	—	214	284	325
.3	9.00	$2.15 \times 10^{-3}$	29.9	66	—	1.0	—	123	162	185
.4	10.05	$4.40 \times 10^{-3}$	59.6	46	—	0.08	0.92	83	108	123
.5	10.68	$7.52 \times 10^{-3}$	97.6	35	—	—	1.0	63	82	93
.6	11.20	$1.65 \times 10^{-2}$	224.0	23	—	—	1.0	40	53	60
C.1	6.65	$8.45 \times 10^{-4}$	5.4	104	0.92	0.08	—	207	276	317
.2	7.82	$2.52 \times 10^{-3}$	17.1	62	0.65	0.35	—	121	160	183
.3	9.12	$4.95 \times 10^{-3}$	32.1	44	0.56	0.38	0.06	85	113	129
.4	9.88	$8.03 \times 10^{-3}$	50.6	34	0.45	0.15	0.40	64	84	96
.5	10.62	$1.72 \times 10^{-2}$	115.5	23	0.35	0.03	0.62	43	56	64
.6	11.20	$3.90 \times 10^{-2}$	247.6	16	0.38	—	0.62	30	39	44

The results of series A in table 17 show a volume of exclusion of about 9 ml per gram clay at low salt level to about — 30 ml at high concentration, the net positive adsorption of P varying from about 41 to 97  $\mu\text{g P}$  per gram clay. The pH was fairly constant throughout the series (varying from 6.8 to 7.2). In figure 28 the amount of P adsorbed is plotted versus the total electrolyte concentration, indicating an influence of the electrolyte level on the P adsorption. The observed increase with increasing salt concentration thus shows that electrostatic forces exert at least a moderating influence on the adsorption of phosphate.

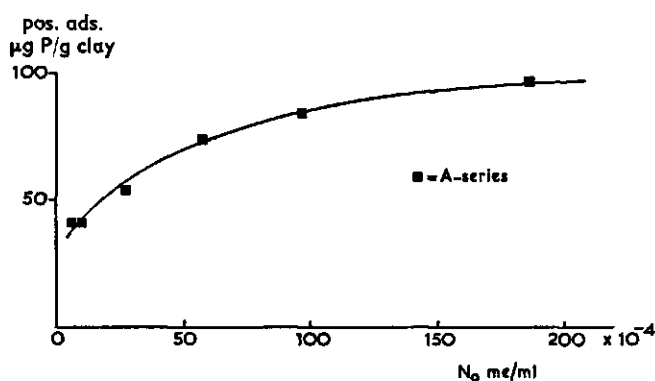


Fig. 28. The influence of total electrolyte level on the adsorption of phosphate by montmorillonite

constant (low), phosphate concentration increasing; Series C: Both phosphate and chloride concentration increasing. The data represent the average values of duplicate measurements

$V_{\text{as}}$ Cl <sup>-</sup> (g clay)	Theoretical $V_{\text{as}}$ for phosphate using a spec. surface area of 700 m <sup>2</sup> /g clay			Theoretical neg. adsorption ( $\mu\text{g P/g clay}$ )				$V_{\text{as}}$ measured (ml/g clay)	Neg. adsorption measured ( $\mu\text{g P/g clay}$ )	Net pos. adsorption ( $\mu\text{g P/g clay}$ )
	H <sub>2</sub> PO <sub>4</sub> <sup>-</sup>	HPO <sub>4</sub> <sup>2-</sup>	PO <sub>4</sub> <sup>3-</sup>	H <sub>2</sub> PO <sub>4</sub> <sup>-</sup>	HPO <sub>4</sub> <sup>2-</sup>	PO <sub>4</sub> <sup>3-</sup>	Total			
6.22	16.80	22.33	25.62	52.6	29.9	—	82.5	9.23	41.3	41.2
4.81	14.77	19.74	22.61	49.9	16.8	—	66.7	6.04	25.6	41.1
7.86	8.26	10.99	12.67	19.4	14.0	—	33.4	— 5.62	—20.3	53.7
5.26	5.74	7.63	8.82	13.6	6.0	—	19.6	—17.47	—55.1	74.7
3.94	4.34	5.81	6.65	7.5	8.2	—	15.7	—21.76	—68.0	83.7
3.02	3.08	4.13	4.76	4.3	5.8	—	10.1	—30.81	—87.0	97.1
	16.17	21.56	24.71	57.2	19.2	—	76.4	7.70	34.1	42.3
	14.98	19.88	22.75	71.2	40.4	—	111.6	10.98	74.4	37.2
	8.61	11.34	12.95	—	338.5	—	338.5	8.92	266.3	72.2
	5.81	7.56	8.61	—	135.2	359.3	494.5	6.18	368.4	126.1
	4.41	5.74	6.51	—	22.4	609.7	632.1	4.78	466.3	165.8
	2.80	3.71	4.18	—	—	937.9	937.9	3.32	743.6	194.3
4.24	14.49	19.32	22.19	62.2	20.7	—	82.8	7.02	37.6	45.2
8.61	8.47	11.20	12.81	29.0	153.0	—	182.0	7.78	132.9	49.1
6.03	5.95	7.91	9.03	—	228.8	29.0	257.8	6.27	201.5	56.3
4.25	4.48	5.88	6.72	—	104.1	221.0	325.1	4.44	224.6	100.5
2.96	3.01	3.92	4.48	—	18.1	496.5	514.6	3.10	357.9	156.7
2.04	2.10	2.73	3.08	—	—	762.7	762.7	2.41	596.8	165.9

#### 4.1.7.3 The influence of pyrocatechol and fluoride on the positive adsorption of phosphate

Pyrocatechol(1-2-dihydroxybenzene) has been shown to have a high affinity for clay minerals (HEMWALL, 1963), which may be attributed to the complex forming properties of this material. It was thought therefore that pyrocatechol might depress the phosphate adsorption by covering the reactive spots on the clay. Thus series A of the foregoing experiment was repeated in 3 series in which clay suspensions were employed after different pretreatments, viz. a shaking procedure with 10, 50 and 100 ppm. pyrocatechol, respectively. In order to check the reproducibility of the measurements one point without pretreatment was repeated. Results are given in table 18.

The influence of fluoride (FIFE, 1959) was tested in a separate experiment. To this purpose parts of the Na-montmorillonite suspension were shaken during one week at fluoride concentration levels of 0.005 and 0.01 N, using NaF. Then series A was repeated again, employing now the fluoride pretreated clays. Results are presented in table 18.

In figure 29 the data are plotted for all pretreatments. The repeat point with unpretreated clay lies exactly on the line of figure 28. It is evident from figure 29 that pyrocatechol does not have any influence on the P adsorption. This indicates that either the affinity of the active spots for phosphate is much higher than for pyrocatechol, or that pyrocatechol is adsorbed on other sites than phosphate.

Table 18. The influence of pyrocatechol and fluoride on the positive adsorption of phosphate by Na montmorillonite (Osage). Series I, II and III: pretreatment with 10, 50 and 100 ppm. pyrocatechol, respectively. Series IV and V: pretreatment with 0.005 and 0.01 me. NaF per ml, respectively. X): repeat point with untreated clay. The data presented are the average values of duplicate measurements

No.	pH	$N_0$ (me./ml)	$\frac{1}{\sqrt{\beta N_0}}$ (Å)	$\mu\text{g P/ml}$ in dialyzate	$d^-$ (Å)	$d^-$ (Å)	Theor. neg. adsorption ( $\mu\text{g P/g clay}$ ) $\text{H}_2\text{PO}_4^-$	Total	$V_{\text{me}}$ measured (ml/g clay)	Neg. adsorption measured ( $\mu\text{g P/g clay}$ )	Net pos. adsorption ( $\mu\text{g P/g clay}$ )
I.1	6.52	$6.50 \times 10^{-4}$	121.0	4.3	240.3	320.0	61.0	15.5	76.5	8.63	39.2
.2	6.54	$2.87 \times 10^{-3}$	57.3	3.5	114.5	152.5	23.6	6.0	29.6	-7.98	57.5
.3	6.50	$5.56 \times 10^{-3}$	41.2	3.1	82.4	109.8	15.2	3.9	19.1	-16.10	69.7
.4	6.52	$1.02 \times 10^{-2}$	30.4	3.0	60.8	81.0	10.7	2.7	13.4	-25.39	89.1
.5	6.50	$1.85 \times 10^{-2}$	22.6	2.7	45.2	60.2	7.2	1.8	9.0	-34.62	102.9
II.1	6.10	$7.51 \times 10^{-4}$	112.3	4.1	223.9	298.7	60.0	5.1	65.1	1.71	58.1
.2	6.06	$2.97 \times 10^{-3}$	56.4	3.3	112.8	150.4	24.6	2.1	26.7	-13.33	70.9
.3	6.02	$5.65 \times 10^{-3}$	40.9	3.0	81.8	109.0	16.2	1.4	17.6	-20.05	77.8
.4	6.00	$9.74 \times 10^{-3}$	31.1	3.0	62.2	82.9	12.1	1.0	13.1	-26.93	92.4
.5	5.96	$1.83 \times 10^{-2}$	22.7	2.8	45.4	60.5	8.3	0.7	9.0	-32.65	99.2
III.1	5.70	$8.33 \times 10^{-4}$	106.7	3.9	213.2	284.0	56.4	3.1	59.5	-0.75	62.5
.2	5.70	$3.03 \times 10^{-3}$	55.8	3.5	111.6	148.8	25.9	1.4	27.3	-9.80	61.2
.3	5.60	$5.73 \times 10^{-3}$	40.5	3.2	81.0	108.2	17.4	1.0	18.4	-15.75	68.6
.4	5.60	$1.02 \times 10^{-2}$	30.4	3.1	60.8	81.0	12.7	0.7	13.4	-23.47	86.1
.5	5.64	$1.74 \times 10^{-2}$	23.2	2.6	46.4	61.8	8.0	0.5	8.5	-33.08	93.4
IV.1	6.98	$1.73 \times 10^{-3}$	73.9	4.1	147.2	195.8	27.2	19.5	46.7	3.64	31.9
.2	6.80	$4.02 \times 10^{-3}$	48.5	3.7	96.8	128.8	17.6	10.0	27.6	-3.91	42.1
.3	6.80	$6.71 \times 10^{-3}$	37.5	3.5	74.9	99.8	12.7	7.2	19.9	-6.13	41.1
.4	6.76	$1.07 \times 10^{-2}$	29.7	3.5	59.4	79.2	10.8	4.8	15.6	-9.66	49.0
.5	6.72	$1.94 \times 10^{-2}$	22.0	3.3	44.0	58.7	7.6	3.4	11.0	-14.47	58.4
V.1	7.00	$5.70 \times 10^{-3}$	40.7	3.8	81.3	108.3	14.0	10.0	24.0	-3.24	36.2
.2	6.98	$7.71 \times 10^{-3}$	35.0	3.7	69.9	93.2	11.6	8.3	19.9	-5.04	38.3
.3	6.92	$1.03 \times 10^{-2}$	30.2	3.5	60.4	80.5	10.2	5.9	16.1	-6.36	38.1
.4	6.92	$1.45 \times 10^{-2}$	25.5	3.5	51.0	68.0	8.8	5.0	13.8	-8.16	42.5
.5	6.88	$2.31 \times 10^{-2}$	20.2	3.4	40.4	53.9	6.7	3.9	10.6	-11.30	49.1
X.	6.58	$1.91 \times 10^{-2}$	22.2	2.8	44.4	59.2	6.9	2.3	9.2	-30.88	95.1

Fluoride shows a considerable influence, the net positive adsorption of phosphate being depressed to about 60 and 50 per cent of the original adsorption, after pretreatment at 0.005 and 0.01 N fluoride, respectively. This, however, does not have

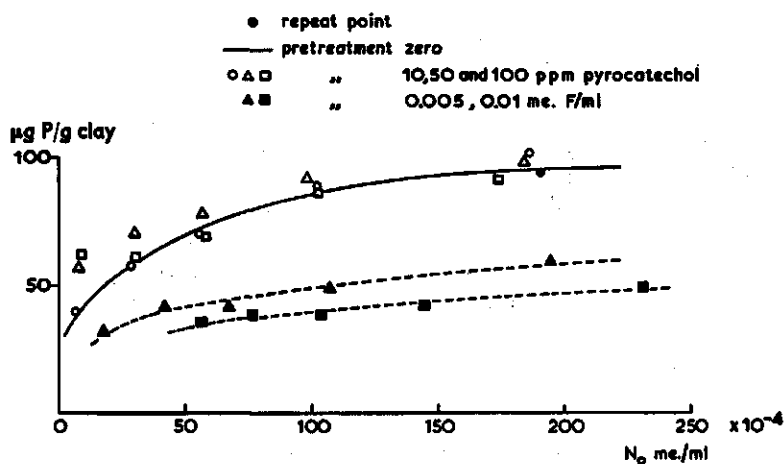


Fig. 29. The influence of pyrocatechol and fluoride on the phosphate adsorption by montmorillonite

much practical meaning with respect to an attempt to depress the phosphate adsorption quantitatively, since for that purpose a rather high fluoride concentration would be required. Accordingly, experiments at low electrolyte levels would then become impossible.

The above experiments, showing the very high affinity of phosphate ions for the clay, are again indicative for the fact that the adsorption mechanism is of the chemisorption type.

#### 4.1.7.4 The influence of sodiumsilicate on the phosphate adsorption

Studies on the availability of phosphate to plants in soils with strong phosphate fixation have indicated that silicate ions may release, to a certain extent, the phosphate retained by the soil (THOMAS, 1930; TOTH, 1939). Thus the montmorillonite suspension used in the adsorption experiments was pretreated at different levels of silicate concentrations, employing a solution of sodiumsilicate. The degree of polymerisation of silicate in this solution was studied according to ALEXANDER (1953), indicating that the silicate was almost quantitatively present in the monomeric form.

Parts of the stock suspension were shaken for one week at  $10^{-3}$  and  $2 \times 10^{-3}$  N silicate, respectively. Both suspensions were used to make up series with a constant phosphate level of about  $4 \times 10^{-4}$  N and increasing total electrolyte concentrations as obtained by NaCl additions (series I and II). Moreover a cross-section of figure



Table 19. The influence of silicate on the positive adsorption of phosphate by Na montmorillonite (Osage). Series I and II: pretreatment at  $10^{-3}$  and  $2 \times 10^{-3}$  N silicate concentration, respectively; Points of series III: pretreatment at  $10^{-4}$ ,  $3 \times 10^{-4}$ ,  $6 \times 10^{-4}$  N silicate concentration, respectively; Series IV: lower phosphate level and pretreatment at 0,  $10^{-4}$ ,  $3 \times 10^{-4}$ ,  $10^{-3}$ ,  $2 \times 10^{-3}$ ,  $5 \times 10^{-3}$  and  $10^{-3}$  N silicate concentration. The data presented are the average values of duplicate measurements

No.	pH	$N_0$ (mc./ml)	$\frac{1}{\sqrt{\beta N_0}}$ (Å)	$\mu\text{g P/ml}$ in dialyate	$d^+$ (Å)	$d^-$ (Å)	$d^{\equiv}$ (Å)	Theor. neg. adsorption ( $\mu\text{g P/g clay}$ )			$V_m$ measured (ml/g clay)	Neg. adsorption measured ( $\mu\text{g P/g clay}$ )	Net pos. adsorption ( $\mu\text{g P/g clay}$ )
								$\text{H}_2\text{PO}_4^-$	$\text{HPO}_4^{2-}$	Total			
I.1	8.24	$1.10 \times 10^{-3}$	92.6	4.9	175.4	231.5	—	4.8	72.5	—	77.3	71.0	6.3
.2	8.26	$3.22 \times 10^{-3}$	54.1	4.3	105.0	139.3	—	2.5	38.5	—	41.0	32.4	8.6
.3	8.50	$5.95 \times 10^{-3}$	39.8	4.0	78.3	103.9	—	1.1	27.6	—	28.7	19.4	9.3
.4	8.51	$1.04 \times 10^{-2}$	30.1	4.0	59.7	79.3	—	0.8	20.9	—	21.7	12.2	9.5
.5	8.10	$1.96 \times 10^{-2}$	21.9	3.9	43.6	57.9	—	1.3	14.1	—	15.4	-2.4	17.8
II.1	9.50	$1.96 \times 10^{-3}$	69.4	2.3	129.5	170.6	194.7	0.2	24.5	2.8	27.5	21.9	5.6
.2	9.54	$3.80 \times 10^{-3}$	49.8	2.4	95.3	126.1	144.3	0.1	19.3	2.5	21.9	16.1	5.8
.3	9.50	$6.42 \times 10^{-3}$	38.3	2.6	74.6	99.0	113.5	0.1	16.3	1.9	18.3	9.7	8.6
.4	9.40	$1.06 \times 10^{-2}$	29.8	2.5	58.7	77.9	89.5	—	12.4	1.2	13.6	7.1	6.5
.5	9.35	$1.95 \times 10^{-2}$	22.0	2.7	—	58.0	66.5	—	10.0	0.9	10.9	3.2	7.7
III.1	6.72	$1.90 \times 10^{-3}$	22.3	2.9	44.5	59.1	—	7.1	2.4	—	9.5	-26.92	86.6
.2	6.90	$1.90 \times 10^{-3}$	22.3	3.1	44.5	59.1	—	5.9	5.2	—	11.1	-19.71	73.0
.3	7.58	$1.90 \times 10^{-3}$	22.3	3.5	44.5	59.1	—	2.7	11.1	—	13.8	-7.02	38.6
IV.1	6.40	$1.87 \times 10^{-3}$	22.5	1.2	44.9	59.9	—	3.2	0.7	—	3.9	-49.07	62.1
.2	6.54	$1.89 \times 10^{-3}$	22.4	1.3	44.7	59.6	—	3.3	0.9	—	4.2	-43.00	59.1
.3	6.85	$1.89 \times 10^{-3}$	22.4	1.4	44.6	59.5	—	3.1	1.7	—	4.8	-28.31	43.8
.4	7.24	$1.87 \times 10^{-3}$	22.5	1.7	44.8	59.7	68.8	2.0	4.5	0.1	6.6	-14.08	30.6
.5	8.26	$1.80 \times 10^{-3}$	22.9	1.9	45.6	60.6	69.7	0.5	7.2	0.2	7.9	-2.58	12.8
.6	9.30	$1.76 \times 10^{-3}$	23.2	1.9	45.9	60.9	70.0	0.1	7.7	0.5	8.3	0.57	7.2
.7	10.20	$1.63 \times 10^{-3}$	24.1	2.0	—	62.2	71.5	—	6.2	3.0	9.2	1.34	6.5
.8	11.00	$1.52 \times 10^{-3}$	24.9	2.0	—	62.4	70.9	—	2.2	7.5	9.7	4.32	1.1

28 was made by maintaining the total salt level constant at about  $2 \times 10^{-2}$  N, using suspensions which had been pretreated at silicate levels of  $6 \times 10^{-4}$ ,  $3 \times 10^{-4}$  and  $10^{-4}$  N, respectively (series III). The results are presented in table 19 and plotted in figure 30.

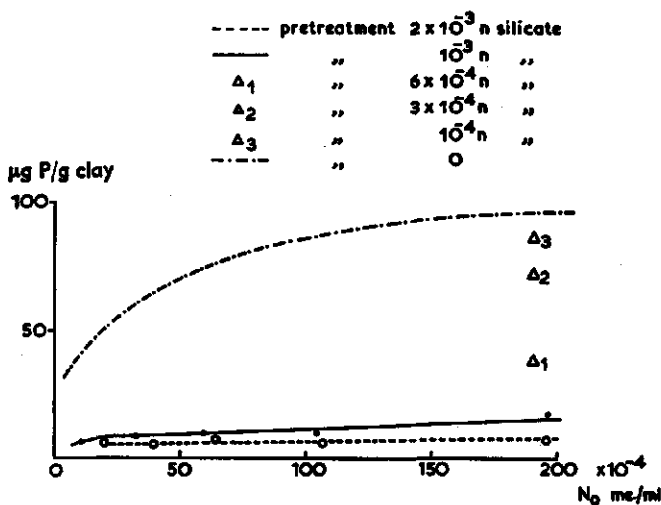


Fig. 30. The influence of sodium silicate on the adsorption of phosphate by montmorillonite

It was found that the P retention decreased to about 20 and 10 per cent of the original adsorption after pretreatments at  $10^{-3}$  and  $2 \times 10^{-3}$  N silicate, respectively. In addition the increasing silicate concentration of series III resulted in a gradual decrease of the P adsorption. However, the lowest value of the net adsorption still amounted to about  $8 \mu\text{g P}$  per gram clay, indicating that a fairly large excess of silicate is required to suppress completely phosphate adsorption by the clay. It was concluded that a decrease of the phosphate level and an increase of the silicate level might lead to a further depression of the P adsorption. Again a cross-section of figure 28 was made, now at a phosphate level of about  $2 \times 10^{-4}$  N, lower concentrations being impractical in view of the P adsorption at the polyethylene bottles (cf section 3.4.1). Silicate pretreatments of 0,  $10^{-4}$ ,  $3 \times 10^{-4}$ ,  $6 \times 10^{-4}$ ,  $10^{-3}$ ,  $2 \times 10^{-3}$ ,  $5 \times 10^{-3}$ , and  $10^{-2}$  N were applied. The results are given as series IV in table 19. Total electrolyte levels turned out to be slightly lower than pre-estimated, viz. varying between  $1.9 \times 10^{-2}$  and  $1.5 \times 10^{-2}$  N. This, however, does not disturb a comparison of the final results since the influence of total electrolyte concentration at this high level is almost negligible in the range of the difference in salt concentration of the two experiments (cf figure 28). The data show that the net adsorption of P could now be decreased to about  $1.1 \mu\text{g P/g}$  clay, which value is near to the experimental error. This then means that under the above conditions even the phosphate ions are behaving in accordance with theoretical predictions as regards anion exclusion.

It should perhaps be stated here that the above experiments were not designed to distinguish between different rates of isotopic equilibration (cf SISSINGH, 1961), if present. The reaction time was chosen such that no further increase of the adsorption could be observed upon an increase of the shaking period. Thus it could be shown that even for systems comparable to point no 8 of series IV equilibration periods of 1, 2 and 3 weeks yielded values of 1.0, 1.3 and 1.1  $\mu\text{g P/g}$  clay, respectively, indicating that one week was ample time for complete equilibration.

The data of table 19 also allow a plot of the P adsorption versus the silicate concentration level of the pretreatments, for the two phosphate levels involved. The relation meant is presented in figure 31. The values of the intercepts with the ordinate, corresponding to the net adsorption of P at zero silicate treatment, reflect again the influence of the phosphate concentration in the equilibrium solution on the magnitude of the P adsorption (cf also the adsorption isotherm of figure 27). The phosphate concentrations mentioned in figure 31 viz.  $4 \times 10^{-4}$  and  $2 \times 10^{-4}$  N, are based upon additions of a sodiumphosphate solution of known normality. Thus these numbers represent the concentrations of the dialyzates in the absence of interaction between phosphate ions and the clay. Since, however, phosphate was positively adsorbed by the clay, the equilibrium concentrations were somewhat lower than those given above, depending on the magnitude of positive adsorption (cf e.g. series IV of table 19).

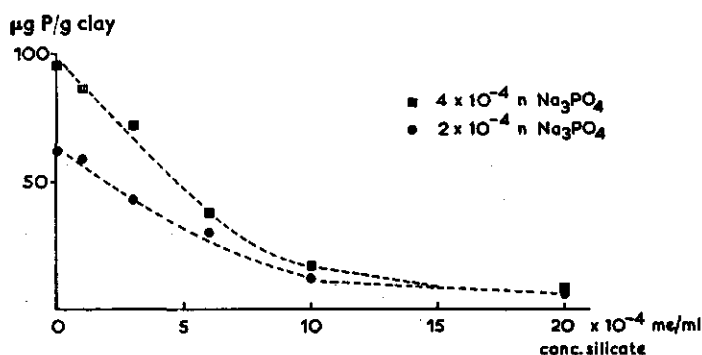


Fig. 31. Decrease of the phosphate adsorption (at two phosphate levels) with increasing silicate concentration

The experiments described so far involved both different silicate treatments and different pH values (the latter varying with silicate level). As was mentioned in section 2.1, the pH of the system may have a considerable influence on the electric charge of clay particles, the charge of the clay edges being dependent upon the  $\text{H}^+$ / $\text{OH}^-$  concentration in solution. Since one could visualize that the increasing negative charge with increasing pH values might affect the P adsorption to a certain extent it appeared necessary to investigate separately the effect of pH and silicate upon the phosphate adsorption.

#### 4.1.7.5 The influence of the pH on the phosphate adsorption

The net positive adsorption of phosphate on Na-montmorillonite was measured over a fairly large range of pH values. To this purpose a variation of pH values was induced by additions of precalculated amounts of HCl, NaCl and NaOH solutions in various combinations to a clay suspension with an initial electrolyte level of about  $4 \times 10^{-4}$  N. Additions were chosen such that the final total electrolyte level amounted to roughly  $2 \times 10^{-2}$  N. A  $\text{Na}_3\text{PO}_4$  solution, tagged with  $\text{P}^{32}$ , was used again to acquire a phosphate concentration around  $4 \times 10^{-4}$  N. Shaking time was limited to 48 hours in this experiment, which was proved to be satisfactory to ensure equilibrium at this salt level. At the same time it was felt that longer shaking periods should be avoided in order to limit decomposition of the clay, especially at the low pH values involved.

To investigate the effect of silicate on the phosphate adsorption over the above pH range, other parts of the mother suspension were shaken during one week (prior to the experiment) at silicate levels of  $8 \times 10^{-4}$  and  $3 \times 10^{-2}$  N. The electrolyte level of the highest pretreatment exceeding already the value desired in the subsequent experiment, it became necessary to reduce the salt concentration by means of dialysis until a sufficiently low electrolyte level was reached to allow preparation of systems with compositions comparable to those of the untreated sample (e.g. about  $10^{-2}$  N silicate). After equilibration pH values were measured in the suspension. Experimental results are shown in table 20 and figure 32.

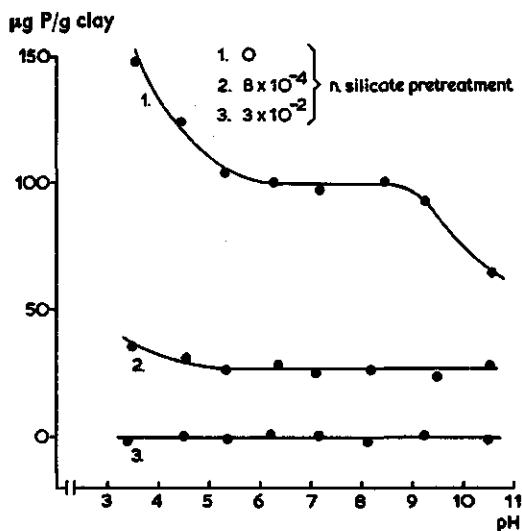


Fig. 32. The adsorption of phosphate on Na-montmorillonite as a function of pH and silicate pretreatment

The untreated clay showed a substantial influence of the pH on the net positive phosphate adsorption, yielding values varying from about 150  $\mu\text{g P/g}$  clay at pH 3.6

to about 65  $\mu\text{g P/g}$  clay at pH 10.6. The amount adsorbed turned out to be fairly constant over a pH range from about 5.5 to 8.5. The increase at low pH can be attributed to an increasing number of positively charged sites at the clay edges and/or to a precipitation as aluminum (and possibly iron) phosphates. The decrease of positive adsorption at high pH values, which is of the same order of magnitude as the increase at low pH, could be caused by an increased negative charge or by the competition between phosphate and hydroxyl ions or by a combination of these two factors (cf also section 4.3.1). According to line 1 of figure 32 the above effects are apparently minor over a quite large pH range.

Table 20. Influence of the pH on the positive adsorption of phosphate on Na montmorillonite. Series I, II and III: pretreatment zero,  $8 \times 10^{-4}$  and  $3 \times 10^{-2}$  normal silicate, respectively. The data presented are the mean values of duplicate measurements

No.	pH	$\mu\text{g P/ml}$ in dialyzate	$N_0$ (me./ml)	Theor. neg. adsorption ( $\mu\text{g P/g}$ clay)	$V_{\text{incl.}}$ measured (ml/g clay)	Apparent pos. adsorption ( $\mu\text{g P/g}$ clay)	Net pos. adsorption ( $\mu\text{g P/g}$ clay)
I.1	3.57	2.3	$1.94 \times 10^{-2}$	6.5	61.47	141.4	147.9
.2	4.45	2.6	$1.96 \times 10^{-2}$	7.3	45.09	117.2	124.5
.3	5.32	2.8	$1.89 \times 10^{-2}$	8.1	34.18	95.7	103.8
.4	6.27	2.8	$1.95 \times 10^{-2}$	8.9	32.58	91.2	100.1
.5	7.18	2.9	$1.97 \times 10^{-2}$	9.8	30.28	87.8	97.6
.6	8.46	2.8	$1.84 \times 10^{-2}$	10.9	32.29	90.4	101.3
.7	9.24	3.1	$2.02 \times 10^{-2}$	11.6	26.39	81.8	93.4
.8	10.60	3.5	$1.93 \times 10^{-2}$	14.8	14.30	50.1	64.9
II.1	3.48	3.7	$1.87 \times 10^{-2}$	10.6	6.65	24.6	35.2
.2	4.54	3.5	$1.85 \times 10^{-2}$	10.1	6.10	21.4	31.5
.3	5.38	3.8	$1.93 \times 10^{-2}$	11.0	4.22	16.0	27.0
.4	6.36	4.0	$2.06 \times 10^{-2}$	12.3	4.09	16.4	28.7
.5	7.10	4.1	$2.00 \times 10^{-2}$	13.7	2.78	11.4	25.1
.6	8.19	3.9	$1.90 \times 10^{-2}$	15.0	2.90	11.3	26.3
.7	9.50	4.2	$1.94 \times 10^{-2}$	16.1	1.88	7.9	24.0
.8	10.52	3.9	$2.03 \times 10^{-2}$	16.1	3.11	12.1	28.2
III.1	3.40	5.0	$2.13 \times 10^{-2}$	13.3	-2.91	-14.6	-1.3
.2	4.50	4.9	$2.04 \times 10^{-2}$	13.4	-2.61	-12.8	0.6
.3	5.35	4.8	$2.05 \times 10^{-2}$	13.4	-2.96	-14.2	-0.8
.4	6.21	4.8	$2.16 \times 10^{-2}$	14.4	-2.74	-13.2	1.2
.5	7.16	4.7	$1.99 \times 10^{-2}$	16.2	-3.27	-15.4	0.8
.6	8.11	5.1	$2.05 \times 10^{-2}$	18.8	-3.95	-20.1	-1.3
.7	9.23	4.9	$2.18 \times 10^{-2}$	17.7	-3.57	-17.5	0.2
.8	10.50	4.9	$2.15 \times 10^{-2}$	19.6	-4.06	-19.9	-0.3

Pretreatment with silicate at a concentration of  $8 \times 10^{-4}$  N (cf line 2 of figure 32) yielded a depression of the P adsorption in the range of intermediate pH values of about 70 %. This checks very well with the data of figure 31, where this same number was found for similar phosphate and silicate levels. It is seen that in this case the variation of P adsorption with varying pH disappears, except for a very small effect at the lowest pH value.

The pretreatment at  $3 \times 10^{-2}$  N silicate (cf line 3 of figure 32) resulted in a quan-

titative prevention of positive phosphate adsorption, regardless of pH value. The small negative values for the net adsorption (cf table 20) are attributed to inaccuracy of the measurements. As was pointed out above the silicate level of this series had a value of about  $10^{-2}$  N after the dialysis procedure. According to data presented before (cf table 19), one should indeed expect a complete suppression of phosphate adsorption at the existing silicate and phosphate levels.

It is interesting to note that the apparent adsorption values of this series still vary with pH in a systematic manner. Because the electrolyte level is roughly the same for all samples, the observed variation must be attributed to the influence of pH. This is in remarkable agreement with the predicted variation of the  $Q$ -values with the pH – the latter determining the relative amounts of mono-, di- and trivalent phosphate ions – as is evidenced by the disappearance of the systematic variation in the net adsorption values (cf last column of series III in table 20).

Results of the present experiment allow the conclusion that at zero silicate treatment the pH of the system has obviously a considerable influence on the magnitude of the phosphate adsorption. After silicate treatment, however, this pH dependency disappears. Thus the results for the  $4 \times 10^{-4}$  N phosphate level, as presented in figure 31, may be ascribed completely to the action of the silicate itself. For, the pH values of the first 5 points (cf series IV of table 19) were in the range where pH effects are non existent (cf figure 32). At the same time the high silicate level of point no 6 was sufficient to suppress the pH influence, which is found in the absence of silicate.

#### 4.1.7.6. *The release of phosphate against silicate as a function of time*

In the experiments described so far the competition between silicate and phosphate ions with respect to adsorption on Na-montmorillonite was studied in such a way that the clay was pre-equilibrated with silicate prior to the phosphate addition. It was the aim of the present experiment to investigate the silicate effect after achieving a contact between phosphate and clay antecedent to the silicate treatment. Thus in this case the reactive sites could be assumed to be occupied, at least in part, by phosphate ions at the moment of silicate addition. Knowledge about the silicate influence on P adsorption under such conditions might be useful in view of the application of silicate fertilizers in soils exhibiting "fixation" of P from phosphate fertilizers.

The rate of the silicate-phosphate exchange reaction presumably being an important factor with respect to the above purpose, the release of phosphate upon silicate treatment was studied as a function of contact time after addition of the competitor. A preliminary experiment indicated that this release is very fast, roughly 80–90 % of the silicate effect being established within a few minutes after the silicate addition. This rendered the application of the dialysis procedure impossible in this case. Instead, centrifugation was used for a separation between clay and equilibrium solution. Accordingly a fairly high electrolyte level was required, viz. about 0.05 N, to ascertain a clear supernatant. At the same time this appeared to be advantageous

with respect to a possible depression of the anion exclusion since at this high electrolyte level the influence of interacting double layers is almost negligible.

The pre-adsorption of phosphate was achieved by addition of a  $\text{Na}_3\text{PO}_4$  solution, tagged with  $\text{P}^{32}$ , to a concentration level of  $4 \times 10^{-4}$  N. A solution of  $\text{NaCl}$  was then used to adjust the total salt level at roughly  $5 \times 10^{-2}$  N. Thereafter the suspension was agitated during one week to allow equilibration. Part of the suspension was then used for measurement of the net positive P adsorption, as described before. This indicated a value of  $102.3 \mu\text{g P/g clay}$ , which value is in good agreement with the line of figure 28 for an electrolyte level of about  $5 \times 10^{-2}$  N.

Silicate treatments were done at fairly low level, viz.  $3 \times 10^{-4}$  and  $6 \times 10^{-4}$  N, in order to avoid a significant alteration of the total electrolyte concentration. Parts of the suspension of pretreated clay were then supplied with appropriate amounts of a sodiumsilicate solution, whereafter the systems were agitated quite vigorously by means of a reciprocating shaker. The systems had been prepared in small polyethylene bottles of 10 ml, one for each contact time and silicate level. After the shaking, these bottles were placed in a centrifuge and separation of the equilibrium solution was effected at a speed of 1,500 rpm.. A preliminary trial indicated that about 70% of the total suspension volume was clear after 1 minute centrifugation at the electrolyte level involved, indicating that indeed contact between silicate ions in solution and the majority of the clay colloid could be assumed to be terminated as soon as

*Table 21. Release of P adsorbed on Na montmorillonite (Osage) after silicate additions at two different levels, as a function of time. The net P adsorption at zero pretreatment amounted to  $102.3 \mu\text{g P/g clay}$ . Series I and II: silicate concentrations of  $3 \times 10^{-4}$  and  $6 \times 10^{-4}$  normal, respectively. The data presented are the mean values of duplicate measurements*

Shaking time in minutes	Series I release		Series II release	
	$\mu\text{g P/g clay}$	percentage of original adsorption	$\mu\text{g P/g clay}$	percentage of original adsorption
1	18.5	18.1	39.1	38.2
5	21.9	21.5	40.3	39.4
15	23.8	23.3	41.4	40.5
60	28.4	27.8	44.5	43.5
120	32.0	31.3	46.3	45.2
600	33.2	32.4	47.2	46.1
1 440	33.4	32.6	47.1	46.0
10 080	33.0	32.2	47.4	46.3

centrifugation was started. Shaking times were chosen as 1, 5, 15, 60, 120, 600, 1,440 and 10,080 minutes. In view of the above, the first two points should be considered to be quite inaccurate as far as the time determination is concerned. After centrifugation, which was extended over 10 minutes to ensure satisfactory settling of the clay particles, the supernatant was used for activity determinations. Assuming a constant value for the specific activity of  $\text{P}^{32}$  in the systems, these count data allowed

the calculation of the increase of the P concentration in solution as a function of time. A comparison with the untreated sample then resulted in the phosphate release, expressed as percentage of the originally adsorbed amount. Results are given in table 21 and plotted for shaking times up to 120 minutes in figure 33.

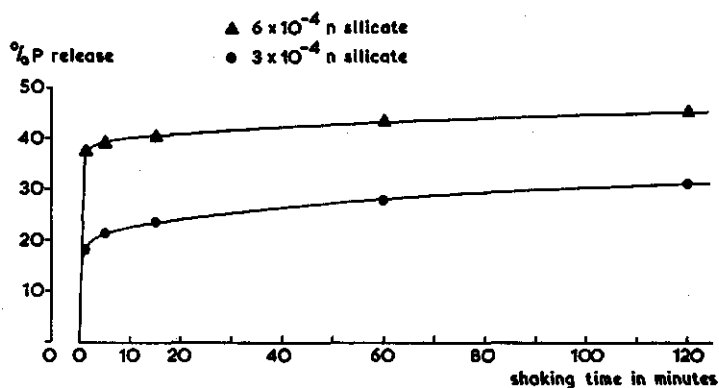


Fig. 33. The release of pre-adsorbed phosphate against silicate as a function of time

It is clearly shown that the replacement was established almost completely during the first 5–10 minutes, especially at the highest silicate level. After a shaking time of 10 hours the amount released reached a constant value, corresponding to the end-point of the reaction. Amounts released were then about 32 % and 46 % of the originally adsorbed amount at the  $3 \times 10^{-4}$  and  $6 \times 10^{-4}$  N silicate levels, respectively. According to figure 31 the percentages depression of P adsorption at these silicate and phosphate concentration levels were found as 30 % and 50 %, respectively. This thus means that the effect of silicate with respect to phosphate adsorption is the same for the experimental conditions chosen, regardless whether the clay has been pretreated with silicate or with phosphate. This then implies that under the conditions studied the exchange reaction between phosphate and silicate appears to be reversible.

#### 4.1.8 Simultaneous determination of the adsorption of three anions on Na-montmorillonite

As has been discussed in Chapter 3 the difference in half life of different radioisotopes may be applied to distinguish between the activities of two radioisotopes when present in the same solution. Although  $\text{Cl}^{36}$  and  $\text{P}^{32}$  would lend themselves best for such a differentiation procedure (cf half lives in table 7) it was found that also  $\text{S}^{35}$  in combination with  $\text{P}^{32}$  may be used to this purpose. Naturally the accuracy of the activity measurements is now slightly lower than that of the single activity



determinations (cf figure 19). Thus one may measure simultaneously the adsorption of chloride, sulfate and phosphate ions, applying the potentiometric titration for chloride and the "double" tracer method for sulfate and phosphate.

In the foregoing experiments it was found that both chloride and sulfate are excluded by the Na-montmorillonite under normal conditions. In order to facilitate a comparison between the results of the three anions the experimental upset was chosen such that also phosphate could be expected to be excluded instead of positively adsorbed. To this purpose the clay was first shaken for one week at a silicate level of about  $8 \times 10^{-3}$  N. Again to facilitate the comparison, it is advantageous to plot the experimental phosphate data as exclusion volume versus the distance of exclusion. Such a plot requires phosphate to be present as ions of the same valency. According to figure 16 about 97 % of total phosphate occurs as divalent ion at pH values of 8.7 to 8.9. After the pretreatment with silicate, the clay suspension was therefore brought at a pH of 8.8 by small additions of a HCl solution. Then the systems were prepared in the normal way by additions of NaCl, Na<sub>2</sub>SO<sub>4</sub> and Na<sub>2</sub>HPO<sub>4</sub> solutions, the two last solutions being labeled with the appropriate radioisotopes.

Table 22. Simultaneous determination of the negative adsorption of 3 anions on Na montmorillonite (Osage)

No.	pH	$N_0(\text{me./ml})$	$1/\sqrt{\beta N_0}$ (Å)	$Q'/\sqrt{\beta N_0}$ (Å)	$Q''/\sqrt{\beta N_0}$ (Å)	$V_{ex}(\text{ml/g clay})$					
						Cl <sup>-</sup>		SO <sub>4</sub> <sup>2-</sup>		HPO <sub>4</sub> <sup>2-</sup>	
1	8.83	$0.94 \times 10^{-3}$	31.7	58.7	76.7	4.15	4.08	5.36	5.16	4.59	4.81
2	8.79	$1.12 \times 10^{-3}$	29.1	53.9	70.5	4.01		4.95		5.03	
						3.50	3.26	4.72	4.61	4.40	4.70
3	8.85	$1.43 \times 10^{-3}$	25.7	47.8	62.3	3.12		4.50		4.99	
						3.31	3.25	3.20	3.34	4.48	4.28
4	8.74	$1.86 \times 10^{-3}$	22.6	42.1	54.9	3.19		3.48		4.08	
						2.82	2.64	3.85	3.83	3.47	3.47
5	8.70	$2.15 \times 10^{-3}$	20.9	39.1	50.8	2.46		3.81		3.47	
						2.48	2.25	4.17	4.07	3.15	3.14
						2.02		3.97		3.13	

The experimental results are shown in table 22 and figure 34. The measured pH values indicated that indeed phosphate could be assumed to be almost quantitatively present in the divalent form. The high silicate concentration, required to prevent positive phosphate adsorption, limited the variation of the total electrolyte level. Values for sulfate and phosphate exclusion were determined by duplicate countings of the samples after a time interval of 480 hours. According to equation (3.15) one finds then:

$$\text{for } P^{32}: A^*(t = 480 \text{ h}) = 0.379 A^*(t = 0)$$

$$\text{for } S^{35}: A^*(t = 480 \text{ h}) = 0.863 A^*(t = 0)$$

Applying equations (3.16) the count rates of both S<sup>35</sup> and P<sup>32</sup> were then calculated and accordingly the values of  $V_{ex}$  were found.

It is seen in figure 34 that the experimental points are in quite good agreement with the 700 m<sup>2</sup>/g line. As was shown already in figure 19, especially the accuracy of the sulfate determination decreases under the conditions chosen, which again is

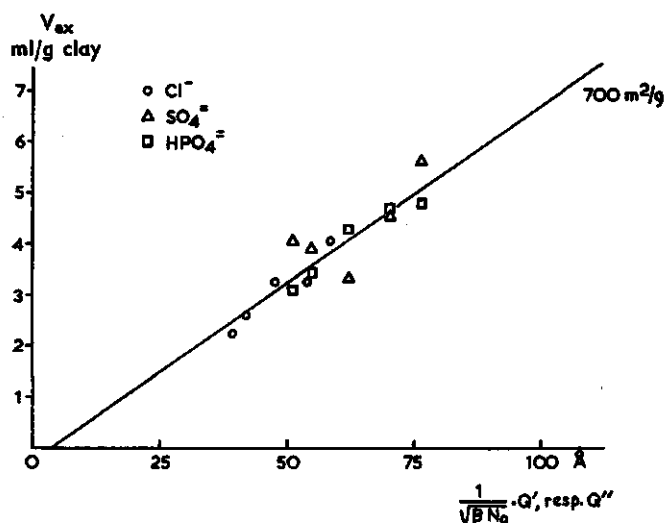


Fig. 34. Simultaneously measured exclusion of three anions by Na-montmorillonite

clearly demonstrated in figure 34. Nevertheless one may conclude that the three anions are all behaving in good accordance with theoretical expectations as regards negative adsorption.

#### 4.1.9 The reduction of the negative adsorption of chloride due to the interaction of double layers

The experiments described so far were all carried out with systems of high liquid content, in which the thickness of the double layer did not exceed the thickness of the water layer around the colloidal particles.

In Chapter 2 considerable attention has been paid to the influence of interacting double layers upon the negative adsorption of anions. It was shown that the reduction of the anion exclusion will not exceed 5 % as long as the reduced thickness of the water layer,  $D/D^*$ , remains larger than about 1.5. As an experimentally accessible parameter for interaction the quantity  $D \cdot \sqrt{\beta N_0}$  was introduced, the decrease of the negative adsorption being larger at smaller values for  $D \cdot \sqrt{\beta N_0}$  (cf figure 9). These model calculations were tested in an experiment in which the exclusion of  $\text{Cl}^-$  by Na-montmorillonite was measured at different degrees of interaction.

Since low values for  $D \cdot \sqrt{\beta N_0}$  are required to attain a detectable decrease of the

anion exclusion, several problems arise with respect to the experimental procedure. In order to ascertain small values of  $D$  one must operate with highly concentrated suspensions. At the same time the salt concentration must be maintained as low as possible to arrive at low values for  $\sqrt{\beta N_0}$ . These factors are acting in opposite direction as regards the fluidity of the suspension. A minimum degree of fluidity, however, is necessary to attain equilibrium between the suspension and the content of the dialysis bag.

As a result of the requirement of a high suspension concentration on the one hand and a low chloride level on the other hand the titration method should be expected to fail in this case, due to lack of accuracy of the concentration determinations under such conditions. This thus necessitated application of the tracer method.  $\text{Cl}^{36}$  not being available with high specific activity at reasonable cost, the low  $\text{Cl}^-$  level required additions of minute amounts of chloride in the labeling solution, resulting in an extended counting time of the samples.

It should be pointed out that if the experiment can be executed successfully with  $\text{Cl}^-$ , it could presumably be performed even better with  $\text{SO}_4^{2-}$ ,  $\text{S}^{35}$  being available at high specific activity. Moreover, the divalent sulfate ion is more sensitive to interaction of double layers, the distance of exclusion exceeding that for chloride under comparable conditions (cf also figure 9).

Prior to the experiment, part of the Na-montmorillonite stock suspension was brought into a pressure membrane apparatus. Applying pressure, the suspension was concentrated and in the mean time the  $\text{Cl}^-$  concentration of the filtrate was measured. During the concentration procedure a mat of clay was formed on the bottom of the apparatus, causing a sieving of the salt. The clay mat was broken with a spatula at regular time intervals and the pressure filtration was continued until a steep decrease in the salt concentration of the filtrate was observed (cf BOLT, 1960 a). In this way a clay paste of about 12 % montmorillonite was obtained. The paste was diluted with distilled water and shaken for quite a long time until a very thick, but still satisfactorily "fluid", homogeneous suspension was obtained. Parts of this suspension were brought into polyethylene bottles together with a small amount of  $\text{Cl}^{36}$  labeling solution. Precalculated amounts of distilled water were then added in order to acquire a range of suspension concentrations. Finally two dialysis bags were added and the systems were agitated during 12 days.

The experimental results are given in table 23. The data of this table have been compiled in the following way. From the clay content of each system - which was determined in triplicate - the value of  $D$  (thickness of water layer) may be calculated if the specific surface area of the colloid is known. For the surface area the value of  $700 \text{ m}^2/\text{g}$  was taken, which had been found in all foregoing experiments. The  $D$  value and the salt concentration of the equilibrium solution then gave  $D \cdot \sqrt{\beta N_0}$ . Accordingly the theoretically expected decrease of the anion exclusion for each system could be found from figure 9. The maximum distance of exclusion (for dilute suspensions) was found in the normal way from the salt concentration and the composition of the equilibrium solution ( $Q' = 2$ ,  $\delta = 4 \text{ \AA}$ , in this case).

If this distance of exclusion is multiplied with the specific surface area one arrives at the volume of exclusion per gram clay, which should be expected for each system

in the absence of interaction. This value was compared to the measured exclusion volume and thus the experimentally determined decrease of the negative adsorption was found. A comparison between the theoretically predicted and the measured values shows an excellent agreement.

Table 23. Comparison between the theoretically expected and the measured decrease of the negative adsorption of  $\text{Cl}^-$  in systems with interacting double layers (Na-Cl-montmorillonite, Osage). The data presented are the mean values of duplicate measurements

No.	Clay content (%)	D (Å)	$N_0$ (me./ml)	$\frac{1}{\sqrt{\beta N_0}}$ (Å)	$D \cdot \sqrt{\beta N_0}$	Theor. expected decrease according to fig. 9 (%)	$d^-$ (Å)	$V_{\infty}$ , theor. assuming a specific surface area of 700 m <sup>2</sup> /g (ml/g clay)	$V_{\infty}$ measured (ml/g clay)	Measured decrease of $V_{\infty}$ (%)
1	6.631	201.2	$1.04 \times 10^{-3}$	95.2	2.11	17	186.4	13.05	10.79	17.3
2	6.020	223.0	$1.07 \times 10^{-3}$	93.9	2.38	12	183.8	12.87	11.36	11.7
3	5.512	244.9	$1.03 \times 10^{-3}$	95.7	2.56	10	187.4	13.12	11.86	9.6
4	5.003	271.3	$1.05 \times 10^{-3}$	94.8	2.86	6	185.6	12.99	12.17	6.3
5	2.218	629.8	$0.95 \times 10^{-3}$	100.3	4	0	196.6	13.76	13.68	0.0

In contrast to the experimental complications described previously in this section, it is mentioned here that the presence of a relatively large amount of clay in each system resulted in a large difference between the apparent volume and the actual volume, thus still allowing an accurate determination of the exclusion volume.

#### 4.1.10 Determination of the chloride exclusion by Clayspur montmorillonite

This experiment was set up to compare the chloride exclusion by the Osage montmorillonite to that by a montmorillonite from a different source. To that purpose

Table 24. Determination of the specific surface area of Clayspur montmorillonite, fraction < 2 $\mu$ . Duplicate measurements refer to different dialysis bags

No.	pH	$N_0$ (me./ml)	$1/\sqrt{\beta N_0}$ (Å)	$d^- (= Q'/\sqrt{\beta N_0} - \delta^-)$ (Å)	$V_{\infty}$ (ml/g clay)	$S (= V_{\infty}/d^-)$ (m <sup>2</sup> /g clay)
1	5.90	$1.03 \times 10^{-3}$	96.2	188.4	12.62 12.73	676
2	5.70	$1.57 \times 10^{-3}$	77.5	151.0	12.85 10.60 10.13	671
3	5.40	$4.44 \times 10^{-3}$	46.1	88.2	9.66 6.02 6.00	680
4	5.31	$6.09 \times 10^{-3}$	37.0	70.0	5.97 4.67 4.68	669
5	5.08	$1.57 \times 10^{-3}$	24.7	45.4	4.69 3.15 3.10	682
					3.04	average 676

the fraction  $< 2\mu$  of Clayspur montmorillonite was employed, using the same method for fraction collection and preparation of the homoionic Na clay as was applied for the Osage sample. The data shown in table 24 were acquired by means of the tracer method, indicating a specific surface area of the Clayspur of  $676 \text{ m}^2/\text{g}$ , which value is very near to that of the Osage montmorillonite.

## 4.2 Experiments with illite

The illite used was a sample separated from a field soil, thus containing organic matter in contrast to the montmorillonites and kaolinite used, which originated from mined deposits. Since the Winsum soil contains a considerable percentage of a very fine fraction (cf KOENIGS, 1961), it was not felt necessary to continue the fraction collection procedure until the complete fraction  $< 2\mu$  had been obtained. Thus parts of the mother suspension were syphoned off until enough clay was collected to work with. It should be kept in mind, however, that for that reason the proportion of the very fine fractions was larger in the suspension used than it would be in the total fraction  $< 2\mu$  (cf also section 4.2.6). The clay was made homoionic with respect to Na by passing the suspension through columns containing Na and Cl resins.

### 4.2.1 Measurement of chloride exclusion. Determination of the specific surface area

In this experiment the fraction of the soil, designed as a fraction  $< 2\mu$ , was used as a whole without pretreatment to remove organic matter.

Since the specific surface area was expected to be considerably smaller than that of the montmorillonite, the suspension concentration used was larger than in the preceding experiments, viz. about 6 %. This implied that the apparent volume was expected to be of roughly the same magnitude as in the montmorillonite experiments, leading to a similar experimental accuracy. Measurements were done with the tracer method, employing  $\text{Cl}^{36}$ ; results are given in table 25.

Table 25. Determination of the specific surface area, employing  $\text{Cl}^{36}$ , of a fraction  $< 2\mu$  of Winsum illite. The data presented are the mean values of duplicate measurements

No.	pH	$N_0$ (me./ml)	$1/\sqrt{\beta N_0}$ (Å)	$d^- = (Q'/\sqrt{\beta N_0} - \delta^-)$ (Å)	$V_{\infty}$ (ml/g clay)	$S (= V_{\infty}/d^-)$ ( $\text{m}^2/\text{g}$ clay)
1	6.10	$1.33 \times 10^{-3}$	84.3	167.6	4.99	298
2	5.90	$4.32 \times 10^{-3}$	46.8	92.6	2.78	300
3	5.82	$5.05 \times 10^{-3}$	43.2	85.4	2.54	297
4	5.70	$8.45 \times 10^{-3}$	33.5	66.0	2.13	319
5	5.54	$1.26 \times 10^{-2}$	27.4	53.8	1.70	316
						average 306

The specific surface area of the clay involved appeared to be 306 m<sup>2</sup>/g, which is a fairly high value in comparison to data for illites given elsewhere. This must be attributed to the presence of a relatively large amount of very fine particles (cf section 4.2.6). It is noted that no decrease in negative adsorption due to double layer interaction was to be expected, although the suspension was fairly concentrated. As may be verified, the value of  $D \cdot \sqrt{\beta N_0}$  remained above 5 in the system with the lowest salt level.

#### 4.2.2 Simultaneous determination of the adsorption of chloride and sulfate in Na-illite systems

With the specific purpose to compare the behavior of chloride and sulfate in illitic systems to that in montmorillonitic ones, 2 series of systems were prepared in which the compositions were comparable to those of the experiment described in section 4.1.3. Thus in series I the total electrolyte level (composed of both chloride and sulfate) was varied, whereas in series II the salt concentration was kept low while increasing quantities, though only trace amounts, of sulfate were added (cf section 4.1.4). It was expected that the values of  $V_{ex}$  in series I should be around the line representing a specific surface area of 300 m<sup>2</sup>/g, whereas in series II any inclusion of sulfate, if present, would be detectable (cf figure 24). Results are given in table 26 and plotted in figure 35.

Table 26. The negative adsorption of Cl<sup>-</sup> and SO<sub>4</sub><sup>2-</sup> as measured according to the potentiometric titration method and the tracer method, respectively, on Na-illite (Winsum, fraction < 2μ). Data presented are mean values of duplicate measurements

Series	No.	pH	N <sub>0</sub> (me./ml)	1/√βN <sub>0</sub> (A)	Q'/√βN <sub>0</sub> (A)	Q''/√βN <sub>0</sub> (A)	V <sub>∞</sub> (ml/g clay)	
							Cl <sup>-</sup>	SO <sub>4</sub> <sup>2-</sup>
I	1	6.56	9.19 × 10 <sup>-4</sup>	112	—	292	—	8.76
	2	6.42	1.14 × 10 <sup>-3</sup>	91	176	234	5.11	7.11
	3	6.28	4.01 × 10 <sup>-3</sup>	49	94	125	2.73	3.73
	4	6.16	9.55 × 10 <sup>-3</sup>	31	60	79	1.83	2.40
	5	6.10	1.68 × 10 <sup>-2</sup>	24	46	61	1.38	1.62
II	1	6.54	7.01 × 10 <sup>-4</sup>	116	—	309	—	9.24
	2	6.60	7.13 × 10 <sup>-4</sup>	115	—	307	—	9.46
	3	6.52	7.10 × 10 <sup>-4</sup>	115	—	307	—	9.20
	4	6.58	6.85 × 10 <sup>-4</sup>	117	—	312	—	9.44
	5	6.50	7.30 × 10 <sup>-4</sup>	114	—	304	—	8.96

For chloride the potentiometric titration was applied, for sulfate the tracer method. The titration method was, however, severely limited in this case since the relatively high suspension concentration necessitated a dilution of the suspension before titration. This, of course, had an adverse influence on the accuracy of the measurements. The titration was found to fail at the lowest electrolyte level, whereas at the second and third chloride point of series I (about 0.6 × 10<sup>-3</sup> and 2 × 10<sup>-3</sup> N chloride, respectively) the duplicates showed quite large differences, although the mean values were in good

accordance with expectations. For these reasons values for chloride have not been determined in series II.

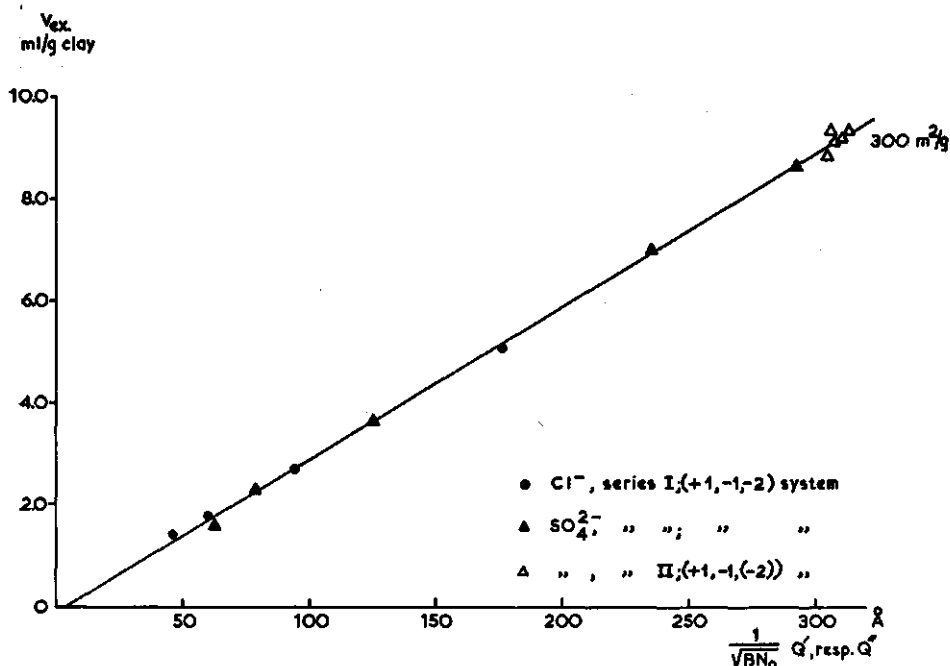


Fig. 35. Simultaneously measured exclusion of chloride and sulfate by Na-illite

It is seen that all points are very near to the line mentioned, which is in agreement with expectations as far as series I is concerned. However, the data showed a complete absence of positive sulfate adsorption, even at the carrier free sulfate level. The explanation for this phenomenon is given by the fact that the field sample of the illite after pretreatment still contained an amount of phosphate sufficiently large to prevent any positive sulfate adsorption. This was substantiated by the observation that the dialyzate of the homoionic Na-illite contained about 0.4 ppm. P, corresponding to roughly  $10^{-5}$  molar phosphate. This concentration should certainly be sufficient to prevent sulfate adsorption, as was shown in section 3.1.5. Moreover, phosphate had in this case the advantage with respect to sulfate competition of being pre-adsorbed, thus covering the reactive sites already at the moment of sulfate addition, whereas in the other experiment both sulfate and phosphate were added at the same time.

### 4.2.3 Determination of the specific surface area after removal of the organic matter

A determination of the organic matter content of the original clay according to KURMIES (1949) indicated a value of 1.86 %.

Part of the Na-illite stock suspension was treated with 30 % peroxide to destroy the organic matter. This treatment causes a decrease of the pH, probably due to the formation of organic acids (of which one may even smell acetic acid). These acids were removed by stirring with equivalent amounts of Na and OH resins until the original pH of the suspension was reached. Then the organic matter free clay was used for specific surface area determination. The results are shown in table 27.

Table 27. Determination of the specific surface area of a fraction  $< 2\mu$  of Winsum illite (tracer method) after removal of the organic matter. The data presented are the mean values of duplicate measurements

No.	pH	$N_0$ (me./ml)	$1/\sqrt{\beta N_0}$ (Å)	$d (= Q'/\sqrt{\beta N_0} - \delta)$ (Å)	$V_{90}$ (ml/g clay)	$S (= V_{90}/d)$ (m <sup>2</sup> /g clay)
1	5.72	$1.51 \times 10^{-3}$	79.5	158.0	4.25	269
2	5.68	$2.06 \times 10^{-3}$	67.8	134.6	3.62	269
3	5.47	$4.77 \times 10^{-3}$	44.6	88.2	2.36	267
4	5.32	$6.82 \times 10^{-3}$	37.2	73.4	2.01	274
5	5.05	$1.61 \times 10^{-2}$	24.5	48.0	1.32	275
						average 271

The specific surface area of the clay decreased upon peroxide treatment from 306 to 271 m<sup>2</sup>/g, yielding a value for the specific surface area of the organic substances on the basis of the above data of about 1,800 m<sup>2</sup> per gram.

Only very few data on the surface area of organic matter can be found in the literature. LYON *et al* (1952) suggested this value to be about 3 to 4 times higher than that of montmorillonite, which then would give roughly 3,000 m<sup>2</sup>/g. This, however, was based upon measured values of the cation exchange capacity. Since there are no indications that the surface charge density of the organic substances equals that of montmorillonite the conclusion on the above basis seems rather premature. According to FLAIG and BEUTELSPACHER (1954) one should visualize the humic substances of soils as spheres, of which the diameter would be about 30–50 Å as calculated from data of diffusion measurements. If one accepts these values the specific surface area is found as 2,000 to 1,200 m<sup>2</sup>/g, respectively, assuming a density of 1. These numbers should be considered as minimum values since they account only for the outer surface of perfect spheres of mentioned size. The values would be greater for irregular shapes, whereas the internal surface would probably contribute to a certain degree.

Although the results of the above experiment may certainly not be used to give a definite number for the specific surface area of organic matter in the present sample,



the measured value of 1,800 m<sup>2</sup> per gram may be regarded as indicative for the order of magnitude. Obviously a number of general validity will hardly exist, as the specific surface area of organic matter will depend on the specific nature of the organic compounds, which may differ with the type of soil.

#### 4.2.4. The adsorption of phosphate on Na-illite before and after removal of the organic matter

The adsorption isotherm of phosphate for Na-illite was determined in the manner as described in section 4.1.7.2. In this case, however, the phosphate concentration in the dialyzates could not be ascertained from count data and calculated values for the specific activity of P<sup>32</sup> since the original sample contained already an unknown amount of phosphate. Therefore the phosphate concentration of the dialyzates was measured colorimetrically (cf section 3.4).

The calculation of the net P adsorption was performed in the same way as is shown in tables 17, 18 and 19. For the specific surface areas of the unpretreated and pretreated clay values of 306 and 271 m<sup>2</sup>/g, respectively, were taken. A summary of the calculated and measured data is given in table 28 and represented as adsorption isotherms in figure 36.

Table 28. The positive adsorption of phosphate on Na-illite (Winsum) before and after removal of the organic matter (series I and II, respectively). The data presented are the mean values of duplicate measurements

No.	pH	N <sub>0</sub> (me./ml)	P conc. in dialyzate (μg P/ml)	Expected neg. adsorption (μg P/g clay)	V <sub>incl.</sub> measured (ml/g clay)	Over-all pos. adsorption (μg P/g clay)	Net pos. adsorption (μg P/g clay)
I.1	6.40	5.03 × 10 <sup>-4</sup>	0.7	5.4	27.73	19.4	24.8
.2	6.42	1.41 × 10 <sup>-3</sup>	1.0	5.3	21.15	21.2	26.5
.3	7.40	4.15 × 10 <sup>-3</sup>	20.5	74.9	7.72	158.2	233.1
.4	8.30	7.91 × 10 <sup>-3</sup>	61.4	161	3.36	207	368
.5	8.94	1.66 × 10 <sup>-2</sup>	169	308	0.69	117	425
II.1	6.28	6.65 × 10 <sup>-4</sup>	0.3	1.9	230.4	69.1	71.0
.2	6.05	1.43 × 10 <sup>-3</sup>	1.5	6.6	100.0	150.0	156.6
.3	6.70	4.32 × 10 <sup>-3</sup>	21.5	56.2	21.50	462.3	519
.4	7.05	7.44 × 10 <sup>-3</sup>	54.0	112	11.02	595.1	707
.5	8.83	1.51 × 10 <sup>-2</sup>	133	216	4.46	594.1	810

These data give a clear demonstration of the fact that an unambiguous interpretation of anion adsorption data requires a correction for anion exclusion. If one would confine oneself to the over-all (apparent) adsorption, which equals the value as it is measured from the inclusion volume and the equilibrium concentration, one would conclude from points 4 and 5 of series I in table 28 that the positive adsorption starts decreasing again at these high phosphate concentration levels. After correction for negative adsorption one finds, however, that the net positive adsorption is still

increasing. A comparable situation was found with respect to several points of table 17, showing an over-all adsorption which was negative, although a net positive adsorption was present.

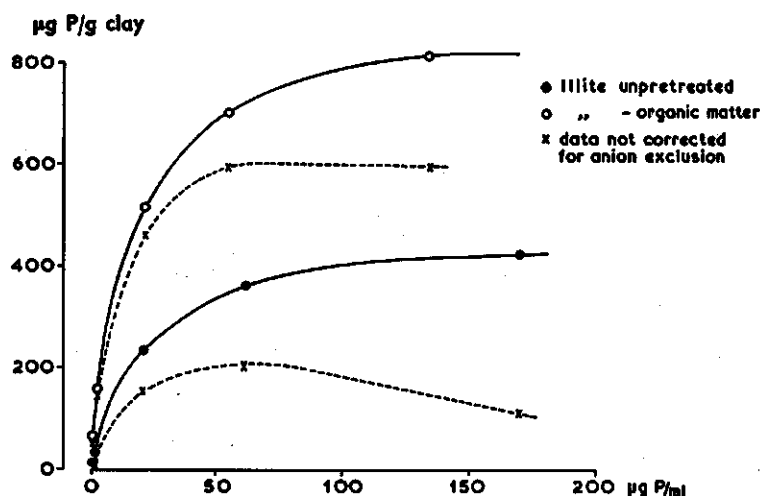


Fig. 36. Phosphate adsorption isotherm for illite, before and after removal of organic matter

The removal of organic matter showed a considerable influence on the phosphate adsorption, the maximum adsorption value for the pretreated sample being roughly two times higher than that for the untreated one. This difference is attributed to the fact that the organic matter in soils probably covers the reactive sites on the clay minerals, at least in part, thus preventing the phosphate adsorption to a certain degree.

Further details on the adsorption isotherms are given in section 4.4.

The effect of the pH was studied in a separate experiment in which the adsorption of phosphate on both the pretreated and untreated illite was measured at different pH values (obtained again by additions of HCl and NaOH). The results are listed in table 29.

Table 29. The net adsorption of phosphate on Na-illite as a function of the pH

	illite untreated				illite - org. matter		
pH	4.58	6.34	8.59	11.64	4.67	6.26	8.41
eq. conc. ( $\mu\text{g P/ml}$ )	51.8	52.6	51.4	59.1	42.0	42.6	42.2
net pos. ads. ( $\mu\text{g P/g clay}$ )	340	354	342	164	654	638	646

It is noted that the amounts adsorbed check well with the adsorption isotherms of figure 36. Apparently no pH influence is present in the pH range from about 4.5

to about 8.5. At extremely high pH values (about 11.5), however, the phosphate adsorption decreased considerably, probably due to the competitive effect of OH ions at this high pH level.

#### 4.2.5 Reduction of the negative adsorption of sulfate in Na-illite systems with interacting double layers

The experimental procedure was identical with that described in section 4.1.9. In this case, however, not the anion exclusion of chloride but that of sulfate was measured. The composition of the systems was chosen such that only trace amounts of sulfate were present, resulting in a  $f^=$  value of 0.0 and accordingly a  $Q_a'$  value of 2.667. The use of almost carrier free  $S^{35}$  allowed lower electrolyte levels than in the comparable  $Cl^-$  experiment. Since clay contents of about 11 % were involved the lowest value of  $D \cdot \sqrt{\beta N_0}$  was about 1.85 against 2.11 in the  $Cl$ -montmorillonite

Table 30. Comparison between the theoretically expected and the measured decrease of the negative adsorption of  $SO_4^{2-}$  in Na-illite systems with interacting double layers. ( $f^= = 0.0$ )

No.	Clay content (%)	$D$ (Å)	$N_0$ (me./ml)	$\frac{1}{\sqrt{\beta N_0}}$ (Å)	$D \cdot \sqrt{\beta N_0}$	Theor. expected decrease according to fig. 9 (%)	$d^=$ (Å)	$V_{\infty}$ expected for spec. surface area of 306 m <sup>2</sup> /g	$V_{\infty}$ measured (ml/g clay)	Measured decrease (%)
1	11.284	256.9	$4.82 \times 10^{-4}$	139.9	1.84	34.5	372.5	11.40	7.40	35.1
2	10.843	268.7	$4.66 \times 10^{-4}$	142.3	1.89	33.0	378.5	11.58	7.78	32.8
3	9.927	296.5	$4.23 \times 10^{-4}$	149.3	1.99	29.0	397.2	12.15	8.70	28.4
4	9.136	325.0	$4.15 \times 10^{-4}$	150.8	2.16	23.5	401.2	12.28	8.93	27.3
5	5.021	618.2	$2.64 \times 10^{-4}$	189.1	3.27	5.5	503.3	15.40	14.52	5.7

experiment. Moreover, the exclusion of a divalent anion is more sensitive towards double layer interaction than that of monovalent anions at the same  $D \cdot \sqrt{\beta N_0}$  values, as may be seen in figure 9. Under the above conditions the maximum expected decrease amounted to about 35 %. Results are given in table 30, indicating that again a very good agreement was found between the theoretically predicted and the measured reduction of the negative adsorption, except perhaps for point no 4.

#### 4.2.6 Determination of the specific surface area of the total fraction $< 2\mu$ of Winsum illite

To this purpose the total fraction  $< 2\mu$  of the Winsum soil was collected by suspending about 300 grams of soil in 10 liter distilled water. Then the fraction was

syphoned off repeatedly until the solution was clear over the depth of syphoning. In this manner about 40 liters suspension with a very low clay content were obtained. This suspension was concentrated by use of Chamberlain filters to a clay concentration of about 6 %, and passed through columns with Na and Cl resins to attain a homoionic Na-Cl-composition. The surface area determination from  $\text{Cl}^-$  exclusion (tracer method) gave results as shown in table 31.

Table 31. Determination of the specific surface area, employing  $\text{Cl}^-$ , of the total fraction  $< 2\mu$  of Winsum illite. The data presented are the mean values of duplicate measurements

No.	pH	$N_0$ (me./ml)	$1/\sqrt{\beta N_0}$ (Å)	$d^- = (Q'/\sqrt{\beta N_0 - \delta^-})$ (Å)	$V_{\text{ex}}$ (ml/g clay)	$S (= V_{\text{ex}}/d^-)$ (m <sup>2</sup> /g clay)
1	6.52	$2.36 \times 10^{-3}$	63.2	125.4	2.06	164
2	6.50	$3.15 \times 10^{-3}$	54.7	108.4	1.76	162
3	6.48	$5.92 \times 10^{-3}$	39.8	78.6	1.32	168
4	6.40	$7.48 \times 10^{-3}$	35.5	70.0	1.11	158
5	6.24	$1.70 \times 10^{-2}$	23.9	46.8	0.72	154
						average 161

The mean value of the surface area of the total fraction  $< 2\mu$  was 161 m<sup>2</sup>/g and thus amounted to only 55 % of the value for the fraction used in the foregoing illite experiments. The difference found is attributed to the presence of a substantial amount of relatively coarse particles in the total fraction  $< 2\mu$ . This was supported by the results of the determination of particle size distribution. It was found that the fraction  $< 0.2 \mu$  constituted about 51 % of the "total" fraction  $< 2\mu$ , as against 83 % of the "incomplete" fraction  $< 2\mu$  used before.

### 4.3 Experiments with kaolinite

#### 4.3.1 The interaction between chloride and Na-kaolinite

The chloride exclusion and the ensuing value of the specific surface area of Dry-branch kaolinite, fraction  $< 2\mu$ , were determined by means of an experiment similar to those described in the foregoing sections.

As regards the influence of pH on the surface charge of clay particles the relevant literature (FRIPIAT *et al*, 1954; CASHEN, 1959; SCHOFIELD, 1949) indicates that, among the common clay minerals, kaolinite is a prime example of such influence. As was mentioned before such a variation in charge may affect the anion interaction, the adsorption then becoming a function of the pH. Although the increase of positive anion adsorption with an increasing number of positive sites at low pH values is self-evident, the interpretation of an influence of pH in the high range values would be more involved. This follows from the fact that anion exclusion is little sensitive

towards the surface density of charge, once a certain minimum value of a surface density of *negative* charge has been reached (cf the value of  $\delta$ , equation 2.2). Thus in as far as the anion-clay interaction is solely of an electrostatic nature (i.e. a combination of Coulombic adsorption at positive sites and exclusion at negative sites) one should expect a gradually diminishing influence of an increase in pH once the positive sites have become obliterated.

On the other hand the chemi-sorption of anions (specifically that on a surface which was electrically neutral or negatively charged prior to the chemi-sorption) might become increasingly sensitive towards increasing pH values. This would result from either a counteraction of chemi-sorption through the built-up of a repulsive electrostatic energy – following the increased negative charge of clay surface and/or adsorbed anion – or from the direct competitive action of (probably also chemi-sorbed) OH ions.

Summarizing one might state that the magnitude of the effect at high pH depends on the nature of the interaction between anion and clay at about neutral pH: if this interaction is a repulsion, increase of pH will exhibit a minor influence only, whereas in the case of positive adsorption a notable decrease of the latter may occur.

Table 32. Determination of the specific surface area of Na kaolinite (Drybranch), fraction  $< 2\mu$ . The data presented are the mean values of duplicate measurements

No.	pH	$N_0$ (me./ml)	$1/\sqrt{\beta N_0}$ (Å)	$d^-$ (Å)	$V_{as}$ (ml/g clay)	Spec. surface area (m <sup>2</sup> /g clay)
1	6.15	$9.80 \times 10^{-4}$	98.4	194.8	0.88	45
2	5.86	$2.99 \times 10^{-3}$	56.2	110.4	0.54	49
3	5.85	$4.90 \times 10^{-3}$	43.9	85.8	0.41	48
4	5.70	$8.72 \times 10^{-3}$	32.9	63.8	0.32	50
5	5.60	$1.28 \times 10^{-2}$	27.2	52.4	0.27	51
mean value						49

Results of the Cl<sup>-</sup> exclusion measurements with Na-kaolinite are presented in table 32. As expected, a minor variation of pH with different salt levels was found. However, exclusion data resulted in values for specific surface area which were very near to each other, with an average value of 49 m<sup>2</sup>/g. This indicates that over the employed pH range from 5.6 to 6.2, any variation of positive surface charges – if the latter were present at all – was negligible.

The influence of low pH values on the electric charge of kaolinite, as evidenced by the change of the interaction with Cl<sup>-</sup>, was measured in a separate experiment. To this purpose a series of systems was prepared in which the total electrolyte level was kept constant at roughly  $10^{-2}$  N, while different levels of H ion concentrations were effected by additions of HCl solutions. The experiment was then conducted in the normal way, employing Cl<sup>36</sup>.

After equilibration the dialyzates were used for the determination of the total

electrolyte level by means of conductivity measurements, whereas at the same time the  $\text{Cl}^-$  concentration was determined potentiometrically. As is shown in table 33 these values were very nearly the same. The net positive chloride adsorption was calculated again from the measured adsorption data corrected for the theoretically expected exclusion values, as based on the measured specific surface area of  $49 \text{ m}^2/\text{g}$

Table 33. The influence of the pH on the positive adsorption of chloride by Na kaolinite (Drybranch). The data presented are the mean values of duplicate measurements

No.	pH	$N_0$ (me./ml)	$\text{Cl}^-$ conc. (me./ml)	$d^-$ (Å)	Theor. neg. adsorption ( $\mu\text{e.}/\text{g}$ clay)	$V_{\text{ex}}$ measured (ml/g clay)	Neg. adsorption measured ( $\mu\text{e.}/\text{g}$ clay)	Net pos. adsorption of chloride ( $\mu\text{e.}/\text{g}$ clay)
1	3.28	$1.02 \times 10^{-3}$	$0.98 \times 10^{-3}$	59.0	2.8	-0.32	-3.1	5.9
2	3.74	$1.02 \times 10^{-3}$	$0.97 \times 10^{-3}$	59.0	2.8	-0.04	-0.4	3.2
3	4.16	$1.06 \times 10^{-3}$	$0.99 \times 10^{-3}$	58.2	2.8	0.12	1.2	1.6
4	4.68	$0.98 \times 10^{-3}$	$0.93 \times 10^{-3}$	59.4	2.7	0.23	2.1	0.6
5	5.01	$1.02 \times 10^{-3}$	$0.95 \times 10^{-3}$	59.0	2.8	0.27	2.6	0.2
6	5.52	$1.10 \times 10^{-3}$	$0.99 \times 10^{-3}$	57.2	2.8	0.28	2.9	-0.1
7	6.13	$1.07 \times 10^{-3}$	$0.98 \times 10^{-3}$	58.0	2.8	0.27	2.7	0.1

(cf table 32). Figure 37 presents a plot of the net positive chloride adsorption versus the pH, showing that over the pH range from 5.2 to about 3.3 the net adsorption increased with about  $6 \mu\text{e. Cl}$  per gram clay.

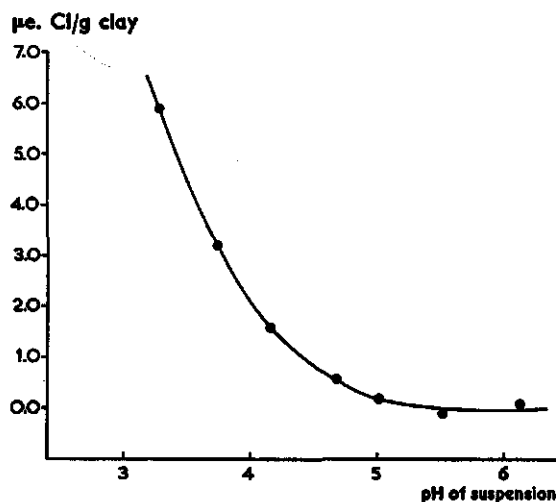


Fig. 37. The positive adsorption of chloride on Na-kaolinite as influenced by the pH

The effect in the high pH range was tested by measurement of  $V_{\text{ex}}$  values in two systems, in which the pH was increased by NaOH additions. The total electrolyte

levels ( $N_0$ ) were found as  $7.05 \times 10^{-3}$  and  $2.37 \times 10^{-2}$  N for the systems with pH values of 8.72 and 9.36, respectively.  $V_{ex}$  values amounted to 0.348 and 0.188 ml/g clay, indicating a specific surface area of 48.9 and 49.5 m<sup>2</sup>/g clay, respectively. Thus it was found that the exclusion of chloride remained constant over a pH range from about 5.5 to about 9.5. In view of the considerations given at the beginning of this section it thus seems obvious that the interaction between chloride and this kaolinite is governed by electrostatic forces only. At the same time it seems unlikely that a positive charge, if present, would remain constant over such a wide pH range. It is concluded that positive (edge) charges are absent above a pH of about 5. It remains possible, however, that these edges become negatively charged above this pH; such an effect would remain undetected with the methods employed.

#### 4.3.2 The positive adsorption of phosphate on Na-kaolinite

Also for Na-kaolinite the adsorption of phosphate was studied in an experiment comparable to those described before. Experimental results are shown in table 34 and plotted as a phosphate adsorption isotherm in figure 38. The general shape of this isotherm is slightly different from the ones for montmorillonite and illite. In this case the adsorption has not yet reached its maximum value at the highest phosphate concentrations employed.

Table 34. The positive adsorption of phosphate on Na-kaolinite (Drybranch). The data presented are the mean values of duplicate measurements

No.	pH	$N_0$ (me./ml)	P conc. in dialyzate ( $\mu\text{g P/ml}$ )	Expected neg. adsorption ( $\mu\text{g P/g clay}$ )	$V_{\text{tot.}}$ measured (ml/g clay)	Over-all pos. adsorption ( $\mu\text{g P/g clay}$ )	Net pos. adsorption ( $\mu\text{g P/g clay}$ )
1	6.51	$5.75 \times 10^{-4}$	0.7	0.9	8.35	5.9	6.8
2	7.06	$1.67 \times 10^{-3}$	3.5	3.0	3.32	11.6	14.6
3	8.69	$4.98 \times 10^{-3}$	30.0	16.2	1.33	39.9	56.1
4	9.80	$9.41 \times 10^{-3}$	83.6	32.4	0.93	77.8	110.2
5	10.61	$1.78 \times 10^{-2}$	163	46.0	0.72	117.4	163.4

#### 4.4 Analysis of the phosphate adsorption data

In order to distinguish between different adsorption mechanisms of phosphate, if present, it was attempted to analyze the phosphate adsorption isotherms presented before. Taking as a point of departure that the adsorption of phosphate on a certain site follows, at least roughly, the Langmuir adsorption equation (COLE, *et al*, 1953; FRIED and SHAPIRO, 1956; OLSEN and WATANABLE, 1957), one may put for such a site:

$$P_a = \frac{b \cdot C \cdot P_m}{1 + b \cdot C} \quad (4.1)$$

with  $P_a$  and  $C$  the adsorbed amount of phosphate and the concentration in solution, respectively;  $P_m$  represents the maximum adsorption value and  $b$  stands for the reaction constant of the adsorption process.

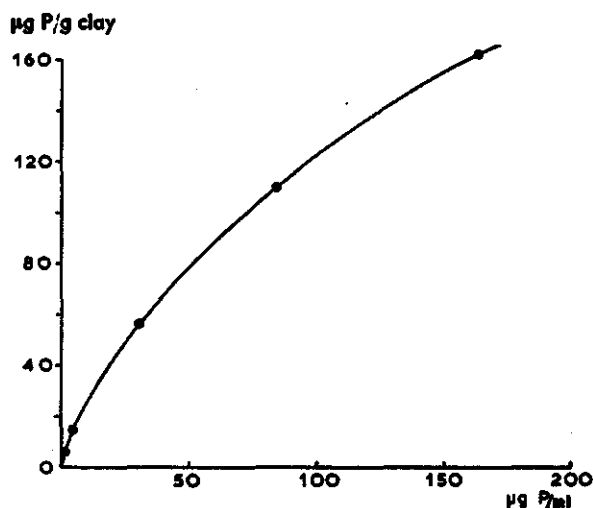


Fig. 38. Phosphate adsorption isotherm for kaolinite

As follows from equation (4.1):

$$P_a = P_m - \frac{1}{b} \cdot P_a/C \quad (4.2)$$

It should perhaps be noted (cf HITCHCOCK, 1926) that the Langmuir equation follows directly from the application of the mass action law to two adsorbates competing for the same adsorber, the constant  $b$  then corresponding to the ratio of the preference factor for the primary adsorbate (i.e.  $P$ ) relative to the competing adsorbate (i.e. possibly OH or silicate, assumed to be at a constant concentration), and the concentration of the latter. The above equation (4.2) is thus principally the same as that derived by SHAPIRO and FRIED (1959), employing mass action considerations, viz.:

$$\text{Soil-P} = -K \cdot \frac{\text{Soil-P}}{(P)} + \sum \text{Soil-P} \quad (4.3)$$

with  $K$  = an apparent dissociation constant,  $(P)$  = phosphate concentration in solution and  $\sum \text{Soil-P}$  = the amount adsorbed when all adsorption sites are saturated with phosphate.

The advantage of plotting the Langmuir equation according to (4.2) becomes obvious when the simultaneous presence of more than one type of adsorbing sites is considered, since such a plot allows a resolution of the resultant adsorption isotherm into the composing isotherms of the separate adsorption mechanisms.



For the case of two different types of adsorption sites one may introduce the quantities  $P_{a1}$ ,  $P_{a2}$  and  $P_a$  for the amounts adsorbed by the two types of sites, and the combined adsorption, respectively. Since the amounts adsorbed are functions of the concentration in solution,  $C$ , one finds at any particular value  $C_p$ :

$$P_a(C_p) = P_{a1}(C_p) + P_{a2}(C_p) \quad (4.4)$$

Plotting now separately the three isotherms according to equation (4.2), i.e.  $P_{a1}$  against  $P_{a1}/C$ ,  $P_{a2}$  against  $P_{a2}/C$  and  $P_a$  against  $P_a/C$  one finds that in all three isotherms the points corresponding to  $C = C_p$  are situated on a line through the origin with a slope equal to  $\tan \theta_p = C_p$ . Indicating the distance of these points to the origin with  $r_1$ ,  $r_2$  and  $R$  one then finds:

$$\begin{aligned} r_1 &= P_{a1} \cdot \sqrt{1 + 1/C_p^2} \\ r_2 &= P_{a2} \cdot \sqrt{1 + 1/C_p^2} \\ R &= P_a \cdot \sqrt{1 + 1/C_p^2} \end{aligned} \quad (4.5)$$

Combining with equation (4.4) one thus concludes:

$$R = r_1 + r_2$$

Accordingly the plot of  $P_a$  against  $P_a/C$  is found from the corresponding plots of  $P_{a1}$  and  $P_{a2}$  by simple addition along lines drawn through the origin.

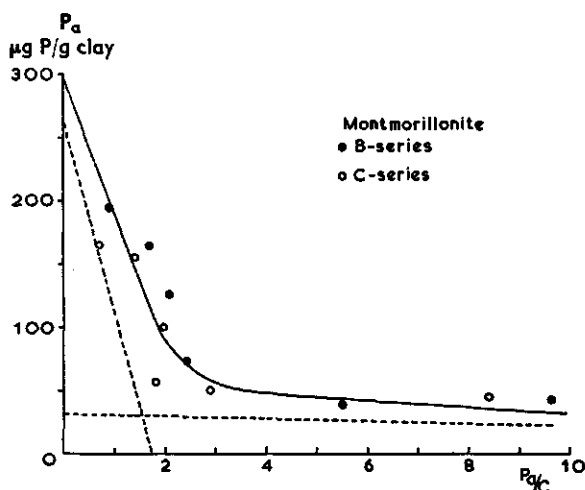


Fig. 39. Analysis of the phosphate adsorption isotherm for montmorillonite

Conversely, a plot of  $P_a$  against  $P_a/C$  may be resolved into the composing isotherms by a reverse procedure in which the lines through the origin are divided into sections corresponding to the distances to the origin of the composing isotherms. Such a division is possible only if the nature of the composing isotherms is known. Assuming these to be linear (consistent with the assumed existence of Langmuir adsorption isotherms) one may, in principle, compute the composing lines from  $2n$  points of the overall adsorption isotherm,  $n$  being the number of primary reaction mechanisms involved. In the case that only two primary reaction mechanisms are present one may show that the resultant isotherm

is a hyperbola, the primary isotherms constituting the asymptotes. Then a graphical procedure may replace the tedious computations suggested above.

This construction of the "primary" lines reads as follows. First the experimental curve is extrapolated to both axes. Next the point of maximum curvature is located and a normal to the curve at that point is constructed. The intersection point of this normal with the replica of the experimental curve drawn at half distance from the origin is then the intersection point of the two asymptotes which are sought. These must then be situated symmetrically with respect to the normal constructed before, while their abscissa and ordinates must sum up to the same of the experimental curve.

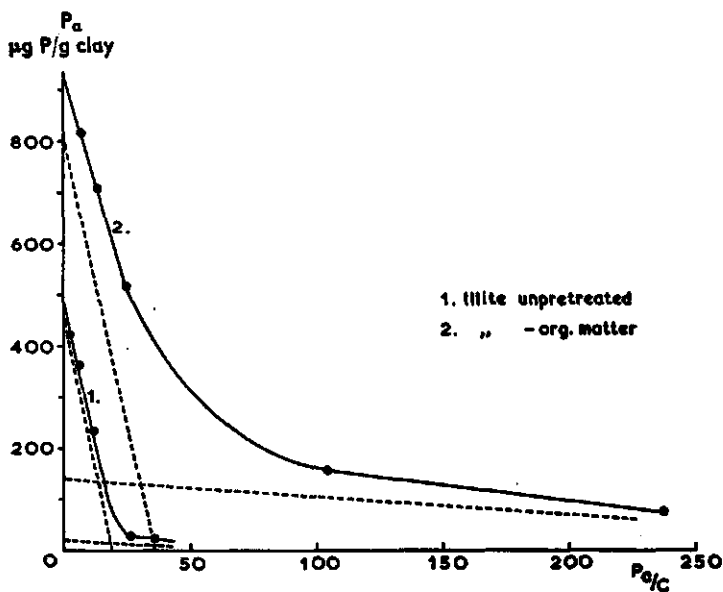


Fig. 40. Analysis of the phosphate adsorption isotherms for both illites

Such a resolution of curves into two straight lines has been applied by several authors, mainly in relation to the uptake of ions by plants, a.o. HAGEN and HOPKINS (1955); FRIED and NOGGLE (1958) and YOSHIDA (1964). This procedure was first proposed by HOFSTEE (1952) with respect to enzyme reactions.

The experimental data corresponding to the adsorption isotherms of figures 27, 36 and 38 were plotted according to equation (4.2) in figures 39, 40 and 41 for montmorillonite, illite before and after removal of organic matter, and kaolinite, respectively. The resulting curves all show a markedly similar shape, viz. a quite strongly curved line which one may easily visualize to be constituted by at least two straight ones.

It should be emphasized that in the present case the above treatment is open for criticism in view of the limited accuracy of the measurements. Thus considering the isotherm for montmorillonite (cf figure 27) one may wonder whether this procedure has any significance since the experimental points are relatively widely scattered

around the adsorption isotherm. On the other hand, the data for the illites and kaolinite (cf figures 36 and 38) yielded adsorption isotherms of which the positions were much more unambiguous; thus the reliability of the proposed treatment may be assumed to be higher for the latter samples. Application of the same procedure to the montmorillonite data in spite of the above objections may be justified by the striking similarity with the other curves.

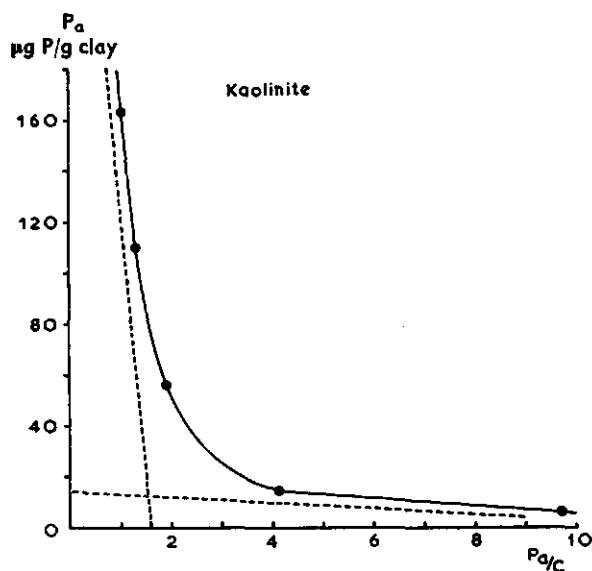


Fig. 41. Analysis of the phosphate adsorption isotherm for kaolinite

The application of this approach to the curves of figures 39, 40 and 41 resulted in the dotted lines indicated in these figures. It thus seems very likely that two reaction mechanisms are involved in the adsorption of phosphate ions on the three types of clay minerals studied, viz. a very strong adsorption and a relatively weak one. An estimate of the reaction constants and maximum adsorption values for the two mechanisms is presented in table 35. It was thus found that the reaction constant of the strong adsorption was about 50–150 times larger than that of the weak adsorption.

Table 35. Reaction constants and maximum values for the adsorption of phosphate on clays

Clay	$b_1$ ( $\mu\text{g P/ml}$ ) <sup>-1</sup>	$b_2$	$P_{m1}$ ( $\mu\text{g P/g clay}$ )	$P_{m2}$
montmorillonite (Osage)	0.9	0.006	30	260
illite unpretreated (Winsum)	2.7	0.045	20	460
illite — organic matter	2.7	0.042	140	800
kaolinite (Drybranch)	0.8	0.005	15	?

It is interesting to note that the reaction constants for both the untreated and pretreated illite samples were almost identical, indicating that the rôle of organic matter with respect to phosphate adsorption was probably limited in this sample to a passive one, just preventing the phosphate ions to be adsorbed, rather than an active interference (e.g. adsorption of phosphate on the organic matter itself). From the  $P_m$  values for both illites one must conclude that proportionally more places suitable for the strong than for the weak adsorption were covered by the organic substances, since removal yielded an increase in  $P_{m1}$  of a factor 7 as against a factor 2 for  $P_{m2}$ .

Considering all phosphate adsorption data described, it seems perhaps warranted to present some suggestions as to the general pattern of the phosphate bonding mechanism itself. It should be stipulated in advance, however, that such suggestions have necessarily a quite tentative character and cannot be completely unambiguous, since the systems used were still of a too complicated nature to allow definite conclusions.

Visualizing the possible adsorption sites for phosphate bonding in the systems studied, these may be enumerated as: organic matter, free aluminum and iron compounds, and reactive sites on the clay minerals themselves. The precipitation of phosphate as calcium phosphate compounds, an important feature in phosphate-soil interaction studies, can be left out of consideration here since the clays involved in the phosphate adsorption experiments were used in the homoionic sodium form.

Organic matter can be ruled out as a possible cause for phosphate adsorption, at least in the form in which it was apparently present in the clay studied (Winsum, fraction  $< 2\mu$ , homoionic Na-form), since removal of the organic matter yielded a considerable increase of the adsorbed amount instead of a decrease. This conclusion does not imply that organic matter, as it may be present in soils, would not be a possible source for phosphate adsorption. Indeed, evidence may be found in the literature for the occurrence of organic phosphate compounds in soils, although little is known about their actual nature. From the experience gained in section 4.2.4 it may be concluded anyhow that the adsorption of phosphate in the organic forms, if present at all, is negligible in comparison to the other possibilities listed above.

As regards the bonding of phosphate to aluminum and iron compounds it may be suggested that this mechanism follows basically the solubility product principle. As was pointed out by Hsu and RENNIE (1962), and Hsu (1964), in that case the action of all forms of Al and Fe, including amorphous aluminum hydroxides and iron oxides or hydroxides, are a concern in governing the phosphate concentration in solution and accordingly the phosphate adsorption. The precipitation as aluminum and iron phosphates is strongly dependent upon the pH of the system, a minimum solubility of aluminum phosphates prevailing in the pH range from roughly 4.5 to 6.5, of iron phosphates from about 3 to 5. It may be assumed that iron probably played a minor role in this respect in the foregoing experiments, because it was not present at a detectable concentration in the dialyzates of the clays.

Considering the effect of the pH on the phosphate adsorption (cf e.g. figure 32),

also the rôle of free aluminum seems illusory at first sight, since one should then expect a much stronger dependency over almost the complete pH range instead of the plateau found. The upper curve of the above figure represents the pH dependency at "zero" silicate treatment. This, however, does not imply that the actual silicate concentration in the systems was zero. On the contrary, dialyzates of clays show under normal conditions invariably the presence of silicate, although at fairly low concentrations. Thus assuming that the silicate level amounted in these unpretreated systems to e.g.  $10^{-5} - 10^{-4}$  N, it seems warranted to conclude that, in line with the pH influence at the other, induced, silicate concentrations, the pH dependency increases with decreasing silicate concentrations. A maximum pH dependency (i.e. over the entire pH range) would thus perhaps occur only in the absence of silicate.

If the precipitation of aluminum phosphates would be of considerable concern in comparison with other reaction mechanisms, one should expect a completely different adsorption - pH curve, viz. a maximum adsorption in the intermediate pH range, with decreasing adsorption values at *both* increasing and decreasing pH.

In opposition to the above it might be reasoned that the observed "strong" adsorption could still be related to the precipitation with free aluminum. The amounts adsorbed according to this mechanism would then be too small in comparison with the total adsorption capacity (cf values of  $P_m$ , in table 35) to exert a noticeable influence. The pH influence upon the total (combined) adsorption could then still deviate from the one expected from solubility considerations. As listed previously,  $P_{m1}$  values indeed amounted to roughly 10 % only of the total phosphate adsorption capacity. Closer consideration indicates, however, that the observed pH effects referred to systems with P concentrations, at which  $P_{m1}$  constituted a major part of the total phosphate adsorption. For lack of further information it is concluded that co-precipitation of P with free Al ions played a minor role in comparison to other bonding mechanisms.

Thus remains the adsorption of phosphate on the clay minerals themselves as the predominant type of bonding under the experimental conditions employed. This bonding should apparently be looked upon much more as a chemical reaction between phosphate and clay rather than as an electrostatic attraction, as was evidenced by e.g. the sulfate-phosphate competition (cf section 4.1.5) and the effect of high pH on the adsorption values. It seems obvious that the adsorption takes place at the clay edges and /or imperfections. It might be considered more or less as an extension of the clay crystal lattice,  $PO_4$  groups functioning in a manner comparable to the silicate groups in the lattice. This hypothesis was supported by the observed influence of organic matter on P adsorption, the organic material presumably also being attached at the edges rather than at the planar sides.

It has indeed been found that  $PO_4$  may replace  $SiO_4$  groups under certain conditions. Thus it was indicated by MASON and BEGGREN (1941) that in phosphorus-bearing minerals  $PO_4$  groups substituted as much as 25 per cent of the  $SiO_4$  groups. According to BLACK (1960), these substitutions were presumably established during the process of lattice crystallization. LOW and BLACK (1950) pointed to the fact that at *high* phosphate levels the surface  $SiO_4$  groups of kaolinite may partially be replaced by  $PO_4$  groups. The present experiments, however, indicated a preference of silicate

above phosphate, which is reasonable if one realizes that the silicate ions will fit better into the crystal lattice. Accordingly, a considerable excess of phosphate would be required in order to attain a measurable phosphate adsorption in the presence of silicate.

If one confines oneself to the aluminosilicate clay minerals of interest here, the general constitution of the mineral lattice may be described as sheets of alumina and silica layers; the alumina layers may be simply alternating with silica layers (1 : 1 type; kaolinite), or be bounded on both sides by silica sheets (2 : 1 type; montmorillonite and illite). Successive Al atoms in the alumina layer share O-atoms with tetra coordinated Si of the upper (or lower) Si layer in addition to sharing OH groups. At the surface of gibbsite they share OH groups only. Now one may visualize that at the edge of a clay mineral, lattice pairs of Al atoms which share normally bonds with OH groups (thus forming the edge-situated aluminum hydroxides), become preferentially bonded to silicate or phosphate groups, if present at satisfactory concentration. The result would then be a bonding between edge-Al and tetra-edges of  $\text{SiO}_4$  or  $\text{PO}_4$ , comparable to the situation in the lattice between the alumina and silica sheets. The position of the tetra-edges, however, is different, viz. not extending the silica layer but the alumina layer. This different position presumably prevents a further extension of the lattice, once all sites are saturated with silicate or phosphate groups.

The above generalized picture is in agreement with the observed phenomena with respect to the adsorption of silicate and phosphate, and probably also of OH (the latter at high pH values).

It may be shown that the amount of phosphate corresponding to the maximum adsorption value can easily be stored at the edges of the clay. The thickness of the elementary aluminosilicate layer amounts to 10 Å for montmorillonite and illite, and 6 Å for kaolinite. The length dimensions of the platelets may have a very wide variation. Electron microscope photographs <sup>1)</sup> of the montmorillonite used showed values of about 2,500 Å, indicating a specific surface area of these platelets of roughly  $12 \times 10^6 \text{ Å}^2$ . According to the specific surface area of the clay (700  $\text{m}^2/\text{g}$ ), the total number of platelets per gram montmorillonite is about  $0.6 \times 10^{16}$ . Assuming the distance between the Al atoms at the edges to be 5 Å (cf WEY, 1956), each platelet contains about 2,000 edge-situated Al atoms, which according to the above given concept may be bonded in pairs to  $\text{PO}_4$  ions. This means that the total number of reactive sites amounts to roughly  $0.6 \times 10^{19}$  per gram montmorillonite, which corresponds to 10  $\mu\text{e}$ . phosphate or about 300  $\mu\text{g}$  P. The total phosphate adsorption capacity of montmorillonite was found as 290  $\mu\text{g}$  P/g clay, indicating that maximum adsorption corresponds to complete coverage of the edges.

According to the ratio between the specific surface area of the montmorillonite and the illite used (700 and 160  $\text{m}^2/\text{g}$ , respectively) one must conclude that the illite

<sup>1)</sup> courtesy of the Stichting Technische en Fysische Dienst voor de Landbouw, Wageningen

minerals consist of 4-5 aluminosilicate layers attached together, amounting to a thickness of the platelets of 40-50 Å. This is confirmed by the results of electron microscopy. As regards the number of reactive sites at the edges, however, these should stay the same for illite and montmorillonite, provided that the longitudinal dimensions are the same. The phosphate adsorption capacity of illite (after removal of organic matter) was roughly 3 times larger than that of montmorillonite (940 against 290 µg P/g clay, respectively). This would imply that the length dimensions of the illite platelets would be 3 times as small as those for the montmorillonite platelets. Electron microscope photographs supported this point, indicating values for the Winsum illite of roughly 800-1,000 Å.

A precise value of the maximum phosphate adsorption on kaolinite could not be given (cf figures 38 and 41). This becomes understandable if one realizes that in kaolinite also one of the planar surfaces exists of AlOH groups. The maximum capacity, calculated on the basis of one P per two Al groups, would then be about 2,700 µg P/g kaolinite, assuming a specific surface area of about 50 m<sup>2</sup>/g. In addition the edges will accomodate a certain amount of P. It would seem logical that for a planar surface the competition between neighbouring phosphate groups will play an important rôle. Thus it could be expected that a definite maximum adsorption value will only be reached very gradually with increasing P concentrations.

The explanation of the occurrence of two different reaction mechanisms in the phosphate adsorption forms a question that remains unanswered.

## 5 The interaction of chloride and phosphate with soils

### 5.1 Chloride interaction measurements

#### 5.1.1 Determination of the specific surface area according to the exclusion of chloride

The specific surface area of soils may be determined according to different methods, a.o. the ethylene glycol retention method (cf section 3.5), the watervapor-adsorption method (HARVEY, 1943; ORCHISTON, 1953), the mechanical analysis method (PURI, 1949), the ortho-phenantroline method (LAWRIE, 1961) and the low-temperature nitrogen adsorption method (BRUNAUER, EMMETT and TELLER, 1938). In a recent article PURI and MURARI (1963) described a comparison between the results of these methods for a large number of soils, indicating a very good agreement between the data of the different methods.

Most of the above mentioned methods are based upon the measurement of the amount of a certain compound, which is positively adsorbed on the outer surface of the soil material. Therefore the results may be ambiguous, especially in those cases where swelling minerals are involved; then the experimental value is strongly dependent upon the swelling status. In addition to lack of certainty with respect to monolayer coverage by the adsorbent, also the value for the surface area covered per unit adsorbent often remains uncertain.

On the other hand, the value for the specific surface area according to anion exclusion is based on the assumption of a fairly uniform distribution of the surface charge, i.e. the absence of regions with very low charge density. For fairly pure clays, this condition is presumably met to a satisfactory degree. In whole soils, including the coarser material, the charge distribution is certainly far from homogeneous. This, however, is probably not important, since the contribution of the coarser particles to total surface area is very small and almost negligible in comparison to that of the finer ones. On the other hand, the anion exclusion measurements might be invalidated by the presence of organic matter and other substances which might interact with anions (e.g. iron compounds). The present experiment was carried out to evaluate the anion exclusion method for the measurement of the specific surface area of soils.

To this purpose the 12 soils (fraction  $< 50\mu$ ), as described in Chapter 3, were employed for measurement of the chloride exclusion (tracer method). In order to prevent a possibly occurring positive adsorption of chloride, all systems were supplied with a  $\text{Na}_3\text{PO}_4$  solution up to a phosphate concentration of  $10^{-4}$  N, regardless of



the amount of phosphate originally present in the soils. Experimental results are given in table 36.

Table 36. Determination of the specific surface area of 12 Dutch soils (fraction  $< 50\mu$ ) according to the negative adsorption of  $\text{Cl}^-$

Soil	No.	pH	$N_0(\text{me./ml})$	$Q'/\sqrt{\beta N_0} (A)$	$V_{ss}(\text{ml/g soil})$	$S(\text{m}^2/\text{g soil})$
1. Sticky soil	1	5.80	$7.81 \times 10^{-3}$	69.5	0.305	46.6
	2	6.10	$9.36 \times 10^{-3}$	63.5	0.279	46.8
	3	5.79	$1.03 \times 10^{-2}$	62.4	0.257	44.0
	4	5.65	$1.18 \times 10^{-2}$	56.5	0.210	40.7
	5	6.04	$2.94 \times 10^{-2}$	35.5	0.139	44.2
					average	44.5
2. Loess soil	1	7.22	$8.85 \times 10^{-3}$	65.3	0.174	28.4
	2	7.20	$8.99 \times 10^{-3}$	64.8	0.183	30.1
	3	7.12	$1.47 \times 10^{-2}$	50.7	0.134	28.6
	4	7.08	$1.72 \times 10^{-2}$	46.8	0.113	26.4
	5	7.04	$5.23 \times 10^{-2}$	26.9	0.064	28.1
					average	28.3
3. Wilhelmina polder soil	1	7.46	$1.85 \times 10^{-2}$	45.2	0.536	124
	2	7.42	$1.93 \times 10^{-2}$	44.2	0.546	129
	3	7.40	$2.03 \times 10^{-2}$	43.1	0.488	119
	4	7.36	$2.20 \times 10^{-2}$	41.4	0.498	126
	5	7.32	$2.60 \times 10^{-2}$	38.1	0.461	128
					average	125
4. Oss soil	1	7.00	$2.31 \times 10^{-2}$	40.4	0.261	71.8
	2	7.00	$2.48 \times 10^{-2}$	39.0	0.256	73.0
	3	6.92	$2.51 \times 10^{-2}$	38.8	0.252	72.4
	4	6.98	$3.05 \times 10^{-2}$	35.2	0.222	71.3
	5	6.85	$3.61 \times 10^{-2}$	32.3	0.209	73.7
					average	72.4
5. River basin clay soil	1	7.10	$1.53 \times 10^{-2}$	49.7	0.878	184
	2	7.11	$1.61 \times 10^{-2}$	48.4	0.840	181
	3	7.04	$1.71 \times 10^{-2}$	47.0	0.819	182
	4	7.04	$1.93 \times 10^{-2}$	44.2	0.763	181
	5	7.01	$2.54 \times 10^{-2}$	38.5	0.666	183
					average	182
6. Griend soil	1	7.82	$1.49 \times 10^{-2}$	50.3	0.357	73.8
	2	7.85	$1.54 \times 10^{-2}$	49.5	0.357	75.2
	3	7.82	$1.61 \times 10^{-2}$	48.4	0.341	73.6
	4	7.84	$1.87 \times 10^{-2}$	44.9	0.320	74.7
	5	7.83	$2.39 \times 10^{-2}$	39.7	0.278	73.8
					average	74.2
7. Munnikeland soil	1	6.20	$1.42 \times 10^{-2}$	51.6	0.269	56.4
	2	6.12	$1.47 \times 10^{-2}$	50.7	0.277	59.3
	3	6.10	$1.62 \times 10^{-2}$	48.3	0.246	55.6
	4	5.84	$1.71 \times 10^{-2}$	46.9	0.230	53.7
	5	5.88	$2.60 \times 10^{-2}$	38.1	0.188	55.1
					average	56.0
8. Randwijk soil	1	7.00	$1.19 \times 10^{-2}$	56.3	0.513	94.4
	2	6.90	$1.23 \times 10^{-2}$	55.4	0.498	93.3
	3	6.91	$1.35 \times 10^{-2}$	52.9	0.471	92.6
	4	6.85	$1.65 \times 10^{-2}$	47.8	0.413	90.2
	5	6.80	$2.36 \times 10^{-2}$	40.0	0.361	95.0
					average	93.1

Table 36 (continued)

Soil	No.	pH	$N_0(\text{me./ml})$	$Q'/\sqrt{\beta N_0} (A)$	$V_{\infty}(\text{ml/g soil})$	$S(\text{m}^2/\text{g soil})$
9. Wolfswaard soil	1	7.44	$1.73 \times 10^{-3}$	46.7	0.399	93.3
	2	7.42	$1.74 \times 10^{-3}$	46.6	0.390	91.6
	3	7.28	$1.93 \times 10^{-3}$	44.2	0.348	86.7
	4	7.32	$2.08 \times 10^{-3}$	42.6	0.349	90.3
	5	7.35	$3.29 \times 10^{-3}$	33.9	0.269	89.8
						average 90.3
10. Y polder soil	1	7.64	$2.30 \times 10^{-3}$	40.5	0.516	134
	2	7.62	$2.30 \times 10^{-3}$	40.5	0.531	138
	3	7.64	$2.36 \times 10^{-3}$	40.0	0.493	130
	4	7.60	$2.54 \times 10^{-3}$	38.5	0.479	131
	5	7.54	$3.27 \times 10^{-3}$	34.0	0.432	135
						average 134
11. N.O.P. soil	1	8.00	$1.65 \times 10^{-3}$	47.8	0.354	77.2
	2	7.96	$1.68 \times 10^{-3}$	47.4	0.349	76.8
	3	7.82	$1.83 \times 10^{-3}$	45.4	0.332	76.5
	4	7.90	$2.03 \times 10^{-3}$	43.1	0.312	75.8
	5	7.92	$2.69 \times 10^{-3}$	37.5	0.277	77.9
						average 76.8
12. Winsum soil	1	6.90	$1.58 \times 10^{-3}$	48.9	0.358	79.8
	2	6.98	$1.73 \times 10^{-3}$	46.7	0.340	79.6
	3	6.70	$1.86 \times 10^{-3}$	45.1	0.325	79.2
	4	6.82	$2.02 \times 10^{-3}$	43.2	0.317	80.9
	5	6.75	$3.11 \times 10^{-3}$	34.8	0.244	79.2
						average 79.7

It was found that under the experimental conditions all soils exhibited an exclusion of chloride, resulting in specific surface area values varying from 28 m<sup>2</sup>/g for the Loess soil to 182 m<sup>2</sup>/g for the River basin clay soil. Table 36 clearly demonstrates that the values within the series of each soil were very nearly the same, indicating a high reproducibility of the measurements. The range of electrolyte levels within each series, however, was much smaller than expected because of an incomplete removal of the salt during the sample preparation. A separate experiment was set up to investigate whether the results obtained also applied to systems at lower electrolyte levels.

### 5.1.2 Specific surface area determination of 3 soils over a wider range of electrolyte levels

The electrolyte level of the original suspension of three soils, viz. the River basin clay soil, the Randwijk soil and the Loess soil, was decreased by means of a dialysis procedure until electric conductivity measurements indicated a salt concentration of about  $2 \times 10^{-4}$  N. Starting with these suspensions, systems were prepared in which the total electrolyte concentration varied from about  $8 \times 10^{-4}$  N to about  $2 \times 10^{-2}$  N. Results of the experiment, conducted again according to the tracer method, are presented in table 37.

Table 37. Repeated specific surface-area determination on 3 soils, employing a wider range of salt concentrations in the equilibrium solution. I: River basin clay soil; II: Randwijk soil; III: Loess soil

No.	$N_0(\text{me./ml})$			$Q'/\sqrt{\beta N_0} (\text{\AA})$			$V_{\infty}(\text{ml/g soil})$					
	I	II	III	I	II	III	I		II		III	
1	$8.10 \times 10^{-4}$	$8.45 \times 10^{-4}$	$8.98 \times 10^{-4}$	216	211	205	3.89	3.83	3.05	2.97	0.493	0.501
2	$1.48 \times 10^{-3}$	$1.80 \times 10^{-3}$	$1.61 \times 10^{-3}$	160	145	153	3.77		2.89		0.509	
3	$3.17 \times 10^{-3}$	$3.63 \times 10^{-3}$	$3.46 \times 10^{-3}$	109	102	104	2.92	2.94	1.31	1.34	0.465	0.465
4	$6.25 \times 10^{-3}$	$6.18 \times 10^{-3}$	$6.44 \times 10^{-3}$	78	78	77	2.96		1.37		0.464	
5	$9.81 \times 10^{-3}$	$9.46 \times 10^{-3}$	$9.27 \times 10^{-3}$	62	63	64	2.15	2.05	0.73	0.84	0.358	0.376
6	$1.82 \times 10^{-2}$	$1.76 \times 10^{-2}$	$1.93 \times 10^{-2}$	46	46	44	1.95		0.95		0.394	
							1.41	1.25	0.72	0.73	0.295	0.294
							1.09		0.73		0.292	
							1.11	1.15	0.521	0.502	0.168	0.170
							1.19		0.483		0.172	
							0.80	0.81	0.361	0.351	0.160	0.164
							0.81		0.340		0.167	

The lines in figure 42 correspond to the values of the specific surface area as measured in the foregoing experiment at high electrolyte level. The points indicate the mean values of the results given in table 37. All points were found to be situated very near to the lines, showing that for the three soils involved the results as measured over a large range of electrolyte levels were identical with those found at high salt concentration.

Although the above observation certainly supported the reliability of the specific surface area data, the conceivable presence of a small positive adsorption of chloride

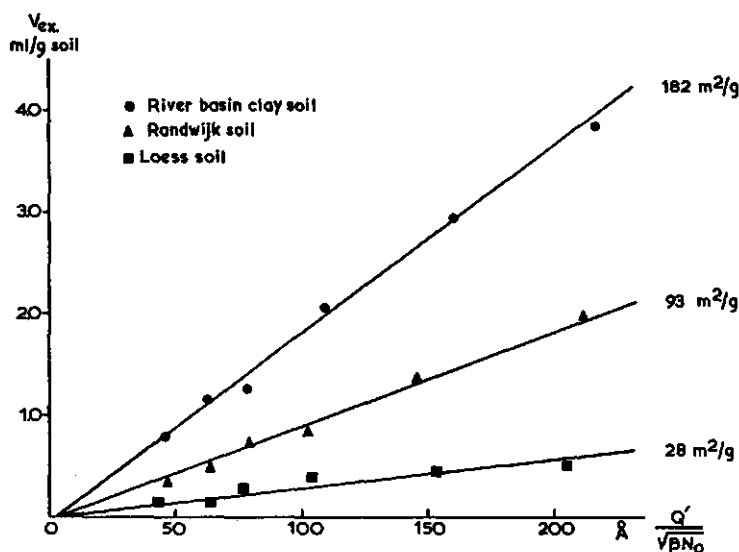


Fig. 42. Comparison between the specific surface area determinations of three soils as measured over a wide range of electrolyte levels and at high salt concentration only

- which could have been masked by the anion exclusion - might have caused a systematic error. Indeed, one could visualize that such a positive adsorption took place in spite of the presence of phosphate. This would most likely be the case in soils with a relatively high content of iron oxides. Obviously, the resulting values for the specific surface area would be too low.

### 5.1.3 The influence of the removal of free iron oxides on the chloride exclusion by Sticky soil and Na-laterite

The influence of the presence of free iron oxides on the adsorption of chloride by soils has been investigated thoroughly by SUMNER (1961). This author indicated that a major part of the observed adsorption in kaolinitic soils should probably be attributed to iron oxides present, instead of to the clay minerals themselves.

Because the iron oxides form an integral part of the soil solid phase, they cannot be removed by means of a mechanical procedure. This necessitates the application of a chemical method. As was found by the above author, the removal of iron oxides by means of the sodium dithionite procedure (MITCHELL and MACKENZIE, 1954) does not affect the properties of the clay minerals.

Table 38. Determination of the specific surface area, as measured according to the exclusion of  $\text{Cl}^-$  in the presence of  $10^{-4}$  normal  $\text{Na}_3\text{PO}_4$ , before and after removal of iron oxides (A and B, respectively). Series I: Sticky soil, a fraction  $< 2\mu$ ; Series II: Laterite, total fraction  $< 2\mu$ . The data presented are the mean values of duplicate measurements

No.	pH	$N_0(\text{me./ml})$	$1/\sqrt{BN_0}(\text{\AA})$	$d^-(\text{\AA})$	$V_m(\text{ml/gram})$	Specific surface area ( $\text{m}^2/\text{g}$ clay)
I.A.1	6.78	$8.62 \times 10^{-4}$	104.7	208.4	3.56	171
.2	6.72	$2.37 \times 10^{-3}$	63.2	125.4	2.08	166
.3	6.70	$6.20 \times 10^{-3}$	39.0	77.0	1.26	164
.4	6.71	$9.85 \times 10^{-3}$	30.5	60.0	1.04	173
.5	6.65	$1.68 \times 10^{-2}$	23.9	46.8	0.77	165
						average 168
I.B.1	6.83	$8.76 \times 10^{-4}$	103.8	206.6	3.64	176
.2	6.77	$2.58 \times 10^{-3}$	60.4	119.8	2.01	168
.3	6.62	$6.61 \times 10^{-3}$	37.8	74.6	1.31	176
.4	6.66	$1.21 \times 10^{-2}$	28.4	55.8	0.92	165
.5	6.63	$1.74 \times 10^{-2}$	23.6	46.2	0.80	173
						average 172
II.A.1	6.82	$1.88 \times 10^{-3}$	70.8	139.6	0.618	44.3
.2	6.80	$3.02 \times 10^{-3}$	55.8	109.6	0.454	41.4
.3	6.73	$5.59 \times 10^{-3}$	41.1	80.1	0.351	43.8
.4	6.65	$9.10 \times 10^{-3}$	32.2	62.4	0.255	40.9
.5	6.62	$1.77 \times 10^{-2}$	23.5	45.0	0.196	43.6
						average 42.8
II.B.1	6.84	$1.85 \times 10^{-3}$	71.4	140.8	0.607	43.1
.2	6.82	$3.10 \times 10^{-3}$	55.2	108.3	0.461	42.6
.3	6.75	$5.47 \times 10^{-3}$	41.5	81.0	0.339	41.9
.4	6.70	$9.12 \times 10^{-3}$	32.1	62.2	0.272	43.8
.5	6.61	$1.79 \times 10^{-2}$	23.3	44.6	0.197	44.2
						average 43.3

Part of the Sticky soil sample, which obviously contained a considerable amount of iron oxides, was used for collection of a fraction  $< 2 \mu$ . Unfortunately not the total fraction  $< 2 \mu$  was separated off, which made a comparison between the results of this fraction and the total fraction  $< 50 \mu$  impossible. Also from a lateritic clay soil (Passar Minggu, Indonesia), the total fraction  $< 2 \mu$  was separated off. This soil contained predominantly fine and poorly crystallized kaolinites, and crystoballite; the reduceable iron content calculated as Fe amounted to 7.8 % (KOENIGS, 1961). The sample was brought to a homoionic Na composition in the normal way.

Parts of the above described suspensions were treated with sodium dithionite to remove iron oxides. Then the measurement of the specific surface area was carried out as before, employing both the unpretreated and pretreated samples of both soils. Again phosphate was added to all systems to a concentration of  $10^{-4}$  N. Results are given in table 38.

Apparently no significant difference was found between the results before and after removal of the iron oxides; this allowed the conclusion that the phosphate additions chosen for the previous experiment were sufficiently large to prevent any positive chloride adsorption, even in soils with iron contents comparable to that of the lateritic soil.

Table 39. The positive adsorption of chloride on Na-laterite (total fraction  $< 2 \mu$ ) in the absence of phosphate. The data presented are the mean values of duplicate measurements

No.	pH	$N_0$ (me./ml)	Cl <sup>-</sup> conc. in dialyzate (me./ml)	$d^-$ (Å)	$V_{ss}$ expected for spec. surface area of 43 m <sup>2</sup> /g (ml/g clay)	$V_{ss}$ measured (ml/g clay)	Deficit of $V_{ss}$ (ml/g clay)	Net pos. adsorption of chloride (μe./g clay)
1	6.63	$8.65 \times 10^{-4}$	$8.57 \times 10^{-4}$	195.8	0.84	-0.92	1.76	1.51
2	6.58	$3.17 \times 10^{-3}$	$3.10 \times 10^{-3}$	108.3	0.47	-0.48	0.95	2.95
3	6.55	$6.38 \times 10^{-3}$	$6.37 \times 10^{-3}$	75.0	0.32	-0.32	0.64	4.08
4	6.32	$1.29 \times 10^{-2}$	$1.24 \times 10^{-2}$	53.8	0.23	-0.13	0.36	4.46
5	6.14	$2.51 \times 10^{-2}$	$2.48 \times 10^{-2}$	37.0	0.16	-0.037	0.197	4.89

For comparison the experiment with the unpretreated laterite was repeated without phosphate addition (cf table 39). In this case an increasing net positive adsorption of chloride was found with increasing chloride concentration in the dialyzate. Since pH values were in the range where kaolinite does not exhibit a net positive adsorption of chloride (cf figure 37), it was concluded that the observed chloride adsorption must be attributed to the presence of free iron oxides in this sample.

#### 5.1.4 Comparison between the results of the ethylene glycol retention method and the anion exclusion method

Specific surface area determinations according to the retention of ethylene glycol

were performed on all 12 soils used before. Parts of the soil suspensions gained after wet sieving were dried at 105° C. Next the samples were ground in a mortar, transferred into weighing flasks and dried in a vacuum desiccator over P<sub>2</sub>O<sub>5</sub>. Then the experiment was performed in exactly the same way as described by BOWER and GOERTZEN (1959), except for the composition of the adsorption complex (homoionic Na instead of homoionic Ca). According to McNEAL (1964) the glycol retention data are less ambiguous when obtained with Na saturated samples. At the same time it facilitated the comparison with the anion exclusion data, which were also determined on the Na saturated soils.

Triplicate samples of each soil were transferred to one desiccator. A sample of Na-montmorillonite (Osage, fraction < 2  $\mu$ ) was included. After equilibration the entire procedure was repeated with new samples, so in fact results were gained in sixfold for each soil.

It is noted that at the endpoint of the experiment, which was not the same for all samples, the specific surface area of the Na-montmorillonite was found as 710 and 695 m<sup>2</sup>/g for the two repeats, respectively; these values are in good agreement with previous experience (cf also table 8 and figure 21).

Results for the soils, indicated as mean values of the two runs, are given in table 40.

*Table 40. Comparison between values for specific surface area and surface charge density as calculated according to the ethylene glycol retention method and according to the anion exclusion method*

Soil	Specific surface area (m <sup>2</sup> /g soil)		Surface charge density (10 <sup>-7</sup> me./cm <sup>2</sup> )	
	eth. glycol method	anion exclusion method	eth. glycol method	anion exclusion method
1. Sticky soil	299 307 315	44.5	0.5	3.2
2. Loess soil	109 118 126	28.3	0.6	2.5
3. Wilhelmina polder soil	255 247 238	125	1.0	2.1
4. Oss soil	398 372 346	72.4	0.6	3.0
5. River basin clay soil	364 384 403	182	1.3	2.8
6. Griend soil	191 203 214	74.2	0.9	2.4
7. Munnikeland soil	225 219 213	56.0	0.8	3.3
8. Randwijk soil	221 239 256	93.1	0.9	2.4
9. Wolfswaard soil	284 293 302	90.3	0.9	2.8
10. Y-polder soil	395 389 384	134	0.8	2.4
11. N.O.P. soil	182 195 208	76.8	0.9	2.3
12. Winsum soil	306 313 320	79.7	0.7	2.9

It is seen that, although the replicates agreed fairly well with each other, there is by no means a good correlation between the data of the ethylene glycol method and those of the anion exclusion method. For a further interpretation and evaluation of both methods, the Winsum soil was taken. For this soil data had been collected according to both methods, for two different size fractions. Comparing the values for Winsum soil and for Winsum clay, it is concluded that the ethylene glycol retention method showed quite strange results. Thus the specific surface area of the fraction  $< 50 \mu$  was even larger than that of the fraction  $< 2 \mu$ , viz. 310 and 277  $\text{m}^2/\text{g}$ , respectively (cf tables 40 and 8).

In contrast, the anion exclusion data showed a much better agreement. Here a value of 161  $\text{m}^2/\text{g}$  was found for the total fraction  $< 2 \mu$  (cf table 31) against 79.7  $\text{m}^2/\text{g}$  for the fraction  $< 50 \mu$ . This then means that according to the particle size distribution (cf table 10) for the Winsum soil the particles  $< 2 \mu$  contribute for 96 % to the total surface area, whereas the contribution of the coarser particles (52.5 % on weight) amounts to only 4 %, which is reasonable.

Another indication for the superior reliability of the anion exclusion data, above those from the ethylene glycol retention, was found from the calculation of the surface charge density. These values were calculated from the C.E.C. and the specific surface area according to both methods (see table 40). It is well known that illite is the most abundant clay mineral in most Dutch clayey soils. The surface charge density of illite is about  $3 \times 10^{-7}$  me./ $\text{cm}^2$ . As is shown in table 40, values for all soils were quite near to  $3 \times 10^{-7}$  me./ $\text{cm}^2$  if the specific surface area according to anion exclusion was used. For the ethylene glycol data, these values were less than about  $1 \times 10^{-7}$  me./ $\text{cm}^2$ .

It is noted once more that the Winsum illite data checked very good for both fractions. Here a value of  $2.9 \times 10^{-7}$  was found for the total fraction  $< 2 \mu$  (very near to the expected value for illite); the same value resulted for the Winsum soil, fraction  $< 50 \mu$ . In contrast, ethylene glycol data would give  $1.7 \times 10^{-7}$  and  $0.7 \times 10^{-7}$  me./ $\text{cm}^2$  for both fractions, respectively.

The discrepancy between both methods remains somewhat problematic. A comparison between the organic matter content as determined according to KURMIES (1949) and the difference in surface area between both methods is presented in figure 43. From this figure an indication is found that the observed differences are related to the organic matter content. Although one might reason that organic compounds (at least if negatively charged) should exert the same influence on both methods, upon closer consideration it seems that the suggested cause for the discrepancy is acceptable. If the organic matter is present as a coiled polymer with a large internal surface, its contribution to the surface area as measured by anion exclusion would perhaps be deficient as regards the internal surface (full development of anion exclusion assumes free expansion of the electric double layer). At the same time it appears equally possible that the glycol retention by organic compounds does attain higher values for surface coverage than that assumed for external surfaces. This then would imply a possible underestimate of total surface area as measured from anion exclusion

(in fact indicating only the mineral surface area and perhaps external area of the organic compounds), whereas the glycol retention could possibly lead to an overestimate.

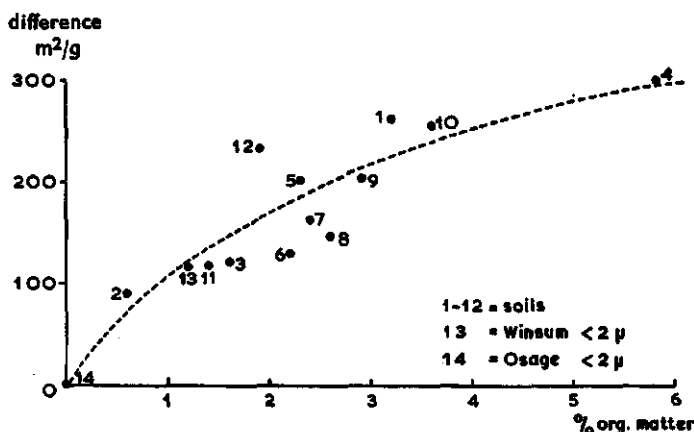


Fig. 43. Relation between the organic matter content and the difference in specific surface area according to the ethylene glycol method and the anion exclusion method

It should be admitted that the above reasoning is not entirely consistent with the experience about the influence of organic matter as gained in section 4.2.3. This same discrepancy between the influence of organic matter when present in clays as opposed to whole soils was observed by GREENLAND and QUIRK (1963, 1964), and BURFORD *et al* (1964), who derived values for specific surface area from the adsorption of cetyl pyridinium bromide. Also these authors interpreted this as the direct result of the difference in nature of the organic substances, which presumably occur in the clay fractions (especially when in Na form) as stretched chains against as coiled polymers in soils.

A more detailed investigation in which special attention should be paid to the rôle of organic matter seems to be required to warrant a more definite evaluation of both methods compared above.

## 5.2 Phosphate adsorption measurements

### 5.2.1. Determination of the phosphate adsorption isotherms

Phosphate being an important plant nutrient, the adsorption isotherms of the soils used above were also studied. Granted that in soils phosphate behavior is influenced by many other factors than the adsorption on soil constituents (e.g. the metabolic activity of soil organisms, and precipitation reactions with iron and aluminum ions), it seems nevertheless that the adsorption isotherms under certain standardized



conditions (Na saturation at a roughly fixed salt level) are of interest. At the same time this study was meant to provide an orientation as regards a comparison between the behavior of phosphate in soils and that in clays.

The experimental technique was principally the same as described in Chapter 4. Since all samples contained originally an unknown amount of phosphate in this case, it was necessary to determine the phosphate concentrations in the dialyzates colorimetrically. The dialyzates of several soils showed a brownish color due to the presence of organic substances. These were removed by treatment with activated charcoal prior to the concentration determination.

Results are given in table 41. In the present experiments the anion exclusion value

Table 41. The adsorption of phosphate on 12 Dutch soils as a function of the phosphate concentration in solution

Soil	No.	pH	$N_0$ (me./ml)	$\mu\text{g P/ml}$ in dialyzate	Expected exclusion ( $\mu\text{g P/g soil}$ )	Inclusion volume measured (ml/g soil)	Over-all pos. adsorption ( $\mu\text{g P/g soil}$ )	Net pos. adsorption ( $\mu\text{g P/g soil}$ )
1. Sticky soil	1	6.12	$0.21 \times 10^{-2}$	0.3	0.19	143.3	43.0	43.2
	2	5.98	$0.32 \times 10^{-2}$	3.2	1.60	45.53	145.7	147
	3	6.42	$0.55 \times 10^{-2}$	21.5	8.12	19.39	416.9	425
	4	7.10	$0.96 \times 10^{-2}$	66	21.19	9.75	643.5	665
	5	7.80	$1.91 \times 10^{-2}$	131	28.55	5.62	736.2	765
2. Loess soil	1	7.20	$0.63 \times 10^{-2}$	4.5	1.15	17.49	78.7	80
	2	7.30	$0.75 \times 10^{-2}$	10.2	2.44	9.63	98.2	101
	3	7.84	$1.08 \times 10^{-2}$	51	10.71	2.59	132.1	143
	4	8.21	$1.57 \times 10^{-2}$	92	16.17	1.64	150.9	167
	5	9.10	$2.69 \times 10^{-2}$	216	30.25	0.84	181.4	212
3. Wilhelm. polder soil	1	7.72	$1.43 \times 10^{-2}$	2.8	2.23	42.01	117.6	120
	2	7.79	$1.43 \times 10^{-2}$	8.6	6.88	17.26	148.4	155
	3	7.90	$1.51 \times 10^{-2}$	36.5	28.74	6.47	236.2	265
	4	8.21	$1.76 \times 10^{-2}$	88	66.21	3.14	276.3	343
	5	8.97	$2.11 \times 10^{-2}$	164	113.12	1.81	296.8	410
4. Oss soil	1	7.02	$2.30 \times 10^{-2}$	0.4	0.13	85.75	34.3	34.4
	2	7.02	$2.47 \times 10^{-2}$	4.7	1.45	66.12	310.8	312
	3	7.05	$2.54 \times 10^{-2}$	18.5	5.76	43.30	801.1	807
	4	7.08	$2.89 \times 10^{-2}$	42.3	12.48	27.36	1157	1170
	5	7.10	$3.80 \times 10^{-2}$	83	21.22	17.02	1413	1434
5. River basin clay soil	1	7.22	$1.22 \times 10^{-2}$	0.8	0.95	45.38	36.3	37.3
	2	7.22	$1.29 \times 10^{-2}$	2.2	2.55	44.27	97.4	100
	3	7.41	$1.40 \times 10^{-2}$	5.9	6.71	25.15	148.4	155
	4	7.63	$1.64 \times 10^{-2}$	14.2	15.26	20.74	294.5	310
	5	8.01	$2.10 \times 10^{-2}$	116	112.07	5.11	592.8	705
6. Griend soil	1	8.04	$1.25 \times 10^{-2}$	1.3	0.67	65.84	85.6	86
	2	8.07	$1.31 \times 10^{-2}$	3.7	1.87	30.54	112.7	115
	3	8.26	$1.44 \times 10^{-2}$	26.0	12.76	5.74	149.2	162
	4	8.38	$1.64 \times 10^{-2}$	67	30.43	3.16	211.7	242
	5	8.99	$2.14 \times 10^{-2}$	156	62.16	1.89	294.8	357
7. Munnike- land soil	1	6.72	$1.61 \times 10^{-2}$	0.3	0.09	73.98	22.2	22.3
	2	6.76	$1.78 \times 10^{-2}$	4.4	1.19	19.32	85.0	86
	3	6.82	$1.96 \times 10^{-2}$	16.5	4.31	11.92	196.7	201
	4	6.90	$2.36 \times 10^{-2}$	60	14.63	5.30	319.6	334
	5	6.95	$3.18 \times 10^{-2}$	153	31.18	2.34	358.0	389

Soil	No	pH	$N_0$ (me./ml)	$\mu\text{g P/ml}$ in dialyzate	Expected exclusion ( $\mu\text{g P/g soil}$ )	Inclusion volume measured (ml/g soil)	Over-all pos. adsorption ( $\mu\text{g P/g soil}$ )	Net pos. adsorption ( $\mu\text{g P/g soil}$ )
8. Randwijk soil	1	7.05	$0.92 \times 10^{-2}$	1.2	0.81	—	—	—
	2	7.05	$0.96 \times 10^{-2}$	3.5	2.30	69.71	243.9	246
	3	7.26	$1.15 \times 10^{-2}$	7.6	5.02	46.32	352.0	357
	4	7.47	$1.43 \times 10^{-2}$	39.0	22.45	12.06	470.3	493
	5	7.83	$1.87 \times 10^{-2}$	138	71.27	3.50	483.0	554
9. Wolfswaard soil	1	7.26	$1.36 \times 10^{-2}$	0.8	0.45	17.94	14.4	14.9
	2	7.30	$1.48 \times 10^{-2}$	2.1	1.14	14.95	31.4	32.5
	3	7.45	$1.77 \times 10^{-2}$	21.6	10.80	8.03	173.5	184
	4	7.66	$2.21 \times 10^{-2}$	65	30.06	3.75	243.8	274
	5	8.15	$3.32 \times 10^{-2}$	194	70.37	1.69	327.8	398
10. Y-polder soil	1	7.61	$1.76 \times 10^{-2}$	1.5	1.16	35.33	53.0	54
	2	7.65	$1.76 \times 10^{-2}$	6.0	4.64	21.04	126.2	131
	3	7.65	$1.80 \times 10^{-2}$	32.4	24.45	5.18	167.8	192
	4	7.80	$2.21 \times 10^{-2}$	86	59.21	2.41	207.3	267
	5	7.96	$2.34 \times 10^{-2}$	146	98.73	1.58	230.7	329
11. N.O.P. soil	1	8.13	$1.44 \times 10^{-2}$	1.0	0.49	21.91	21.9	22.4
	2	8.20	$1.43 \times 10^{-2}$	9.8	4.88	6.61	64.8	70
	3	8.32	$1.61 \times 10^{-2}$	38.4	18.14	2.16	82.9	101
	4	8.55	$1.85 \times 10^{-2}$	92	41.05	1.22	112.2	153
	5	8.89	$2.38 \times 10^{-2}$	165	65.92	0.81	133.6	200
12. Winsum soil	1	6.75	$1.26 \times 10^{-2}$	1.4	0.91	21.60	30.2	31.1
	2	6.80	$1.33 \times 10^{-2}$	5.1	2.28	13.81	70.4	73
	3	6.80	$1.66 \times 10^{-2}$	24.9	9.97	7.79	194.0	195
	4	6.94	$2.10 \times 10^{-2}$	57	20.95	5.41	308.4	329
	5	7.40	$3.31 \times 10^{-2}$	147	47.79	3.06	449.8	497

constituted often only a minor part of the total adsorption value, due to the relatively high electrolyte level and the small specific surface area. Nevertheless, in certain cases the negative adsorption formed a substantial part of the final result.

The adsorption isotherms for all soils are presented in figure 44. The values for the adsorbed amounts (at comparable concentration in solution) were roughly of the same order of magnitude except for the Oss soil (and perhaps also for the Sticky soil and the River basin clay soil). Since these (at least the Oss and Sticky soil) have a relatively high iron content, it seems likely that the higher adsorption values must be ascribed to the formation of iron phosphate compounds (cf also section 5.2.2).

Applying the HOFSTEE plot to the adsorption data it was found again that all soils exhibited at least two different adsorption mechanisms, except for the Oss soil and the Randwijk soil. As an example, figure 45 represents such a plot for one of the samples, viz. the N.O.P. soil. The above treatment was not applicable to the Oss data, since in that case  $P_e$  values were found to increase with increasing  $P_e/C$  values. The plot for the Randwijk data yielded a fairly straight line, indicating the occurrence of one adsorption mechanism only with a reaction constant of about 0.2 ml/ $\mu\text{g P}$ .

The reaction constants and maximum adsorption values are presented in table 42. The adsorption values were expressed both per gram soil and per  $\text{m}^2$  surface area

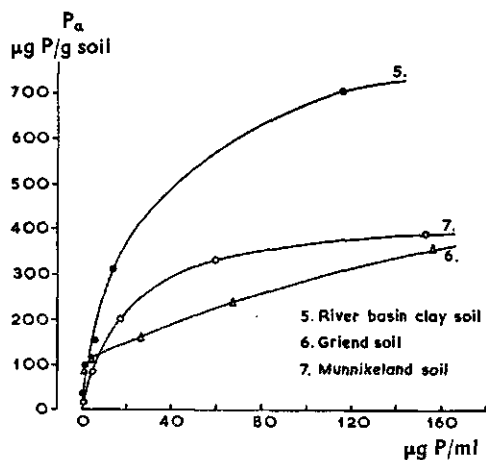
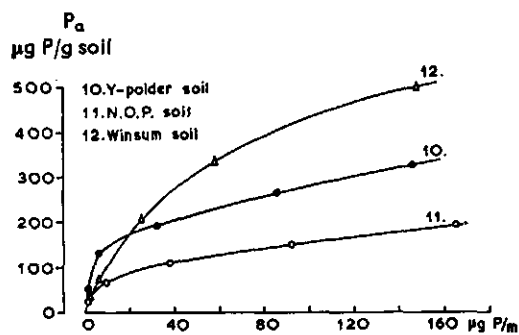
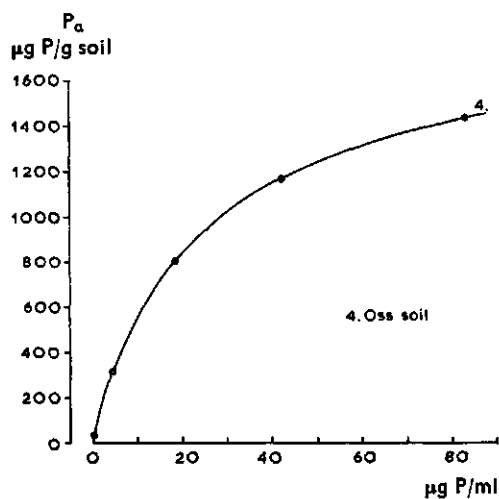
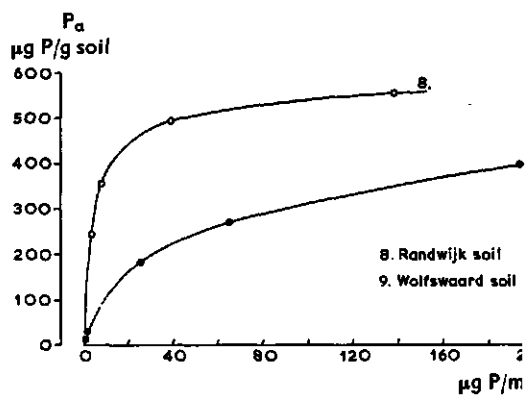
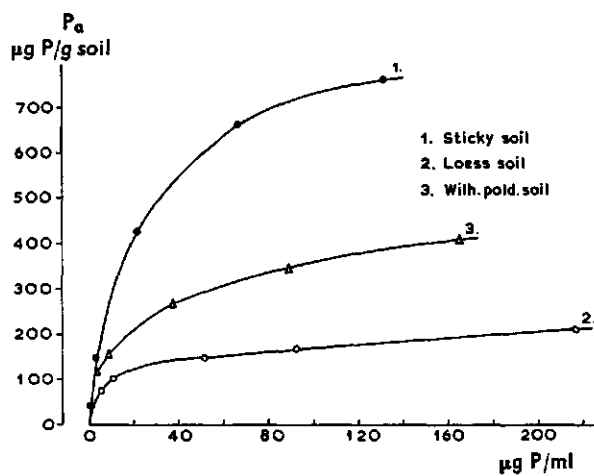


Fig. 44. The phosphate adsorption isotherms for 12 Dutch soils

Table 42. Reaction constants and adsorption maxima of the phosphate adsorption by 12 Dutch soils

Soil	$(\mu\text{g P/ml})^{-1}$		$\mu\text{g P/g soil}$			$\mu\text{g P/m}^2 \text{ surface}$		
	$b_1$	$b_2$	$P_{m1}$	$P_{m2}$	$P_m$	$P_{m1}$	$P_{m2}$	$P_m$
1. Sticky soil	2.8	0.033	70	825	895	1.6	18.5	20.1
2. Loess soil	1.9	0.013	60	195	255	2.1	6.9	9.0
3. Wilh. p. soil	0.93	0.013	140	400	540	1.1	3.2	4.3
4. Oss soil	—	—	—	—	1600	—	—	22.0
5. River b.c. soil	1.1	0.029	60	850	910	0.3	4.7	5.0
6. Griend soil	1.2	0.005	100	535	635	1.3	7.3	8.6
7. Munnikeland soil	2.8	0.046	25	405	430	0.4	7.3	7.7
8. Randwijk soil	—	—	—	—	580	—	—	6.2
9. Wolfswaard soil	0.09	0.007	185	415	600	2.0	4.6	6.6
10. Y-polder soil	0.31	0.006	150	390	540	1.1	2.9	4.0
11. N.O.P. soil	0.56	0.008	50	230	280	0.7	2.9	3.6
12. Winsum soil	0.48	0.012	40	700	740	0.5	8.8	9.3

(as derived from the anion exclusion measurements). The last column of this table indicates that the phosphate adsorption capacities per unit surface area were roughly the same for all soils, viz. about 4–9  $\mu\text{g P/m}^2$ , except for the Sticky soil and the Oss soil (roughly 20  $\mu\text{g P/m}^2$ ). Again this is ascribed to the presence of iron compounds in these soils, which causes a phosphate adsorption or precipitation in addition to the normal adsorption by the soil colloids.

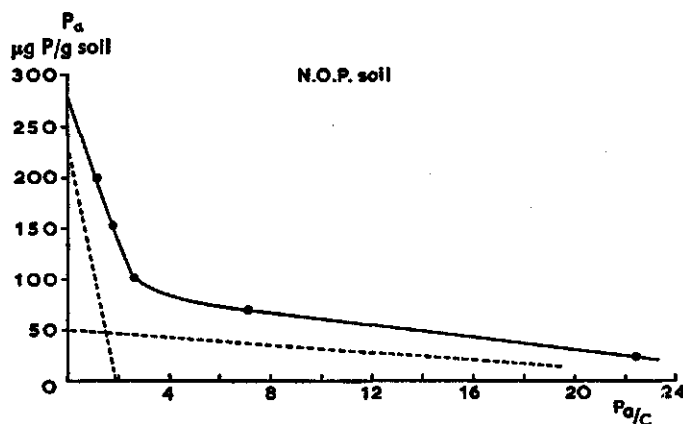


Fig. 45. Analysis of the phosphate adsorption isotherm for N.O.P. soil

### 5.2.2 The influence of pH on the phosphate adsorption by two soils

It might be reasoned that the significance of the adsorption isotherms presented in the foregoing section is very limited because of the possible influence of the pH on the adsorption values. As has been described in Chapter 4, such an influence was

absent in the case of pure clays in the pH range of about 4.5 to 8.5. In soils the situation might be different, however, due to the presence of other compounds interfering with phosphate adsorption. In order to investigate this point, the phosphate adsorption on two soils, viz. the Oss soil and the Munnikeland soil, was measured as a function of the pH.

Results are shown in table 43, indicating that with respect to the Munnikeland soil the adsorption values remained constant over a pH range from about 4.7 to 8.2. The Oss soil, however, showed a marked influence of the pH, at least in the low pH range. Adsorption values were roughly the same at pH 6.8 and 8.5, but increased with about 80 % at pH 4.2. This must certainly be attributed, at least in part, to the precipitation of iron phosphates.

Table 43. The adsorption of phosphate on Oss soil and Munnikeland soil as a function of pH

Soil	pH	$N_0$ (me./ml)	$\mu\text{g P/ml}$ in dialyzate	expected neg. adsorption ( $\mu\text{g P/g soil}$ )	$V_{inc}$ measured (ml/g soil)	Over-all pos. adsorption ( $\mu\text{g P/g soil}$ )	Net pos. adsorption ( $\mu\text{g P/g soil}$ )
Oss							
1	4.21	$2.45 \times 10^{-2}$	20.2	6	92.1	1,860	1,866
2	6.83	$2.52 \times 10^{-2}$	34.2	11	31.64	1,082	1,093
3	8.47	$2.40 \times 10^{-2}$	35.1	11	28.60	1,004	1,015
Munnikeland							
1	4.74	$2.01 \times 10^{-2}$	46.3	12	6.18	286	298
2	6.89	$1.95 \times 10^{-2}$	45.1	12	6.61	298	310
3	8.15	$2.08 \times 10^{-2}$	44.6	12	6.68	298	310

Comparing the phosphate adsorption capacities of the soils with the values that would be expected on the basis of the clay content and the maximum adsorption value of the untreated illite (thus assuming again that illite is the most important clay mineral in the soils), one finds that about one third to one half of the measured adsorption maxima can be accounted for by the adsorption on the clay. Thus although the phosphate adsorption on clays forms a substantial part of the total adsorption in soils, it seems evident that other factors play an important rôle in soils. In this respect the effect of aluminum, iron, and possibly also of organic matter, is suggested again. A separate study on the interaction of phosphate with these compounds is required for a good understanding of the phosphate bonding by soils.

Aside from the latter it appears that the isotherms provide a first orientation of the phosphate adsorption characteristics of the soils studied, over the pH range of most interest in soil systems.

## Summary

The interaction between soil colloids and anions usually comprises simultaneously two different phenomena, viz. negative and positive anion adsorption. The negative adsorption (anion exclusion) results from the repulsion of anions by the predominantly negatively charged colloidal substances in soils. Such a repulsion leads to a decrease of the anion concentration close to the colloid as compared to the concentration in the equilibrium solution (i.e. the solution present at such a distance from the charged surface that the influence of the latter on the concentration distribution of the ions has become negligible). In turn, the positive anion adsorption is caused in part by positively charged sites usually also present on certain soil colloids – presumably at the edges of clay mineral crystals. In addition chemi-sorption of certain anions appears to occur.

The resultant of the above interaction mechanisms is the experimentally accessible adsorption value. Experimental data may thus indicate an anion exclusion or a positive adsorption, depending on the relative magnitude of the two phenomena involved. It should be kept in mind that in case of a detectable cation exchange (adsorption) capacity of a soil, anion exclusion is certainly present; in practice this applies to all soil systems. As a result, an experimentally observed absence of interaction between anions and soil must imply an (accidental) equality of negative and positive anion adsorption. At the same time, the experimental adsorption value must always be augmented with the ever-present anion exclusion in order to find the correct value for the amount which is positively adsorbed. This necessitates a distinction between the over-all adsorption and the net (positive) adsorption. The over-all (or apparent) adsorption is represented by the experimental value, and may thus be positive or negative. The net adsorption is found from the value of the over-all adsorption after correction for anion exclusion.

A precise knowledge of the negative adsorption is thus required for a correct interpretation of anion adsorption measurements. In addition, such knowledge is of interest because anion exclusion plays an important rôle in salt transport phenomena, and it forms the basis of a method for the determination of the specific surface area of soil colloids.

Chapter 2 presents calculations on anion exclusion. The GOUY-CHAPMAN theory of the electric double layer was taken as a point of departure. In contrast to earlier calculations, the derivations presented here are valid for all mixed ionic systems, containing both mono- and divalent cations and anions. An approximation with

satisfactory accuracy was introduced for the calculation of the negative adsorption of trivalent anions. These derivations are applicable to systems with a relatively high liquid content. Expressions were also derived for systems with interacting double layers. The effect of interaction was expressed in anion exclusion values relative to the non-interaction case.

The anion exclusion was indicated in the above derivations as an equivalent distance of exclusion, i.e. the distance from the charged surface over which anions would have to be absent, if all anions were distributed at equilibrium concentration. This distance of exclusion was expressed as a function of three variables, viz. 1°: a factor  $Q$ , which is a function only of the equivalent fractions of the different ions in the equilibrium solution; 2°: the total electrolyte level of the equilibrium solution,  $N_0$ ; 3°: a factor  $\delta^-$ , which was introduced in the derivations for mathematical convenience and which is related to the surface charge density of the colloid. The  $Q$ -values were calculated separately for different anions and are presented graphically for a wide range of fractional compositions. The value of  $\delta^-$  is found in practice with satisfactory accuracy from an approximate equation. Exact values for  $\delta^-$  were also calculated for both the interaction and the non-interaction case. The validity of the suggested approximation was checked by a comparison between exact and approximate values of  $\delta^-$ .

Finally, attention has been paid in Chapter 2 to the possible mechanisms governing positive anion adsorption.

In Chapter 3 experimental methods are discussed. The experimentally accessible measure for anion exclusion is given by the volume of exclusion,  $V_{ex}$ , in ml per gram colloid. Analogous to the distance of exclusion,  $V_{ex}$  represents the volume that is apparently free of anions if all anions would be present at equilibrium concentration. The volume of exclusion per total system is found as the difference between the actual liquid volume,  $V_{tot}$ , and the volume in which the anions appear to be distributed at equilibrium concentration,  $V_{app}$ . It is evident that in case of positive adsorption exceeding the value of anion exclusion, the apparent volume will be larger than the actual volume, resulting in a volume of inclusion,  $V_{inc}$ .

$V_{tot}$  may be found from weighing data, assuming a solution density of 1.00 gram per ml. Usually, and especially so in case of anion exclusion,  $V_{ex}$  amounts to a fraction only of the total volume. Thus the determination of  $V_{app}$  must be carried out with the highest possible accuracy in order to limit the error in the final result. Consequently, in this Chapter considerable attention has been paid to the errors in the determinations.

When studying the interaction between chloride ions and soil colloids, different procedures may be applied for the determination of  $V_{ex}$ , viz. the potentiometric titration and the isotopic dilution. With respect to sulfate and phosphate studies only the last mentioned method was applied. A procedure for a simultaneous determination of the adsorption of three anions is described.

At very low phosphate levels a considerable adsorption of phosphate was found

at materials other than the soil colloids (e.g. the polyethylene bottles in which the systems were equilibrated). It was established in a separate experiment what minimum phosphate level was required to allow neglect of this adsorption.

The required separation between equilibrium solution and suspension was obtained by the use of dialysis bags. Equilibrium between the solutions inside and outside the bags was attained by agitation with an end-over-end shaker.

In the absence of positive adsorption, a plot of the experimental  $V_{ex}$  values against the calculated, not for  $\delta^-$  corrected, distance of exclusion should yield a straight line with a slope equal to the specific surface area of the colloid involved and with an intercept equal to  $\delta^-$ . Values for the distance of exclusion were calculated for each system by using the  $Q$ -values of Chapter 2, in combination with the total electrolyte concentration as measured from electric conductivity data. If positive adsorption is also present, deviations from the above straight line are found. The net (positive) adsorption is calculated as the product of the deficit in  $V_{ex}$  and the equilibrium concentration of the anion concerned.

In the phosphate experiments a somewhat different technique was applied for the calculation of the adsorbed amounts. To this purpose the distribution of total P over mono-, di- and trivalent phosphate ions as function of the pH was calculated. Then the expected exclusion of each of these species could be found, the sum of these values representing the total expected negative adsorption. Net positive adsorption of phosphate was then found in the same way as described above.

A description is given of the measurement of the specific surface area according to the retention of ethylene glycol.

The materials used in the experiments, viz. fairly pure clays and 12 Dutch clayey soils, are described in Chapter 3.

Chapter 4 presents the experimental results obtained with clays. The surface area determinations according to the exclusion of anions (chloride) resulted in acceptable values. The measurements at mixed ionic composition agreed with theoretical expectations.

A positive adsorption of sulfate on montmorillonite was found at very low sulfate concentrations. This positive adsorption could be suppressed by minute additions of phosphate. The illite did not exhibit positive sulfate adsorption; the phosphate concentration in the original sample (field sample) was sufficiently high to prevent such adsorption.

The adsorption of phosphate on montmorillonite was studied in detail, indicating evidence for chemi-sorption of phosphate. Silicate was found to be a strong competitor for phosphate. Certain silicate additions resulted in a complete suppression of phosphate adsorption. It was shown that this effect must be attributed to silicate itself and not to the increase of the pH, following increasing silicate additions. The exchange of pre-adsorbed phosphate against added silicate was found to be established for about 80 % within a few minutes after the silicate addition. It was concluded that the bonding of phosphate on the clays studied was governed by at least two different



reaction mechanisms. A quantitative account could be given for the maximum adsorption values.

The influence of the removal of organic matter from the illite indicated that these organic substances probably covered part of the reactive sites on the clay, thus partially preventing the adsorption of phosphate ions.

The results of the simultaneous determination of the adsorption of three anions were in accordance with expectations within experimental accuracy.

A very good agreement was found between the theoretically predicted and the measured decrease of anion exclusion due to the interaction of double layers at high clay content.

The kaolinite exhibited an increasing positive adsorption of chloride with decreasing pH values below pH 4.5. The observed influence of the pH on both the chloride and phosphate adsorption leads to the conclusion that the chloride adsorption resulted from electrostatic attraction whereas the phosphate adsorption was caused mainly by chemi-sorption.

The interaction between chloride and phosphate and the 12 soils (fraction  $< 50 \mu$ ) is described in Chapter 5. In the presence of  $10^{-4}$  N  $\text{Na}_3\text{PO}_4$ , chloride was found to be excluded by all soils, yielding values for the specific surface area. The phosphate addition was sufficiently high to prevent any positive adsorption of chloride, even in soils with high iron content.

A great discrepancy was found between the results of the specific surface area determinations according to the anion exclusion method and the ethylene glycol retention method. Using the data for different fractions of the Winsum sample, it could be reasoned that the anion exclusion data were more reliable than the ethylene glycol data. The difference should probably be attributed to the presence of organic matter.

Finally phosphate adsorption isotherms have been measured for all soils. Again it was found that the adsorption of phosphate was governed by at least two reaction mechanisms.

## Samenvatting

De interactie tussen bodemcolloïden en anionen omvat meestal twee gelijktijdig optredende verschijnselen, nl. negatieve en positieve adsorptie van anionen. De negatieve adsorptie (anionenexclusie) is het gevolg van de afstoting tussen anionen en de overwegend negatief geladen colloïdale bestanddelen in de grond. Deze afstoting heeft tot gevolg dat de anionenconcentratie dicht bij het colloïd lager is dan in de evenwichtoplossing (d.i. de oplossing welke aanwezig is op een zodanige afstand van het geladen colloïd-oppervlak, dat de invloed er van op de concentratieverdeling van de ionen verwaarloosbaar is). De positieve adsorptie wordt deels veroorzaakt door positief geladen plekken, welke meestal eveneens aanwezig zijn aan het oppervlak van bepaalde bodemcolloïden, bijvoorbeeld aan de randen van kleikristallen. Tevens kan chemisorptie van bepaalde anionen voorkomen.

De resultante van beide genoemde interactie-mechanismen is de adsorptiewaarde, welke experimenteel wordt bepaald. Meetwaarden kunnen dus zowel anionenexclusie als positieve adsorptie aangeven, afhankelijk van de relatieve waarden van beide verschijnselen. Anionenexclusie treedt altijd op wanneer de kationenadsorptiecapaciteit van een grond van meetbare grootte is; deze conditie geldt voor vrijwel alle bodemsystemen. Dit betekent, dat een experimenteel waargenomen afwezigheid van interactie tussen anionen en grond wijst op een (toevallige) gelijkheid van de negatieve en de positieve anionenadsorptie. Om dezelfde reden dient de experimenteel gevonden adsorptie te worden vergroot met de altijd aanwezige anionenexclusie, teneinde de juiste waarde te vinden van de hoeveelheid, welke positief is geadsorbeerd. Het bovenstaande maakt een onderscheid noodzakelijk tussen de z.g. schijnbare adsorptie (in het voorgaande aangeduid als "over-all" of "apparent adsorption") en de netto-adsorptie. De schijnbare adsorptie vertegenwoordigt dan de meetwaarde, terwijl de netto-adsorptie die waarde is, welke gevonden wordt nadat op de meetwaarde een correctie is toegepast voor anionenexclusie.

Een juist inzicht in het verschijnsel van de negatieve adsorptie is derhalve noodzakelijk om een correcte interpretatie van anionen-adsorptiemetingen mogelijk te maken. Bovendien is de kennis van dit verschijnsel van belang, aangezien anionenexclusie mede bepalend is voor het zouttransport in poreuze media en het de basis vormt van een methode ter bepaling van het soortelijk oppervlak van bodemcolloïden.

In Hoofdstuk 2 werd dan ook op uitgebreide wijze aandacht geschonken aan de berekening van anionenexclusie. Hierbij werd uitgegaan van de GOUY-CHAPMAN theorie van de diffuse dubbellaag, zoals deze al eerder werd toegepast bij beschou-

wingen over negatieve adsorptie van anionen. In tegenstelling tot vroeger gebruikte berekeningen zijn de hier afgeleide betrekkingen van toepassing op alle mengsystemen, waarin zowel een- als tweewaardige kationen en anionen aanwezig zijn. Voor drie-waardige anionen kon met voldoende nauwkeurigheid gebruik worden gemaakt van een benaderende berekeningsmethode. Bovengenoemde betrekkingen werden afgeleid voor systemen met een relatief hoog vloeistofgehalte. Tevens werden een aantal berekeningen uitgevoerd voor systemen met interactie van dubbellagen. Het effect van interactie werd hierbij uitgedrukt als de relatieve waarde van de negatieve adsorptie in vergelijking tot de waarden bij afwezigheid van interactie.

In al deze berekeningen werd de anionenexclusie uitgedrukt als een "equivalente afstand van exclusie"; dit is die afstand vanaf het geladen oppervlak over welke geen anionen aanwezig zouden zijn, indien alle anionen in het systeem op evenwichtsconcentratie verspreid worden gedacht. De exclusie-afstand blijkt een functie te zijn van drie variabele grootheden, nl. 1°: een factor  $Q$ , waarvan de waarde alleen wordt bepaald door de relatieve concentraties van kationen en anionen in de evenwichtsooplossing; 2°: de totale elektrolytconcentratie van de evenwichtsooplossing,  $N_0$ ; 3°: een grootheid  $\delta^-$ , welke ter vereenvoudiging werd ingevoerd in de berekeningen en welke verband houdt met de oppervlakte-ladingsdichtheid van het colloïd. Waarden van  $Q$  werden afzonderlijk berekend voor verschillende anionen en zijn grafisch weergegeven voor een groot aantal mogelijke samenstellingen van de evenwichtsooplossing. De waarde van  $\delta^-$  kan voldoende nauwkeurig worden berekend met behulp van een benaderingsformule. Exacte waarden van  $\delta^-$  werden afgeleid, zowel voor systemen met als voor systemen zonder interactie van dubbellagen. De bruikbaarheid van de voorgestelde benaderingsformule werd gecontroleerd door een vergelijking te maken tussen de exacte en de benaderde waarden van  $\delta^-$ .

Tot slot werd in hoofdstuk 2 enige aandacht geschonken aan de mogelijke adsorptiemechanismen in geval van positieve adsorptie van anionen.

De meetmethodiek werd besproken in hoofdstuk 3. De experimenteel te bepalen maat voor de negatieve adsorptie wordt gegeven door het volume van exclusie,  $V_{ex}$ , in ml per gram colloïd. In analogie met de afstand van exclusie vertegenwoordigt  $V_{ex}$  het volume dat vrij zou zijn van anionen, indien alle anionen op evenwichtsconcentratie aanwezig zouden zijn. Het exclusie volume voor het totale systeem wordt gevonden als het verschil tussen het werkelijke vloeistofvolume,  $V_{tot}$ , en het schijnbare volume, waarin de anionen op evenwichtsconcentratie verdeeld lijken te zijn,  $V_{app}$ . Het zal duidelijk zijn dat in het geval van een optredende positieve adsorptie, welke de negatieve overtreft, het schijnbare volume groter is dan het werkelijke volume, resulterende in een volume van inclusie,  $V_{inc}$ .

$V_{tot}$  kan worden bepaald uit weeggegevens, uitgaande van een soortelijk gewicht van de vloeistoffase van 1,00 gram per ml. Aangezien, althans in het geval van anionen-exclusie,  $V_{ex}$  meestal slechts een zeer klein deel van het totale volume uitmaakt, dient de bepaling van  $V_{app}$  met de grootst mogelijke nauwkeurigheid te geschieden teneinde de fout in de bepaling van  $V_{ex}$  tot een redelijk niveau te beperken. In hoofdstuk 3

wordt aandacht geschonken aan de te verwachten fouten in de metingen.

Voor de bepaling van  $V_{ex}$  staan verschillende methoden ter beschikking indien de interactie tussen chloorionen en bodemcolloïden wordt onderzocht, nl. de potentiometrische titratie-methode en de isotopen-verdunningsmethode. Voor de overige anionen welke werden bestudeerd, nl. sulfaat en fosfaat, werd steeds laatstgenoemde methode toegepast. Aangegeven wordt, hoe simultaan de adsorptie van drie anionen kan worden bepaald, nl. door middel van de titratie-methode voor chloor en door een speciale toepassing van de isotopenmethode (gebaseerd op verschillen in half-waarde tijd) voor sulfaat en fosfaat.

Aangezien bij zeer lage fosfaatconcentraties de adsorptie van fosfaat aan andere materialen dan de bodemcolloïden (b.v. de polyethyleen flessen waarin de systemen tot evenwicht werden gebracht) een aanzienlijke rol ging spelen, werd in een afzonderlijk experiment nagegaan welk minimum fosfaatk niveau vereist was teneinde genoemde adsorptie te kunnen verwaarlozen.

De isolatie van de evenwichtsooplossing uit de suspensie werd bewerkstelligd door het toevoegen van dialyze-zakjes, gevuld met gedistilleerd water, aan de systemen. Evenwicht tussen oplossing binnen en buiten de zakjes werd verkregen door schudden.

Bij het uitzetten van de gemeten  $V_{ex}$  waarden tegen de niet voor  $\delta^-$  gecorrigeerde afstand van exclusie wordt (bij afwezigheid van positieve adsorptie) een rechte lijn gevonden. De helling hiervan is gelijk aan het soortelijk oppervlak van het colloïd en het intercept is gelijk aan  $\delta^-$ . Voor elk systeem kon de exclusie-afstand worden berekend door gebruik te maken van de in hoofdstuk 2 afgeleide  $Q$ -waarden, in combinatie met de waarde van de elektrolyet-concentratie in de evenwichtsooplossing; deze laatste werd gevonden door meting van het specifiek elektrisch geleidingsvermogen in de dialyzaten. Bij aanwezigheid van positieve adsorptie wijken de proefresultaten af van bovengenoemde rechte lijn. De netto (positieve) adsorptie kan dan worden berekend als het produkt van het tekort in  $V_{ex}$  met de evenwichtsconcentratie van het betreffende anion.

Aangezien in de experimenten met fosfaat rekening gehouden moest worden met de verdeling van het toegevoegde  $P^{32}$  over fosfaationen van verschillende waardigheid, werd bij deze experimenten een enigszins afwijkende berekeningstechniek toegepast om de geadsorbeerde hoeveelheden te vinden. Hiertoe werd de verdeling van totaal P over een-, twee- en driewaardige fosfaationen berekend als functie van de in de systemen gemeten pH waarden. Vervolgens werd de verwachte exclusie voor elk dezer ionen berekend. De totale verwachte negatieve adsorptie van fosfaat is de som van deze exclusiewaarden voor de verschillende species. Netto (positieve) adsorptie van fosfaat werd dan gevonden als het verschil tussen de totale verwachte fosfaatexclusie en de schijnbare adsorptie.

De experimenten werden uitgevoerd aan vrij zuivere kleien en aan gronden. Als kleien werden de drie voornaamste kleimineralen gekozen, nl. montmorilloniet (Osage), illiet (Winsum) en kaoliniet (Drybranch). In de proeven met gronden werden 12 Nederlandse gronden gebruikt. Een beschrijving van de gebruikte materialen wordt in dit hoofdstuk gegeven.

Hoofdstuk 4 vermeldt de proefresultaten, welke werden verkregen met kleien. De oppervlakmetingen volgens de anionenexclusiemethode resulteerden in aanmerkelijke waarden. De metingen bij gemengde bezetting waren in overeenstemming met de theoretische verwachtingen.

Bij zeer lage sulfaatconcentraties werd aan de montmorilloniet een positieve sulfaat-adsorptie gemeten, welke geheel verdween na toevoeging van geringe hoeveelheden fosfaat. De illiet vertoonde onder overeenkomstige omstandigheden geen positieve sulfaatadsorptie, aangezien hier het oorspronkelijk in het monster (veldmonster) aanwezige fosfaat reeds voldoende was om sulfaatadsorptie tegen te gaan.

De fosfaatadsorptie aan montmorilloniet werd uitvoerig bestudeerd, waarbij aanwijzingen werden gevonden voor een optredende chemisorptie. Alhoewel ook fluoride de fosfaatadsorptie enigermate bleek te onderdrukken, werd de sterkste concurrentie gevonden tussen silicaat en fosfaat. Bepaalde toevoegingen van silicaat maakten een totale onderdrukking van fosfaatadsorptie mogelijk. Dit effect bleek voornamelijk te moeten worden toegeschreven aan de werking van silicaationen zelf en niet aan de verhoogde pH bij grotere toevoegingen van silicaat. Een tijdproef toonde aan dat de uitwisseling van geadsorbeerd fosfaat tegen toegevoegd silicaat voor ongeveer 80 % verloopt binnen enkele minuten na toevoeging.

Er werden aanwijzingen gevonden dat de binding van fosfaat aan alle onderzochte kleien verloopt volgens tenminste twee verschillende reactiemechanismen. De gevonden adsorptiecapaciteiten konden kwantitatief worden verklaard.

Het effect van verwijdering van organische stof uit de illiet toonde aan, dat deze organische bestanddelen waarschijnlijk een gedeelte van de bindingsplaatsen op de klei afdekken en daardoor gedeeltelijk de adsorptie van fosfaationen verhinderen.

De resultaten van een gelijktijdige bepaling van de adsorptie van drie anionen waren binnen de te verwachten nauwkeurigheid in overeenstemming met de theorie.

Een zeer goede overeenstemming werd gevonden tussen de berekende en de gemeten verkleining van de negatieve adsorption van anionen ten gevolge van interactie van dubbellagen.

De kaoliniet vertoonde een toename van de positieve chlooradsorptie bij afnemende pH waarden vanaf pH 4,5. Uit de invloed van de pH op de chloor- en de fosfaat-adsorptie kon worden geconcludeerd, dat de chlooradsorptie het gevolg is van elektrostatische binding terwijl de fosfaatadsorptie voornamelijk veroorzaakt wordt door chemische binding.

De interactie tussen de anionen chloride en fosfaat en de 12 gronden (fractie  $< 50 \mu$ ) wordt beschreven in hoofdstuk 5. Chloride bleek, in de aanwezigheid van  $10^{-4}$  N  $\text{Na}_3\text{PO}_4$ , door alle gronden te worden geëxcludeerd, waardoor het mogelijk was het soortelijk oppervlak te berekenen volgens de anionenexclusiemethode. De fosfaat-toevoeging bleek voldoende groot om positieve adsorptie van chloride tegen te gaan, zelfs indien de grond rijk was aan ijzeroxiden. De oppervlaktebepaling zoals deze voor drie van de gronden werd uitgevoerd over een uitgestrekt zouttraject leverde dezelfde resultaten, welke werden gevonden bij hoog zoutniveau.

Een vergelijking tussen de oppervlaktemetingen volgens de methode van anionen-exclusie en volgens de ethyleenglycolmethode gaf aanzienlijke verschillen te zien tussen de meetresultaten. De waarden verkregen uit de retentie van ethyleenglycol waren aanmerkelijk groter dan de anionenexclusiewaarden. Aan de hand van de fractieverdeling en de oppervlakteladingsdichtheid van de Winsummonsters kon worden aangetoond, dat de anionenexclusiegegevens voor de fracties  $< 2 \mu$  en  $< 50 \mu$  goed met elkaar overeenstemden; dit was niet het geval voor de ethyleenglycol-resultaten. Het gevonden verschil kan mogelijk worden toegeschreven aan de aanwezigheid van organische stof.

Tenslotte werd voor elk der gronden een fosfaatadsorptie-isotherm gemeten. Hierbij bleek, dat ook de adsorptie van fosfaat aan de grondmonsters verloopt volgens tenminste twee verschillende reactiemechanismen.

## Acknowledgement

This study formed part of a program of fundamental research on the adsorption characteristics of clays and soils by the Laboratory of Soils and Fertilizers of the State Agricultural University, Wageningen. The author is very much indebted to Prof. Dr. G. H. BOLT, under which guidance the investigations have been performed.

The necessary funds for the purchase of the radioisotopes used were supplied by the International Atomic Energy Agency, Vienna.

The assistance in the ordering and delivery of the radioisotopes received from the Institute for the Application of Atomic Energy in Agriculture (ITAL), Wageningen, is gratefully acknowledged.

## Literature

- ALEXANDER, G. B. 1953 The reaction of low molecular weight silicic acids with molybdic acid; *J. Am. Chem. Soc.* 75, 5655.
- BABCOCK, K. L. 1963 Theory of the chemical properties of soil colloidal systems at equilibrium; *Hilgardia* 34, 419.
- BAILAR, J. C. 1956 Chemistry of the coordination compounds; Reinhold Publishing Corp., New York.
- BLACK, C. A. 1960 Soil-plant relationships; John Wiley and Sons, Inc, New York; Sec. pr.
- BOLT, G. H. 1954 Physico-chemical properties of the electric double layer on planar surfaces; Ph. D. Thesis, Cornell University.
- BOLT, G. H. 1955 Analysis of the validity of the Gouy-Chapman theory of the electric double layer; *J. Coll. Sci.* 10, 206.
- BOLT, G. H. and B. P. WARKENTIN 1956 Influence of the method of sample preparation on the negative adsorption of anions in montmorillonite suspensions; Trans. VIe Congrès Intern. de la Science du Sol, Paris.
- BOLT, G. H. 1957 Determination of the charge density of silica sols; *J. Phys. Chem.* 61, 1166.
- BOLT, G. H. and B. P. WARKENTIN 1958 The negative adsorption of anions by clay suspensions; *Koll. Zeitschr.*, 156 Bd, Heft 1, 41.
- BOLT, G. H. 1960 Cations in relation to clay surfaces; Proc. 7th Intern. Congr. Soil Sci.; Madison, 321.
- BOLT, G. H. and M. J. FRISSEL 1960 The preparation of clay suspensions with specified ionic composition by means of exchange resins; *Soil Sci. Soc. Am. Proc.* 24, 172.
- BOLT, G. H. 1961a The pressure filtrate of colloidal suspensions; I Theoretical considerations; *Koll. Zeitschr.*, 175 Bd, Heft 1, 33.
- BOLT, G. H. 1961b The pressure filtrate of colloidal suspensions; II Experimental data on homoionic clays; *Koll. Zeitschr.*, 175 Bd, Heft 1, 144.
- BOLT, G. H. and F. A. M. DE HAAN 1963 Determination of ion exchange characteristics of soils and clays; Report Research Contract No 123/RB between I.A.E.A., Vienna, and Lab. of Soils and Fertilizers, Wageningen (available on request).
- BOLT, G. H. and F. A. M. DE HAAN 1964 Diffusion of alkali chlorides in clay-water systems; A discussion of a report by G. R. Dutt and P. F. Low; *Soil Sci.* 97, 344.



- BOLT, G. H. and B. G. M. PIETERS 1964 Assessing the activity concentrations of  $\beta$ -emitters by means of the end-window G. M. tube; *Anal. Chim. Act.* 31, 64.
- BOWER, C. A. and F. B. GESCHWEND 1952 Measure of surface area and interlayer swelling; *Soil Sci. Soc. Am. Proc.* 16, 342.
- BOWER, C. A. and J. D. GOERTZEN 1959 Surface area of soils and clays by an equilibrium ethylene glycol method; *Soil Sci.* 87, 289.
- BRELAND, H. L. and F. A. SIERRA 1962 A comparison of the amounts of phosphorus removed from different soils by various extractants; *Soil Sci. Soc. Am. Proc.* 26, 348.
- BROWN, A. S. 1934 A type of silver chloride electrode suitable for use in dilute solutions; *J. Am. Chem. Soc.* 56, 646.
- BRUNAUER, S., P. H. EMMETT and E. TELLER 1938 Adsorption of gases in multimolecular layers; *J. Am. Chem. Soc.* 60, 309.
- BURFORD, J. R. *et al.* 1964 Influence of organic materials on the determination of the specific surface areas of soils; *J. Soil Sci.* 15, 192.
- CASHEN, G. H. 1959 Electric charges of kaolin; *Trans. Far. Soc.* 55, 477.
- CHANG, M. L. and G. W. THOMAS 1963 A suggested mechanism for sulfate adsorption by soils; *Soil Sci. Soc. Am. Proc.* 27, 281.
- CHAO TSUN TIEN, M. E. HARWARD and S. C. FONG 1962 Adsorption and desorption phenomena of sulfate ions in soils; *Soil Sci. Soc. Am. Proc.* 26, 234.
- CHAO TSUN TIEN, M. E. HARWARD and S. C. FONG 1963 Cationic effects of sulfate adsorption by soils; *Soil Sci. Soc. Am. Proc.* 27, 35.
- COLE, C. V., S. R. OLSEN and C. O. SCOTT 1953 The nature of phosphate sorption by calcium carbonate; *Soil Sci. Soc. Am. Proc.* 17, 352.
- DAVIS, L. E. 1945 Theories of base-exchange equilibria; *Soil Sci.* 59, 379.
- DERYAGUIN, B. V. and N. K. MELNIKOVA 1958 Mechanism of moisture equilibrium and migration in soils. Highway Research Board, Spec. Rep. 40, Int. Symp. 1958, 43.
- DUTT, G. R. and P. F. LOW 1962 Diffusion of alkali chlorides in clay-water systems; *Soil Sci.* 93, 233.
- DYAL, R. S. and S. B. HENDRICKS 1950 Total surface of clays in polar liquids as a characteristic index; *Soil Sci.* 69, 421.
- EDELMAN, C. H. 1950 Soils of the Netherlands; Amsterdam.
- ENSMINGER, L. E. 1954 Some factors affecting the adsorption of sulfate by Alabama soils; *Soil Sci. Soc. Am. Proc.* 18, 259.
- ERIKSSON, E. 1952 Cationic exchange equilibria on clay minerals; *Soil Sci.* 74, 103.
- FIFE, C. V. 1959 An evaluation of ammoniumfluoride as a selective extractant for aluminum-bound soil phosphate: II Preliminary studies on soils; *Soil Sci.* 87, 83.
- FLAIG, W. and H. BEUTELSPACHER 1954 Physikalische Chemie der Huminsäuren; *Lbk. Tijdschrift* 66, 306.
- FRIED, M. and L. A. DEAN 1952 A concept concerning the measurement of available soil nutrients; *Soil Sci.* 73, 263.
- FRIED, M. and R. E. SHAPIRO 1956 Phosphate supply pattern of various soils; *Soil Sci. Soc. Am. Proc.* 20, 471.

- FRIED, M. and J. C. NOGGLE 1958 Multiple site uptake of individual cations by roots as affected by hydrogen ions; *Plant Physiol.* 33, 139.
- FRINK, C. R. and M. PEECH 1963 Hydrolysis of the aluminum ion in dilute aqueous solutions; *Inorg. Chem.* 2, 473.
- FRIPIAT, J. J., M. C. GASTUCHE and G. VANCOMPERNOLLE 1954 Les groupes hydroxyles de surface de la kaolinite et sa capacité d'échange ionique; *Actes et Comptes rendus du Ve Congrès Int. de la Science du Sol*, Vol II, 401.
- FRIPIAT, J. J. 1957 Progrès apportés par la chimie de surface à la connaissance des argiles; *Bull. Soc. Française de Céramique*, No A4-A5, 111.
- FRISSEL, M. J. 1961 The adsorption of some organic compounds, especially herbicides, on clay minerals; Ph. D. Thesis, Utrecht.
- GAARDER, T. 1930 Die Bindung von Phosphorsäure im Erdboden; *Medd. Nr 14 Kgl. vestl. Forstl. Fors-Stat.*
- GAINES, G. L. and H. C. THOMAS 1953 Adsorption studies on clay minerals, II; *J. Chem. Phys.* 21, 714.
- GAPON, E. N. 1933 On the theory of exchange adsorption in soils; *J. Gen. Chem. U.S.S.R.* 3, 144.
- GREENLAND, D. J. and J. P. QUIRK 1963 Determination of surface areas by adsorption of cetyl pyridinium bromide from aqueous solution; *J. Phys. Chem.* 67, 2886.
- GREENLAND, D. J. and J. P. QUIRK 1964 Determination of the total specific surface areas of soils by adsorption of cetyl pyridinium bromide; *J. Soil Sci.* 15, 178.
- HAAN, F. A. M. DE, and G. H. BOLT 1963 Determination of anion adsorption by clays; *Soil Sci. Soc. Am. Proc.* 27, 636.
- HAAN, F. A. M. DE, G. H. BOLT and B. G. M. PIETERS 1964 Application of radioactive K-isotopes to the determination of K-adsorption and -release characteristics of potassium containing materials; *Int. J. Applied Radiation and Isotopes*, 15, 221.
- HAAN, F. A. M. DE 1964 The negative adsorption of anions (anion exclusion) in systems with interacting double layers; *J. Phys. Chem.* 68, 2970.
- HAAN, F. A. M. DE 1965 Determination of the specific surface area of soils on the basis of anion exclusion measurements; *Soil Sci.* (in print).
- HAGEN, C. E. and H. T. HOPKINS 1955 Ionic species in orthophosphate absorption by barley roots; *Plant Physiol.* 30, 193.
- HARVEY, E. N. 1943 Surface areas of porous materials calculated from capillary radii; *J. Am. Chem. Soc.* 65, 2343.
- HASEMAN, J. F., E. H. BROWN and C. D. WHITT 1950 Some reactions of phosphate with clays and hydrous oxides of iron and aluminum; *Soil Sci.* 70, 257.
- HENDRICKS, S. B. 1941 Base exchange of the clay mineral montmorillonite for organic cations and its dependence upon adsorption due to v. d. Waals forces; *J. Phys. Chem.* 45, 65.
- HEMWALL, J. B. 1957 The role of soil clay minerals in phosphorus fixation; *Soil Sci.* 83, 101.

- HEMWALL, J. B.
- HITCHCOCK, D. I.
- HOFSTEE, B. H. J.
- HOLMES, R. M. and S. J. TOTY
- HSU, P. H. and C. I. RICH
- HSU, P. H. and D. A. RENNIE
- HSU, P. H.
- ILER, R. K.
- JACKSON, M. L.
- JENNY, H.
- KAMPATH, E. J., W. L. NELSON and J. W. FITTS
- KELLEY, W. P.
- KEMPER, W. D.
- KERR, H. W.
- KLAARENBECK, F. W.
- KOENIGS, F. F. R.
- KRISNAMOORTHY, C. and R. OVERSTREET
- KURMIES, B.
- LAGERWERFF, J. V. and G. H. BOLT
- LARSEN, S.
- LAWRIE, D. C.
- LIU, M. and G. W. THOMAS
- LOW, P. F. and C. A. BLACK
- 1963 The adsorption of 4-tert-butylpyrocatechol by soil clay minerals; *Proc. Int. Clay Conf.* Stockholm, Vol 1, 319.
- 1926 The formal identity of Langmuir's adsorption equation with the law of mass action; *J. Am. Chem. Soc.* 48, 2870.
- 1952 On the evaluation of the constants  $V_m$  and  $K_m$  in enzyme reactions; *Science* 116, 329.
- 1957 Physico-chemical behavior of clay-conditioner complexes; *Soil Sci.* 84, 479.
- 1960 Aluminum fixation in a synthetic cation exchanger; *Soil Sci. Soc. Am. Proc.* 24, 21.
- 1962 Reactions of phosphate in aluminum systems; *Can. J. Soil Sci.* 42, 197.
- 1964 Adsorption of phosphate by aluminum and iron in soils; *Soil Sci. Soc. Am. Proc.* 28, 474.
- 1955 The colloid chemistry of silica and silicates; Cornell University Press, Ithaca, New York.
- 1963 Aluminum bonding in soils: a unifying principle in soil science; *Soil Sci. Soc. Am. Proc.* 27, 1.
- 1936 Simple kinetic theory of ionic exchange; *J. Phys. Chem.* 40, 501.
- 1956 The effect of pH, sulfate and phosphate concentrations on the adsorption of sulfate by soils; *Soil Sci. Soc. Am. Proc.* 20, 463.
- 1948 Cation exchange in soils; New York.
- 1961 Movement of water as effected by free energy and pressure gradients; *Soil Sci. Soc. Am. Proc.* 25, 255 and 260.
- 1928 The identification and composition of the soil alumina-silicate active in base exchange and soil activity; *Soil Sci.* 26, 385.
- 1946 Over Donnan-evenwichten bij solen van Arabische gom; Ph. D. Thesis, Utrecht.
- 1961 The mechanical stability of clay soils as influenced by the moisture conditions and some other factors; Ph. D. Thesis, Wageningen.
- 1949 Theory of ion exchange relationships; *Soil Sci.* 68, 307.
- 1949 Humusbestimmung nach dem Bichromat-verfahren ohne Kaliumjodid; *Zeitschr. Pfl. ernähr. Düng. Bodenk.* 44, 121.
- 1959 Theoretical and experimental analysis of Gapon's equation for ion exchange; *Soil Sci.* 87, 217.
- 1952 The use of  $P^{32}$  in studies on the uptake of phosphorus by plants; *Plant and Soil* 4, 1.
- 1961 A rapid method for the determination of approximate surface areas of clays; *Soil Sci.* 92, 188.
- 1961 Nature of sulfate retention by acid soils; *Nature* 192, 384.
- 1950 Reactions of phosphate with kaolinite; *Soil Sci.* 70, 273.

- LYON, T. L., H. O. BUCKMAN and N. C. BRADY  
MAGISTADT, O. C., M. FIREMANN and B. MABRY  
MARTIN, R. T.
- MASON, B. and T. BERGGREN
- MATTSON, S.
- MATTSON, S.
- McAULIFFE, C. D., N. S. HALL, L. A. DEAN and S. B. HENDRICKS
- McNEAL, B. L.
- MEHLICH, A.
- MITCHELL, B. D. and R. C. MACKENZIE
- MORTENSEN, L. J.
- ØIEN, A., G. SEMB and K. STEENBERG
- OLPHEN, H. VAN
- OLSEN, S. R. and F. S. WATANABLE
- ORCHISTON, H. D.  
PRATT, P. F., L. D. WHITTIG and B. L. GROVER  
PURI, A. N.
- PURI, B. R. and K. MURARI
- RAGLAND, J. L. and N. T. COLEMAN
- RUSSELL, R. SCOTT, J. B. RICKSON and S. N. ADAMS
- SCHOFIELD, R. K.
- SCHOFIELD, R. K.
- 1952 The nature and properties of soils; 378, The MacMillan Company, New York.
- 1944 Comparison of base exchange equations founded on the law of mass action; *Soil Sci.* 57, 371.
- 1955 Ethylene glycol retention by clays; *Soil Sci. Soc. Am. Proc.* 19, 160.
- 1941 A phosphate-bearing spessartite garnet from Wodgina, Western Australia; *Geol. Förr., Stockholm, Förhandl.* 63, 413.
- 1927 Anionic and cationic adsorption by soil colloidal materials of varying  $\text{SiO}_2/\text{Al}_2\text{O}_3 + \text{Fe}_2\text{O}_3$  ratios; *Trans. Int. Congr. Soil Sci.*, Washington, 2, 199.
- 1942 Laws of ionic exchange; *Lantbr. Högsk. Ann.* 10, 56.
- 1947 Exchange reactions between phosphates and soils: Hydroxylic surfaces of soil minerals; *Soil Sci. Soc. Am. Proc.* 12, 119.
- 1964 Effect of exchangeable cations on glycol retention by clay minerals; *Soil Sci.* 97, 96.
- 1961 Influence of sorbed hydroxyl and sulfate on soil pH, neutralization of acidity, calcium release and cation exchange capacity; *Agr. Abstr. Am. Soc. Agr.*, Madison, Wisc. 13.
- 1954 Removal of free iron oxide from clays; *Soil Sci.* 77, 173
- 1959 Adsorption of hydrolyzed polyacrylonitrile on kaolinite; *Soil Sci. Soc. Am. Proc.* 23, 199.
- 1959 Comparison of leaching and fixation of K and Rb in soils using the isotopes  $\text{K}^{40}$  and  $\text{Rb}^{86}$ ; *Soil Sci.* 88, 284.
- 1951 The rheological properties of drilling fluids; Ph. D. Thesis, Delft.
- 1957 A method to determine a phosphorus adsorption maximum of soils as measured by the Langmuir isotherm; *Soil Sci. Soc. Am. Proc.* 21, 144.
- 1953 Adsorption of water vapour: I; *Soil Sci.* 76, 453.
- 1962 Effect of pH on the sodium-calcium exchange equilibria in soils; *Soil Sci. Soc. Am. Proc.* 26, 227.
- 1949 Soils, Their Physics and Chemistry; Reinhold Publishing Corp., New York.
- 1963 Studies in surface area measurements of soils, I Comparison of different methods; *Soil Sci.* 96, 331.
- 1960 The hydrolysis of aluminum salts in clay and soil systems; *Soil Sci. Soc. Am. Proc.* 24, 457.
- 1954 Isotopic equilibria between phosphates in soil and their significance in the assessment of fertility by tracer methods; *J. Soil Sci.* 5, 85.
- 1946 Ionic forces in thick films of liquid between charged surfaces; *Trans. Far. Soc.* 42 B, 219.
- 1947 Calculation of surface areas from measurements of negative adsorption; *Nature* 160, 408.

- SCHOFIELD, R. K. 1949 Effect of pH on electric charges carried by clay particles; *J. Soil Sci.* 1, 1.
- SCHOFIELD, R. K. and A. WORMALD 1954 The hydrolysis of aluminum salt solutions; *J. Chem. Soc.* 4445.
- TAYLOR 1963 Potassium-exchange behavior of an illite; *Neth. J. Agr. Sci.* 11, 13.
- SCHOUWENBURG, J. CH. VAN and A. C. SCHUFFELEN 1959 Relative release and retentiveness of soil phosphates; *Soil Sci. Soc. Am. Proc.* 23, 195.
- SHAPIRO, R. E. and M. FRIED 1961 Componenten van het fosfaat in de grond welke betrokken zijn bij de fosfaatvoorziening van de plant; Ph. D. Thesis, Wageningen.
- SISSINGH, H. A. 1961 The influence of precipitated iron oxides on the surface properties of clays and soils; Ph. D. Thesis, Wadham College.
- SUMNER, M. E. 1962 Isotopic exchange of potassium in an illite under equilibrium conditions; *Soil Sci. Soc. Am. Proc.* 26, 541.
- SUMNER, M. E. and G. H. BOLT 1930 The effect of colloidal silica on the absorption of phosphoric acid by plants; *Science* 71, 422.
- THOMAS, W. 1962 Soil chemistry as an aid in interpretation of soil genetics and morphology; *Virg. Agr. Exp. Stat.*
- THOMAS, G. W. 1939 The stimulating effects of silicates on plant yields in relation to anion displacement; *Soil Sci.* 47, 123.
- THOT, S. J. 1932 Der Kationen- und Wasserhaushalt des Mineralbodens; Berlin.
- VAGELER, P. 1932 Equilibria of the base-exchange reactions of bentonites, permutites, soil colloids and zeolites; *Soil Sci.* 33, 95.
- VANSELOW, A. P. 1959 Reaction of phosphate with allophane and halloysite; *Soil Sci.* 87, 325.
- WADA, K. 1956 Etude de la rétention des anions phosphoriques par les argiles: montmorillonite et kaolinite; *Ann. Agron.* 1, 1.
- WEY, R. 1951 Equilibria in ion exchange; I Influence of the proportions of exchanging ions; *Act. Agr. Scand.* 2, 190.
- WIKLANDER, L. 1952 Equilibria in ion exchange; II Influence of the mode of replacement; *Act. Agr. Scand.* 11, 3, 197.
- WIKLANDER, L. 1964 Interrelationships between potassium and magnesium absorption by oats; Ph. D. Thesis, Wageningen.
- YOSHIDA, F.

## Appendix I

### Derivations for systems with mono- and divalent cations and anions

1 The expression for the negative adsorption of the *monovalent anion* in such a system is found in the following way:

By dividing both the numerator and the denominator of the integral in equation (2.9) by  $(u-1)$  one finds:

$$\begin{aligned}
 \frac{\Gamma^-}{(1-f^-)N_0} &= \pm \frac{\sqrt{2}}{\sqrt{\beta N_0}} \cdot \int_{\infty}^1 \frac{du}{u\sqrt{f^{++}u^2+2u+f^-}} - \delta^- \\
 &= \pm \frac{\sqrt{2}}{\sqrt{\beta N_0}} \cdot \left[ -\frac{1}{\sqrt{f^-}} \cdot \sinh^{-1} \frac{2\sqrt{f^{++}f^-}u^2+2f^-u+f^-f^-}{u\sqrt{4-4f^{++}f^-}} \right]_1^{\infty} - \delta^- \\
 &= \pm \frac{\sqrt{2}}{\sqrt{\beta N_0}} \cdot \left[ -\frac{1}{\sqrt{f^-}} \cdot \sinh^{-1} \frac{\sqrt{f^-} \cdot \sqrt{f^{++}u^2+2u+f^-}}{u\sqrt{1-f^{++}f^-}} \right]_1^{\infty} - \delta^- \\
 &= \pm \frac{\sqrt{2}}{\sqrt{\beta N_0}} \\
 &\quad \cdot \left\{ -\frac{1}{\sqrt{f^-}} \sinh^{-1} \frac{\sqrt{f^{++}} \cdot \sqrt{f^-}}{\sqrt{1-f^{++}f^-}} + \frac{1}{\sqrt{f^-}} \sinh^{-1} \frac{\sqrt{f^-} \cdot \sqrt{f^{++}+2+f^-}}{\sqrt{1-f^{++}f^-}} \right\} - \delta^-.
 \end{aligned} \tag{2.10}$$

Because of the positive value of the negative adsorption the formula for the monovalent anion becomes:

$$\begin{aligned}
 \frac{\Gamma^-}{(1-f^-)N_0} &= \frac{\sqrt{2}}{\sqrt{\beta N_0}} \\
 &\quad \cdot \left\{ \frac{1}{\sqrt{f^-}} \left( \sinh^{-1} \frac{\sqrt{f^-} \cdot \sqrt{f^{++}+2+f^-}}{\sqrt{1-f^{++}f^-}} - \sinh^{-1} \frac{\sqrt{f^-} \cdot \sqrt{f^{++}}}{\sqrt{1-f^{++}f^-}} \right) \right\} - \delta^-
 \end{aligned} \tag{2.14}$$

2 The derivation of the expression for the *divalent anion* runs in a similar way.

$$\begin{aligned}
 \frac{\Gamma^-}{f^-N_0} &= \pm \frac{\sqrt{2}}{\sqrt{\beta N_0}} \cdot \int_{\infty}^1 \frac{(u+1)du}{u^2\sqrt{f^{++}u^2+2u+f^-}} - \delta^- \\
 &= \pm \frac{\sqrt{2}}{\sqrt{\beta N_0}} \cdot \left\{ \int_{\infty}^1 \frac{udu}{u^2\sqrt{f^{++}u^2+2u+f^-}} + \int_{\infty}^1 \frac{du}{u^2\sqrt{f^{++}u^2+2u+f^-}} \right\} - \delta^-
 \end{aligned} \tag{2.13}$$

$$\begin{aligned}
&= \pm \frac{\sqrt{2}}{\sqrt{\beta N_0}} \cdot \left\{ \int_{-\infty}^1 \frac{du}{u\sqrt{f^{++}u^2+2u+f^-}} - \left[ \frac{\sqrt{f^{++}u^2+2u+f^-}}{f^-u} \right]_1^{\infty} \right. \\
&\quad \left. - \frac{1}{f^-} \cdot \int_{-\infty}^1 \frac{du}{u\sqrt{f^{++}u^2+2u+f^-}} \right\} - \delta^- \\
&= \pm \frac{\sqrt{2}}{\sqrt{\beta N_0}} \cdot \left\{ \frac{f^- - 1}{f^-} \cdot \int_{-\infty}^1 \frac{du}{u\sqrt{f^{++}u^2+2u+f^-}} - \left[ \frac{\sqrt{f^{++}u^2+2u+f^-}}{f^-u} \right]_1^{\infty} \right\} - \delta^-
\end{aligned}$$

The integral of this equation has been solved already at the derivation of the expression for the monovalent anion.

Furthermore

$$- \left[ \frac{\sqrt{f^{++}u^2+2u+f^-}}{f^-u} \right]_1^{\infty} = \frac{\sqrt{f^{++}+2+f^-}}{f^-} - \frac{\sqrt{f^{++}}}{f^-}$$

Thus finally the expression for the divalent anion is found as:

$$\begin{aligned}
\frac{\Gamma^-}{f^-N_0} &= \frac{\sqrt{2}}{\sqrt{\beta N_0}} \cdot \left\{ \frac{\sqrt{f^{++}+2+f^-}}{f^-} - \frac{\sqrt{f^{++}}}{f^-} - \frac{1-f^-}{f^-} \right. \\
&\quad \cdot \frac{1}{\sqrt{f^-}} \left( \sinh^{-1} \frac{\sqrt{f^-} \cdot \sqrt{f^{++}+2+f^-}}{\sqrt{1-f^{++}f^-}} - \sinh^{-1} \frac{\sqrt{f^{++}} \cdot \sqrt{f^-}}{\sqrt{1-f^{++}f^-}} \right) \left. \right\} - \delta^- \quad (2.15)
\end{aligned}$$

After substitution of the terms within accolades in the equations (2.14) and (2.15), multiplied by  $\sqrt{2}$ , by  $Q'_a$  and  $Q''_a$ , respectively, the expressions for the negative adsorption of the anions in this system may be represented by:

$$\frac{\Gamma^-}{(1-f^-)N_0} = \frac{1}{\sqrt{\beta N_0}} \cdot Q'_a - \delta^- \quad (2.16) \text{ for the monovalent anion and}$$

$$\frac{\Gamma^-}{f^-N_0} = \frac{1}{\sqrt{\beta N_0}} \cdot Q''_a - \delta^- \quad (2.17) \text{ for the divalent anion.}$$

Using equations (2.14) and (2.15)  $Q_a$  values can be calculated for all different values of  $f^{++}$  and  $f^-$ .

The performance of these calculations for the limiting value of  $f^- (= 0)$  requires the use of series expansions for certain terms appearing in the equations (2.14) and (2.15).

### 3 The calculation of $Q_a$ values at the condition $f^- = 0$ .

To this purpose the series expansion of the inversed hyperbolic sine is used.

$$\begin{aligned}
Q'_s &= \frac{\sqrt{2}}{\sqrt{f''}} \cdot \left( \sinh^{-1} \frac{\sqrt{f''} \cdot \sqrt{f^{++}+2+f''}}{\sqrt{1-f^{++}f''}} - \sinh^{-1} \frac{\sqrt{f^{++}} \cdot \sqrt{f''}}{\sqrt{1-f^{++}f''}} \right) \\
&= \frac{\sqrt{2}}{\sqrt{f''}} \cdot \frac{\sqrt{f''} \cdot \sqrt{f^{++}+2+f''}}{\sqrt{1-f^{++}f''}} - \frac{1}{6} \cdot \frac{\sqrt{2}}{\sqrt{f''}} \cdot \frac{\sqrt{(f'')^3} \cdot \sqrt{(f^{++}+2+f'')^3}}{\sqrt{(1-f^{++}f'')^3}} \\
&\quad - \frac{\sqrt{2}}{\sqrt{f''}} \cdot \frac{\sqrt{f^{++}} \cdot \sqrt{f''}}{\sqrt{1-f^{++}f''}} + \frac{1}{6} \cdot \frac{\sqrt{2}}{\sqrt{f''}} \cdot \frac{\sqrt{(f^{++})^3} \cdot \sqrt{(f'')^3}}{\sqrt{(1-f^{++}f'')^3}} \\
&= \frac{\sqrt{2} \cdot (\sqrt{f^{++}+2+f''} - \sqrt{f^{++}})}{\sqrt{1-f^{++}f''}} - \frac{\sqrt{2}}{6} \cdot f'' \cdot \frac{\sqrt{(f^{++}+2+f'')^3} - \sqrt{(f^{++})^3}}{\sqrt{(1-f^{++}f'')^3}}
\end{aligned}$$

Thus one finds for  $f^{++} = 0$  and  $f'' = 0$ :  $Q'_s = 2.000$

for  $f^{++} = 1$  and  $f'' = 0$ :  $Q'_s = 1.035$

In a similar way one arrives for  $Q''_s$  at:

$$\begin{aligned}
Q''_s &= \sqrt{2} \\
&\cdot \left\{ \frac{\sqrt{f^{++}+2+f''}}{f''} - \frac{\sqrt{f^{++}}}{f''} - \frac{1-f''}{f''} \cdot \frac{\sqrt{f^{++}+2+f''}}{\sqrt{1-f^{++}f''}} + \frac{1-f''}{f''} \cdot \frac{\sqrt{f^{++}}}{\sqrt{1-f^{++}f''}} \right. \\
&\quad \left. + \frac{1}{6} \cdot \frac{(1-f'')\sqrt{(f^{++}+2+f'')^3}}{\sqrt{(1-f^{++}f'')^3}} - \frac{1}{6} \cdot \frac{(1-f'')\sqrt{(f^{++})^3}}{\sqrt{(1-f^{++}f'')^3}} \right\} \\
Q''_s &= \sqrt{2} \cdot \left\{ \frac{1}{f''} \cdot \sqrt{f^{++}+2+f''} \cdot \left( 1 - \frac{1}{\sqrt{1-f^{++}f''}} \right) + \frac{\sqrt{f^{++}+2+f''}}{\sqrt{1-f^{++}f''}} \right. \\
&\quad \left. - \frac{1}{f''} \cdot \sqrt{f^{++}} \cdot \left( 1 - \frac{1}{\sqrt{1-f^{++}f''}} \right) - \frac{\sqrt{f^{++}}}{\sqrt{1-f^{++}f''}} \right. \\
&\quad \left. + \frac{1}{6} \cdot \frac{(1-f'')\sqrt{(f^{++}+2+f'')^3}}{\sqrt{(1-f^{++}f'')^3}} - \frac{1}{6} \cdot \frac{(1-f'')\sqrt{(f^{++})^3}}{\sqrt{(1-f^{++}f'')^3}} \right\}
\end{aligned}$$

Now the series expansion of  $1/\sqrt{1-f^{++}f''}$  is introduced, which reads:

$$1 + \frac{1}{2}f^{++}f'' + \frac{3}{8}(f^{++}f'')^2 + \dots$$

Thus the term  $1 - 1/\sqrt{1-f^{++}f''}$  equals  $-\{\frac{1}{2}f^{++}f'' + \frac{3}{8}(f^{++}f'')^2 + \dots\}$

Substituting  $\sqrt{F}$  for  $\sqrt{f^{++}+2+f''}$  and introducing the above series expansion one finds:

$$\begin{aligned}
Q''_s &= \sqrt{2} \cdot \left[ -\frac{1}{f''} \cdot \sqrt{F} \cdot \left\{ \frac{1}{2}f^{++}f'' + \frac{3}{8}(f^{++}f'')^2 \right\} + \sqrt{F} \cdot \left\{ 1 + \frac{1}{2}f^{++}f'' + \frac{3}{8}(f^{++}f'')^2 \right\} \right. \\
&\quad \left. + \frac{1}{f''} \cdot \sqrt{f^{++}} \cdot \left\{ \frac{1}{2}f^{++}f'' + \frac{3}{8}(f^{++}f'')^2 \right\} - \sqrt{f^{++}} \cdot \left\{ 1 + \frac{1}{2}f^{++}f'' + \frac{3}{8}(f^{++}f'')^2 \right\} \right]
\end{aligned}$$



$$\begin{aligned}
& + \frac{1-f^-}{6\sqrt{(1-f^{++}f^-)^3}} \cdot (F\sqrt{F}-f^{++}\sqrt{f^{++}}) \Big] \\
& = \sqrt{2} \cdot \left[ -\sqrt{F} \cdot \left\{ \frac{1}{2}f^{++} + \frac{3}{8}(f^{++})^2 \cdot f^- \right\} + \sqrt{F} \cdot \left\{ 1 + \frac{1}{2}f^{++}f^- + \frac{3}{8}(f^{++}f^-)^2 \right\} \right. \\
& + \sqrt{f^{++}} \cdot \left\{ \frac{1}{2}f^{++} + \frac{3}{8}(f^{++})^2 \cdot f^- \right\} - \sqrt{f^{++}} \cdot \left\{ 1 + \frac{1}{2}f^{++}f^- + \frac{3}{8}(f^{++}f^-)^2 \right\} \\
& \left. + \frac{1-f^-}{6\sqrt{(1-f^{++}f^-)^3}} \cdot (F\sqrt{F}-f^{++}\sqrt{f^{++}}) \right]
\end{aligned}$$

Resubstituting for  $F$  one finds at the condition  $f^- = 0$ :

$$\begin{aligned}
Q_a'' &= \sqrt{2} \cdot [(\sqrt{f^{++}+2}-\sqrt{f^{++}}) \cdot (1-\frac{1}{2}f^{++}) + \frac{1}{6}\{(f^{++}+2)\sqrt{f^{++}+2}-f^{++}\sqrt{f^{++}}\}] \\
&= \sqrt{2} \cdot \left\{ (\sqrt{f^{++}+2}) \cdot \left( 1-\frac{1}{2}f^{++} + \frac{f^{++}+2}{6} \right) - \sqrt{f^{++}} \cdot (1-\frac{1}{2}f^{++} + \frac{1}{6}f^{++}) \right\} \\
&= \sqrt{2} \cdot \{ (\sqrt{f^{++}+2}) \cdot (\frac{4}{3}-\frac{1}{2}f^{++}) - \sqrt{f^{++}} \cdot (1-\frac{1}{2}f^{++}) \}
\end{aligned}$$

Thus for  $f^{++} = 0$  and  $f^- = 0$ :  $Q_a'' = 2 \cdot \frac{4}{3} = 2.667$

for  $f^{++} = 1$  and  $f^- = 0$ :  $Q_a'' = \sqrt{2} \cdot (\sqrt{3}-\frac{1}{2}) = 1.507$

For all other values of  $f^{++}$  and  $f^-$ ,  $Q_a$  may be calculated by using directly the terms within accolades in equations (2.14) and (2.15), multiplied by  $\sqrt{2}$  (cf table 1 and figure 2).

## Appendix II

Derivations for systems containing monovalent cations and mono-, di-, and trivalent anions (+1, -1, -2, -3)

1 In this case one finds for the *monovalent anion*:

$$\begin{aligned} & \frac{\Gamma^-}{(1-f^+ - f^{\equiv})N_0} \\ &= \pm \frac{1}{\sqrt{\beta N_0}} \cdot \int_{-\infty}^1 \frac{(1-1/u)du}{\sqrt{u^3 - (2 - \frac{1}{2}f^+ - \frac{2}{3}f^{\equiv})u^2 + (1-f^+ - f^{\equiv})u + \frac{1}{2}f^+ + \frac{1}{3}f^{\equiv}u^{-1}}} - \delta^- \\ &= \pm \frac{1}{\sqrt{\beta N_0}} \cdot \int_{-\infty}^1 \frac{(u-1)du}{\sqrt{u^5 - (2 - \frac{1}{2}f^+ - \frac{2}{3}f^{\equiv})u^4 + (1-f^+ - f^{\equiv})u^3 + \frac{1}{2}f^+u^2 + \frac{1}{3}f^{\equiv}u}} - \delta^- \end{aligned} \quad (2.18)$$

Dividing both the numerator and denominator by  $(u-1)$ :

$$= \pm \frac{1}{\sqrt{\beta N_0}} \cdot \int_{-\infty}^1 \frac{du}{\sqrt{u^3 + (\frac{1}{2}f^+ + \frac{2}{3}f^{\equiv})u^2 + \frac{1}{3}f^{\equiv}u}} - \delta^- \quad (2.19)$$

The third power polynomial in  $u$  of equation (2.19) is substituted by  $B$ , thus:

$$Q'_b = \int_{-\infty}^1 \frac{du}{\sqrt{B}}$$

Solution of this integral requires the roots of  $B$ , which may be found as:

$$\begin{aligned} B &= u\{u^2 + (\frac{1}{2}f^+ + \frac{2}{3}f^{\equiv})u + \frac{1}{3}f^{\equiv}\} \\ &= u[\{u + (\frac{1}{2}f^+ + \frac{1}{3}f^{\equiv})\}^2 + \frac{1}{3}f^{\equiv} - (\frac{1}{2}f^+ + \frac{1}{3}f^{\equiv})^2] \\ &= (u - \alpha_1)\{(u - r)^2 + s^2\} \end{aligned}$$

with  $\alpha_1 = 0$

$$r = -(\frac{1}{2}f^+ + \frac{1}{3}f^{\equiv})$$

$$s = \sqrt{\frac{1}{3}f^+ - (\frac{1}{2}f^+ + \frac{1}{3}f^{\equiv})^2}$$

Since  $-s^2$  is the discriminant of  $u^2 + (\frac{1}{2}f^+ + \frac{2}{3}f^{\equiv})u + \frac{1}{3}f^{\equiv} = 0$  the roots are imaginary if

$$\sqrt{\frac{1}{3}f^+ - \frac{1}{3}f^{\equiv}} > \frac{1}{2}f^+$$

In figure 3 it is shown for which combinations of  $f^-$  and  $f^=$  the discriminant equals zero, is smaller than zero and is larger than zero, respectively. This figure indicates that the roots are imaginary in most cases and therefore the solution is first confined to combinations for which  $s^2 > 0$ .

The integral to be solved may be transformed now into:

$$Q'_b = \int_{\infty}^1 \frac{du}{\sqrt{B}} = \frac{-(a+b)}{c} \cdot F(\varphi, k)$$

in which:  $a = -r + s \operatorname{tg} \theta$

$$b = +r + s \cot \theta$$

$$c = \sqrt{\frac{4s^3}{\sin^3 2\theta}}$$

$$k = |\sin \theta| \quad \text{with } \theta = \frac{1}{2} \operatorname{arc} \operatorname{tg} \frac{s}{\alpha_1 - r}; \quad 0 < \theta < \pi/2$$

$\varphi$  may be found by substituting the integration limits of  $u$  into:

$$u = \frac{a \cos \varphi + b}{1 - \cos \varphi}$$

Because  $\alpha_1 = 0$  in this case it may easily be shown that  $a = b$ , as:

$$\operatorname{tg} 2\theta = \frac{2}{\cot \theta - \operatorname{tg} \theta} = \frac{2s}{b - a - 2r}$$

$$\operatorname{tg} 2\theta = \frac{s}{\alpha_1 - r} = \frac{2s}{-2r}$$

Thus  $b - a = 0 \rightarrow a = b$

The final expression of  $Q'_b$  may now be written as:

$$Q'_b = \frac{-2a}{c} \cdot F(\varphi, k) \quad (2.21)$$

If  $s^2 < 0$  the equation:  $u^2 + (\frac{1}{2}f^- + \frac{2}{3}f^=)u + \frac{1}{3}f^= = 0$  has two real roots, which means that three real roots ( $\alpha_1, \alpha_2, \alpha_3$ ) are found for  $B$ .

In that case

$$Q'_b = 2\lambda \cdot F(\varphi, k) \quad (2.22)$$

with  $\lambda = 1/\sqrt{\alpha_1 - \alpha_3}$  and  $k^2 = (\alpha_2 - \alpha_3)/(\alpha_1 - \alpha_3)$

$\varphi$  is now found by substituting the integration limits into:

$$u = \frac{\alpha_1 - \alpha_2 \sin^2 \varphi}{1 - \sin^2 \varphi}$$

It is noted that  $F(\phi, k)$  in equation (2.22) represents an incomplete elliptic integral with integration limits  $\phi$  and  $\pi/2$ . Its value is found by diminishing the value of the complete elliptic integral,  $F(\pi/2, k)$ , with the value of the incomplete elliptic integral with integration limits 0 and  $\phi$ .

Under the condition that  $f''$  and/or  $f'''$  equal zero, the solutions become less complicated, since equation (2.19) is transformed now into "degraded" elliptic integrals, according to:

a if both  $f''$  and  $f'''$  equal zero

$$\begin{aligned}\frac{\Gamma^-}{N_0} &= \pm \frac{1}{\sqrt{\beta N_0}} \cdot \int_{\infty}^1 \frac{du}{\sqrt{u^3}} - \delta^- \\ &= \pm \frac{1}{\sqrt{\beta N_0}} \cdot \int_{\infty}^1 -2du^{-\frac{1}{2}} - \delta^- \\ &= \frac{2}{\sqrt{\beta N_0}} - \delta^-\end{aligned}$$

Thus in this case  $Q'_b$  is found as 2, which, of course, checks with the  $Q'_a$  value under the same condition. (If  $f^{++}$  and  $f''$  both equal zero  $Q'_a = 2$ , cf table 1).

b if  $f'''$  equals zero

$$\frac{\Gamma^-}{(1-f'')N_0} = \pm \frac{1}{\sqrt{\beta N_0}} \cdot \int_{\infty}^1 \frac{du}{u\sqrt{u+\frac{1}{2}f''}} - \delta^-$$

which is identical with equation (2.10) for  $f^{++} = 0$ .

As indicated above  $Q'_b$  values may be calculated for all combinations of  $f''$  and  $f'''$  (cf table 2 and figure 4).

2 For the negative adsorption of the *divalent anion* in this system one finds:

$$\frac{\Gamma^-}{f''N_0} = \pm \frac{1}{\sqrt{\beta N_0}} \cdot \int_{\infty}^1 \frac{(u+1)du}{u\sqrt{u^3 + (\frac{1}{2}f'' + \frac{2}{3}f''')u^2 + \frac{1}{3}f'''u}} - \delta^-$$

Using the same substitution for the third power polynomial in  $u$  as before:

$$= \pm \frac{1}{\sqrt{\beta N_0}} \cdot \int_{\infty}^1 \frac{(u+1)du}{u\sqrt{B}} - \delta^- \quad (2.24)$$

$$= \pm \frac{1}{\sqrt{\beta N_0}} \cdot \left\{ \int_{\infty}^1 \frac{du}{\sqrt{B}} + \int_{\infty}^1 \frac{du}{u\sqrt{B}} \right\} - \delta^- \quad (2.25)$$

$$= \frac{1}{\sqrt{\beta N_0}} \cdot Q''_b - \delta^- \quad (2.26)$$

Thus  $Q''_b$  values consist of the summation of the two integrals of equation (2.25).

The first integral has been solved already in section 1 of Appendix II, whereas the second integral may be found as:

$$\int \frac{du}{u\sqrt{B}} = \frac{a+b}{c \cdot a} \cdot F(\varphi, k) - \frac{(a+b)^2}{c \cdot a \cdot b} \cdot \int \frac{d\varphi}{(1+a/b \cdot \cos \varphi)\sqrt{1-k^2 \sin^2 \varphi}} \quad (2.25a)$$

in which all symbols have the meaning as described in the foregoing section. Since  $a = b$  the last part of equation (2.25 a) may be transformed as follows:

$$\begin{aligned} & - \frac{(2a)^2}{c \cdot a^2} \cdot \int \frac{d\varphi}{(1+\cos \varphi)\sqrt{1-k^2 \sin^2 \varphi}} \\ & = - \frac{4}{c} \left\{ \frac{1-\cos \varphi}{\sin \varphi} \sqrt{1-k^2 \sin^2 \varphi} + F(\varphi, k) + E(\varphi, k) \right\} \end{aligned}$$

Finally one finds for  $Q_b''$  the expression:

$$Q_b'' = Q_b' + \left\{ -\frac{2}{c} \cdot F(\varphi, k) + \frac{4}{c} \cdot E(\varphi, k) - \frac{4}{c} \cdot \left( \frac{1-\cos \varphi}{\sin \varphi} \cdot \sqrt{1-k^2 \sin^2 \varphi} \right) \right\} \quad (2.27)$$

In the case that  $B$  has three real roots the solution of the second integral of equation (2.25) reads:

$$\int \frac{du}{u\sqrt{B}} = 2\lambda \cdot \{ -E(\varphi, k) - \cot \varphi \sqrt{1-k^2 \sin^2 \varphi} \}$$

Then the expression for  $Q_b''$  is found as:

$$Q_b'' = 2\lambda \cdot \{ F(\varphi, k) - E(\varphi, k) - \cot \varphi \sqrt{1-k^2 \sin^2 \varphi} \} \quad (2.27a)$$

With the use of equations (2.27) and (2.27 a)  $Q_b''$  values may be calculated for all combinations of  $f^+$  and  $f^-$  (cf table 2 and figure 5).

If both  $f^+$  and  $f^-$  equal zero the negative adsorption of the divalent anion in this system is found as:

$$\begin{aligned} \frac{\Gamma^-}{f^- N_0} &= \pm \frac{1}{\sqrt{\beta N_0}} \cdot \left\{ \int_{\infty}^1 \frac{du}{\sqrt{u^3}} + \int_{\infty}^1 \frac{du}{u\sqrt{u^3}} \right\} - \delta^- \\ &= \pm \frac{1}{\sqrt{\beta N_0}} \cdot \left\{ \int_{\infty}^1 -2du^{-\frac{1}{2}} + \int_{\infty}^1 -\frac{1}{3}du^{-\frac{3}{2}} \right\} - \delta^- \\ &= \frac{2.667}{\sqrt{\beta N_0}} - \delta^- \end{aligned}$$

(cf table 2)

3 The negative adsorption of the *trivalent anion* in this system is found as:

$$\begin{aligned}\frac{\Gamma^{\equiv}}{f^{\equiv} N_0} &= \pm \frac{1}{\sqrt{\beta N_0}} \cdot \int_{\infty}^1 \frac{(u^2 + u + 1) du}{u^2 \sqrt{u^3 + (\frac{1}{2}f^{\equiv} + \frac{2}{3}f^{\equiv})u^2 + \frac{1}{3}f^{\equiv}u}} - \delta^- \\ &= \pm \frac{1}{\sqrt{\beta N_0}} \cdot \int_{\infty}^1 \frac{(u^2 + u + 1) du}{u^2 \sqrt{B}} - \delta^- \quad (2.29)\end{aligned}$$

$$= \pm \frac{1}{\sqrt{\beta N_0}} \cdot \left\{ \int_{\infty}^1 \frac{du}{\sqrt{B}} + \int_{\infty}^1 \frac{du}{u\sqrt{B}} + \int_{\infty}^1 \frac{du}{u^2\sqrt{B}} \right\} - \delta^- \quad (2.30)$$

The summation of the first and second integral has been executed for the calculation of  $Q_b''$  values.

The third integral may be converted to the foregoing integrals by means of a recurrence procedure.

If the integral  $\int u^t \cdot du/\sqrt{B}$  is defined as  $J_t$ , the integrals already solved are represented by  $J_0$  and  $J_{-1}$ , respectively. Thus  $Q_b'''$  is then found as the summation of  $J_0$  plus  $J_{-1}$  plus  $J_{-2}$ . The recurrence procedure for  $J_t$  in this case reads:

$$(2t+5) \cdot J_{t+3} + (2t+4) \cdot (\frac{1}{2}f^{\equiv} + \frac{2}{3}f^{\equiv}) \cdot J_{t+2} + (2t+3) \cdot \frac{1}{3}f^{\equiv} \cdot J_{t+1} = [2(u)^{t+1} \cdot \sqrt{B}]_1^{\infty}$$

For the transformation of  $J_{-2}$  the value  $-3$  is substituted for  $t$ , resulting in:

$$-J_0 - 2(\frac{1}{2}f^{\equiv} + \frac{2}{3}f^{\equiv}) \cdot J_{-1} - f^{\equiv} \cdot J_{-2} = [2u^{-2}\sqrt{u^3 + (\frac{1}{2}f^{\equiv} + \frac{2}{3}f^{\equiv})u^2 + \frac{1}{3}f^{\equiv}u}]_1^{\infty}$$

Since  $J_0$  and  $J_{-1}$  are known for different values of  $f^{\equiv}$  and  $f^{\equiv}$  the problem has been solved now in principle, thus:

$$J_{-2} = \frac{-J_0 - (f^{\equiv} + \frac{4}{3}f^{\equiv}) \cdot J_{-1}}{f^{\equiv}} - \left[ \frac{2\sqrt{u^3 + (\frac{1}{2}f^{\equiv} + \frac{2}{3}f^{\equiv})u^2 + \frac{1}{3}f^{\equiv}u}}{u^2 \cdot f^{\equiv}} \right]_1^{\infty}$$

As  $Q_b'$  is represented by  $J_0$  and values for  $Q_b''$  consist of the summation  $J_0 + J_{-1}$  (cf. sections 1 and 2, respectively, of this appendix)  $J_{-1}$  may be substituted by  $(Q_b'' - Q_b')$ . Thus finally one arrives at the equation:

$$Q_b''' = \frac{2\sqrt{1 + \frac{1}{2}f^{\equiv} + f^{\equiv}}}{f^{\equiv}} - \frac{1 - f^{\equiv}}{f^{\equiv}} \cdot Q_b' - \frac{f^{\equiv} + \frac{4}{3}f^{\equiv}}{f^{\equiv}} \cdot (Q_b'' - Q_b') \quad (2.32)$$

Equation (2.32) allows the calculation of  $Q_b'''$  values for all combinations of  $f^{\equiv}$  and  $f^{\equiv}$  (cf table 2 and figure 6).

### Appendix III

#### Approximate approach for the negative adsorption of the trivalent anion in a quintuple system

As was described in section 2.1.3 the expression for the negative adsorption of the trivalent anion in this case reads:

$$\frac{\Gamma^{\equiv}}{f^{\equiv} N_0} \approx \pm \frac{\sqrt{2}}{\sqrt{\beta N_0}} \cdot \left\{ \int_{\infty}^1 \frac{du}{u\sqrt{A}} + \int_{\infty}^1 \frac{du}{u^2\sqrt{A}} + \int_{\infty}^1 \frac{du}{u^3\sqrt{A}} \right\} - \delta^- \quad (2.38)$$

with  $A = f^{++}u^2 + 2u + f^=$ .

The recurrence procedure is now:

$$(2t+4) \cdot f^{++} \cdot J_{t+2} + (2t+3) \cdot J_{t+1} + (2t+2) \cdot f^= \cdot J_t = [2(u)^{t+1} \cdot \sqrt{A}]_1^{\infty}$$

Substituting  $-3$  for  $t$ :

$$-2f^{++} \cdot J_{-1} - 6J_{-2} - 4f^= \cdot J_{-3} = [2u^{-2}\sqrt{f^{++}u^2 + 2u + f^=}]_1^{\infty}$$

$$J_{-3} = \frac{\sqrt{f^{++} + 2 + f^=}}{2f^=} - \frac{f^{++}}{2f^=} \cdot J_{-1} - \frac{3}{2f^=} \cdot J_{-2}$$

$J_{-1}$  may be replaced by  $Q'_a/\sqrt{2}$  and  $J_{-2}$  by  $(Q''_a - Q'_a)/\sqrt{2}$ .

Thus the expression for  $Q'''_c$  becomes:

$$Q'''_c = \sqrt{2} \cdot \left\{ \frac{\sqrt{f^{++} + 2 + f^=}}{2f^=} + \frac{2f^= - f^{++}}{2f^=} \cdot \frac{Q'_a}{\sqrt{2}} + \frac{2f^= - 3}{2f^=} \cdot \frac{(Q''_a - Q'_a)}{\sqrt{2}} \right\} \quad (2.40)$$

## Appendix IV

### Derivation of the expressions for the negative adsorption of anions in systems with interacting double layers

The derivations are given for a system of the composition (+1, -1, -2). In this case the negative adsorption of the mono- and divalent anion is described by:

$$\frac{\Gamma^-}{(1-f^-)N_0} = \frac{Q'_i}{\sqrt{\beta N_0}} - \delta^- \quad (2.47)$$

and

$$\frac{\Gamma^{--}}{f^- N_0} = \frac{Q''_i}{\sqrt{\beta N_0}} - \delta^- \quad (2.49)$$

in which

$$Q'_i = \int_{-\infty}^{u_0} \frac{du}{\sqrt{I}} - \int_{-\infty}^{u_0} \frac{du}{u\sqrt{I}} \quad (2.44a)$$

and

$$Q''_i = \int_{-\infty}^{u_0} \frac{du}{\sqrt{I}} - \int_{-\infty}^{u_0} \frac{du}{u^2\sqrt{I}} \quad (2.46a)$$

$I$  stands for a third power polynomial in  $u$  of which the roots,  $\alpha_1, \alpha_2, \alpha_3$ , are known functions of  $u_c$  and  $f^-$  (cf section 2.1.4).

#### 1 THE MONOVALENT ANION

The solution of the first integral of (2.44a) is:

$$\int_{-\infty}^{u_0} \frac{du}{\sqrt{I}} = \frac{2}{\sqrt{\alpha_1 - \alpha_3}} \cdot F(\varphi, k) \quad \text{with } k = \sqrt{\frac{\alpha_2 - \alpha_3}{\alpha_1 - \alpha_3}};$$

$\varphi$  is found by substituting the integration limits into:

$$u = \frac{-\alpha_2 \sin^2 \varphi + \alpha_1}{-\sin^2 \varphi + 1}$$



Executing this for the limits  $u_c$  and  $\infty$ ,  $\varphi$  is found to be  $0^\circ$  and  $90^\circ$ , respectively. Thus  $F(\varphi, k)$  is in this case a complete elliptic integral of the first kind,  $F(\pi/2, k)$ . The solution of the second integral of equation (2.44a) is:

$$\int_{\infty}^{u_c} \frac{du}{u\sqrt{I}} = \frac{2}{-\alpha_2\sqrt{\alpha_1-\alpha_3}} \cdot \left\{ -F(\varphi, k) + \frac{\alpha_1-\alpha_2}{\alpha_1} \cdot \Pi\left(\varphi, -\frac{\alpha_2}{\alpha_1}, k\right) \right\}$$

Combining this with the solution of the first integral one finds, after substitution of  $u_c$  for  $\alpha_1$ :

$$Q'_i = \frac{2}{\sqrt{u_c-\alpha_3}} \left(1 - \frac{1}{\alpha_2}\right) \cdot F(\pi/2, k) + \frac{2(u_c-\alpha_2)}{\alpha_2 u_c \sqrt{u_c-\alpha_3}} \cdot \Pi(\pi/2, \rho, k) \quad (2.48)$$

in which  $\Pi(\pi/2, \rho, k)$  stands for a complete elliptic integral of the third kind with  $\rho = -\alpha_2/u_c$ .

## 2 THE DIVALENT ANION

The expression for  $Q'_i$  requires the solution of the second integral of (2.46a). This integral may be converted to the ones appearing in (2.44a) by applying the recurrence procedure as described in Appendix II. One then finds:

$$J_{-2} = \frac{1}{f''} \cdot J_1 - \frac{1-f''}{f''} \cdot J_{-1}$$

Thus

$$\begin{aligned} Q'_i &= J_0 + \frac{1-f''}{f''} \cdot J_{-1} - \frac{1}{f''} \cdot J_1 \\ &= \frac{2}{\sqrt{\alpha_1-\alpha_3}} \left\{ \left(1 + \frac{1-f''}{\alpha_2 f''} - \frac{\alpha_1}{f''}\right) \cdot F(\varphi, k) + \frac{\alpha_1-\alpha_3}{f''} \cdot E(\varphi, k) - \frac{1-f''}{f''} \cdot \frac{\alpha_1-\alpha_2}{\alpha_1 \alpha_2} \right. \\ &\quad \left. \cdot \Pi(\varphi, \rho, k) \right\} \end{aligned}$$

Replacing  $\alpha_1$  by  $u_c$ :

$$\begin{aligned} &= \frac{2}{\sqrt{u_c-\alpha_3}} \left\{ \left(1 + \frac{1-f''}{\alpha_2 f''} - \frac{u_c}{f''}\right) \cdot F(\pi/2, k) + \frac{u_c-\alpha_3}{f''} \cdot E(\pi/2, k) - \frac{1-f''}{f''} \cdot \frac{u_c-\alpha_2}{\alpha_2 u_c} \right. \\ &\quad \left. \cdot \Pi(\pi/2, \rho, k) \right\} \quad (2.50) \end{aligned}$$

As the elliptic integral of the third kind has never been tabulated its value must be found by means of a series expansion. This series expansion reads for a complete elliptic integral of the third kind:

$$\begin{aligned} \Pi(\pi/2, \rho, k) = & \frac{\pi}{2} \left[ 1 - \frac{1}{2}\rho \left( 1 - \frac{1}{2} \cdot \frac{k^2}{\rho} \right) + \frac{3}{8}\rho^2 \left( 1 - \frac{1}{2} \cdot \frac{k^2}{\rho} + \frac{3}{8} \cdot \frac{k^4}{\rho^2} \right) \right. \\ & - \frac{5}{16}\rho^3 \left( 1 - \frac{1}{2} \cdot \frac{k^2}{\rho} + \frac{3}{8} \cdot \frac{k^4}{\rho^2} - \frac{5}{16} \cdot \frac{k^6}{\rho^3} \right) \\ & \left. + \frac{35}{128}\rho^4 \left( 1 - \frac{1}{2} \cdot \frac{k^2}{\rho} + \frac{3}{8} \cdot \frac{k^4}{\rho^2} - \frac{5}{16} \cdot \frac{k^6}{\rho^3} + \frac{35}{128} \cdot \frac{k^8}{\rho^4} \right) - \dots \right] \end{aligned}$$

### A Derivation of the expressions to the neglect of the divalent anions

Under the condition that  $f'' \simeq 0$  the roots of  $I$  are found as  $u_c$ ,  $1/u_c$  and 0, respectively.

#### A1 The monovalent anion

In this case  $\Pi(\pi/2, \rho, k)$  may again be converted into an elliptic integral of the second kind as  $\rho = -k^2$ , according to:

$$\Pi(\pi/2, -k^2, k) = \frac{1}{1-k^2} \cdot E(\pi/2, k)$$

Thus now one finds for  $Q'_i$ :

$$Q'_i(f'' = 0) = \frac{2}{\sqrt{\alpha_1}} \cdot F(\pi/2, k) - \frac{2}{\alpha_2 \sqrt{\alpha_1}} \cdot F(\pi/2, k) + \frac{2}{\alpha_2 \sqrt{\alpha_1}} \cdot \frac{\alpha_1 - \alpha_2}{\alpha_1} \cdot \frac{1}{1-k^2} \cdot E(\pi/2, k)$$

Since in this case  $\alpha_1 = u_c$ ,  $\alpha_2 = 1/u_c$  and  $k = 1/u_c$  this may be written as:

$$Q'_i(f'' = 0) = \frac{2}{\sqrt{u_c}} (1 - u_c) \cdot F\left(\pi/2, \frac{1}{u_c}\right) + 2\sqrt{u_c} \cdot E\left(\pi/2, \frac{1}{u_c}\right) \quad (2.51)$$

#### A2 The divalent anion

Applying again the recurrence procedure one finds for:

$$\int_{-\infty}^{u_c} \frac{du}{u^2 \sqrt{I}} = J_{-2} = \frac{2}{3} \left( u_c + \frac{1}{u_c} \right) \cdot J_{-1} - \frac{1}{3} J_0$$

According to equation (2.46a):

$$\begin{aligned} Q'_i(f'' = 0) &= J_0 - J_{-2} \\ &= \frac{4}{3} J_0 - \frac{2}{3} \left( u_c + \frac{1}{u_c} \right) \cdot J_{-1} \\ &= \frac{4}{3} \cdot \frac{2}{\sqrt{\alpha_1}} \cdot F(\pi/2, k) - \frac{2}{3} \left( u_c + \frac{1}{u_c} \right) \frac{2}{\alpha_2 \sqrt{\alpha_1}} \cdot F(\pi/2, k) \end{aligned}$$

$$+ \frac{2}{3} \left( u_c + \frac{1}{u_c} \right) \frac{2(\alpha_1 - \alpha_2)}{\alpha_1 \alpha_2 \sqrt{\alpha_1}} \cdot \frac{1}{1 - k^2} \cdot E(\pi/2, k)$$

Replacing again  $\alpha_1$  by  $u_c$  and  $\alpha_2$  and  $k$  by  $1/u_c$  one finds:

$$Q_i''(f'' = 0) = \left\{ \frac{8}{3\sqrt{u_c}} - \frac{4\sqrt{u_c}}{3} \left( u_c + \frac{1}{u_c} \right) \right\} \cdot F\left(\pi/2, \frac{1}{u_c}\right) + \frac{4\sqrt{u_c}}{3} \left( u_c + \frac{1}{u_c} \right) \cdot E\left(\pi/2, \frac{1}{u_c}\right) \quad (2.52)$$

### A3 The trivalent anion

The expression of  $Q_i$  for this anion is now found as:

$$Q_i''' = \int_{\infty}^{u_c} \frac{du}{\sqrt{I}} - \int_{\infty}^{u_c} \frac{du}{u^3 \sqrt{I}} \\ = J_0 - J_{-3}$$

The expression for  $J_{-3}$  is again found from a recurrence procedure, viz.:

$$J_{-3} = -\frac{3}{5} \cdot J_{-1} + \frac{4}{5} \left( u_c + \frac{1}{u_c} \right) \cdot J_{-2}$$

Thus:

$$Q_i'''(f'' = f''' = 0) = J_0 + \frac{3}{5} \cdot J_{-1} - \frac{4}{5} \left( u_c + \frac{1}{u_c} \right) \cdot J_{-2}$$

Substituting the value for  $J_{-2}$  found in the above:

$$= J_0 + \frac{3}{5} \cdot J_{-1} - \frac{4}{5} \left( u_c + \frac{1}{u_c} \right) \left\{ -\frac{1}{3} \cdot J_0 + \frac{2}{3} \left( u_c + \frac{1}{u_c} \right) \cdot J_{-1} \right\} \\ = \left\{ 1 + \frac{4}{15} \left( u_c + \frac{1}{u_c} \right) \right\} \cdot J_0 + \left\{ \frac{3}{5} - \frac{8}{15} \left( u_c + \frac{1}{u_c} \right)^2 \right\} \cdot J_{-1} \\ = \left[ \left\{ 1 + \frac{4}{15} \left( u_c + \frac{1}{u_c} \right) \right\} \cdot \frac{2}{\sqrt{u_c}} + \left\{ \frac{3}{5} - \frac{8}{15} \left( u_c + \frac{1}{u_c} \right)^2 \right\} \cdot 2\sqrt{u_c} \right] \cdot F\left(\pi/2, \frac{1}{u_c}\right) \\ - \left\{ \frac{3}{5} - \frac{8}{15} \left( u_c + \frac{1}{u_c} \right)^2 \right\} \cdot 2\sqrt{u_c} \cdot E\left(\pi/2, \frac{1}{u_c}\right) \quad (2.53)$$

**B Derivation of the expressions for systems in which the anionic concentrations are all negligible in comparison to the cationic concentrations**

### B1 The monovalent anion

In this case the expression for  $Q_i'$  reads:

$$\begin{aligned}
Q'_i(N_0^{z-} = 0) &= \int_{\infty}^{u_0} \frac{(1-1/u)du}{u\sqrt{u-u_c}} \\
&= \int_{\infty}^{u_0} \frac{du}{u\sqrt{u-u_c}} - \int_{\infty}^{u_0} \frac{du}{u^2\sqrt{u-u_c}} \\
&= \left(1 - \frac{1}{2u_c}\right) \cdot \int_{\infty}^{u_0} \frac{du}{u\sqrt{u-u_c}} \\
&= \left(1 - \frac{1}{2u_c}\right) \cdot \frac{2}{\sqrt{u_c}} \cdot \frac{\pi}{2} \\
&= \left(1 - \frac{1}{2u_c}\right) \cdot \frac{\pi}{\sqrt{u_c}}
\end{aligned} \tag{2.54}$$

B2 The divalent anion

$$\begin{aligned}
Q''_i(N_0^{z-} = 0) &= \int_{\infty}^{u_0} \frac{(1-1/u^2)du}{u\sqrt{u-u_c}} \\
&= \int_{\infty}^{u_0} \frac{du}{u\sqrt{u-u_c}} - \int_{\infty}^{u_0} \frac{du}{u^3\sqrt{u-u_c}} \\
&= \int_{\infty}^{u_0} \frac{du}{u\sqrt{u-u_c}} - \frac{3}{4u_c} \cdot \int_{\infty}^{u_0} \frac{du}{u^2\sqrt{u-u_c}}
\end{aligned}$$

Substituting the value found above for the second integral of this equation:

$$\begin{aligned}
Q''_i(N_0^{z-} = 0) &= \left(1 - \frac{3}{8u_c^2}\right) \cdot \int_{\infty}^{u_0} \frac{du}{u\sqrt{u-u_c}} \\
&= \left(1 - \frac{3}{8u_c^2}\right) \cdot \frac{\pi}{\sqrt{u_c}}
\end{aligned} \tag{2.55}$$

B3 The trivalent anion

$$\begin{aligned}
Q'''_i(N_0^{z-} = 0) &= \int_{\infty}^{u_0} \frac{(1-1/u^3)du}{u\sqrt{u-u_c}} \\
&= \int_{\infty}^{u_0} \frac{du}{u\sqrt{u-u_c}} - \int_{\infty}^{u_0} \frac{du}{u^4\sqrt{u-u_c}} \\
&= \int_{\infty}^{u_0} \frac{du}{u\sqrt{u-u_c}} - \frac{5}{6u_c} \cdot \int_{\infty}^{u_0} \frac{du}{u^3\sqrt{u-u_c}}
\end{aligned}$$

Substituting for the second integral the value derived at B2) one finds:

$$Q'''_i(N_0^{z-} = 0) = \left(1 - \frac{5}{16u_c^3}\right) \cdot \frac{\pi}{\sqrt{u_c}} \tag{2.56}$$